The role of microRNAs in renal fibrosis

Aleksandra Krupa MSc

Thesis presented for the degree of Philosophiae Doctor

March 2010

Institute of Nephrology School of Medicine Cardiff University Heath Park Campus Cardiff CF14 4XN United Kingdom UMI Number: U584462

All rights reserved

INFORMATION TO ALL USERS

The quality of this reproduction is dependent upon the quality of the copy submitted.

In the unlikely event that the author did not send a complete manuscript and there are missing pages, these will be noted. Also, if material had to be removed, a note will indicate the deletion.



UMI U584462

Published by ProQuest LLC 2013. Copyright in the Dissertation held by the Author.

Microform Edition © ProQuest LLC.

All rights reserved. This work is protected against unauthorized copying under Title 17, United States Code.



ProQuest LLC 789 East Eisenhower Parkway P.O. Box 1346 Ann Arbor, MI 48106-1346 I dedicate this thesis to Doctor Krystyna Boroń, who let me start my contribution to the kidney research field when I was six.

ACKNOWLEDGMENTS

I wish to express my gratitude to my supervisor, Dr Donald Fraser, for constant support and guidance throughout my PhD. In addition, I would like to thank him for explaining to me the English meaning of 'I sort of agree with you', which has since become my favourite phrase. I am also very grateful to my second supervisor and the most perfect person I have ever met, Professor Aled Phillips, for enhancing my motivation all the way through my studies.

I would also like to show my genuine appreciation to the Head of the Department, Professor John Williams, and other staff members and students in the Institute of Nephrology. In particular, I am thankful to the excellent Lab Manager, Dr Ruth MacKenzie, for her invaluable help and patience; Dr Timothy Bowen and Dr Robert Steadman for their helpful suggestions; Dr Robert Jenkins, Dong Dong Luo, and Dr John Martin for technical advice and expert assistance; and Girish Bommayya, Chantal Colmont, and Rasha Bennagi for more or less scientific, but always inspiring discussions.

Also, I am very grateful to the two Central Biotechnology Services staff members: Dr Claudia Consoli, who let me assist her while she performed qRT-PCR-based microRNA profiling experiment on FFPE renal biopsy samples, and Mrs Megan Musson, who showed me how to check RNA quality using Agilent's 2100 bioanalyser.

A very special thank you goes to Dr Małgosia Bzowska, Dr Krzysztof Guzik, and Dr Jasiek Smagur from the Jagiellonian University, Kraków, Poland, for helping me realise there might be a place in the world for me; and then for letting me go and find my own way. I owe them my eternal gratitude.

Finally, I would like to thank my Mum for continuous encouragement, whether she was happy with my choices or not; my Absolutely Best Friends for their patience and understanding; and my little Nephew for being the most lovely distraction during the writing up period.

SUMMARY

This thesis examines the role of microRNAs in renal fibrosis. MicroRNAs constitute a large family of approximately 22-nucleotide-long non-coding RNAs, that in animal cells regulate gene expression posttranscriptionally. At the start of the project, microRNAs were emerging as potentially important factors in various physiological and pathological processes; however, there was very little known about their expression and function in the kidney, in particular in tubulointerstitial fibrosis. In this thesis, global microRNA expression has been analysed in vitro in proximal tubular epithelial cells, and in vivo in formalin-fixed, paraffin-embedded kidney biopsy samples from patients with diabetic nephropathy. Among microRNAs altered by profibrotic stimuli, the greatest difference has been found in expression of miR-192, which is downregulated in severe diabetic nephropathy. Further examination of miR-192 in kidney biopsy samples has revealed that its expression correlates well with renal function and inversely correlates with fibrosis. A possible function of miR-192 has been then studied in vitro in proximal tubular epithelial cells. It has been found that treatment of the cells with the profibrotic cytokine TGF-beta1 downregulates miR-192. Moreover, manipulation of miR-192 expression has shown that miR-192 is involved in E-cadherin regulation. The mechanism of that regulation has been investigated, pointing to two transcriptional repressors of E-cadherin, ZEB1 and ZEB2, as direct targets of miR-192. The presented data suggest that, in the kidney, miR-192 may prevent epithelial-to-mesenchymal transition, known to contribute to renal fibrosis. In parallel, global microRNA downregulation in proximal tubular epithelial cells has been attempted. However, knockdown of Dicer or TRBP, proteins involved in microRNA processing, has not been sufficient to induce changes in microRNA expression. The possible explanations have been discussed. Finally, microRNA role in direct regulation of TGF-beta1 synthesis has been investigated. In particular, human microRNAs similar to viral hsv-miR-LAT, reported to directly target TGF-beta1 mRNA, have been tested.

PUBLICATIONS AND PRESENTATIONS ARISING FROM THIS THESIS

Publications

Zhang M., Lee C.H., Luo D.D., **Krupa A.**, Fraser D.J., Phillips A.O. Polarity of response to transforming growth factor-beta 1 in proximal tubular epithelial cells is regulated by beta-catenin. *J Biol Chem.* 2007 Sep 28;282(39):28639-47 (Epub 2007 Jul 9).

Krupa A., Jenkins R., Luo D.D., Lewis A., Phillips A.O., Fraser D.J. Loss of microRNA-192 promotes fibrogenesis in diabetic nephropathy. *J Am Soc Nephrol*. In Press (Epub 2010 Jan 7).

Michael D.R., Phillips A.O., **Krupa A.**, Webber J., Altaher A., Neville R.D., Kim M., Bowen T. Regulation of the expression of the human hyaluronan synthase 2 antisense RNA, HAS2AS (submitted).

Martin J., Krupa A., Bennagi R., Phillips A.O., Fraser D.J. Post-transcriptional regulation of transforming growth factor-beta 1 by its 3' UTR (in preparation).

Presentations

- 2006: **Krupa A.**, Phillips A.O., Fraser D.J. Glucose alters microRNA expression in proximal tubular epithelial cells (poster presentation). 5th Annual Meeting of the Cardiff Institute of Tissue Engineering and Repair in Abergavenny, Wales.
- 2007: **Krupa A.**, Phillips A.O., Fraser D.J. The role of microRNA in glucose-induced changes in proximal tubular epithelial cell phenotype (poster presentation). Annual Science Meeting of the Metabolism, Regeneration & Repair (MR2) Interdisciplinary Research Group in Cardiff, Wales.
- 2008: **Krupa A.**, Phillips A.O., Fraser D.J. MicroRNA expression and function in proximal tubular cells (oral presentation). 20th Meeting of the European Renal Cell Study Group in Gregynog, Wales.
 - **Krupa A.**, Lewis A., Phillips A.O., Fraser D.J. The role of miR-192 in renal fibrosis (oral presentation). 7th Annual Meeting of the Cardiff Institute of Tissue Engineering and Repair in Abergavenny, Wales.
- 2009: **Krupa A.**, Lewis A., Phillips A.O., Fraser D.J. The role of microRNAs in renal fibrosis (oral presentation). 4th Annual Meeting of the Bristol RNA Club in Bristol, England.

INDEX

List of figures and tables	
Abbreviations	5
CHAPTER ONE: Introduction	7
1.1 The kidney	
1.1.1 Kidney structure	
1.1.2 Kidney function	
1.1.3 Renal diseases	
1.2 Diabetic nephropathy	
1.2.1 Factors contributing to development and progression of diabetic	
nephropathy	14
1.2.2 The clinical course of diabetic nephropathy	
1.2.3 Pathological changes in diabetic nephropathy	
1.2.4 Molecular basis of tubulointerstitial fibrosis in diabetic	
nephropathy and other chronic kidney diseases	18
1.3 Control of gene expression	
1.3.1 Transcriptional control	
1.3.2 Posttranscriptional control	
1.3.3 Posttranslational control.	
1.4 MicroRNAs in regulation of gene expression	
1.4.1 MicroRNA discovery	
1.4.2 MicroRNA expression	
1.4.3 Biogenesis of microRNAs in animals	
1.4.4 Modes of action of animal microRNAs	
1.4.5 MicroRNA role in health and disease	
1.5 MicroRNAs in the kidney and in fibrotic diseases	
1.6 Aim of this thesis	
CHAPTER TWO: Methods	
2.1 Samples	
2.1.1 Cell culture	
2.1.1.1 Cell lines	
2.1.1.2 Culture conditions	
2.1.1.3 Determination of cell number and viability	
2.1.1.4 Cell stimulations	
2.1.1.5 Transfections	61
2.1.2 Tissue samples	76
2.2 RNA analysis	
2.2.1 RNA extraction, quantification, and quality control	77
2.2.1.1 Cell culture samples	77
2.2.1.2 Tissue samples	82
2.2.2 Messenger RNA detection	85
2.2.2.1 Reverse transcription	
2.2.2.2 Quantitative polymerase chain reaction	
2.2.2.3 Quantitative RT-PCR data analysis	88
2.2.3 MicroRNA detection	89
2.2.3.1 MicroRNA profiling	89
	92

2.3 Protein analysis	98
2.3.1 Western blot	98
2.3.2 Immunofluorescence	102
2.3.3 Enzyme-linked immunosorbent assay	
2.3.4 Luciferase activity	105
2.4 Bioinformatics	
2.4.1 MicroRNA target prediction	106
2.4.2 Identification of human microRNAs similar to miR-LAT	107
2.4.3 Other applications	108
2.5 Statistical analysis	
CHAPTER THREE: Changes in microRNA expression in response	
to profibrotic stimuli in vitro and in vivo	128
3.1 Introduction	129
3.2 Results	
3.2.1 MicroRNA expression in proximal tubular epithelial cells	
3.2.2 MicroRNA expression in kidney biopsies from patients	
with diabetic nephropathy	134
3.3 Discussion	137
3.3 Discussion	,,,,,,,,,,,,,,,,,,,,,,,,,,,,,,,,,,,,,,,
CHAPTER FOUR: Attempts to repress expression or function of all	
microRNAs in proximal tubular epithelial cells	158
4.1 Introduction	159
4.2 Results	162
4.2.1 Transient knockdown of Dicer or TRBP using siRNA	
4.2.2 Long-term knockdown of Dicer or GW182 with shRNA	165
4.3 Discussion	167
CHAPTER FIVE: MicroRNA function in the kidney: the role	
of miR-192 in EMT	179
5.1 Introduction	180
5.2 Results	184
5.2.1 Characterisation of HK-2 cell response to TGF-beta	
5.2.2 Manipulation of miR-192 (and miR-200b) expression	
in HK-2 cells	185
5.3 Discussion	
CHAPTER SIX: Role of microRNAs in posttranscriptional regulation	
of TGF-beta synthesis	206
6.1 Introduction	
6.2 Results	
6.2.1 In silico search for human microRNAs similar to miR-LAT	
6.2.2 Expression of miR-608 and miR-663 in HK-2 and U937 cells	209
6.2.3 Effects of enforced expression of miR-608 and miR-663 in HK-2	
cells on TGF-beta	
6.2.4 Function of exogenous miR-LAT in HK-2 cells	
6.3 Discussion	
CHAPTER SEVEN: General discussion	
CHAFTER SEVENT UCHCIAI UISCUSSIOII	23
References	238
Annendix: Buffers and Reagents	258

LIST OF FIGURES AND TABLES

Figures

1.1	The kidney	49
1.2	Control of gene expression in eukaryotic organisms	50
1.3	The canonical microRNA biogenesis pathway	
2.1	The siSTRIKE U6 vector	.110
2.2	The pGL3-Control vector	
2.3	Construction of reporter plasmids with ZEB1 or ZEB2 3'UTRs	
	downstream the luciferase CDS	. 112
2.4	Selection of an optimal transfection method for plasmid DNA delivery to	
	HK-2 cells	
2.5	HK-2 cell resistance to puromycin	
2.6	RNA extraction using mirVana miRNA Isolation Kit	. 115
2.7	Comparison of two RNA isolation methods	
2.8	Preliminary analysis of RNA isolated from FFPE renal biopsy samples	
2.9	Amplification plot features	. 118
2.10	Schematic overview of the stem-loop qRT-PCR microRNA detection	110
	system	. 119
2.11		. 120
2.12	Design and validation of SYBR Green-based stem-loop qRT-PCR	
	for microRNA detection	. 121
3.1	Preliminary experiments done before the start of my project.	. 143
3.2	Expression of selected microRNAs in HK-2 cells cultured in medium with	
	high glucose concentration	. 145
3.3	TGF-beta secretion by HK-2 cells cultured with 25 mM glucose	
3.4	MicroRNA profiling in proximal tubular cells	. 148
3.5	Expression of selected microRNAs in HK-2 cells stimulated with TGF-	1.40
	beta	. 149
3.6	Expression of newly selected microRNAs in HK-2 cells stimulated with	150
	TGF-beta	. 150
3.7	Expression of miR-192 and miR-21 in HK-2 cells stimulated with	
	profibrotic stimuli	. 151
3.8	Quantification and quality control of RNA isolated from FFPE renal	
	biopsy tissue from patients with diabetic nephropathy	. 152
3.9	TaqMan Low Density Array determination of microRNA expression in	
	renal biopsy tissue from patients with diabetic nephropathy	. 154
3.10	Expression of miR-192 in individual kidney biopsies and its correlation	
	with severity of kidney disease	. 155
4.1	Transient Dicer knockdown – time course	
4.2	Sequential transfection with siRNA silencing Dicer	. 170
4.3	Transient Dicer knockdown – dose response	. 171
4.4	Transient Dicer knockdown using three siRNAs against Dicer	
4.5	Transient Dicer knockdown at the protein level	. 173
4.6	Transient knockdown of Dicer and TRBP	
4.7	Long-term Dicer knockdown	
4.8	Selection of single lines that stably express shRNA silencing Dicer	. 176
4.9	GW182 knockdown	

5.1	Characterisation of HK-2 response to TGF-beta by qRT-PCR	195
5.2	Characterisation of HK-2 response to TGF-beta by qRT-PCR – time course	
5.3	Inhibition of miR-192 or miR-200b in HK-2 cells	
5.4	Transient overexpression of miR-192 and miR-200b in HK-2 cells	198
5.5	Stable overexpression of miR-192 and miR-200b in HK-2 cells	
5.6	Stable overexpression of miR-192 – kinetics	
5.7	Comparison of three shRNAs expressed by control cells in stable	
	transfection experiments	201
5.8	Expression of E-cadherin in single lines that stably overexpress miR-192	
	- at the mRNA level	202
5.9	Expression of E-cadherin in single lines that stably overexpress miR-192	
	- at the protein level	203
5.10	Regulation of ZEB1 and ZEB2 expression by miR-192	204
5.11	Expression of other EMT markers in single lines that stably overexpress	
	miR-192	205
<i>-</i> 1	II MODIL	220
6.1	Human TGF-beta transcript	220
6.2	Predicted interactions between microRNAs and TGF-beta mRNA	221
6.3	Validation of the commercial TaqMan qRT-PCR assay for miR-608	222
	detection	222
6.4	Expression of miR-608 in HK-2 and U937 cells	223
6.5	Validation of the miR-663 stem-loop qRT-PCR system designed for this	, 004
	project	224
6.6	Expression of miR-663 in HK-2 and U937 cells	225
6.7	TGF-beta expression in HK-2 following transfection with synthetic	226
	miR-608	226
6.8	Transfection with synthetic miR-608 or miR-663	
6.9	Effects of miR-608 and/or miR-663 on TGF-beta and SMAD3	
6.10	Effect of miR-608 on TGF-beta at the protein level	
6.11	Effect of synthetic miR-LAT on TGF-beta and SMAD3	
6.12	Effect of synthetic miR-LAT on SMAD-dependent transcription	
6.13	Effect of miR-608 and miR-663 on TGF-beta mRNA – summary	232
Tab	oles	
1.1	The stages of chronic kidney disease	51
1.2	MicroRNAs in the kidney and in renal non-malignant diseases	
1.3	Summary of microRNA profiling experiments using renal cell carcinoma	
	samples	53
	0 11 11 11 11	100
2.1	Small RNA used in this study	122
2.2	Plasmids generated for this study and sequences of the oligonucleotides	100
• •	used in cloning	
2.3	Patient characteristics	
2.4	Quantitative PCR assays used in this study	
2.5	Antibodies used for immunofluorescence and Western blot	127
3.1	Selection of microRNAs for further analysis	156
3.2	Selection of microRNAs potentially regulated by TGF-beta	157
_	· , , , , , , , , , , , , , , , , , , ,	

ABBREVIATIONS

ACE Angiotensin-converting enzyme

ACTB Beta-actin

B2M Beta-2-microglobulin

bp Base pair

BSA Bovine serum albumin

CBS Central Biotechnology Services, Cardiff University School of Medicine

cDNA Complementary DNA

CDS Coding sequence
C_T Threshold cycle

CTGF Connective tissue growth factor

DGCR8 DiGeorge syndrome critical region gene 8

DMSO Dimethyl sulfoxide

ECL Enhanced chemiluminescence
EDTA Ethylenediamine-tetraacetic acid
eGFR Estimated glomerular filtration rate

eIF6 Eukaryotic translation initiation factor 6
ELISA Enzyme-linked immunosorbent assay
EMT Epithelial-to-mesenchymal transition

Exp5 Exportin-5

FCS Fetal calf serum

FFPE Formalin-fixed, paraffin-embedded

GAPDH Glyceraldehyde-3-phosphate dehydrogenase

GW182 Glycine-tryptophan protein of 182 kDa (official symbol TNRC6A)

h Hour

HGF Hepatocyte growth factor

HPRT1 Hypoxanthine phosphoribosyltransferase 1

HRP Horseradish peroxidase

ICAM-1 Inter-cellular adhesion molecule 1

IGF-1 Insulin-like growth factor 1

IL-1 Interleukin 1

IRES Internal ribosome entry site

miRISC MicroRNA-induced silencing complex

MMP Matrix metalloproteinase
NMD Nonsense-mediated decay

nt Nucleotide

NTC Non-template control

PAGE Polyacrylamide gel electrophoresis

PAI-1 Plasminogen activator inhibitor 1

PBS Phosphate-buffered saline

PCR Polymerase chain reaction

PDGF Platelet-derived growth factor

piRNA Piwi-interacting RNA

PMA 12-O-Tetradecanoylphorbol 13-acetate

qRT-PCR Quantitative reverse transcription – polymerase chain reaction

RPLP0 Large ribosomal protein P0

RT Reverse transcription

SBE SMAD-binding element

SDS Sodium dodecyl sulfate

SEM Standard error of the mean

shRNA Short hairpin RNA

siRNA Short interfering RNA

TBP TATA box-binding protein

TBS Tris-buffered saline

TFRC Transferrin receptor

TGF-beta Transforming growth factor-beta

TIMP-1 Tissue inhibitor of metalloproteinases 1

Tm Melting temperature

TNF Tumour necrosis factor

TRBP HIV-1 transactivating response RNA-binding protein

uPA Urokinase-type plasminogen activator

UTR Untranslated region

VCAM-1 Vascular cell adhesion molecule 1

ZEB1 Zinc finger E-box binding homeobox 1 (also known as δEF1)

ZEB2 Zinc finger E-box binding homeobox 2 (also known as SIP1)

CHAPTER ONE:

INTRODUCTION

1.1 The kidney

The human kidneys are two relatively small but vital organs, located at the end of the rib cage, one on each side of the spine, behind the peritoneal cavity (Figure 1.1A). Their main roles are removal of waste products from the blood, maintenance of homeostatic balance in the body, and secretion of important hormones. In order to perform their tasks, the kidneys have evolved over thousands of years into organs of an unusually sophisticated anatomy and physiology.

1.1.1 Kidney structure

The kidneys are bean-shaped, in a normal adult about 10 cm long, 6 cm wide and 3 cm thick, and together constitute approximately 0.5% of total body weight. The outer part of the kidney is known as the renal cortex, whereas the inner bit is the renal medulla (Figure 1.1B). Each kidney is attached to the renal artery, the renal vein, nerves, and the ureter. Above the kidney is situated the adrenal gland [1].

The nephron

The basic structural and functional unit of the kidney is the nephron (Figure 1.1C). Each nephron starts with the renal corpuscle, composed of a cluster of blood vessels supported by the mesangium, together called the glomerulus, located within

a chamber-like structure known as the Bowman's capsule. The renal corpuscle is attached to the renal tubule, encircled by the peritubular capillaries. The tubule walls are made of epithelial cells that specialise in transport of small molecules, with varying properties in distinct sections of the tubule, which are consecutively: proximal convoluted tubule, loop of Henle, distal convoluted tubule, and collecting duct (shared by several nephrons) [1].

A healthy kidney contains typically more than one million nephrons. The vast majority of them are located almost entirely in the renal cortex, apart from loops of Henle and collecting ducts which descend into the medulla [1].

1.1.2 Kidney function

The most basic function of the kidneys is the removal of waste products and toxins from blood. Accordingly, despite their relatively small mass, the kidneys are supplied with 20-25% of total arterial blood pumped by the heart. Every day the kidneys filter approximately 200 litres of blood. This makes them particularly valuable sensors of plasma concentrations of important minerals, glucose, oxygen, and hydrogen ions. Certain mechanisms have evolved, enabling the kidneys not only to sense, but also react to unusual composition of the blood, so that the optimal concentrations are restored. Their role in maintaining the bodily fluid homeostasis is so significant that the kidney is considered one of the main homeostatic devices of the human body [1].

Urine formation and maintenance of homeostasis

There are three fundamental processes, occurring in nephrons, that result in both urine formation and maintenance of electrolyte and water balance. These are filtration, reabsorption, and tubular secretion.

Filtration

Filtration takes place in the renal corpuscle. Blood enters the glomerulus under pressure, so that the water and small molecules from the blood are forced into Bowman's capsule through a layer of glomerular endothelial cells, basement membrane, and podocytes. The gaps in the filtration barrier are too small to let bigger molecules (> 50-70 kDa) and the blood cells through. Consequently, the filtrate, which now flows from the Bowman's capsule to the renal tubule, has a very similar composition to the blood plasma, but lacks the majority of plasma proteins [1].

Reabsorption

In the tubule, useful substances are returned from the filtrate back to the blood in a process known as reabsorption. This occurs in two steps. The substances are first transported from the tubule to the interstitium (connective tissue surrounding the nephron), and then to the peritubular capillaries. That is driven by active transport, osmosis and diffusion, and differs in various parts of the tubule. For instance, the proximal tubule specialises in reabsorption of glucose, amino acids, and vitamins, and also claims back the majority of inorganic salts and water. The process continues in the next tubule sections, with more focus on sodium and water reabsorption. In particular the loop of Henle with the following distal tubule are perfectly suited to

reclaim as much water as possible and form very concentrated urine due to the very smart counter-current multiplier system [1].

Tubular secretion

The tubular secretion is the auxiliary process, in which some particular substances, toxic or present in excess in blood, are secreted directly from the peritubular capillaries to the tubular fluid. It has the greatest role in maintaining constant pH of the blood (by secretion of more hydrogen ions, combined with ammonia, when the blood becomes acidic), but is also used to excrete some poisons (like antibiotics) and excess potassium [1].

Having passed through the entire nephron, the urine is formed, ready to exit the kidney and eventually the organism. It contains only substances that cannot be used by the body, either because of their nature or because they are present in a great excess. On top of the already clever system, which in most circumstances would be sufficient to keep the right fluid balance in the body, there are additional mechanisms to adjust the contents of the urine to the physiological needs at the particular moment (for review see [2]).

Secretion of hormones

In addition to regulatory roles exerted through urine formation, the kidneys also influence the body functions by release of hormones. The most important of them are erythropoietin, or EPO, stimulating production of erythrocytes in the bone marrow; calcitriol, the active form of vitamin D, regulating calcium metabolism; and renin,

a key component of the renin-angiotensin-aldosterone system, which controls blood pressure [1].

1.1.3 Renal diseases

Considering their importance and complexity, it is not surprising that the impairment of the kidney functions has serious consequences for the organism. The most fundamental is dysfunction of other tissues and organs caused by the waste products accumulating in the blood. Without appropriate treatment, that will very likely lead to a prompt death.

Sadly, in Western countries renal diseases are becoming increasingly widespread. It has been estimated that 1 in 10 people has some kind of kidney disease, and 1% of them will in due course develop end stage renal disease and will need renal replacement therapy (either dialysis or transplantation) to stay alive [3].

Although the final tragic outcome, the end stage renal disease, characterised by the loss of nephrons and deposition of extracellular matrix, is common for all sorts of non-malignant kidney diseases if they are not stopped at an earlier stage, the initial causes vary greatly. Renal disease may start with hypertension, glomerulonephritis (inflammation in the glomerulus, usually resulting from an infection or autoimmune reaction), formation of large cysts gradually replacing the normal tissue (like in the most frequent inherited kidney disease known as polycystic kidney disease), or overuse of medicines or "street" drugs [4]. The most common cause, however, is poorly controlled diabetes [4].

1.2 Diabetic nephropathy

Diabetes mellitus is a condition characterised by the presence of elevated glucose levels in blood. This may be caused by lack of insulin production (type I diabetes, ~5-10% patients with diabetes mellitus), or, most often, inability to respond to insulin (type II diabetes). Over time hyperglycaemia causes significant anomalies in the vasculature [5], which lead to micro- and macrovascular complications of diabetes: nephropathy, retinopathy, neuropathy, and atherosclerosis.

In Europe approximately 3.5% of the population have been diagnosed with diabetes, and the frequency of diabetes is growing rapidly [6]. Approximately one third of the diabetic patients (both type I and II diabetes) suffer from kidney disease [7]. Diabetic nephropathy is therefore the most common single cause of end stage renal disease and accounts for 20% of all patients requiring renal replacement therapy in the UK [8]. Furthermore, the mortality is higher in diabetic patients in comparison with non-diabetic patients [8]. This creates an urgent need to design more effective therapies for diabetic nephropathy, most likely based on better understanding of mechanisms driving the disease.

1.2.1 Factors contributing to development and progression of diabetic nephropathy

Only about 30% of patients with diabetes develop nephropathy [7]. There are a few factors known to increase the risk of kidney disease in both type I and II diabetic patients. The most widely acknowledged are poor glycaemic control and hypertension.

Glycaemic control

Substantial epidemiological data suggest that the development of diabetic nephropathy is related to poor glycaemic control. It has been also demonstrated that strict glycaemic control is effective in prevention of development and progression of diabetic nephropathy at early stages [9]. Whether or not it can also slow down progression or cause reversal of the advanced disease is more controversial. It has been reported, however, that ten years after pancreas transplantation in patients with type I diabetes and nephropathy, some morphological alterations of diabetic nephropathy, such as increased thickness of the basement membranes and mesangial expansion, decreased [10]. This suggests that at least in some cases and after a long time (more than five years) control of blood glucose may cause regression of diabetic nephropathy.

Blood pressure

In the later stages, it is the degree of hypertension that correlates best with the rate of progression of diabetic nephropathy [11]. Additionally, it has been demonstrated that aggressive treatment of hypertension with angiotensin-converting enzyme (ACE) inhibitors significantly delays the progression [12]. Although lowering of blood pressure by the ACE inhibitors has a great impact on renal function itself, it is clear now that blockade of the renin-angiotensin system is also beneficial for diabetic nephropathy patients in other ways, independent of its antihypertensive effects [13]. The possible mechanisms will be discussed later in this chapter.

Other factors

A few other factors have been linked to development or quick progression of diabetic nephropathy. These include hypercholesterolaemia, dietary protein intake, obesity, and cigarette smoking [14]. There is also strong evidence suggesting that genetic factors play an important role. The likelihood of developing nephropathy in those patients who have a sibling or parent with diabetic nephropathy is substantially increased, and this cannot be completely explained by environmental factors [15]. Furthermore, the incidence of diabetic nephropathy varies according to ethnicity [15]. So far, however, success in identifying genes responsible for development and progression of diabetic nephropathy has been limited, mostly by the modest data collections and small number of candidate genes examined. A recent genome-wide association study, using DNA samples from approximately 2000 patients for each of seven major diseases (including type I and II diabetes mellitus, but not diabetic

nephropathy), is a perfect demonstration of how to approach the problem [16]. Hopefully, a similar work will be done to identify genetic loci for diabetic nephropathy susceptibility.

1.2.2 The clinical course of diabetic nephropathy

Clinically incipient nephropathy manifests initially as persistent microalbuminuria (i.e. albumin excretion: 20-200 mg per day). Then, persistent proteinuria occurs (i.e. total protein excretion > 200 mg per day) and is an indication of overt diabetic nephropathy. Following the onset of proteinuria, there is a progressive decline in kidney function, leading to end stage renal disease. The rate of progression is heavily influenced by glycaemic and blood pressure control, as well as the other factors mentioned above [14]. In approximately 50% of patients with overt nephropathy the progression is quick and the kidney function is nearly lost in less than five years [17].

A routinely used measure of kidney function is estimated glomerular filtration rate (eGFR), which is calculated using the following equation [18]:

eGFR =
$$186*(S_{Cr})^{-1.154}*(Age)^{-0.203}*(0.742 \text{ if female})*(1.210 \text{ if African-American})$$

(ml/min per 1.73 m²)

where S_{Cr} is serum creatinine concentration in mg per 100 ml, and age is in years.

Creatinine is a waste product of the muscle, and in patients with impaired kidney function removal of creatinine from blood is not effective, so elevated creatinine levels are commonly detected. After adjustment for patient age, sex, and race, creatinine concentration is an indication of the stage of kidney disease (Table 1.1). Normal eGFR is about 120 ml/min in young adults and declines with age [18].

1.2.3 Pathological changes in diabetic nephropathy

The changes seen in diabetic kidneys are comparable in patients with type I and II diabetes, and are also similar to, but in some aspects distinguishable from, those found in non-diabetic chronic renal diseases [19].

The earliest histopathological change in diabetic nephropathy is renal hypertrophy [20]. This may be explained by both mesangial and interstitial expansion. Whereas the expansion within the renal corpuscle is caused mainly by matrix deposition, the interstitial expansion is a result of hypertrophy of interstitial cells [21]. In the course of the disease, further damage in both the renal corpuscle and tubulointerstitium is observed. In addition to the mesangial expansion, the corpuscular changes include glomerular basement membrane thickening, glomerular sclerosis, and, at later stages of the disease, also loss of podocytes [20]. In the tubulointerstitium fibrosis develops. The tubular basement membrane thickens [21]. Tubules and peritubular capillaries are gradually replaced by extracellular matrix and interstitial cells. The latter include, apart from usual fibroblasts and resident macrophages, myofibroblasts and infiltrating immune cells [22].

1.2.4 Molecular basis of tubulointerstitial fibrosis in diabetic nephropathy and other chronic kidney diseases

The tubulointerstitium comprises the tubular epithelium, vascular structures, and interstitium, and accounts for 85 to 90% of the kidney volume [23]. After realisation that the degree of tubulointerstitial fibrosis correlates best with the rate of progression of chronic kidney disease, the mechanisms underlying this process have become a subject of intensive studies.

To facilitate discussion, the pathophysiology of tubulointerstitial fibrosis is sometimes divided into three sequential phases [19]: cellular activation and injury, profibrotic signalling, and the fibrogenic phase.

Cellular activation and injury

During the initial phase of fibrogenic cascade, tubular cells are exposed to bioactive molecules not present in the normal ultrafiltrate. These consist mainly of proteins and, in diabetic nephropathy, also glucose in unusually high concentrations, coming from the plasma or injured glomeruli [24]. Some of those molecules are directly toxic to the tubular cells and contribute to further renal injury. An example of such a protein is the iron-binding protein transferrin, which facilitates generation of reactive oxygen species in the Haber-Weiss Fenton reaction. Accordingly, transferrin-bound iron is toxic for tubular cells *in vitro* [25], and iron-deficient mice were more resistant to kidney damage caused by anti-glomerular basement membrane antibodies [26]. Another example is the complement system. Once in the tubule, the complement

proteins may destroy the tubular cells via formation of the membrane attack complex [27]. A toxic effect may also be exerted by proteins from the glomerular filtrate indirectly. For instance, albumin, immunoglobulin G, and transferrin have been shown to induce secretion of vasoactive peptides, such as endothelin-1, which cause vasoconstriction and consequently tubular damage due to ischemia [28].

Constituents of the tubular fluid may also trigger inflammation in the interstitium. Albumin and transferrin have been reported to stimulate secretion of monocyte chemoattractant protein-1 [29]; while a mixture of serum proteins, especially 30-100 kDa fraction, has been shown to induce expression of the complement C3 gene by cultured tubular epithelial cells [30]. These, together with endothelial cells of peritubular capillaries, additionally facilitate leucocyte migration into the interstitium by exposure of adhesion molecules on the cell surface (e.g. ICAM-1, VCAM-1) [31]. Profound changes in gene expression in the activated cells of the tubulointerstitium result in display of unusual antigens in MHC I, which may elicit T-cell-mediated immune response that adds to the tubulointerstitial inflammation [32].

In addition to injury and inflammation, the abnormal contents of the glomerular filtrate may also directly cause fibrosis of the tubulointerstitium. Profibrotic cytokines such as transforming growth factor-beta (TGF-beta, discussed in detail in the next section) or insulin-like growth factor 1 (IGF-1) may enter the tubule, bind to their receptors on the tubular cells, and cause production of extracellular matrix [24]. Also elevated glucose concentration in diabetic patients may have similar effect [33]. Additionally, it has been shown that TGF-beta induces epithelial-to-mesenchymal transition (EMT) of tubular cells, which lose contact with other epithelial cells and migrate into the interstitium to become myofibroblasts [34]. These cells specialise

in production of large amounts of matrix components as well as profibrotic cytokines, and their presence in renal interstitium is a feature of progressive kidney disease [35].

The profibrotic signalling phase

As a result of the events described above, a number of regulatory molecules are released by the cells of the tubulointerstitium. It is widely accepted that amongst these, a key potentiator of renal fibrosis is TGF-beta.

TGF-beta

TGF-beta is a prototype of a multifunctional cytokine. Its activities include regulation of extracellular matrix synthesis and degradation, control of EMT, context-specific inhibition or activation of cell proliferation, induction of apoptosis, and modulation of immune responses [34, 36].

Increased expression of TGF-beta has been reported in practically all human and experimental models of renal fibrosis, including patients suffering from diabetic nephropathy [37, 38], and diabetic rodents [39]. In addition, transgenic mice with enforced TGF-beta expression in the liver, resulting in elevated plasma concentration of TGF-beta, develop glomerular and interstitial fibrosis [40]. Conversely, inhibition of TGF-beta by antibodies, antisense oligonucleotides, soluble TGF-beta type II or III receptor, the TGF-beta inhibitor decorin, or TGF-beta latency-associated peptide prevents fibrosis in animal models [41].

Both resident renal cells and infiltrating immune cells can produce TGF-beta in response to several stimuli, which include glucose, angiotensin II, endothelin 1, ischemia, insulin, IGF-1, platelet-activating factor, thromboxane, and medications

such as cyclosporine [19]. Additionally, TGF-beta may also induce its own expression [42].

Three human TGF-beta genes have been identified: TGF-beta1, TGF-beta2, and TGF-beta3. The sequences of the mature TGF-beta molecules are similar, with 70 to 75% of conserved amino acids [38]. Although their effects on cells are comparable [43], they differ greatly in their spatial and temporal expression patterns. This can be explained by differences in regulatory sequences of the three genes [38]. The most commonly studied in the context of renal fibrosis is the first one, which later in this thesis will be referred to as TGF-beta.

TGF-beta is secreted as a latent precursor molecule (LTGF-beta) [38]. It requires activation into a mature form for receptor binding and activation of signal transduction pathways. *In vitro*, activation may be achieved for example by treatment with plasmin, furin, glycosidase, transglutaminase, metalloproteinase 9, acidic pH, or thrombospondin [19]. How this activation occurs in the kidney is unclear, but it seems to be an important step in the regulation of TGF-beta bioactivity.

Active TGF-beta binds to specific receptors found on most cell types [19]. Typically, the active TGF-beta binds to the TGF-beta type II receptor, a serine/threonine kinase that recruits and phosphorylates the TGF-beta type I receptor. Together they phosphorylate proteins of the SMAD family: SMAD2 and SMAD3, which then in concert with SMAD4 migrate into the nucleus, where they act directly as transcription factors, or modulate activity of other transcription factors [44].

Genes regulated by TGF-beta include matrix genes, inhibitors of matrix-degrading enzymes, matrix-binding integrins, and chemoattractants for monocytes [19]. TGF-beta also controls genes responsible for EMT in tubular cells, and in fibroblasts – transformation into myofibroblasts [19].

Other profibrotic factors

In addition to TGF-beta, activated tubular and interstitial cells produce a few other important factors that have a profibrotic effect. One of them, connective tissue growth factor (CTGF), is thought to act downstream of TGF-beta, and induce fibroblast proliferation, matrix protein synthesis, and integrin expression [45]. It has been detected in human biopsy samples in areas of chronic damage [46], and in a mouse model of diabetic nephropathy [47].

Angiotensin II, on the other hand, is known to be a potent stimulator of TGF-beta production by renal cells [48]. Additionally, its TGF-beta-independent effects may include induction of collagen gene expression in tubular cells and interstitial fibroblasts, and vasoconstriction, contributing to tubulointerstitial ischemia [19, 49]. As mentioned in 1.2.1, ACE inhibitors have been proven beneficial for patients with renal fibrosis, an effect independent of hypertension control. This has been confirmed in several animal models of kidney disease [19]. Furthermore, it has been shown that mice genetically deficient in angiotensinogen develop less renal fibrosis after unilateral ureteral obstruction [50].

Very similar properties to angiotensin II has endothelin 1, which also stimulates production of TGF-beta by renal cells, causes vasoconstriction, and directly regulates matrix accumulation [19, 51]. In agreement, endothelin 1 receptor blockers have been reported to decrease the severity of tubulointerstitial damage in rat models of renal disease [52], whereas transgenic mice overexpressing endothelin 1 have been shown to develop glomerulosclerosis, tubulointerstitial fibrosis, and renal cysts, but not hypertension [53].

Another molecule upregulated in fibrotic renal diseases is platelet-derived growth factor (PDGF). It has been shown to induce the appearance of myofibroblasts

in the interstitium [54], and has also been implicated in regulation of TGF-beta synthesis [55].

The role of proinflammatory cytokines, such as tumour necrosis factor (TNF) or interleukin 1 (IL-1), in the fibrogenic response is not completely clear. Their role in acute renal injury is well established [56, 57], but it has been suggested they may have some profibrotic effects as well. For instance, IL-1 receptor antagonist has been shown to reduce tubulointerstitial fibrosis in rats with crescentic nephritis [58]. Whether this was a direct effect of IL-1 on the fibrogenic response is questionable.

Antifibrotic factors

It is conceivable that, together with extensive production of fibrosis-promoting molecules, activated cells of the tubulointerstitium may synthesise also antifibrotic factors. In keeping with this hypothesis, increased expression of hepatocyte growth factor (HGF) has been noted in areas of tubular damage in human kidney biopsies [59]. Subsequent experiments revealed that HGF has antifibrotic properties. In a mouse model of chronic kidney disease, for example, recombinant HGF decreases renal production of **PDGF** and TGF-beta, reduces number of myofibroblasts, and generally inhibits tubulointerstitial fibrosis **[60]**. Disappointingly, it has been also shown that HGF-overexpressing mice develop cystic renal disease and glomerulosclerosis [61], so its potential use in a therapy would certainly require a great caution.

The fibrogenic phase

As a result of signalling from the profibrotic molecules mentioned above, a new set of genes is expressed by cells of the tubulointerstitium. In general, these are genes that lead to extracellular matrix accumulation along tubular basement membranes and in the interstitial space. Matrix accumulation is thought to occur due to its increased synthesis and decreased degradation.

Increased matrix synthesis

There are two lines of evidence suggesting that the increase in extracellular matrix during progressive renal fibrosis is a result of increased matrix production. Firstly, more mRNA of matrix genes can be detected. Secondly, matrix components not found in the normal kidney appear [19].

The matrix typically found in the fibrotic kidney comprises of matrix proteins (various collagens, a few splice variants of fibronectin, laminin), proteoglycans, and polysaccharides (mainly hyaluronan) [19]. *In situ* hybridisation studies suggest that their main source are interstitial myofibroblasts [62]. In addition to providing structural support, the unusual matrix may also significantly influence behaviour of the neighbouring cells (e.g. control further production of profibrotic genes directly or by sequestration of growth factors, including TGF-beta), or attract immune cells to the scar [19].

Decreased matrix degradation

Normal kidney cells produce several matrix degrading proteases, which are believed to help maintain normal kidney architecture. Amongst the most important are

the large group of matrix metalloproteinases (MMPs). A common feature of renal fibrosis is a strong induction of one of the natural MMP inhibitors, the tissue inhibitor of metalloproteinases 1 (TIMP-1) [63]. TIMP-1 is synthesised in response to TGF-beta and some other growth factors, cytokines, endotoxin, and thrombin by various tubulointerstitial cell types, including fibroblasts, macrophages, and tubular epithelial cells [19]. Surprisingly, genetic deficiency of TIMP-1 does not rescue a mouse from renal fibrosis [63]. It has been suggested that in this model the three other TIMPs may compensate for the lack of TIMP-1, so more studies are needed before any conclusion can be drawn.

A member of another group of proteases, the serine protease plasmin, has also been studied in the context of renal fibrosis. The first role assigned to plasmin was degradation of fibrin, but it can also directly degrade some components of the basement membrane and extracellular matrix, as well as activate MMPs, which are normally secreted as inactive zymogens [19]. Plasmin itself is synthesised as inactive plasminogen, and in the kidney it is typically activated by another serine protease, the urokinase-type plasminogen activator (uPA). Its natural inhibitor, the plasminogen activator inhibitor 1 (PAI-1), is inducible by TGF-beta in proximal tubular epithelial cells, fibroblasts and myofibroblasts [64, 65] and is profoundly upregulated in several models of renal fibrosis [66]. Moreover, PAI-1-deficient mice develop less fibrosis than wild-type mice in response to protein overload or ureteral obstruction [67].

Ultimately, if the fibrogenic cascade is not stopped, extracellular matrix replaces nephrons and the kidney cannot function any longer.

Despite great progress in medical technologies, the number of patients with end stage renal disease is steadily growing. Advances in fundamental biology, in particular those in the field of gene expression regulation, may offer new approaches to chronic kidney disease treatment and/or diagnosis.

1.3 Control of gene expression

In a multicellular organism all cells, as a general rule, have the same DNA, yet the different cell types produce distinct sets of proteins, and therefore differ greatly in terms of structure and function. The mechanisms by which a specific subset of genes are expressed in each cell operate at many levels. Figure 1.2 shows the steps of the eukaryotic DNA-to-protein pathway which may potentially be regulated. These include transcription, mRNA maturation and export from the nucleus, degradation of the mRNA in the cytoplasm, translation, and posttranslational modifications influencing the protein activity [68].

Since many human diseases, including diabetic nephropathy, result from altered gene expression, understanding how the gene expression is regulated seems essential and holds great medical promise.

1.3.1 Transcriptional control

Regulation at the level of transcription is vital for expression of any gene. In eukaryotic organisms this is a complex issue, like the process of transcription itself. There are a few stages required for initiation of transcription, all of which are subject to regulation by numerous activators and repressors.

The order of events leading to the start of transcription differs from gene to gene, but in most cases eventually RNA polymerase II and general transcription factors assemble at the promoter region of the gene. A protein complex known as Mediator

links all of them with gene-specific regulatory proteins (often acting over very large distances), as well as with chromatin-modifying proteins, which can allow better access to the DNA present in chromatin [69]. The total number of proteins necessary for the initiation of transcription in a eukaryotic cell exceeds one hundred [68].

Among proteins that interact with DNA, it is the gene regulatory proteins that are responsible for turning genes on or off in an individual manner. Unlike the few general transcription factors, abundant in every nucleated cell and needed for all genes transcribed by RNA Polymerase II, there are thousands of different gene regulatory proteins, with diverse expression patterns and regulatory capabilities [70]. Their mechanisms of action vary greatly. Predominantly they control the assembly of the general transcription factors, Mediator, and the polymerase at the promoter, or they alter local chromatin structure. They may achieve all that by their ability to recognise and bind to short specific sequences of DNA, and then by making use of DNA looping (as the regulatory sequences sometimes are located even several thousands nucleotide pairs apart from the promoter) and unique properties of protein-protein interactions [71, 72].

The regulatory proteins are usually divided into two groups: activators and repressors of transcription, although there are known examples of proteins that may enhance or inhibit transcription depending on the availability of other factors within the cell [73]. The cooperation of the gene regulatory proteins seems to be very important for the final outcome. Quite often gene activator proteins act synergistically. In some cases they can bind DNA only after they have formed a complex with other regulators. Then again, one of the mechanisms used by the repressors is blocking the action of the activators. Thus, the occurrence and rate of transcription are determined by a whole spectrum of proteins, facilitating adequate

eukaryotic cell response to numerous and complicated signals that come from the environment.

Apart from the gene regulatory proteins, which have been extensively studied for many years, it becomes apparent now that also other molecules, like non-coding RNAs, may be involved in regulation of transcription [74]. Some, such as XIST RNA which drives the inactivation of one of the X chromosomes in female cells, cause global repression of transcription through heterochromatin formation [75]. The others, for example small non-coding RNA molecules (siRNAs, microRNAs), may regulate transcription of specific genes in a sequence-dependent manner [76]. The mechanism is not completely understood yet, but some lines of evidence suggest that small RNAs are able to interact with non-coding transcripts that overlap gene promoters. By that they guide chromatin reorganisation in the vicinity of the promoters, which results either in transcriptional activation or silencing of specific genes [76].

Furthermore, DNA itself can be modified (mainly by methylation of cytosine in the sequence CG), usually causing gene silencing. Interestingly, modifications of either DNA or histones can be preserved during cell division, so that the new cells do not express certain genes, similarly to the parent cell [77], adding to the complexity of the transcriptional control.

1.3.2 Posttranscriptional control

Although critical for gene expression, occurrence of transcription of a particular gene does not guarantee that the protein encoded by that gene will be produced or active in the cell. In the case of many genes, especially those responsible for quick and accurate

responses to changes in the environment, posttranscriptional and posttranslational control is of great importance [78]. There are several opportunities for posttranscriptional regulation of gene expression, i.e. between the start of transcription and the end of translation, in eukaryotic cells.

RNA processing in the nucleus

In eukaryotes, transcription elongation is tightly coupled to RNA processing. Transcription is only the first of a few steps needed to generate mRNA. Other essential steps are modifications of the both transcript ends, and removal of intron sequences in a process known as splicing [79].

Among the modifications of the transcript ends, 3' end processing in particular leaves some opportunities for regulation. The 3' end of a eukaryotic mRNA is not formed by the termination of transcription by the RNA polymerase. Instead, during transcription additional factors are recruited to cleave the transcript and finish it with a polyA tail [80]. A cell may control the site of this cleavage [81], and thus possibly change the end of the eventual protein or at least the 3'-untranslated region (3'UTR) of the mRNA, which, as I shall discuss later in this chapter, may be of great consequence for the transcript translation or stability.

An additional chance to alter the final mRNA (and the resulting protein) is splicing. In the case of many mRNA precursors, various permutations of exon inclusion and skipping can lead to several variations of final mRNA being generated from a single gene. This is described as alternative splicing [82]. In humans it has been estimated that nearly 95% of multi-exon genes produce multiple transcripts in this way [82]. In some cases alternative splicing occurs constitutively, with different final

forms chosen by chance, because of an intron sequence ambiguity. Very often, however, this is a regulated event. The regulation may be either negative, when a regulatory factor prevents the splicing machinery from accessing a particular splicing site, or positive, if a regulatory molecule attracts the splicing machinery to a weak splicing site [82].

Another way used by cells to alter the mature mRNA is called RNA editing. Most surprisingly, it changes the nucleotide sequences of the primary transcripts [83]. In mammals the most common types of editing include deamination of adenine to create inosine, and deamination of cytosine giving uracil [83]. Both types of editing change the base-pairing properties of the bases, and therefore may have a great impact on the amino acid sequence of the protein (if the change is located within the coding sequence) and other posttranscriptional regulatory mechanisms. The process is carried out by a different set of enzymes for each type of editing, recognising precisely the sites which need to be modified [83]. Their expression varies between different tissues, being responsible, as has been shown for a few genes, for expression of different protein isoforms in those tissues [84].

Export of mRNA from the nucleus and localisation in the cytoplasm

Only a small proportion of RNA that is synthesized ever leaves the nucleus. The quality control system of RNA production ensures that only completely processed RNA is exported, whereas incompletely processed or damaged RNA stays in the nucleus, where eventually gets degraded [85]. However, there are known examples of incompletely processed transcripts that are selectively transported to the cytoplasm in a regulated manner. In the best-studied example, during HIV-1

infection, this is controlled by a protein which binds specifically to viral unprocessed transcript and then interacts with a nuclear export receptor, causing the transcript translocation through the nuclear pore [86].

Once in the cytoplasm, mRNA that passes the nonsense-mediated decay (NMD) assessment, which is responsible for degradation of mRNAs containing premature termination signals [87], gets translated. The future localisation of the protein is very often determined by signal sequences within the mRNA. In many cases they are present in the coding region of the mRNA and direct the newly translated protein to the right cell compartment after start of translation [88]. Sometimes, however, especially in large polarized cells, mRNA itself is transported to a particular part of the cell prior to translation. In the known examples, it is 3'UTR of mRNAs that is responsible for their transport and often also inhibition of translation until the mRNA reaches its destination [89]. The exact mechanisms are not well-understood yet, but it is clear that the localisation of mRNA may be influenced by presence of certain proteins (such as those responsible for recognition or directional movement of mRNAs) or 3'UTR modifications during the transcript processing.

mRNA stability and translation

Number of copies of an mRNA available for translation may be controlled at the levels of transcription, transcript processing and intracellular transport, and also its turnover. Degradation and translation rate of a particular mRNA depend on multiple positive and negative regulatory signals. Interestingly, both processes seem to be closely interrelated: poorly translated transcripts are more likely to be degraded,

as polyA tail shortening and decapping enzymes, crucial for mRNA destabilisation, directly compete with the translational machinery [90].

Information necessary for regulation of specific mRNA stability and translation is very often located in untranslated regions (UTRs) of the mRNA. These are lengths of sequence 5' and 3' to the coding sequence (CDS, that part of the mRNA coding for protein). Specific motifs within UTRs are recognised and interpreted by factors present in cells, including proteins and non-coding RNA molecules [91].

Among factors regulating mRNA degradation and translation, a particularly important example are recently discovered small RNAs, called microRNAs, which bind to mRNA and reduce protein output. I shall discuss them in detail later in this chapter. Other well-described modes of translational regulation include alternative choice of translation initiation site, use of the so-called internal ribosome entry sites (IRES) for cap-independent translation, and enzymatic extension of the polyA tail (cytoplasmic polyadenylation) [92, 93]. These can have important consequences

(cytoplasmic polyadenylation) [92, 93]. These can have important consequences for protein output. For example, alternative sites of translation initiation may result in synthesis of proteins with different N-terminus or selection of another open reading frame, IRES-mediated translation is not susceptible to most general inhibitors of translation, and enzymatic extension of polyA tail may increase half-life of the mRNA and stimulate its translation [92, 93].

1.3.3 Posttranslational control

Finally, it often happens that a polypeptide chain, following translation, requires some kind of modification for activity, or alternatively needs to be temporarily inactivated. This is particularly beneficial step for regulation of genes which may be needed immediately in response to a signal. The required protein is ready in the cell and gains its special properties typically in a single reaction.

The most usual posttranslational modifications include addition of functional groups, such as phosphate, acetyl, methyl groups, various lipids and carbohydrates [94]. There might be also modifications changing the chemical nature of amino acids (e.g. glutamine or asparagine may be converted into glutamic acid or aspartic acid, respectively [94]), involving formation of disulfide bridges within a protein, or proteolytical cleavage. A classic example of the latter two is insulin, which is synthesised as a larger inactive protein called proinsulin and becomes active after folding, formation of two disulfide bridges, and specific cleavage and removal of a large part of proinsulin by a proteolytic enzyme [95, 96]. Proteolytical cleavage of the first methionine residue (encoded by the AUG start codon) from newly produced polypeptide chains is also very common, so that mature proteins rarely begin with the methionine [97].

Another possibility to regulate gene expression after translation is control of a protein localisation. Enzymes, in particular, may be kept in a cell compartment apart from their potential but undesirable substrates, until they may be required (like for example proteases in neutrophil granules) [98].

Lastly, when there is a need to reduce amount of a certain protein in a cell, ubiquitin may be covalently linked to it, directing the protein for degradation by proteasomes [94].

1.4 MicroRNAs in regulation of gene expression

In the past few years, hardly any area of biology has been transformed so deeply as RNA molecular biology. In particular, it was the discovery of small, 20-30 nucleotide long, RNA species: microRNAs (miRNAs), short interfering RNAs (siRNAs), and piwi-interacting RNAs (piRNAs), that contributed greatly to the revolution. Among them, microRNAs have been shown to play an important role in regulation of expression of a large proportion of genes in almost all eukaryotic organisms investigated so far in both somatic and germline lineages. Rapid advances in understanding their biogenesis and mechanisms of action, together with microRNA expression patterns available now for many tissues and clinical conditions, have profound implications for basic biology as well as disease diagnosis and treatment.

1.4.1 MicroRNA discovery

The discovery of short non-coding RNAs as regulators of gene expression started about 17 years ago, when researchers screening for genes that control developmental timing in the nematode *Caenorhabditis elegans* found the first microRNA, lin-4, able to inhibit translation of mRNA of a different gene, lin-14, by binding to complementary sites within its 3'UTR [99, 100]. Although this was considered a beautiful and interesting finding, it was the discovery in the year 2000 that another microRNA involved in larval development in *C. elegans*, let-7, was conserved from

nematodes to mammals, that made the importance of that new class of gene expression regulators widely appreciated [101, 102].

1.4.2 MicroRNA expression

Since the discovery of let-7, many more microRNAs have been identified in worms, flies, mammals and plants. There are even known examples of eukaryotic unicellular organisms, in which microRNAs can be found [103]. Furthermore, certain viruses also express microRNAs [104].

Many microRNAs are well conserved in evolution, being probably part of crucial ancient pathways of gene regulation, whereas other microRNAs are more restricted in their phylogenetic distribution [105]. Comparisons of animals with increasingly complicated bodies suggest that the number of microRNA genes is correlated with developmental complexity; according to the miRBase release 14 [106], there have been 718 human microRNAs identified, 216 in zebrafish, and 174 in the genome of *C. elegans*.

Furthermore, some microRNAs have unique tissue-specific or developmental expression patterns, which are especially intensively studied in humans, so that in many cases it is possible now to identify tissue of origin on the basis of the microRNA profile of the sample [107].

1.4.3 Biogenesis of microRNAs in animals

The biogenesis of microRNAs, although similar among different classes of organisms, differs to a certain extent. All the experiments in this thesis were performed on human cells or tissues; therefore, here I will focus on the discoveries made in animal systems. The overview of the canonical pathway of microRNA biogenesis in animals is shown on Figure 1.3, and described in some detail below.

Transcription of primary microRNAs (pri-microRNAs)

Transcription of microRNA genes is usually performed by RNA polymerase II, resulting in capped and polyadenylated primary microRNA transcripts (pri-microRNA) [108]. There are some animal microRNAs individually generated from separate transcription units. The majority, however, are produced from transcription units that generate more than one product: a few microRNAs, or alternatively one or more microRNAs and a protein (with microRNAs most typically located within introns) [109]. A wide range of RNA polymerase II-associated transcription factors, together with promoter methylation status, regulate microRNA gene transcription, facilitating their expression in specific conditions and cell types [110, 111].

Nuclear processing by Drosha and export of pre-microRNA

Within the pri-microRNA, the mature microRNA is localised to an approximately 70-nucleotide long fragment that can form a stem-loop hairpin structure, known as precursor microRNA (pre-microRNA). Once the pri-microRNA is transcribed, the so-called Microprocessor complex, the essential part of which constitute the RNase III enzyme Drosha and its co-factor DiGeorge syndrome critical region gene 8 (DGCR8), recognises and cleaves it specifically so that the pre-microRNA is liberated [112].

Once the pre-microRNA is excised from the primary transcript, it is recognised by the nuclear export factor Exportin-5 (Exp5), which, together with Ran-GTP, transports it through the nuclear pore to the cytoplasm [113].

Cytoplasmic processing by Dicer and miRISC loading

Following the nuclear export, pre-microRNA is processed by the second RNase III-type protein Dicer, which cleaves off the loop and releases about 22-base-pair-microRNA duplex [114]. Subsequently, with help of the proteins including Dicer, TRBP and PACT, the double-stranded RNA unwinds and one of the strands (the guide strand or mature microRNA) is selectively loaded into a large complex, called the microRNA-induced silencing complex (miRISC). This contains an Argonaute protein as the main component [108]. Then, the microRNA is ready to perform its function.

Although it has been thought for a long time that the processing pathway described above is universal for all animal microRNAs, it is becoming clear that processing of different microRNAs may differ substantially, and there is more than a single way to produce a mature microRNA. For example, some intronic microRNAs called mirtrons, do not require processing by Drosha. Their precursors form a hairpin-like pre-microRNA immediately after splicing [115, 116]. Among Drosha-dependent microRNAs, on the other hand, there is a large group of microRNAs that are processed by the Microprocessor complex (i.e. Drosha and DGCR8 alone). There is also a subset of microRNAs that are processed by a larger and more efficient complex, containing additionally the RNA helicases p68 and p72, double-stranded RNA-binding proteins, heterogeneous nuclear ribonucleoproteins and Ewing's sarcoma proteins [117, 118]. Furthermore, TGF-beta signalling has been shown to specifically increase the rate of pri-miR-21 processing by recruitment of p68 and SMAD protein to the Microprocessor complex [119]. Finally, individual microRNA precursors may be a subject of RNA editing, which could then affect the processing [120, 121] or specificity of the resulting mature microRNA [122].

1.4.4 Modes of action of animal microRNAs

The initially described and best-studied microRNA function in animals is posttranscriptional repression of gene expression. To accomplish this, a mature microRNA that has been loaded into the miRISC complex recognises and binds to specific mRNA targets. The choice of the targets depends on the presence, usually within their 3'UTRs, of sequences at least partially complementary to the microRNA.

Due to the structure of the miRISC complex, the 5' end of the microRNA (termed 'seed') is particularly well exposed and therefore plays the major role in the target recognition [123].

In animals, the great majority of microRNA:mRNA interactions are based on imperfect complementarity, and result in inhibition translation and/or the mRNA destabilisation [124]. The exact mechanism of translational repression by microRNA is still unclear. Some reports suggest that microRNAs affect the initiation stage of translation (by competition for cap binding, competition for eIF6, or block of mRNA circularisation) while others point at inhibition of elongation (by ribosome drop-off) [124]. These discrepancies cannot be simply explained by technical or experimental differences. They rather reflect the fact that different microRNAs use distinct mechanisms to inhibit translation, or alternatively that mechanism may be cell type- or stage-dependent.

In contrast to the first studies, showing that microRNAs reduce protein output without influencing the amount of the target mRNA, it has since become clear that in many cases lower protein synthesis is accompanied by loss of the mRNA [125]. Further investigations have revealed that microRNAs can direct their target mRNAs to the cytoplasmic foci called P-bodies, where the mRNAs are not translated but, following decapping and polyA tail removal, slowly degraded by exonucleases [126]. In addition to what appears to be their major action: mRNA destabilisation and inhibition of translation through binding to the 3'UTRs, animal microRNAs have been also implicated in other kinds of regulation of gene expression. For instance, it has been reported that they can activate or repress translation of specific genes in a cell-cycle-stage-dependent manner [127]. Moreover, two independent groups have found examples of microRNAs that activate translation of specific target

mRNAs by binding to their 5'UTRs [128, 129]. A functional microRNA-binding site has been also identified within a CDS [130]. Interestingly, a recent computational analysis suggests that conserved and very likely functional microRNA-binding sites are common in 5'UTRs and CDSs of animal mRNAs [131]. Finally, following discoveries of the role of siRNAs and plant microRNAs in regulation of transcription, a few animal microRNAs involved in transcriptional gene silencing have been identified [132, 133].

1.4.5 MicroRNA role in health and disease

Since only a very short sequence on the target mRNA is necessary for recognition by a microRNA, it has been speculated, and since experimentally confirmed, that one gene may be regulated by more than just one microRNA. Conversely, one microRNA can target many different mRNAs [105]. A highly convincing confirmation of the latter comes from two studies that use mass spectrometry to analyse a few thousand proteins at once. They show that about one thousand of them are changed, in most cases subtly, by introduction or inhibition of a single microRNA in a cell [125, 134]. In line with the prediction that they regulate about 30% of human genes, microRNAs emerge as one of the most important regulatory systems, greatly contributing to the complexity of gene expression. It is not surprising then that they play important roles in nearly all biological processes, physiological as well as pathological, investigated so far.

The failed attempts to generate a Dicer knockout mouse (the embryos died 7.5-12 days after fertilisation) are a highly convincing demonstration of importance

of microRNAs early in mammalian development [135]. Subsequent numerous studies examining inactivation of Dicer in selected tissues or manipulation of expression of individual microRNAs have shown that microRNAs play crucial roles also in late development and normal function of various organs [136-138].

Predictably, microRNAs have been also linked to a range of human diseases, from cancer through neurodegenerative diseases to immune disorders, as reviewed elsewhere [139]. Their role in cancer has been studied particularly intensively. Deregulation of microRNA expression is remarkably widespread in cancers. Typically, most of them are downregulated [140]. Interestingly, such expression pattern closely resembles that of early mammalian development, suggesting an important role in cellular differentiation [140]. To confirm that the change in microRNA expression actually played a role in cancer, global downregulation of microRNA expression in a cancer cell line was studied. This resulted in increased colony formation in culture, and increased tumour growth in nude mice [141]. Not all microRNAs, however, have tumour suppressor properties. Some microRNAs act as oncogenes. The best-established example is miR-21, which targets apoptosis related genes [142]. The enormously quick progress in microRNA research is very likely to bring some new diagnostic, prognostic, and therapeutic strategies against cancer and other diseases soon.

1.5 MicroRNAs in the kidney and in fibrotic diseases

As microRNAs became a subject of intensive studies just recently, at the beginning of the project in 2006 there was very little microRNA data available specifically relevant to the kidney or fibrotic diseases. Therefore, it is important to recognise that the vast majority of work discussed in this section has been published towards the end or after my own practical studies.

MicroRNAs in the kidney

To date, microRNA expression profile in the kidney has been characterised in human and mouse tissue [143-146]. One of those reports suggested that some microRNAs, namely miR-192, miR-194, miR-204, miR-215, and miR-216, are enriched in the kidney when compared with other tissues [143]. Moreover, microRNA expression profiles have been also studied separately in renal cortex and medulla [147]. In that experiment, the authors not only demonstrated a differential expression of several microRNAs in those regions, but also linked that to the differences in expression of their target genes [147].

Recent work clearly shows that microRNAs are functional in the kidney. Conditional Dicer knockout in murine podocytes leads to proteinuria and finally death within a few weeks after birth [148-150] and is associated with various abnormalities exhibited by podocytes and glomeruli. However, specific microRNAs and their targets responsible for the damage have not been identified.

In addition to their role in normal renal physiology, microRNAs have been also implicated in a variety of kidney disorders. The first report regarding the role of microRNAs in diabetic nephropathy appeared in 2007 [151]. The authors demonstrated an increase in miR-192 expression in glomeruli isolated from animal models of diabetic nephropathy. Moreover, they found that miR-192 upregulation by TGF-beta in murine mesangial cells led to increased collagen 1-alpha 2 synthesis. The proposed mechanism included a direct inhibition of ZEB2, one of the transcriptional repressors of collagen 1-alpha 2, by miR-192 [151]. A recent study from the same laboratory shows that in addition to the collagen gene, miR-192 indirectly regulates expression of two other microRNAs, miR-216a and miR-217, both of which target PTEN, an inhibitor of Akt activation [152].

Another group looking at a role of microRNAs in diabetic nephropathy has reported that miR-377 is upregulated both in a mouse model of diabetic nephropathy, and in mesangial cells stimulated with TGF-beta or high concentration of glucose [153]. The upregulation of miR-377 resulted in an increase in the matrix protein fibronectin via downregulation of p21-activated kinase and superoxide dismutase.

So far, there has been no data published on microRNA expression in diabetic nephropathy in humans. Similarly, the role of microRNAs in proximal tubular epithelial cell response to profibrotic factors has not been well-explored yet. The only work devoted to this subject that I am aware of has been presented at the American Society of Nephrology Meeting in November 2008 [154]. The authors reported that TGF-beta causes significant downregulation of miR-192 and miR-215 in mesangial and proximal tubular epithelial cells, but not in podocytes. Furthermore, they found that miR-192 and miR-215 were decreased in the kidney of diabetic mice.

Several studies aimed to investigate microRNA functions in other renal pathologies. A number of microRNAs have been found to be deregulated in a rat model of polycystic kidney disease [155]. Additionally, expression of a few selected microRNAs (the miR-200 family, miR-205, and miR-192) has been examined in patients with immunoglobulin A nephropathy [156] and hypertensive nephrosclerosis [157]. The authors have reported significant changes in expression of some of the tested microRNAs in those conditions and found very weak but significant correlations between their expression and clinical parameters. For more details of the role of microRNAs in renal non-malignant diseases see Table 1.2.

Due to a greater availability of renal tumour tissue and overwhelming evidence that microRNAs are very important in cancers, renal cancer has been the most intensively studied kidney disease in that context so far. A few groups have performed microRNA expression profiling experiments to find microRNAs differentially expressed in renal cell carcinoma [158-162] (for summary see Table 1.3). Although each study has identified a subgroup of microRNAs that are altered in renal tumours, the overlap between the results is unexpectedly small. This may be in part explained by differences in experimental design or techniques. In particular, small number of tissue samples tested in individual studies may be responsible for the discrepancy. Additionally, the use of non-tumourous tissue adjacent to tumours as control provokes a question, whether the microRNA expression profile considered "normal" in those studies is the same as of the kidney from a healthy person. Overall, the results suggest that it is too early now to rely on a microRNA expression pattern for diagnosis of renal cancers.

Finally, two independent groups have investigated microRNA expression in acute rejection after renal transplantation [163, 164]. Considering the differences between the two studies, it is not very surprising that microRNAs identified as under-or overexpressed in acute rejection biopsies also differ greatly. The first group compared microRNA expression in the renal allograft after acute transplant rejection (n=3) with non-tumourous tissue adjacent to renal tumours (n=3) [163]. The second study included more samples (twelve acute rejection samples and twenty one controls), and used normal renal allograft tissue as a control [164]. Furthermore, the authors have demonstrated that acute rejection and allograft function can be predicted based on allograft microRNA expression profile. They have also shown that a few of the overexpressed microRNAs are highly expressed in monocytes and lymphocytes, suggesting that the observed altered microRNA expression pattern in acute rejection is caused by infiltrating immune cells [164].

MicroRNAs in fibrotic diseases

In addition to renal fibrosis, there are dozens of other fibrotic diseases, characterised by excessive production and deposition of extracellular matrix. They include for instance pulmonary fibrosis, liver cirrhosis, scleroderma, atherosclerosis and myocardial fibrosis. Some data on the role of microRNAs in those diseases have been already published.

The best-established example is miR-133 function in cardiac disease. It has been reported that miR-133 is downregulated in two rodent models of heart disease and in human pathological left ventricular hypertrophy [165]. Furthermore, the authors have demonstrated that CTGF, a powerful inducer of extracellular matrix

production (see 1.2.4), is a direct target of miR-133 [165]. Consistent with this, another group has shown that miR-133 knockout mice develop severe fibrosis and heart failure [166].

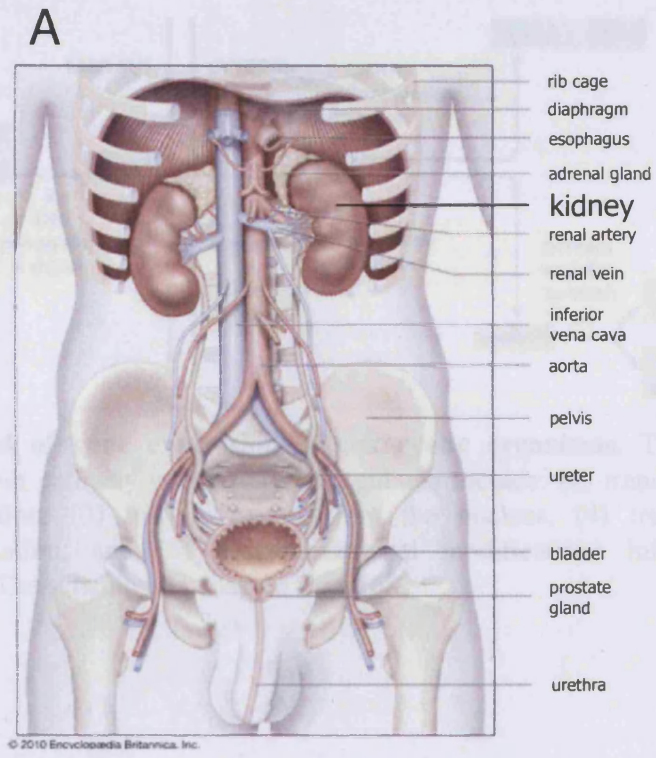
Although such findings are certainly interesting, they are usually less relevant to my work than the kidney-related data. This is because of different microRNA expression patterns in the kidney and other organs/tissues, i.e. many of the microRNAs identified to be important in those diseases are not expressed in the kidney.

1.6 Aim of this thesis

When I started the project, there was no published data regarding microRNA function in renal fibrosis, while mounting evidence suggested that microRNAs are enormously important factors in regulation of gene expression, and they contribute to various physiological and pathological processes. The aim of this thesis was to establish if they play an important role also in the kidney, in particular in renal fibrosis.

Specifically, in this thesis I addressed the following questions:

- Which microRNAs are expressed in the kidney or in cultured proximal tubular epithelial cells, and which are altered by profibrotic stimuli (microRNA profiling experiments)?
- What is the function of all expressed microRNAs in proximal tubular epithelial cells (global downregulation of all microRNAs by knockdown of microRNA-processing enzymes)?
- What is the function of the differentially expressed microRNAs (manipulation of expression of individual microRNAs)?
- Is TGF-beta directly regulated by microRNAs?



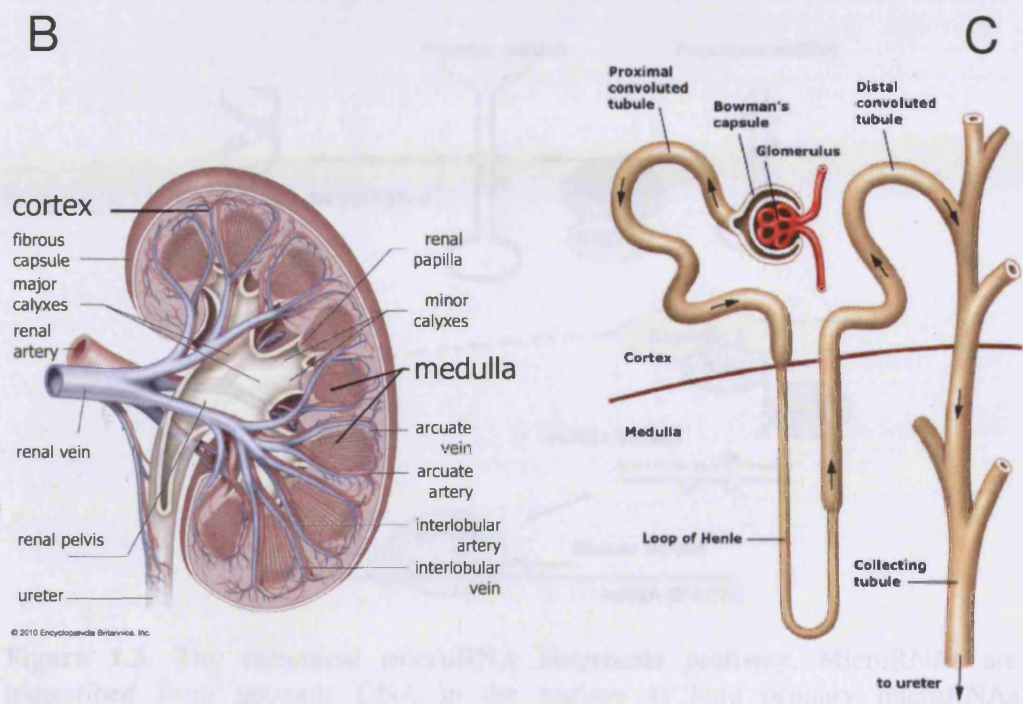


Figure 1.1. The kidney. (A) Human kidneys *in situ*. (B) Cross-section of the right kidney revealing the renal cortex and medulla. (C) Nephron. The renal corpuscule (glomerulus, Bowman's capsule) and the renal tubule (proximal convoluted tubule, loop of Henle, distal convoluted tubule) are shown. The illustrations were adapted from Encyclopædia Britannica Online [167] (A,B) or UpToDate [168] (C).

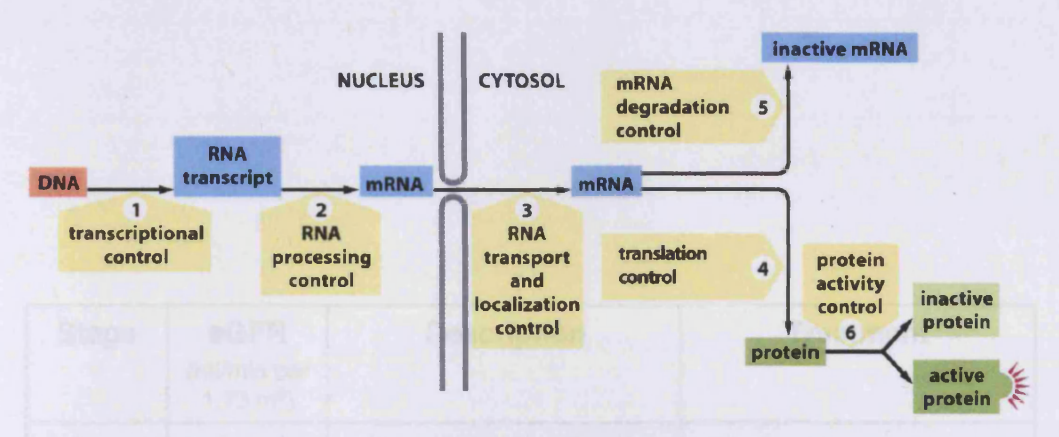


Figure 1.2. Control of gene expression in eukaryotic organisms. The steps of the DNA-to-protein pathway which may be regulated include: (1) transcription, (2) mRNA maturation, (3) mRNA export from the nucleus, (4) translation, (5) mRNA degradation, and (6) post-translational modifications influencing the protein activity. The scheme was adapted from [68].

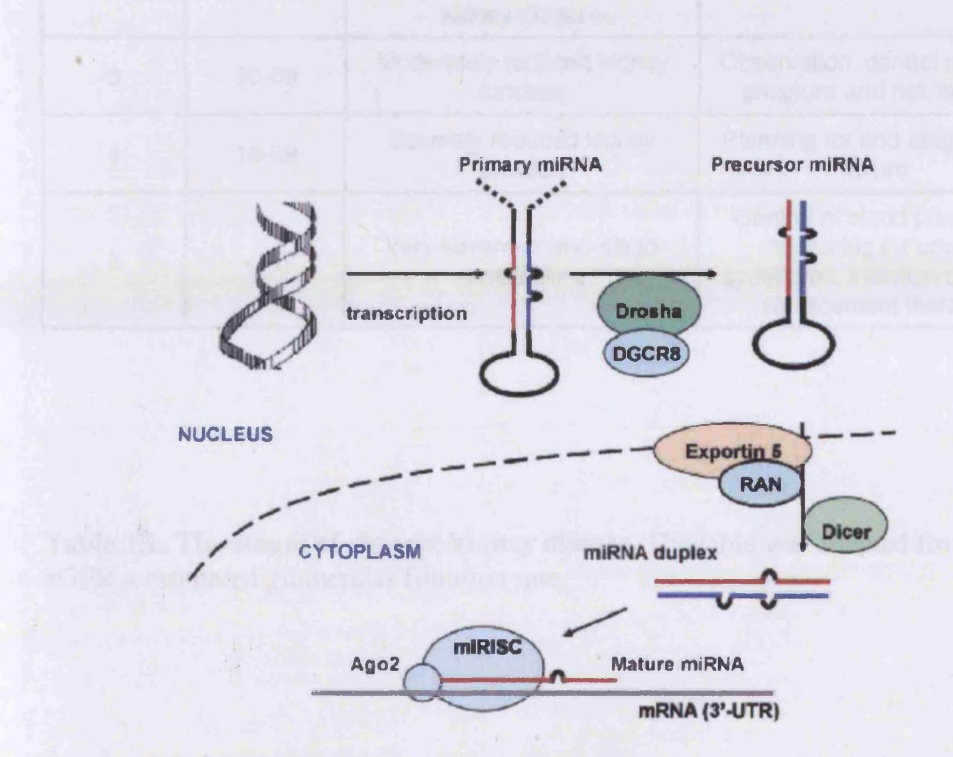


Figure 1.3. The canonical microRNA biogenesis pathway. MicroRNAs are transcribed from genomic DNA in the nucleus as long primary microRNAs (pri-microRNA). They are processed by Drosha in association with DGCR8 into ~70 nt precursor microRNAs (pre-microRNA), which are then exported through the nuclear pore by Exportin-5. In the cytoplasm, pre-microRNAs are cleaved by Dicer into double-stranded RNA complexes. The mature microRNAs (single-stranded RNA) are incorporated into the miRISC complexes and are ready to interact with specific mRNA targets. The scheme was adapted from [169].

Stage	eGFR (ml/min per 1.73 m²)	Description	Treatment	
1	90+	Normal kidney function, but urine findings, structural abnormalities, or genetic trait point to kidney disease	Observation, control of blood	
2	60-89	Mildly reduced kidney function, and other findings (as for stage 1) point to kidney disease	Observation, control of blood pressure and risk factors	
3	30-59	Moderately reduced kidney function	Observation, control of blood pressure and risk factors	
4	15-29	Severely reduced kidney function	Planning for end-stage renal failure	
5	< 15	Very severe or end-stage renal failure	Control of blood pressure, monitoring for uremic symptoms, initiation of renal replacement therapy	

Table 1.1. The stages of chronic kidney disease. The table was adapted from [170]. eGFR – estimated glomerular filtration rate.

Kidney disease	MicroRNA	Expression/Function	Ref		
	miR-192, -194, -204, -215, -216	Enriched in the kidney.	[143]		
-	miR-192, -194, -203, -450, -34a	Enriched in the cortex.	[147]		
	let-7e, miR-24, -30c, -27a, -23, -27b, -200b, -99a, -125a, -200c,-125b	Enriched in the medulla.			
Diabetic nephropathy	miR-192	Upregulated in glomeruli of diabetic mice; upregulated by TGF-beta in mesangial cells; directly targets ZEB2; increases collagen 1-alpha 2 synthesis in mesangial cells.			
	miR-215	Downregulated by TGF-beta in mesangial cells.			
	miR-377	Upregulated in the kidey of diabetic mice; upregulated by high concentration of glucose and TGF-beta in mesangial cells; directly targets PAK1, SOD1, and SOD2; causes increase in fibronectin in mesangial cells.	[153]		
	miR-192, -215	Downregulated in the kidney of diabetic mice; downregulated by TGF-beta in mesangial and proximal tubular epithelial cells.	[154]		
	miR-216a, -217	Upregulated in glomeruli of diabetic mice; upregulated by TGF-beta in mesangial cells; directly target PTEN.	[152]		
Polycystic kidney disease	miR-31, -217, -34b, -126*, -7, -128, -136, -99a, -448, -380, -20, -96, -7b, -379, -203, -147, -196a, -335, -216, -30a, -181b, -346, -377	Downregulated in the kidney of a rat model of polycystic kidney disease.	[155]		
	miR-21	Upregulated in the kidney of a rat model of polycystic kidney disease.			
lgA	miR-200c	Downregulated in renal biopsy samples.	[156]		
nephropathy	miR-141,-205,-192	Upregulated in renal biopsy samples.			
Hypertensive nephrosclerosis	miR-200a, -200b, -141, -429, -205, -192	Upregulated in renal biopsy samples.	[157]		

Table 1.2. MicroRNAs in the kidney and in renal non-malignant diseases.

Type of experiment (total number of	Number of samples		Downregulated microRNAs	Upregulated microRNAs	Ref
microRNAs tested)	C*	N*	(total number)	(total number)	
Hybridisation-based microarray (245)	20	3	-	(4) miR-28, miR-185, miR-27, let-7f	[158]
Hybridisation-based microarray (470)	16	6	(37; top 10 are shown) miR-141, miR-200c, miR-138, miR-514, miR-411, miR-183, miR-381, miR-184, miR-648, miR-368	(6) miR-373*, miR-210, miR-452*, miR-122a, miR-224, miR-155	[159]
Hybridisation-based microarray (331)	11	11	(26; examples are shown) miR-214, miR-422a, miR-145, miR-320, miR-494	(50; examples are shown) miR-27a, miR-221, miR-34a, miR-103, miR-143, miR-15a, miR-16, miR-17_5p, miR-24, let-7g, miR-21	[160]
Hybridisation-based microarray (677)	3	3	(12) miR-200c, miR-720, miR-150, miR-214, miR-1826, miR-182, miR-200b, miR-199a, miR-532_5p, miR- 378, miR-191, miR- 26a	(21; top 10 are shown) miR-122, miR-210, miR-101, miR-19b, miR-489, miR-20b, miR-340, miR-15a, miR-424, miR-106a	[161]
qRT-PCR-based array (384)	28	28	(26; top 10 are shown) miR-141, miR-200c, miR-514, miR-429, miR-377, miR-135a, miR-154, miR-200a, miR-200b, miR-204	(9) miR-185, miR-34a, miR-34b, miR-224, miR-592, miR-21, miR-142_3p, miR-155, miR-210	[162]

 $^{^{\}star}$ C – cancer, N – normal (adjacent non-tumourous) tissue

Table 1.3. Summary of microRNA profiling experiments using renal cell carcinoma samples.

CHAPTER TWO:

METHODS

2.1 Samples

2.1.1 Cell culture

2.1.1.1 Cell lines

HK-2

The vast majority of *in vitro* experiments were performed on the human proximal tubular epithelial cell line HK-2 (human kidney-2) [171]. This cell line was established by transduction of primary proximal tubule cells from adult human kidney with human papilloma virus (HPV 16) E6/E7 genes. These genes facilitate proliferation, but do not change cells as profoundly as for example malignant transformation. Typically, cells immortalised by them retain many features of the primary cells. In particular, they are not tumourigenic in experimental animals, do not grow in soft agar, and exhibit contact inhibition [171, 172].

HK-2 cells have previously been shown to be very much like the primary proximal tubular cells in terms of both their phenotype and function. For instance, they are positive for alkaline phosphatase, gamma-glutamyltranspeptidase, leucine aminopeptidase, acid phosphatase, cytokeratin, integrin alpha-3 beta-1, and fibronectin; but negative for factor VIII-related antigen, 6.19 antigen and CALLA endopeptidase. They also exhibit characteristic for proximal tubular cells sodium-dependent, phlorizin-sensitive sugar transport, and produce more cAMP in response

to parathyroid, but not to antidiuretic, hormone. Moreover, many aspects of proximal tubular cell biology, including those relevant directly to this project, have been studied in this laboratory in both HK-2 and the primary cells, always giving similar results [173, 174].

U937

Posttranscriptional regulation of TGF-beta by an unknown mechanism, similar to microRNA action, was reported in U937 cell line 20 years ago [175]. For that reason, U937 cells were used in the present study, together with HK-2 cells, when investigating the potential role of microRNAs in TGF-beta regulation (Chapter Six). The U937 cell line was derived by Sundstrom and Nilsson in 1974 from malignant cells obtained from the pleural effusion of a patient with histiocytic lymphoma [176]. The cells resemble monocytes, and can differentiate into macrophage-like cells after stimulation with phorbol esters, vitamin D₃, gamma interferon, TNF, and other factors [177-179].

2.1.1.2 Culture conditions

Both cell lines were cultured at 37°C in a humidified incubator (Cell House 170, Heto Holten, Derby, UK) in an atmosphere of 5% CO₂. Conditions for culture differ between HK-2 and U937 cell lines, and were as follows.

HK-2

A single frozen aliquot of HK-2 cells were obtained from ATCC (LGC Standards, Teddington, UK). After three passages, stock cells were prepared as described below and stored in liquid nitrogen. Cells were used in experiments up to the passage 30.

Cells were maintained in a 1:1 mixture of Dulbecco's Modified Eagle's Medium (GIBCO/Invitrogen, Paisley, UK) and Ham's F12 (Sigma, Poole, UK), supplemented with 10% (v/v) fetal calf serum (FCS) (biosera, Ringmer, UK), 20 mM HEPES, 2 mM L-glutamine, 5 µg/ml insulin, 5 µg/ml transferrin, 5 ng/ml sodium selenite, and 0.4 µg/ml hydrocortisone (Sigma). Fresh growth medium was added to cells every three days until confluent. Then they were used in experiments, or subcultured at the ratio 1:5.

For subculture, cells were incubated at 37°C with trypsin/EDTA 10x solution (Sigma), diluted with PBS (1:10). After ten minutes, equal volume of culture medium containing 10% (v/v) FCS was added, cell suspension transferred to a tube, and centrifuged for seven minutes at 150 rcf at room temperature. The cells were resuspended in culture medium and seeded into new culture flasks or plates.

To store frozen in liquid nitrogen, cells were detached from a culture flask with trypsin/EDTA, as described above. After centrifugation cells were resuspended in culture medium supplemented with 10% (v/v) DMSO and 20% (v/v) FCS, and transferred to CryoTube Vials (Nunc/VWR International, Leics, UK). Following

incubation for 30 minutes at room temperature to allow DMSO enter the cells, the tubes were moved to -80°C. Next day, they were transferred to liquid nitrogen.

U937

U937 cells of unknown passage number were in use in the department. Unstimulated U937 cells grow in suspension. They were cultured in Roswell Park Memorial Institute 1640 medium (GIBCO) supplemented with 2 mM L-glutamine, 20 mM HEPES, and 5% (v/v) FCS. Cell density was maintained between 10⁴ and 10⁶ cells/ml. Fresh medium was added every three days.

For subculturing, cells were collected from the culture flask and gently centrifuged in a long tube for seven minutes at 70 rcf at room temperature, so that any dead cells or cell debris remained in the supernatant and could be discarded. Cells from the pellet were resuspended in the culture medium and part of them (usually 1/20) transferred to a new flask.

2.1.1.3 Determination of cell number and viability

To determine total cell number and proportion of dead cells, Trypan Blue stain (BDH Chemicals, Poole, UK) was used in conjunction with a hemocytometer. Trypan Blue is a negatively charged dye, which does not react with cells unless the membrane is damaged. Thus, it can be used to distinguish between live and dead cells. The procedure was as follows. Cells in suspension were mixed with 0.4% (w/v) Trypan Blue in PBS. Approximately 10 µl was transferred to both chambers

of Neubauer hemocytometer by capillary action. Cells were observed under microscope (using 100x magnification) and counted in 5 of 9 squares (1 mm x 1 mm) in each chamber. Of cells touching the outer lines, only cells touching top and bottom lines were calculated. Viable and non-viable cells were counted separately. If there were fewer than 20 or more than 50 cells per square, the dilution of the samples was adjusted and the procedure repeated. To calculate the density of cells in the original suspension (cells/ml), average number of cells per square was multiplied by dilution factor and by 10⁴.

The second method used for examination of relative cell number and/or viability was AlamarBlue assay. This employs a non-toxic. cell permeable. and non-fluorescent dye, resazurin, converted to the pink and fluorescent dye resorufin in response to metabolic activity of cultured cells. The fluorescent and colorimetric signal is proportional to the number of living cells in the sample. To perform the assay, cells were incubated at 37°C with 10% (v/v) solution of AlamarBlue reagent (BioSource/Oxford Biosystems, Oxon, UK) in culture medium. Typically, after one hour the medium was transferred to a black 96-wellplate (100 µl/well) and the fluorescent signal was monitored using 544 nm excitation wavelength and 590 nm emission wavelength. Medium with 10% (v/v) AlamarBlue reagent, kept in the incubator for one hour before the measurement, was used as a blank.

2.1.1.4 Cell stimulations

Stimulation of HK-2 cells with profibrotic factors

Two main profibrotic factors were used in this study. The first one was the elevated concentration of glucose, 25 mM instead of normal 5 mM, in the culture medium. This is a concentration in the order of that detected in the blood of diabetic patients, and is a standard concentration adopted by many investigators in the study of pathological changes elicited by glucose.

The second profibrotic stimulus was recombinant TGF-beta (R&D Systems, Abingdon, UK). It was used at the final concentration of 10 ng/ml unless stated otherwise. Previous work from this department has characterised phenotypic changes in HK-2 cells in response to TGF-beta, with maximal changes observed at this dose [174].

Additionally, in some experiments PMA also known as TPA (12-O-Tetradecanoylphorbol 13-acetate, Sigma) at the concentration of 160 nM was used to stimulate cells. This mostly applies to experiments in which TGF-beta secretion to medium was examined, so the use of TGF-beta as a stimulus was not ideal, and an alternative profibrotic stimulus was required.

In each case, confluent HK-2 cells were growth-arrested (kept in the medium without FCS) for 48 hours before addition of the profibrotic factor, also in FCS-free medium. The duration of the stimulation varied from one hour to seven days, depending on the experiment design. In longer experiments, medium was replaced every 48 hours. Unstimulated cells were used as a control. They were treated similarly; the only deliberate difference was lack of the stimulus in their medium.

U937 monocyte differentiation into macrophages

U937 cells at the density 5 x 10^5 cells/ml in medium with 5% (v/v) FCS were plated (900 μ l/well on a 12-well-plate) and PMA in FCS-free medium (1.6 μ M, 100 μ l/well) was added, so that the final concentration was 160 nM. After 48 hours, cells were stuck to the plastic and bigger, and their number was visibly smaller than in the corresponding control wells, in keeping with PMA-dependent transformation/activation [177].

2.1.1.5 Transfections

HK-2 cells are easy to transfect, like many other adherent and quickly proliferating cell lines. Previously, in this laboratory, they have been successfully transfected with small RNA and plasmid DNA using cationic liposomal or polyamine-based reagents.

Transient transfections with small RNA molecules

For this project HK-2 cells were transfected with three distinct classes of small RNA molecules. These were: siRNAs, synthetic microRNAs, and microRNA inhibitors (anti-microRNAs). All were purchased from Ambion (Ambion/Applied Biosystems, Warrington, UK). Details of the small RNAs used in the study are given in Table 2.1.

Transfection reagents

The small RNAs were delivered to the cells using siPORT Amine (Ambion). Efficiency of the transfection was occasionally confirmed by use of a very effective siRNA designed to silence CD44 (i.e. cause cleavage and subsequent degradation of its mRNA). In these experiments the remaining CD44 mRNA was typically less than 5% of the control expression, as assessed by quantitative RT-PCR (see 2.2.2), suggesting that at least 95% of the cells were successfully transfected (Figure 6.8A).

Transfection procedure

Cells were trypsinised as described above (see 2.1.1.2). After centrifugation they were resuspended in culture medium containing 10% (v/v) FCS, at the density 10⁵ cells/ml. During preparation of transfection complexes, the cell suspension was stored at 37°C. Small RNAs were diluted in Opti-MEM I medium (Invitrogen). When transfection was performed in 12-well-plates, typically 30 pmol of small RNA was mixed with Opti-MEM I at the total volume of 50 µl, so that the final concentration (after the transfection complexes are mixed with cells) was 30 nM, as recommended by the manufacturer. In a separate tube, 5 µl siPORT Amine was added to 45 µl of Opti-MEM I medium, and incubated for exactly ten minutes at room temperature. Then, diluted RNA and diluted siPORT Amine were mixed and incubated another ten minutes to allow transfection complexes to form. Subsequently, 100 µl of the transfection complexes were transferred to culture plate wells, and 900 µl of the cell suspension was added. Transfected cells were incubated at 37°C until ready to assay.

Transient transfections with DNA plasmids

Two main kinds of plasmids were used (see Table 2.2). The first group constitute plasmids for expression of relatively short RNA molecules: short hairpin RNAs (shRNA) or microRNA precursors (pre-microRNA). These plasmids were generated as described below, based on siSTRIKE vector (Figure 2.1A, Promega, Southampton, UK), utilizing the human U6 promoter, which is recognised by the RNA polymerase III.

Reporter plasmids represent the second kind. The plasmid containing four SMAD-binding elements (SBEs) in the promoter region of the firefly luciferase gene, useful to study TGF-beta signaling, was a kind gift from Aristidis Moustakas, Ludwig Institute for Cancer Research, Uppsala University, Uppsala, Sweden [180]. Two other plasmids with 3'UTR of ZEB1 or ZEB2 downstream the firefly luciferase coding sequence, to study posttranscriptional regulation of those genes, were constructed as described below by modification of the pGL3 plasmid (Figure 2.2A, Promega). As a control for transfection efficiency in reporter assays, a plasmid encoding *Renilla* luciferase under a strong constitutive promoter (SV40), the pRL plasmid (Promega), was routinely cotransfected with the firefly luciferase-expressing reporter plasmids (ratio 1:9).

Construction of siSTRIKE U6-based plasmids for expression of shRNAs
or pre-microRNAs

The plasmids for expression of shRNA or pre-microRNA were generated by ligation of annealed DNA oligonucleotides A and B (for sequences see Table 2.2) into the siSTRIKE U6 vector, in accordance with the manufacturer's advice.

Oligonucleotide design

The first oligonucleotide (A) contained the overhang ACCG (complementary to the sticky ends in the siSTRIKE U6 plasmid; the G nucleotide is the transcription start site); a hairpin sequence (for shRNA expression this is ~19-nucleotide-long fragment of the mRNA target sequence, the recommended loop sequence AAGTTCTCT, and the sequence complementary to the target; for pre-microRNA-expressing plasmids this is the pre-microRNA sequence as found in the miRBase release 10 [106]); the U6 termination sequence (TTTTT); an additional C residue (to form a new *Pst*I restriction site upon ligation of the insert; to distinguish the plasmids containing the insert from those without it).

The second oligonucleotide (B) began with the overhang TGCA (complementary to the sticky ends in the siSTRIKE U6), and the rest of the sequence was complementary to the oligonucleotide A, except for the last four nucleotides.

Oligonucleotide annealing

The oligonucleotides A and B were annealed by incubation at 90°C for three minutes, followed by incubation at 37°C for 15 minutes in the Oligo Annealing Buffer (Promega) at the final concentration of 40 ng/µl each.

After the annealing, the oligonucleotides formed double-stranded DNA with 5' overhangs (different on each end), complementary to the overhangs in siSTRIKE U6, to enable effective and directional ligation.

Ligation of the annealed oligonucleotides into siSTRIKE U6 vector

The annealed oligonucleotides (4 ng each) were mixed with the linear siSTRIKE U6 vector (50 ng) and T4 DNA ligase (3 units, Promega) in the Rapid Ligation Buffer (Promega) in the total volume of $10~\mu l$. Ligation was carried out for one hour at room temperature.

Transformation of Escherichia coli

Chemically competent *Escherichia coli* (BIOLINE, London, UK) were thawed on ice. Subsequently, 2.5 µl of ligation reaction was added to 50 µl of bacteria suspension, and incubated on ice for 30 minutes. The tube was then placed at 42°C for 45 seconds, and chilled on ice for two minutes. Following addition of 500 µl SOC medium (Invitrogen), the tube was incubated for one hour at 37°C with shaking. Usually, 100 µl of cell transformation mixture was spread on an YTx2 agar plate containing 100 µg/ml ampicilin, and incubated at 37°C overnight.

Plasmid amplification in E. coli and purification

Plasmids were purified using HiSpeed Plasimd Purification Kit (QIAGEN, Crawley, UK), according to manufacturer's instructions. Briefly, a selected colony from the agar plate was transferred to a tube containing 5 ml YTx2 broth with 100 μg/ml ampicilin, and incubated in an orbital shaker at 37°C for four to eight hours. Then, 800 µl of the bacterial culture was mixed with 200 µl of glycerol, and stored frozen at -80°C. The rest (~4 ml) was moved to a conical with 100 ml YTx2 broth with ampicilin. After overnight incubation at 37°C with vigorous shaking, bacteria were centrifuged for 30 minutes at 3000 rcf at 4°C. The bacterial pellet was resuspended in 6 ml of resuspension buffer (Buffer P1), and 6 ml of lysis buffer (Buffer P2) was added. After five minutes at room temperature, 6 ml of cold neutralization buffer (Buffer P3) was added. The mixture was poured into the barrel of the QIAfilter Cartridge, and left for ten minutes, until a precipitate (containing proteins, genomic DNA, and detergent) formed a layer on top of the solution. The cell lysate was then filtered into a HiSpeed Tip, pre-equilibrated with 4 ml of equilibration buffer (Buffer QBT). The filtrate was allowed to enter the resin by the gravity flow. Subsequently, the HiSpeed Tip was washed with 20 ml of wash buffer (Buffer QC), and DNA was eluted with 5 ml of elution buffer (Buffer OF). The DNA was precipitated by addition of 3.5 ml of room temperature isopropanol. After five minutes, the eluate/isopropanol mixture was filtered through a QIAprecipitator module. The DNA in the QIAprecipitator was then washed with 2 ml of 70% (v/v) ethanol, dried by pressing air through the QIAprecipitator, and eluted with 500 µl of water. All plasmids were stored at -20°C.

Verification of the plasmid identity

A new *Pst*I restriction site is created in the siSTRIKE U6 plasmid as a result of a successful ligation. The plasmid before ligation already contains one *Pst*I site. Thus, the plasmids containing the inserts after digestion with *Pst*I give two products (~3.0 and 1.4 kbp). The diagnostic digestion of newly created plasmids with *Pst*I was routinely performed as follows.

Plasmid concentration was quantified with a UV spectrophotometer, as described in more detail for RNA (see 2.2.1.1), except that in the equation used for calculation of DNA concentration, A_{260nm} is multiplied by the factor of 50 rather than 40 (total RNA) or 33 (small RNA). Usually 1 µg of plasmid DNA was digested with 20 units of *Pst*I in the recommended buffer at 37°C for four hours. Then, the samples were separated on a 1% (w/v) agarose gel as described in detail for RNA electrophoresis (see 2.2.1.1). Samples without the enzyme were processed similarly and run on the same gel. A typical outcome is shown on Figure 2.1B.

Additionally, in all cases, the plasmid sequences were confirmed by sequencing by the Sequencing Service at the University of Dundee.

Construction of pGL3-based reporter plasmids with 3'UTR of ZEB1 or ZEB2

Modification of pGL3 vector

As a preparatory step before generation of reporters with ZEB1 or ZEB2 3'UTR downstream of luciferase coding sequence, pGL3 vector, which originally has only one restriction site downstream of the firefly luciferase CDS (for *XbaI*), was modified to facilitate directional cloning.

Digestion of pGL3 vector with XbaI was performed like the siSTRIKE U6 plasmid digestion with PstI described above. After the digestion XbaI was inactivated by incubation at 60°C for 20 minutes. A short insert (two annealed oligonucleotides, see Table 2.2), containing one restriction site for EcoRI and destroying the second restriction site for XbaI, was ligated as described above into the XbaI-digested pGL3 vector. E. coli transformation with the ligation products, followed by plasmid amplification and purification, was carried out as described above.

As the insert could be ligated into the plasmid in both directions with equal probability, the inserts additionally contained part of the *Psh*AI restriction site, which formed the full functional *Psh*AI restriction site only when ligated in the desired direction, i.e. with *Xba*I restriction site followed by the *Eco*RI site. The second *Psh*AI restriction site was already present in the pGL3 vector, so the properly modified pGL3 vector (called later pGL3-*XbaI/Eco*RI) would give two bands on a gel (576 bp and 4711 bp) when digested with *Psh*AI, one band (distinct from the undigested plasmid) when incubated with *Xba*I, and one band (distinct from the undigested plasmid) after digestion with *Eco*RI (Figure 2.2B)

Insertion of ZEB1 or ZEB2 3'UTR into the modified pGL3 vector

To generate the reporters with ZEB1 or ZEB2 3'UTR downstream of the firefly luciferase CDS, based on the pGL3-XbaI/EcoRI vector, those regions (~1.7 or ~1.4 kbp, respectively) were PCR-amplified from HK-2 cell genomic DNA.

The genomic DNA was isolated from $\sim 6 \times 10^6$ unstimulated HK-2 cells, which were trypsinised and centrifuged as described above (see 2.1.1.2), and resuspended in 400 μ l Digestion Buffer and 4 μ l Protease (both from the RecoverAll Total Nucleic

Acid Isolation Kit, Ambion, used mainly for isolation of RNA from FFPE samples, see 2.2.1.2). After overnight incubation at 50°C, the cell lysate was mixed 1:1 (v/v) with basic-phenol:chloroform containing 1% (v/v) isoamyl alcohol, and centrifuged for five minutes at 13000 rcf at room temperature. The upper (aqueous) phase was collected and mixed with 500 μl of chloroform, and centrifuged again. DNA from the aqueous phase was precipitated in a new tube by addition of 500 μl of isopropanol. After one hour at 4°C, the precipitate was pelleted by centrifugation for three minutes at 13000 rcf at 4°C, washed twice with 70% (v/v) ethanol, air-dried for 15 minutes, and 100 μl of water was added, before dissolving in water overnight at 4°C. Subsequently, the genomic DNA concentration was measured as described above for plasmid DNA, and stored frozen at -20°C in small aliquots.

The genomic DNA was used subsequently as a template for amplification of ZEB1 and ZEB2 3'UTR by PCR. For the PCR, high-fidelity Platinum Pfx DNA Polymerase (Invitrogen) was used, together with the recommended buffer. The optimal PCR conditions were slightly different for ZEB1 and ZEB2 3'UTRs, and were as follows (per 50 μ l reaction):

Components	Plasmid pGL3-XbaI/EcoRI	
	ZEB1 3'UTR	ZEB2 3'UTR
10x PCR Buffer	10 µl	5 µl
2.5 mM dNTP	6 µl	6 μl
50 mM MgSO ₄	1 μl	1 μ1
Water	19 μΙ	14 μl
Pfx Polymerase	1 μl	1 μl
Genomic DNA	10 μl (80 ng/μl)	20 μl (10 ng/μl)
10 μM F-PCR-primer	1.5 μl	1.5 μl
10 μM R-PCR-primer	1.5 μl	1.5 µl

The PCR-primers (listed in Table 2.2) for ZEB2 3'UTR contained XbaI and EcoRI restriction sites, and for ZEB1 3'UTR – SpeI and EcoRI (XbaI could not be used, because there is additional XbaI site within the ZEB1 3'UTR; SpeI generates the same sticky ends as XbaI, but recognises different sequence).

The cycling conditions were as recommended by the manufacturer. The template was denatured for three minutes at 94°C. That was followed by 30 (ZEB1) or 35 cycles (ZEB2) of: 15 seconds at 94°C, 30 seconds at 55°C, two minutes at 68°C. Finally, the reactions were chilled at 4 °C.

The PCR products were gel-purified using the QIAquick Gel Extraction Kit (QIAGEN) according to manufacturer's instructions. Briefly, the PCR products were separated on a 1% (w/v) agarose gel, as described for RNA (see 2.2.1.1). The DNA bands were excised from the gel using a clean scalpel. The fragments were weighed, and three volumes of Buffer QG were added to one volume of gel (assuming that 1 mg of gel is ~1 µl). Following ten minute incubation at 50°C, one volume of isopropanol (Sigma) was added. To bind DNA, the samples were transferred to a QIAquick spin column placed in a centrifuge tube, and centrifuged for one minute at 13000 rcf. The flow-through was discarded and the column washed with 750 µl of Buffer PE. The DNA was finally eluted with 50 µl of water.

The purified PCR products were digested with the appropriate restriction enzymes, as described above for digestion with *PstI*. Subsequently, they were incubated for 30 minutes at 37°C with shrimp alkaline phosphatase, to prevent ligation of two or more inserts. Then, the enzyme was inactivated by ten minute incubation at 65°C, and the cut PCR products were gel-purified again with the QIAquick Gel Extraction Kit, as described above, except that the DNA was eluted with 30 instead of 50 µl of water.

The modified pGL3 (pGL3-XbaI/EcoRI) plasmid was digested with XbaI and EcoRI, and gel-purified. Subsequently, 1 µl of pGL3-XbaI/EcoRI was mixed with 7 µl of the PCR products (3'UTR of ZEB1 or ZEB2, with appropriate sticky ends). The ligation, transformation of E. coli, and all the following steps were performed as described above. Confirmation that the obtained plasmids are as expected came initially from the digestion of the plasmids with XbaI and EcoRI (ZEB2 3'UTR), or BamHI and PstI (ZEB1 3'UTR, choice of restriction enzymes explained in the figure legend) and estimation of size of the cut fragments (Figure 2.3). Ultimately, their sequence was confirmed by the Sequencing Service at the University of Dundee.

Transfection reagents

As there are a few commercially available transfection reagents for DNA plasmid delivery, before starting the main experiments, I compared four of them in terms of transfection efficiency and their effect on HK-2 cells: FuGENE 6 (Roche, Burgess Hill, UK), Lipofectamine LTX with or without PLUS Reagent, and Lipofectamine 2000 (all from Invitrogen) (Figure 2.4). The results suggested that the best transfection reagent for my experiments will be Lipofectamine LTX together with PLUS Reagent, as it is much more effective than FuGENE 6, and does not cause any visible effect on HK-2 cell viability, unlike Lipofectamine 2000.

Transfection procedure

Lipofectamine LTX with (or without) PLUS Reagent

One day before transfection, cells were trypsinised and plated on a 12-well-plate, so that they were ~70% confluent at the time of transfection. For each transfection sample, 1 µg of plasmid DNA was diluted in 200 µl Opti-MEM I. After mixing, 1 µl of PLUS Reagent was added (or not). The sample was mixed and incubated for five minutes at room temperature. Then, 2.5 µl of Lipofectamine LTX was added to the tube. The sample was mixed and incubated for 30 minutes at room temperature. Subsequently, 200 µl of the transfection mix was added to wells with cells, and they were incubated at 37°C until ready to assay.

Lipofectamine 2000

One day before transfection, cells were trypsinised and plated on a 12-well-plate, so that they were ~90% confluent at the time of transfection. For each transfection sample, 1.6 µg of plasmid DNA was diluted in 100 µl Opti-MEM I medium. In a separate tube, 4 µl of Lipofectamine 2000 was diluted in 100 µl Opti-MEM I. After five minutes, the diluted DNA and diluted Lipofectamine 2000 were combined and incubated for 20 minutes at room temperature. Then, the transfection complexes were added to cells in 800 µl FCS-free medium per well. Before testing, the cells were incubated at 37°C for 48 hours.

FuGENE 6

One day before transfection, cells were trypsinised and plated on a 12-well-plate, so that they were ~70% confluent at the time of transfection. For each transfection

sample, 1.5 µl of FuGENE 6 was mixed with 50 µl FCS-free HK-2 cell medium. After five minutes, 0.5 µg of plasmid DNA was added, and transfection complexes were allowed to form for 15 minutes at room temperature. Subsequently, 50 µl of transfection mix was added to cells in 500 µl FCS-free medium per well. The cells were then incubated for 48 hours at 37°C.

Transient transfections with small RNAs and with DNA plasmids

Occasionally, there was a need to cotransfect HK-2 cells with both small RNAs and DNA reporter plasmids.

Transfection reagents

Of the transfection reagents available, only Lipofectamine 2000 has been recommended for transfection of small RNA molecules and/or DNA plasmids. The design of the experiments facilitated assessment of the efficiency of delivery of both the small RNAs and the plasmids.

Transfection procedure

One day before transfection, cells were trypsinised and plated on a 12-well-plate, so that they were ~80% confluent at the time of transfection. For each transfection sample, 1 μ g of plasmid DNA and 40 pmol of small RNA were diluted in 100 μ l Opti-MEM I medium. In a separate tube, 4 μ l of Lipofectamine 2000 was diluted in 100 μ l Opti-MEM I. After five minutes, the diluted nucleic acids and diluted Lipofectamine 2000 were combined and incubated for 20 minutes at room

temperature. Subsequently, the transfection complexes were added to cells in $800~\mu l$ medium with 10%~(v/v) FCS. The cells were then incubated at 37° C before testing.

Stable transfections

In some experiments, prolonged expression of shRNA or pre-microRNA was desired. As these were expressed from the siSTRIKE U6 plasmid, which contains a puromycin resistance gene, it was possible to establish modified HK-2 cell lines that stably express the desired RNA molecules.

Characterisation of the toxic effect of puromycin on HK-2 cells

As a prerequisite for stable transfections, the toxic effect of puromycin on HK-2 cells was examined (Figure 2.5). The cells were seeded on 96-well-plates in various densities (from 3 to 12 thousand cells per well), and (immediately or 24 hours later) they were treated with increasing concentrations of puromycin within the recommended range for mammalian cell lines: 1-10 μ g/ml. Their viability was assessed 72 hours after addition of puromycin by the AlamarBlue assay (as described in 2.1.1.3). The puromycin concentration of 9 μ g/ml was chosen for the subsequent selection of stably transfected cells.

Transfection reagents and procedure

Transfection was carried out exactly as described above for transient transfection with DNA plasmids using Lipofectamine LTX and PLUS Reagent.

Selection of transfected cells

Stably transfected cells were selected by addition of puromycin (9 µg/ml) to medium 48 hours after transfection, and were kept in medium with puromycin afterwards. Untransfected cells (or in some experiments cells transfected with plasmids without the puromycin resistance gene) were used as a negative-control. All these cells died within one week after addition of puromycin, as did the large proportion of cells transfected with siSTRIKE U6-based vector. Many of the latter cells died later, presumably because of the protective effect of the transient expression of the puromycin resistance gene. Approximately three weeks after transfection, stably transfected cells formed colonies, and there were enough cells for storage in liquid nitrogen, and for precise calculation of cell number.

Isolation of single lines

The cells were plated to a mean density of 0.5 cells per well on 96-well-plates, and cultured until colonies were easily visible under the microscope (approximately three weeks). Then, typically, six different wells were selected (forming large or small cell colonies, as the RNA expressed could potentially affect cell growth/proliferation). 100 µl of Trypsin/EDTA was added to the chosen wells. Following 15 minutes at 37°C, equal volume of culture medium (containing 10% (v/v) FCS and puromycin) was added, and the cells were transferred to a 12-well-plate containing 1 ml of the complete medium. A few days later, when they became confluent, they were transferred to bigger cell culture dishes, to facilitate subsequent preparation of samples for liquid nitrogen storage (see 2.1.1.2), cell line characterisation by qRT-PCR (see 2.2.2 and 2.2.3.2), and cell maintenance for later experiments.

2.1.2 Tissue samples

Formaldehyde-fixed, paraffin-embedded (FFPE) kidney biopsy samples of 40 patients with diabetic nephropathy, previously characterised by Lewis et al. [181] were examined.

In the previous work, a computer search was performed on the archive of the Histopathology Department, University Hospital of Wales, to identify renal biopsies with the term diabetes in the diagnosis list. After leaving out the biopsies that showed dual pathology and transplant kidney biopsies, 40 renal biopsies taken between 1992 and 2000 were included in the study.

Official biopsy reports were obtained on all the samples, providing information about renal function, defined as the eGFR (see 1.2.2), at the time of the biopsy, and in the following years if possible. Additionally, in the preceding study, the samples were characterised structurally. In particular, fibrosis scores were determined using the grading system of Shih [182].

Patients were divided into three groups [181]. Those who had chronic kidney disease stage 5 (see 1.2.2) or requiring renal replacement therapy within six months of their renal biopsy were referred to as late presenters. Patients who had deterioration of > 5ml/min/year in their eGFR in follow up (which also equated to a > 10% change in the starting eGFR), were termed progressors, and those who did not satisfy these criteria were termed non-progressors. Mean duration of follow up was longer for non-progressors than progressors (6.11±2.75 years vs. 3.67±2.85 years), suggesting that differences between groups did not reflect an inadequate period of follow-up.

The patient information, including age, sex, date of the biopsy, eGFR at the time of the biopsy, subsequent change in eGFR, fibrosis score, is given in Table 2.3.

2.2 RNA analysis

2.2.1 RNA extraction, quantification, and quality control

2.2.1.1 Cell culture samples

RNA extraction

Some of the traditional methods for RNA isolation are not suitable for small RNA analysis. Therefore, the RNA extraction method commonly used in this laboratory (TRI Reagent, Sigma) was compared with the method designed specially to recover small RNAs (mirVana miRNA Isolation Kit, Ambion).

RNA extraction with TRI Reagent

TRI Reagent is an improved version of the RNA isolation reagent developed by Chomczynski [183]. It combines phenol and guanidine thiocyanate to facilitate the immediate inhibition of RNase activity. A biological sample is lysed in TRI Reagent and the lysate is separated into aqueous and organic phases by chloroform addition and centrifugation. RNA remains in the aqueous phase, whereas DNA and proteins relocate to the interphase or the organic phase, respectively. RNA is precipitated from the aqueous phase by addition of isopropanol, washed with ethanol and solubilised. The detailed procedure was as follows.

At the end of the experiment, cells were washed with PBS, and TRI Reagent was added to the wells (600 μl/well on 12-well-plates, or 1 ml/well on 6-well-plates). After ten minutes at room temperature, the lysate was transferred to a tube, and chloroform (Sigma) was added (200 μl to 600 μl of the lysate, or 300 μl to 1 ml). Following vigorous vortexing, the sample was incubated for five minutes at room temperature, and then centrifuged for 45 minutes at 13000 rcf at 4°C. The upper (aqueous) phase was transferred to a new tube and mixed with 400 μl or equal volume (whichever is greater) of isopropanol (Sigma). The sample was then kept overnight at -80°C. The precipitated RNA was pelleted by centrifugation for 45 minutes at 13000 rcf at 4°C, and the pellet was washed three times with 1 ml of 70% (v/v) ethanol. After final centrifugation (15 minutes at 13000 rcf at 4°C), the pellet was airdried for 15 minutes in the fume hood, and resuspended in 20-35 μl of water (so that the RNA concentration was approximately 200 ng/μl). The RNA was then stored at -80°C.

RNA isolation with mirVana miRNA Isolation Kit

RNA isolation with the mirVana miRNA Isolation Kit starts with an organic extraction step, similar to the previous method. Then, RNA is immobilised and further purified on a glass-fiber filter. Depending on the ethanol concentration used in the immobilisation step, total, large (> 200 nt) or small (< 200 nt) RNA fractions can be obtained.

Total RNA isolation

To isolate total RNA using this method, after a wash with PBS, cells were lysed with 600 μl of Lysis/Binding Solution, and transferred to a tube. 60 μl of miRNA Homogenate Additive was added and the sample mixed vigorously. After ten minutes on ice, 600 μl of Acid-Phenol:Chloroform was added and the sample was vortexed for one minute. The sample was centrifuged for ten minutes at 10000 rcf at room temperature. The upper (aqueous) phase was transferred to a new tube, and mixed with 1.25 volumes of room temperature 100% ethanol. The mixture (700 μl at the time) was transferred onto a Filter Cartridge in a centrifuge tube. After centrifugation for 15 seconds at 10000 rcf, RNA was bound to the filter, while the other substances passed through and were discarded. That was repeated until all the sample mixture had passed through the filter. RNA bound to the filter was washed once with 700 μl Wash Solution 1, and then twice with 500 μl Wash Solution 2/3. RNA was eluted with 100 μl pre-heated to 95°C water and stored at -80°C until needed.

Small or large RNA isolation

To obtain small (< 200 nt) or large (> 200 nt) RNA fractions, after organic extraction (as described above for total RNA isoloation), the aqueous phase was mixed with 1/3 volume of room temperature 100% ethanol. The mixture was placed onto a Filter Cartridge in a centrifuge tube. After centrifugation for 15 seconds at 10000 rcf, large RNA was bound to the filter, while small RNA, because of relatively low ethanol concentration in the mixture, passed through. The large RNA fraction was recovered from the filter using the procedure for total RNA. The small RNA in the filtrate was mixed with 2/3 volumes of room temperature 100% ethanol, and applied to a new

Filter Cartridge. With a higher concentration of ethanol, small RNA molecules were now bound to the filter, and were washed and eluted as described above for total RNA. To confirm that the obtained fractions contained RNA of the expected size, the isolated RNA was separated on an agarose gel as described below (Figure 2.6).

For comparison of the two methods, total RNA obtained with either of them was quantified as described below, and 1 µg of each sample was separated on an agarose gel (Figure 2.7A). Additionally, a model microRNA, miR-16, was quantified by qRT-PCR (see 2.2.3.2) in both the RNA preparations (Figure 2.7B). No difference was seen in the small RNA fraction on the gel and in miR-16 expression by qRT-PCR. Thus for the majority of subsequent experiments RNA was isolated using the cheaper option, TRI Reagent. mirVana miRNA Isolation Kit was used for preparation of RNA for microRNA profiling using the mirVana miRNA Bioarrays (see 2.2.3.1).

RNA quantification and quality control

RNA concentration was measured using a UV spectrophotometer. Absorbance at the wavelength 260 nm (A_{260nm}) was assessed to calculate the nucleic acid concentration, using the following equations (for total and small RNA preparations):

[RNA] =
$$A_{260nm}$$
* 40 * dilution factor

Total RNA

 $(\mu g/ml)$

[RNA] =
$$A_{260nm}$$
* 33 * dilution factor (µg/ml)

Small RNA

To ensure accuracy, the samples were diluted prior to the measurement, so that the absorbance value fell between 0.1 and 1.0.

In addition to the reading at 260 nm, the absorbance at 280 nm (A_{280nm}) was also measured. The ratio of A_{260nm} to A_{280nm} indicated whether the sample was heavily contaminated with other molecules, such as proteins. Only the samples with a ratio above 1.5 were used for further analysis.

Alternatively, RNA concentration in diluted samples was measured using a more sensitive, fluorescence-based method, Quant-iT RNA Assay (Invitrogen). The assay is highly selective for RNA and exhibits a linear detection range between 5 ng and 100 ng RNA. The quantification was performed according to the manufacturer's instructions. Briefly, Quant-iT RNA reagent was mixed with Quant-iT RNA buffer 1:200. To 200 μl of that mixture 1-20 μl of RNA standards or my RNA samples were added. After two minute incubation at room temperature, fluorescence was measured with the Qubit fluorometer (excitation/emission wavelengths: ~644/673 nm).

To determine RNA integrity, 0.5 to 1 μ g of RNA was routinely separated on 3% (w/v) agarose gel. Before loading the RNA samples into the gel, they were mixed with the gel loading buffer (Ambion). The gel was prepared by dissolving of agarose in TAE buffer (Promega) containing 0.5 μ g/ml ethidium bromide. Electrophoresis was carried out in TAE buffer usually for one hour at 100 V. The presence of ethidium bromide in the gel made possible subsequent visualisation of RNA in UV light. Typically, two strong distinct bands (28S and 18S rRNA) were visible.

2.2.1.2 Tissue samples

RNA extraction

RNA extraction from 40 FFPE kidney biopsy samples (see 2.1.2) was performed using the RecoverAll Total Nucleic Acid Isolation Kit (Ambion), especially designed for isolation of RNA and DNA from FFPE samples. Prior to the main experiment, this method was tested on 4 FFPE renal biopsy samples not included in the study.

For RNA isolation with the RecoverAll Total Nucleic Acid Isolation Kit, FFPE samples were processed according to the manufacturer's instructions. Briefly, they were deparaffinised using a series of xylene and ethanol washes. Subsequently, they were digested with a protease. Then, RNA was purified using a rapid glass-fiber filter methodology, including an on-filter treatment with a DNase, and were eluted into water. The detailed procedure was as follows.

The FFPE renal tissue blocks were cut into 20 µm sections (as recommended for maximum microRNA recovery), using a microtome in the Histopathology Department by the Cardiff University School of Medicine Central Biotechnology Services (CBS). From each sample, five sections were taken, the outer one was discarded, and RNA was isolated from the remaining four slices.

To remove paraffin, the sections were incubated with 1 ml of 100% xylene (Sigma) for three minutes at 50°C, and then centrifuged for two minutes at 13000 rcf at room temperature. The pellet was washed twice with 1 ml of 100% ethanol, and air-dried for 15 minutes.

Subsequently, $400 \,\mu l$ of Digestion Buffer and $4 \,\mu l$ of Protease were added per sample, and the samples were incubated at $50 \,^{\circ}\text{C}$ for three hours.

For RNA isolation, 480 μ l of Isolation Additive was added to each sample, mixed, and then 1.1 ml of 100% ethanol was added. The mixture (700 μ l at the time) was placed onto a Filter Cartridge in a centrifuge tube. After centrifugation for 30 seconds at 10000 rcf, the nucleic acids present in the mixture were bound to the filter, while the other substances passed through and were discarded. That was repeated until all the sample mixture was through the filter.

The nucleic acids bound to the filter were washed once with Wash 1 buffer, and then with Wash 2/3 buffer. DNA was removed from the preparation by incubation with $60 \,\mu l$ of DNase mix (containing $6 \,\mu l$ of 10x DNase Buffer, $4 \,\mu l$ DNase, and $50 \,\mu l$ water) for 30 minutes at room temperature.

The filter was washed again with Wash 1 buffer, and then twice with Wash 2/3 buffer. RNA was eluted by addition of water pre-heated to 95°C (2x 30 µl). Small aliquots of all the samples were taken for quality control, and the rest was stored at -80°C until analysis.

RNA quantification and quality control

As the RNA amount isolated from FFPE kidney biopsies was expected to be very small, to assess RNA yield and quality in the samples, microfluidics analysis was performed by CBS. For that, they used Agilent's 2100 bioanalyser together with the RNA PicoChip Kit (Agilent Technologies, Stockport, UK). Each RNA chip contains an interconnected set of microchannels that is used for separation of nucleic acid fragments based on their size as they are driven through it electrophoretically. The data obtained by this method are analogous to those from RNA agarose gels,

but as little as 0.2 ng of RNA is sufficient for the analysis. Moreover, it also estimates RNA concentration of a sample.

Additionally, to determine suitability of the samples for microRNA detection by qRT-PCR, expression of miR-16, known to be expressed in many tissues and cell lines, including HK-2 cells, was analysed by qRT-PCR (see 2.2.3.2).

Before proceeding with array-based quantitation of microRNAs, detailed analysis of the 4 extra FFPE samples was performed, to establish that the extraction procedure was effective, and to determine an optimal method for quality control of subsequent samples. Firstly, the RNA concentrations were determined by PicoChip, and compared with the values obtained with the Quant-iT RNA Assay (see 2.2.1.1) (Figure 2.8A,B).

Subsequently, relative expression of miR-200b and miR-16 was evaluated by qRT-PCR. A constant ratio of miR-200b to miR-16 was seen in the samples (Figure 2.8C,D). Moreover, for both microRNAs, 5x and 25x dilution of the samples resulted in expected ~5x and ~25x reduction in microRNA expression (Figure 2.8F), suggesting that the assays work properly and no PCR inhibitors are present in RNA preparations.

Finally, the qRT-PCR assay for miR-16 quantification developed for this study, used for miR-16 detection in all the 40 FFPE samples, gave almost identical results to the miR-16-specific TaqMan assay supplied by Applied Biosystems (Figure 2.8C,E). That was further confirmed using the both assays on HK-2 cell RNA samples (Figure 2.11D).

2.2.2 Messenger RNA detection

Messenger RNA (mRNA) was measured in cell culture samples by two-step quantitative reverse transcription – polymerase chain reaction (qRT-PCR).

2.2.2.1 Reverse transcription

Reverse transcription (RT) was performed using High-Capacity cDNA Reverse Transcription Kit (Applied Biosystems). Briefly, 1 µg of total RNA in 10 µl of water was added to 10 µl of the RT mix containing: 3.2 µl water, 2 µl 10x RT Buffer, 2 µl 10x Random Primers, 0.8 µl 100 mM dNTP Mix, 1 µl RNase Inhibitor, and 1 µl MultiScribe Reverse Transcriptase. Two types of negative control for RT step were used:

- Non-template control (RT-NTC), which did not contain RNA;
- RT-negative control, which did not contain MultiScribe Reverse Transcriptase.

The following thermal profile in a thermal cycler was used: ten minutes at 25°C, two hours at 37°C, five seconds at 85°C, and cooling to 4°C.

After the reaction, samples (cDNA) were diluted (5x) by addition of 80 µl of water, and used in quantitative polymerase chain reaction (qPCR) or stored at -20°C, as recommended by the manufacturer.

2.2.2.2 Quantitative polymerase chain reaction

There are two main chemistries used to detect PCR products in qPCR:

- TaqMan chemistry, which uses a fluorogenic probe, binding specifically to the target mRNA between the PCR-primers;
- SYBR Green chemistry, which uses SYBR Green dye, binding non-specifically to double-stranded DNA.

Both types of qPCR were used in the study. For a full list of the TaqMan assays and primers used see Table 2.4.

TaqMan assays

Master mix for every gene tested was prepared by combining together a gene-specific set of PCR-primers and TaqMan probe (designed and supplied by Applied Biosystems) (1 µl/reaction), water (5 µl/reaction), and 2x TaqMan Universal PCR Master Mix (Applied Biosystems) (10 µl/reaction), containing a thermostable DNA polymerase, deoxynucleotides, optimized concentration of ions, and the passive reference dye ROX.

Gene-specific master mix was distributed to appropriate wells on an Optical 96-Well Fast Plate (Applied Biosystems) (16 μ l/well). Subsequently, 5x diluted cDNA (or water for PCR-NTC) was added (4 μ l/well).

The plate was sealed with a MicroAmp Optical Adhesive Film (Applied Biosystems) and qPCR performed on an Applied Biosystems 7900HT Fast Real-Time PCR

System, using the recommended conditions: ten minutes at 95°C, followed by 40 cycles of 15 seconds at 95°C and one minute at 60°C.

SYBR Green-based assays

The SYBR Green-based assays were performed as described for TaqMan assays, with a few modifications:

- SYBR Green-containing master mix (Power SYBR Green Master Mix, Applied Biosystems) was used.
- Instead of the primer/TaqMan probe mix, PCR-primers (custom DNA oligonucleotides obtained from Invitrogen) were used at the final concentration of 300 nM each.
- After the last PCR cycle, the fluorescence was measured while the temperature was slowly increasing from 60 to 95°C for subsequent melting curve analysis (to ensure that only a single PCR product is present).

Primer design

The majority of SYBR Green-based assays used for this project were designed using the Primer3 program [184] and BLAST [185]. The mRNA sequences were taken from the NCBI database. In case of genes known to have two or more splicing variants, the primers were designed in a common part, so that all mRNA variants are detected. The length of the PCR product was ideally between 75 and 150 bp (and for all primer pairs designed, it was 50-200 bp). The annealing temperature for all the designed primers was 60°C, so that the standard cycling conditions could be used, and TaqMan assays could be run together with SYBR Green-based assays on one plate. To avoid

detection of genomic DNA, if possible, primers were in different exons or bound to exon-exon junctions.

New pairs of primers were routinely tested for PCR efficiency. For that qPCR was performed on serially diluted cDNA (usually 5x). Relation between C_T (see 2.2.2.3) and template starting copy number was plotted. After addition of the logarithmic trendline, the PCR efficiency was calculated using the following formula (from Stratagene/Agilent Technologies Technical Toolbox, modified):

Efficiency =
$$-1+e^{(-1/\text{slope})}$$

Only the pairs with the efficiency between 90 and 110% (as recommended by Applied Biosystems), and giving a single PCR product, as determined by melting curve analysis, were used in experiments.

2.2.2.3 Quantitative RT-PCR data analysis

For qPCR data analysis, Applied Biosystems SDS v2.3 software and Microsoft Excel were used. Relative expression was calculated using the $2^{-\Delta\Delta CT}$ method [186]. C_T , or the threshold cycle, is a number of PCR cycles needed to detect fluorescence associated with the amplification of a specific product (Figure 2.9). If efficiency of the reaction is 100%, with every PCR cycle the number of copies of the product is doubled. Therefore, one cycle difference (ΔC_T =1) between two samples means that there was initially 2-fold difference in expression of a particular gene between those samples. The difference of two cycles (ΔC_T =2) means 4-fold (2^2) difference in expression, ΔC_T =3 means 8-fold (2^3) difference, and so on.

To normalise for differences in the starting amount of RNA in RT between the samples (or inaccuracy during subsequent steps), in addition to a gene of interest (target gene), expression of a gene not influenced by experimental treatment (endogenous control) is assessed.

In the first step of the $2^{-\Delta\Delta CT}$ method, for each sample the difference between C_T obtained for a target gene and C_T for an endogenous control is calculated $(\Delta C_T = C_T^{TARGET} - C_T^{ENDOGENOUS})$. Subsequently, one sample is chosen as a calibrator (its expression will be equal 1), and $\Delta\Delta C_T$ is calculated by subtraction of $\Delta C_T^{CALIBRATOR}$ from ΔC_T of every other sample. The last step is calculation of $2^{-\Delta\Delta CT}$, which for each sample will give the target gene expression, normalised to the endogenous control, relative to the calibrator.

2.2.3 MicroRNA detection

2.2.3.1 MicroRNA profiling

There are two main types of arrays used currently to examine expression of large number of microRNAs in biological samples. These are hybridisation-based microarrays and qPCR-based arrays (so called TaqMan Low-Density Arrays). Both were used in this study.

MicroRNA profiling in HK-2 cells using mirVana miRNA Bioarrays

The qPCR-based microRNA arrays became available in 2008. Therefore, the only option for early microRNA profiling experiments was a hybridisation-based array. That was carried out twice by Asuragen Services (formerly Ambion Services, Austin, US), using the mirVana miRNA Bioarrays platform (Ambion).

Before the start of my studies, microRNA expression was analysed in control HK-2 cells and those cultured with high concentration of glucose (25 mM) for 48 or 96 hours, using the mirVana miRNA Bioarrays v1. The analysis was repeated one year later, after review of the data from the first microRNA microarrays with Asuragen. They suggested a potential technical error with the high-glucose arrays and agreed to repeat the microRNA profiling on new samples (control and 25 mM glucose for 48 hours), using new version (v2) of Ambion mirVana miRNA Bioarrays. Version 2 included probes to all human (328), mouse (266), and rat (238) miRNAs in the miRBase release 8.0 [106], 152 additional unpublished human miRNAs, and 61 control probes for accurate data normalization.

Stimulation of HK-2 cells was carried out as described above (see 2.1.1.4). Subsequently, total RNA was isolated using the mirVana miRNA Isolation Kit (see 2.2.1.1). Approximately 30 µg of total RNA for each sample (control and high-glucose-treated HK-2 cells, in triplicate) was sent frozen to Asuragen.

Sample preparation by Asuragen included quality assessment of the supplied total RNA, and microRNA enrichment using the flashPAGE Fractionator and Reaction Clean-up Kit (Ambion). The 3' ends of RNA molecules were then labeled using the mirVana miRNA Labeling Kit (Ambion), according to the manufacturer's instructions. Amine-modified nucleotides were incorporated during polyadenylation

reaction. Subsequently, Cy3 succinimide esters were conjugated to the amine moieties on the small RNAs. Hybridisation to the mirVana miRNA Bioarrays was performed using the mirVana miRNA Bioarray Essentials Kit (Ambion). The Cy3 fluorescence was scanned at excitation wavelength of 532 nm, using a GenePix 4200AL scanner (Molecular Devices). The fluorescent signal associated with the probes and local background was extracted using GenePix Pro (version 6.0, Molecular Devices). Thresholding, signal scaling, and normalization were performed using algorithms selected by Asuragen.

MicroRNA profiling in tissue samples by TaqMan Low-Density Arrays

Since the amount of RNA isolated from FFPE kidney biopsy samples was not sufficient for microRNA profiling using hybridisation-based arrays, a qPCR-based array was used. The TaqMan Low-Density Array Human MicroRNA Panel v1.0 (Applied Biosystems) is a 384-well microfluidic card that contains primers and probes for 365 different human microRNAs. It is used in conjunction with the Human Multiplex RT Set v1.0 (Applied Biosystems), so that all 365 microRNAs (if they are expressed) are reverse-transcribed in eight separate RT reactions, using eight distinct RT-primer pools (containing up to 48 RT-primers each). The principles of microRNA detection by this method are analogous to the detection of individual microRNAs by stem-loop qRT-PCR, and are explained below (see 2.2.3.2). The microRNA profiling using this method in FFPE kidney biopsy samples from patients with diabetic nephropathy was performed by CBS.

The procedure was in accordance with the manufacturer's instructions. Briefly, for each group of patients (non-progressors, n=9; progressors, n=9; late presenters,

n=4), total RNA, isolated and quantified as described above (see 2.2.1.2), was pooled. Multiplex reverse transcription reactions (with 8 different sets of microRNA-specific RT-primers) were carried out using 25 ng of the pooled RNA. Each RT reaction was diluted 62.5x with water, and 55 μl was combined with 55 μl of TaqMan 2x Universal PCR Master Mix. Subsequently, 100 μl of the mixture for each of 8 Multiplex RT pools was loaded into appropriate filling ports of the microfluidic card. The array was then centrifuged and mechanically sealed with the Applied Biosystems sealer device. qPCR was carried out on an Applied Biosystems 7900HT Fast Real-Time PCR System, using the recommended cycling conditions. The relative microRNA expression was calculated as described above for mRNA quantification by qRT-PCR (see 2.2.2.3). Detection limit was set to C_T=33, according to the manufacturer's recommendations.

2.2.3.2 Individual microRNA detection

There are several methods available for individual microRNA detection. These are mainly northern blot, solution hybridisation, and RT-PCR-based methods. As RT-PCR-based methods are thought to be more sensitive, can better differentiate between similar sequences, do not involve using radiolabeled reagents, and also can be quantitative, they were considered first for the project.

Due to the small size of microRNAs (~22 nt), they cannot be detected in a common RT-PCR reaction, routinely used for mRNA detection. Recently, two ingenious quantitative RT-PCR systems, suitable even for detection of very short RNA molecules, have been described [187, 188]. These are stem-loop qRT-PCR (used

originally in Applied Biosystems TaqMan MicroRNA Assays) and polyadenylation-based qRT-PCR (Invitrogen NCode miRNA Detection System).

MicroRNA detection by stem-loop qRT-PCR

This involves two steps (Figure 2.10):

- RT with a microRNA-specific RT-primer. This primer contains a few nucleotides complementary to the 3' end of the mature microRNA, and a long unrelated sequence forming a stem-loop structure, so that it cannot interact with other RNA molecules present in the RT reaction.
- qPCR with one PCR-primer identical with the 5' end of microRNA, and the second identical with a part of the long stem-loop RT-primer. Fluorescence signal, needed for quantitative detection, comes from a TaqMan probe, binding to the junction between the microRNA and RT-primer.

The detailed procedure was as follows.

To prepare RT master mix, 4.16 μl water, 1.5 μl 10x Reverse Transcription Buffer, 0.15 μl 100 mM dNTP, 0.19 μl 20 u/μl RNase Inhibitor, 1 μl 50 u/μl MultiScribe Reverse Transcriptase, and 3 μl 5x RT-primer per one reaction were combined. 10 μl of the RT master mix was then added to 5 μl of RNA, typically containing 10 ng total RNA, and incubated on ice for at least five minutes. Negative controls used at this step were RT-NTC (with water instead of RNA) and RT-negative control (without MultiScribe Reverse Transcriptase). The following thermal cycler profile was used: 30 minutes at 16°C, 30 minutes at 42°C, five minutes at 85°C, and cooling to 4°C.

The cDNA was diluted with water 1:3, and 4 μ l were used in qPCR, performed as described for mRNA detection with TaqMan assays (see 2.2.2.2). The data were analysed using the $2^{-\Delta\Delta CT}$ method [186] (see 2.2.2.3).

The accuracy of microRNA detection with this system was assessed for three microRNAs of varying abundance levels in HK-2 cells according to the microarray results: miR-16 (the highest expression), miR-29a, and miR-128a (the lowest expression) (Figure 2.11A). For miR-16 and miR-29a assays, relationship between the fluorescence signal and the RNA amount used for reaction (between 2 and 250 ng) was as expected, with the efficiency of the reactions close to 100% (Figure 2.11B). The efficiency was calculated as described above (see 2.2.2.2). In case of the assay for miR-128a, the least abundant of the selected microRNAs, the signal was not strictly dependent on RNA amount used in RT, especially when higher concentrations of RNA were used. To minimize competition of miR-128a with other RNA molecules, small RNA fraction (< 200 nt), isolated with mirVana miRNA Isolation Kit (see 2.2.1.1), was used in qRT-PCR instead of total RNA (Figure 2.11C). That modification, however, was not sufficient to allow for quantitative miR-128a detection in HK-2 cells. Therefore, for subsequent experiments microRNAs of relatively high expression in HK-2 cells were preferentially chosen, and the efficiency of new assays was routinely estimated.

Design of SYBR Green-based stem-loop qRT-PCR assays for microRNA detection

In order to examine expression of recently described microRNAs (like those studied in Chapter Six), for which no pre-designed qRT-PCR assays were available, stem-loop qRT-PCR assays were designed in house. In those new assays, the protocol

and the reagents from the commercial system were used, except for microRNA-specific primers for RT and PCR, and SYBR Green-containing qPCR master mix (Power SYBR Green Master Mix, Applied Biosystems).

As it was conceivable that those new microRNAs may not be expressed by HK-2 cells, the first assay was designed for detection of miR-16, which is highly expressed and easily measured with the TaqMan assay in HK-2 cells. Assays for other microRNAs were designed later in a similar manner, except for miR-663, which is highly GC-rich and requires special conditions, as described below. For all primer sequences see Table 2.4.

Design of miR-16-specific stem-loop RT-primer and PCR-primers

Sequence of the mature human miR-16 (as deposited in the miRBase [106]) is as follows:

5' UAGCAGCACGUAAAUAUUGGCG 3'

Optimisation experiments showed that, for this microRNA, the RT-primer worked best if it contained in its 3' end 5 nucleotides complementary to 3' end of miR-16 (in bold).

The rest of the primer is intended to increase the length of miR-16 cDNA, so that it can be subsequently detected by qPCR. Chen et al. [187] have reported that these RT-primers work better (in terms of both specificity and sensitivity), if the long part forms a secondary structure, such as a stem-loop.

For good PCR efficiency, this structure is not supposed to be stable during qPCR (i.e. at 60°C or above), one of the PCR-primers should interfere effectively with its re-formation, and bind only to one site on the RT-primer complement. This suggested that a more complicated secondary structure than a simple stem-loop may be superior.

Therefore, a random sequence, not highly similar to any human mRNA, as confirmed by BLAST [185], served as a base for design of a DNA oligonucleotide, forming a stem-double-loop structure with one mismatch in the stem at the temperature of the RT reaction (42°C). This was confirmed by MFOLD [189] (Figure 2.12A). The oligonucleotide, combined with the 5 nucleotides complementary to miR-16, created the miR-16-specific RT-primer (from 5' to 3'):

ATCAAGCGTCGCAGGAACATCACCCACATGTTACGATTGATCGCCA (46 nt)
This primer was used in RT at the optimised final concentration of 50 nM.

For detection of the 63-nucleotide-long miR-16 cDNA by qPCR, two primers were designed. The first (forward) primer has identical sequence (with T instead of U) as the mature miR-16, except that it does not include the last two nucleotides: TAGCAGCACGTAAATATTGG. Ideally, there would be no overlap between RT- and PCR-primer, however the already very low annealing temperature of that forward PCR-primer (50.6°C, calculated using Primer Express, Applied Biosystems) did not allow for further shortening.

The second (reverse) PCR-primer is identical with a part of RT-primer (in italics): AGCGTCGCAGGAACATCA. Most of this fragment of the RT-primer localises to the mismatched region and forms the loops, so the PCR-primer would bind only to one strand and prime only in the desired direction. Moreover, the reverse PCR-primer binding may prevent the formation of the secondary structure within the template.

Validation of the new assay for miR-16

First of all, the amplification of a single product was confirmed by melting curve (see 2.2.2.2) (Figure 2.12C) and agarose gel (see 2.2.1.1) analyses. The latter also showed that the product is approximately of the expected size: 59 bp. Subsequently, efficiency of the new SYBR Green-based stem-loop qRT-PCR assay for miR-16 was tested, and was 98% (Figure 2.12D). Additionally, its performance was compared with the TaqMan assay in both HK-2 cell culture samples (Figure 2.12D) and renal tissue samples (Figure 2.8C,E), giving almost identical results.

Design of miR-663 assay

Since miR-663 is very GC-rich (AGGCGGGGCGCGCGGGACCGC), it was very likely that at temperatures used in a standard stem-loop qRT-PCR it would interact with other RNA species and form stable double-stranded RNA structures, interfering with the detection. Therefore, the procedure was altered as follows.

The RT-primer was longer (60 nt vs. 46 nt) and the secondary structure was more stable (Tm 78.3°C vs. 61.7°C) than of the primer used for miR-16 detection (Figure 2.12B). This allowed for an additional step before RT: sample RNA and the stem-loop RT-primer were mixed together and heated for five minutes at 65°C, then chilled. The RT mix was then added and the RT reaction was carried out for one hour at 42°C. In the following qPCR, the annealing/extension step was set at 75°C instead of standard 60°C; otherwise the RT-primer would form a stable secondary structure that would affect the efficiency of the reaction.

The primer sequences are given in Table 2.4, and the performance of the assay was evaluated in Chapter Six.

Polyadenylation-based qRT-PCR

Before trying to design stem-loop qRT-PCR assays for newly described microRNAs, the other microRNA detection method, NCode SYBR Green qRT-PCR Kit (Invitrogen), was tested. This was a modification of qRT-PCR, which employed a polyadenylation reaction prior to RT [188].

Unfortunately, the system did not work as expected. Assays for miR-16 and miR-29a were far less sensitive than the TaqMan assays (approximately 10-cycle increase in C_T for both microRNAs). Furthermore, fluorescence signal depended neither on the concentration of RNA used for RT, nor cDNA in qPCR. In addition, strong signal was observed in negative controls without the polyadenylation step. Therefore, the method was not used for this project.

2.3 Protein analysis

2.3.1 Western blot

Detection of Dicer by Western blot was used to evaluate performance of Dicer-specific siRNA. Additionally, this method was used (together with Immunofluorescence, see 2.3.2) to assess E-cadherin expression in HK-2 cells stably overexpressing miR-192 at the protein level.

Cell lysis

Whole cell extracts were prepared with RIPA Lysis Buffer (Santa Cruz Biotechnology, Heidelberg, Germany). After washing cells with cold PBS, RIPA Lysis Buffer was added (200 µl/well on 6-well-plates), and incubated for 15 minutes on ice with frequent agitation. Then, the lysate was transferred to a tube and centrifuged for 30 minutes at 16000 rcf at 4°C. The supernatant was then collected, divided into aliquots, and stored frozen at -80°C until needed.

Protein quantification by Bradford Assay

The BioRad Protein Assay, based on the method of Bradford, is a dye-binding assay in which the absorbance maximum for an acidic solution of Coomassie Brilliant Blue G-250 dye shifts from 465 nm to 595 nm when binding to protein occurs.

To quantify proteins in the lysates, the standard curve of bovine serum albumin (BSA) was prepared (2-fold serial dilutions in the range: 1000-15.6 ng/ μ l) and the lysates appropriately diluted. Bradford Reagent 5x was diluted with water 1:5, and $200 \,\mu$ l/well added to a 96-well-plate containing in separate wells 5 μ l of water (blank), BSA standards, or samples (all in triplicate). Absorbance at 595 nm was measured five minutes later, using a FLUOstar OPTIMA plate reader.

SDS-PAGE

Sodium dodecyl sulfate-polyacrylamide gel electrophoresis (SDS-PAGE) was performed by the method of Laemmli [190].

Composition of the resolving and stacking gels was as follows:

Components	Resolving gel 7.5% (w/v)	Stacking gel
Water	7.275 ml	6.1 ml
Buffer	1.5 M Tris-HCl pH 8.8 3.75 ml	0.5 M Tris-HCl pH 6.8 2.5 ml
10% (w/v) SDS	150 μ1	100 μl
Mix of Acrylamide 29.2% (w/v) and Bisacrylamide 0.8% (w/v)	3.75 ml	1.3 ml
10% Ammonium Persulphate (0.05 g in 500 μl water)	75 µl	75 µl
TEMED	7.5 µl	10 μl

Protein samples were thawed on ice, a constant amount (usually 15 µg) mixed with 3x Reducing Loading Buffer (see Appendix), and heated at 95°C for five minutes. Then, samples were cooled on ice, and loaded in the gel. Additionally, 15 µl of a mix of dye-conjugated standards (See Blue Plus Two, Invitrogen) was loaded in one of the wells. The electrophoresis was carried out in a BioRad Mini Protein II apparatus, in Running Buffer (see Appendix), at 100 V for 20 minutes and subsequently at 150 V for one hour.

Protein transfer to a nitrocellulose membrane

The separated proteins were transferred onto a nitrocellulose membrane (GE Healthcare, Amersham, UK), using a BioRad Mini Blot II apparatus. The membrane, filter paper, and pads were pre-soaked in Transfer Buffer (see Appendix). The transfer cassette was assembled in the following order:

(negative charge)-pad-paper-gel-membrane-paper-pad-(positive charge)

The cassette was placed in the holder, and then in the transfer apparatus filled to the top with pre-chilled Transfer Buffer, and containing an ice pack and stirring bar. The transfer was performed for 1-1.5 hours at 100 V.

Incubation with antibodies

The nitrocellulose membrane was blocked (to prevent non-specific antibody binding) for one hour with 5% (w/v) skimmed milk in Tris-buffered saline (TBS) pH 7.4 containing 0.1% (v/v) Tween-20. Subsequently, the membrane was incubated overnight at 4°C with primary antibodies in TBS with 1% (w/v) BSA and 0.1% (v/v) Tween-20. After three washes with 0.1% (v/v) Tween-20 in TBS (15 minutes each), the membrane was transferred to appropriate horseradish peroxidase (HRP)-conjugated secondary antibody solution in TBS with 1% (w/v) BSA and 0.1% (v/v) Tween-20. Following one hour incubation at room temperature, and three more washes, the membrane was ready for the detection step.

For details about the antibodies and dilutions used in this study see Table 2.5.

Detection

Antibody binding was visualised using enhanced chemiluminescence (ECL) detection (Luminogen, GE Healthcare). The substrate for HRP was prepared by mixing reagents A and B, and added to the drained membrane and left for one minute. Then, the membrane was wrapped in cling film and exposed to Amersham Hyperfilm ECL (GE Healthcare) for 0.5-15 minutes, as required.

Membrane stripping and reprobing

To ensure equal protein load in each lane, membranes were stripped by incubation in Stripping Buffer (see Appendix) at 50°C for 30 minutes. Adequacy of the stripping was confirmed by lack of signal from the membrane after incubation with HRP substrate and 30 minute exposure to a film. After extensive washes and quick blocking, the membrane was reprobed with anti-GAPDH antibody. Incubation with appropriate secondary antibody and detection were performed as described above.

2.3.2 Immunofluorescence

Immunofluorescence was used to confirm increase of E-cadherin at the protein level in cells stably overexpressing miR-192.

Cells on glass Lab-Tek Chamber Slides (Nunc) were washed with FCS-free medium, and fixed with 3.7% (w/v) PFA in PBS containing 1 mM CaCl₂ for ten minutes at room temperature. After three washes with PBS, the slides were blocked with 1% (w/v) BSA in PBS for 45 minutes at room temperature. E-cadherin was probed with a murine monoclonal antibody (HECD-1, abcam) diluted 1:50 with 0.1% (w/v) BSA in PBS. Following overnight incubation at 4°C, the slides were washed three times with 0.1% (w/v) BSA in PBS, and incubated for one hour at room temperature with Alexa Fluor 555-conjugated anti-mouse secondary antibody (Molecular Probes/Invitrogen) diluted 1:1000 in PBS containing 0.1% (w/v) BSA. The slides were washed twice with 0.1% (w/v) BSA in PBS. Hoechst 33258 (Sigma) was used at the concentration of 0.5 μg/ml to stain nuclei. After the final wash, the glass coverslip was mounted on the slide using FluorSave Reagent (Calbiochem/Merck Chemicals, Nottingham, UK). Cells were observed on a Leica DMLA fluorescent microscope, and pictures were taken with a Zeiss Axiocam MRc digital camera.

2.3.3 Enzyme-linked immunosorbent assay

A commercially available TGF-beta enzyme-linked immunosorbent assay (ELISA) development kit (R&D Systems) was used to quantify TGF-beta secreted to the medium by HK-2 cells. The antibodies in the kit recognise TGF-beta1, and the cross-reactivity with TGF-beta2 and TGF-beta3 is below 1%, as determined by the manufacturer.

Ultra High Binding 96-well-plates (Immulon, Thermo Fisher Scientific, Loughborough, UK) were coated with anti-TGF-beta capture antibody (2 μ g/ml in PBS, 100 μ l/well) overnight at room temperature. Wells were washed three times with 0.05% (v/v) Tween-20 in PBS, using a Denley Wellwash 4 plate washer. The plate was blocked with 200 μ l 5% (v/v) Tween-20 in PBS for one hour at room temperature.

During that incubation, samples and standards were prepared. The antibodies in the kit recognise the active form of TGF-beta. Previous work in this laboratory suggested that if there is any active TGF-beta in HK-2 cell medium, it is below the detection limit of this method, therefore all cell culture supernatant samples were acid-activated before detection. To each 100 μ l of sample 20 μ l of 1 M HCl was added. After ten minutes, the samples were neutralised with 20 μ l of 1.2 M NaOH in 0.5 M HEPES. In parallel, supplied TGF-beta standards were serially diluted (2-fold dilutions in the range: 2000-31.25 pg/ml) in Reagent Diluent (1.4% (w/v) delipidised BSA, 0.05% (v/v) Tween-20 in PBS).

The standards and acid-activated samples were transferred to the plate (100 µl/well) and incubated for two hours at room temperature. Following three washes, anti-TGF-beta detection antibody was added (300 ng/ml in Reagent Diluent, 100 µl/well). After 2 hours, the plate was washed three times, and HRP-conjugated streptavidin was added (diluted 1:200 in Reagent Diluent, 100 µl/well). The plate was incubated in the dark for 20 minutes, then washed three times. Finally, HRP substrate, freshly prepared by mixing equal volumes of Reagent A with Reagent B, was added. The plate was incubated in the dark for 20 minutes and the reaction was stopped by addition of Stop Solution (2 M H₂SO₄). The absorbance was read at 450 nm. TGF-beta concentrations in the samples were calculated using a standard curve.

2.3.4 Luciferase activity

All reporter plasmids used in this study utilised firefly (*Photinus pyralis*) luciferase CDS, and were routinely cotransfected with a control plasmid coding for *Renilla* (*Renilla reniformis*) luciferase. Firefly and *Renilla* luciferases, because of their distinct evolutionary origins, have different structures and substrate requirements. It is therefore possible to discriminate between their respective bioluminescent reactions. With the Dual-Luciferase Reporter Assay System (Promega), the activities of both luciferases can be measured sequentially in a single sample. The detailed procedure, recommended by the manufacturer, was as follows.

Transfected cells were washed with PBS, and 200 µl of Passive Lysis Buffer (diluted 1:5 in water) was added per well (12-well-plate). After 30 minutes at room temperature with constant agitation, the lysates were transferred to tubes. For each sample, 20 µl aliquot was transferred to a well on a white 96-well-plate. Subsequently, 100 µl of Luciferase Assay Reagent II (substrate for firefly luciferase) was added, and luminescence measured for five seconds on a FLUOstar OPTIMA plate reader. That was followed by addition of 100 µl of Stop & Glo Reagent (quenching the previous reaction and providing a substrate for *Renilla* luciferase), and measurement of luminescence for five seconds. Lysates from untransfected cells were used to determine the background. Unless stated otherwise, the presented results are ratio of firefly to *Renilla* luciferase activities.

2.4 Bioinformatics

2.4.1 MicroRNA target prediction

To find microRNAs that may regulate a gene of interest, or to identify potential targets of a particular microRNA, microRNA target prediction programs are commonly used. One of the most popular programs, PicTar [191], was used in this study to help to identify microRNAs potentially involved in tubulointerstitial fibrosis. The PicTar algorithm may be summarised as follows. Input to PicTar consists of multiple alignments of 3'UTRs from eight vertebrate genomes, and a set of mature microRNAs. PicTar starts the identification of the microRNA targets by searching the 3'UTRs for the perfect and imperfect complementarities to the microRNA 'seed' regions (defined here as seven nucleotides starting with the first or second nucleotide from the 5' end). Then, free energy of the putative microRNA:target site complexes is calculated. Highly probable sites that survive the optimal free energy filter and are conserved between species are then scored. The model accounts for synergistic effect of multiple binding sites of one microRNA, or several microRNAs acting together. Additionally, it takes into consideration microRNA and target gene expression profiles. The estimated false positive rate for PicTar is approximately 30%.

2.4.2 Identification of human microRNAs similar to miR-LAT

For identification of human microRNAs similar to the viral microRNA miR-LAT, which could similarly bind to the GC-rich region of TGF-beta 3'UTR, a few on-line tools were employed.

To begin with, the miRBase Sequence Database release 9.1 [106] was searched for mature microRNAs of similar sequence to miR-LAT, using SSEARCH, an implementation of the Smith-Waterman algorithm [192]. SSEARCH does a rigorous search for similarity between a query sequence and a group of sequences of the same type. Compared to BLAST, it is much slower. However, it may be the most sensitive method available for similarity searches. It is recommended for finding a short sequence within a library, in this case the miRBase Sequence Database.

The chance that the identified microRNAs interact with TGF-beta 3'UTR was assessed using RNA22 [193], a microRNA target prediction program. RNA22 uses a different approach to microRNA target discovery than PicTar. This is so called pattern-based approach. It first finds common motifs ("patterns") in a set of microRNAs (354, at the time of the original publication of the method). Then, it predicts possible microRNA binding sites in a given target sequence, and assigns candidate microRNAs to those sites.

To visualise the potential interactions of the identified microRNAs with 3'UTR of TGF-beta, RNAfold program from Vienna RNA Secondary Structure Package [194] was used. The program reads an input RNA sequence, calculates its minimum free energy structure, and produces a graph of this structure. As it can

process only one RNA molecule at a time, microRNA and its binding site within TGF-beta 3'UTR were linked with the linker sequence GCGGGGACGC, used similarly in RNA22 program [193].

2.4.3 Other applications.

Construction/modification of plasmids (see 2.1.1.5) was facilitated by the on-line tools available at New England BioLabs website (http://www.neb.com). Particularly useful was the NEBcutter, which finds restriction sites in a given sequence. Additionally, NEB Enzyme Finder made possible quick searches of the restriction enzyme database for a particular recognition sequence, an overhang produced after cleavage, or simply enzyme name to find its recognition sequence and recommended digestion conditions.

To identify a suitable endogenous control for microRNA expression studies in renal biopsy samples, or mRNA analysis of HK-2 cell response to TGF-beta, geNorm VBA applet for Microsoft Excel [195] was used. geNorm determines the most stable reference genes from a set of tested genes in a given set of samples. It calculates the gene expression stability measure M for a reference gene as the average pairwise variation V for that gene with all other tested reference genes. Stepwise exclusion of the gene with the highest M value allows ranking of the tested genes according to their expression stability. The underlying principles and calculations are described in Vandesompele et al. [195].

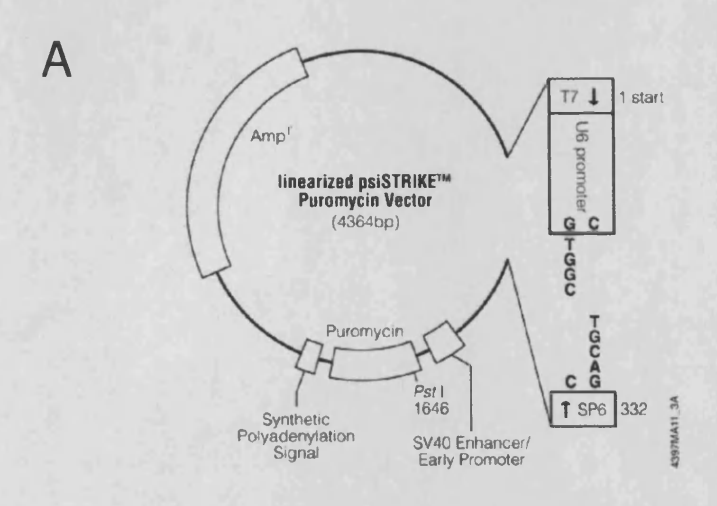
The use of Primer3, NCBI database, the miRBase Sequence Database, BLAST, Primer Express, and MFOLD for primer design was described above (see 2.2.2.2 for primers for mRNA detection, or 2.2.3.2 for stem-loop microRNA qRT-PCR assays).

2.5 Statistical analysis

The statistical analysis of data from the microRNA profiling experiment using mirVana miRNA Bioarrays (see 2.2.3.1) was carried out by Asuragen, as part of the microRNA Standard Service Premium. To check if there were any differentially expressed microRNAs between control HK-2 cells and cells cultured in high-glucose medium, t-test was performed for every microRNA. A multiplicity correction was conducted to control false discovery rate at 5% using a step-up approach, as described by Benjamini and Hochberg [196].

Pearson Correlation Coefficients were calculated for fibrosis score or eGFR and miR-192 in kidney biopsies from patients with diabetic nephropathy using SPSS version 14.0 software.

Statistical evaluation was otherwise by t-test, using Microsoft Excel, with p < 0.05 assumed to be significant.



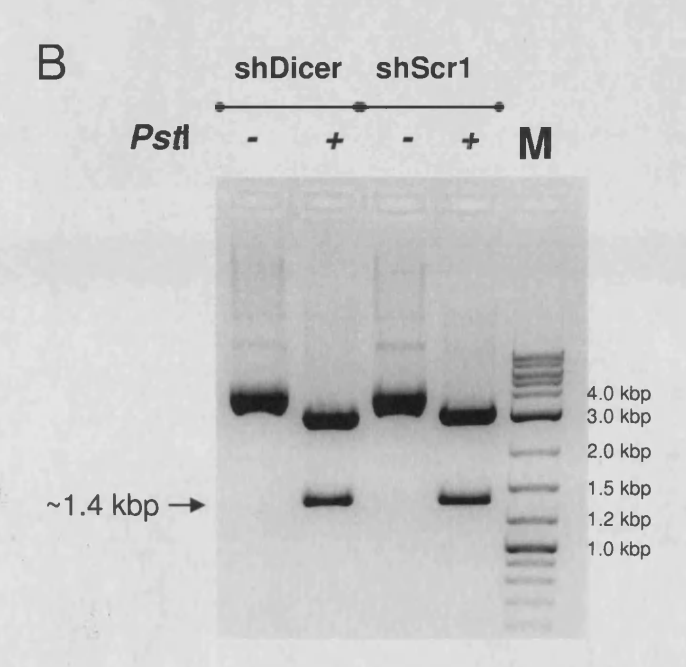
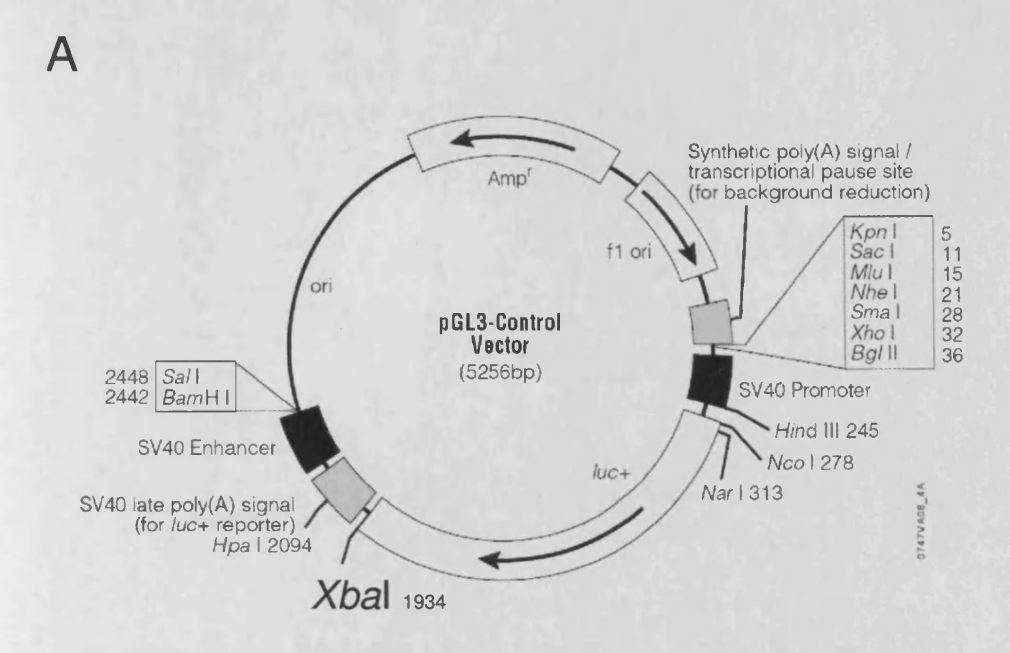


Figure 2.1. The siSTRIKE U6 vector (Promega). (A) Plasmid map. (B) Typical result of the diagnostic digestion with PstI. A second PstI restriction site is created in the plasmid as a result of a successful ligation. Two products (\sim 3 kbp and \sim 1.4 kbp) of the digestion with PstI indicate that the plasmid contains the insert.



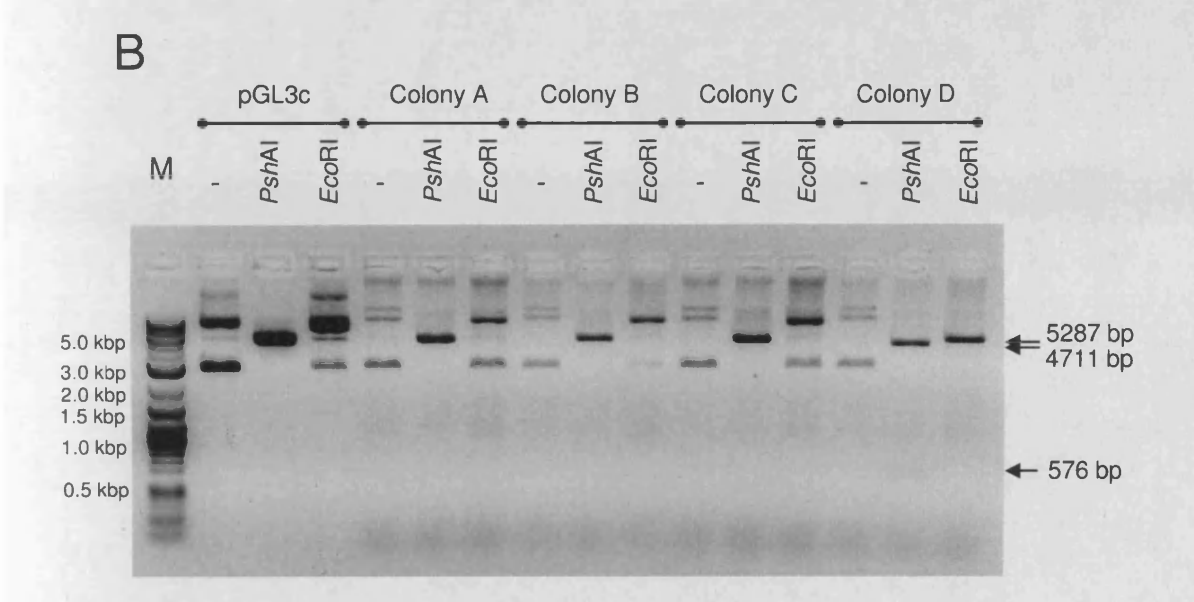
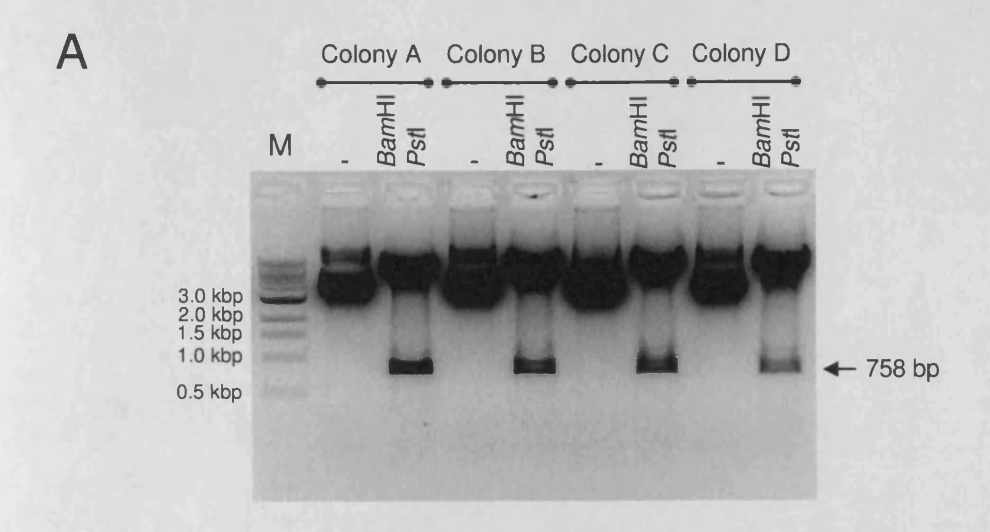


Figure 2.2. The pGL3-Control vector (Promega). (A) Plasmid map. (B) Identification of the properly modified plasmid containing sequential XbaI/EcoRI restriction sites instead of XbaI site downstream the luciferase CDS. Unlike the unmodified pGL3-Control, the desired plasmid would be cut once by EcoRI. Additionally, a second PshAI restriction site would appear in plasmids with XbaI preceding EcoRI (rather than the other way round, which was equally probable), giving two products: 576 bp and 4711 bp. Of the four tested colonies, only Colony D contained the expected plasmid.



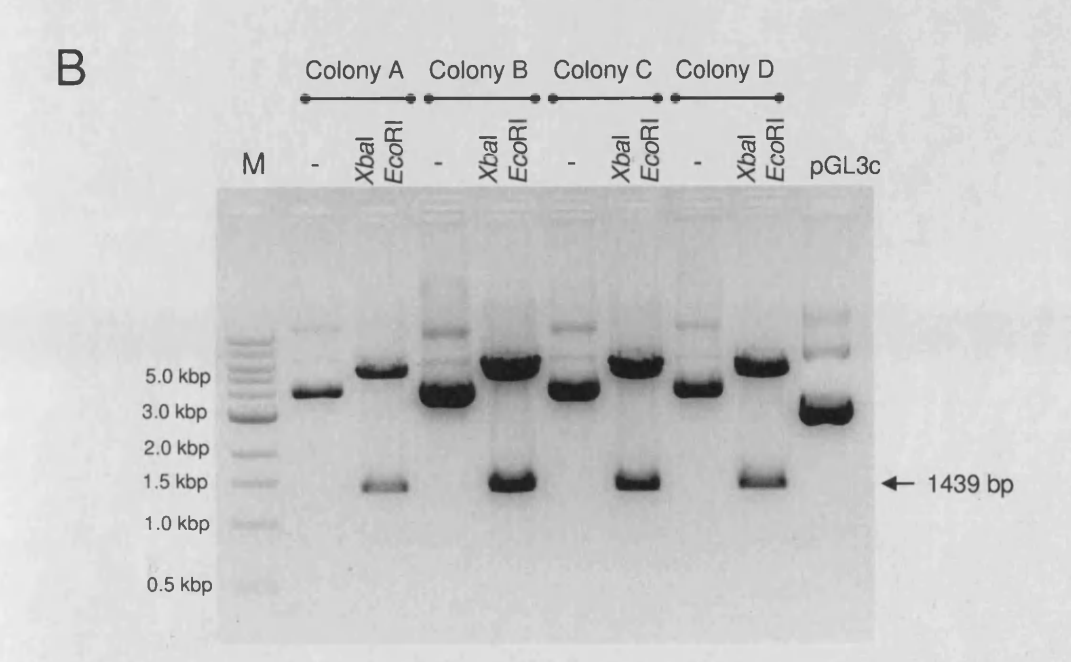


Figure 2.3. Construction of reporter plasmids with ZEB1 or ZEB2 3'UTRs downstream the luciferase CDS. ZEB1 and ZEB2 3'UTRs were PCR-amplified from genomic DNA and ligated into the pGL3-XbaI/EcoRI plasmid using XbaI and EcoRI sites. To confirm the ligation of the insert, the new plasmids were cut with BamHI and PstI for ZEB1 3'UTR (A), or XbaI and EcoRI for ZEB2 3'UTR (B). The later digestion released ~1.4 kbp ZEB2 3'UTR insert from the plasmids. Since ZEB1 3'UTR contains a XbaI site, the PCR product was digested with SpeI and the ligation destroyed the XbaI site. Therefore, PstI site from the ZEB1 3'UTR together with BamHI site on the plasmid (758 bp apart after successful ligation) were used. All tested plasmids were as desired.

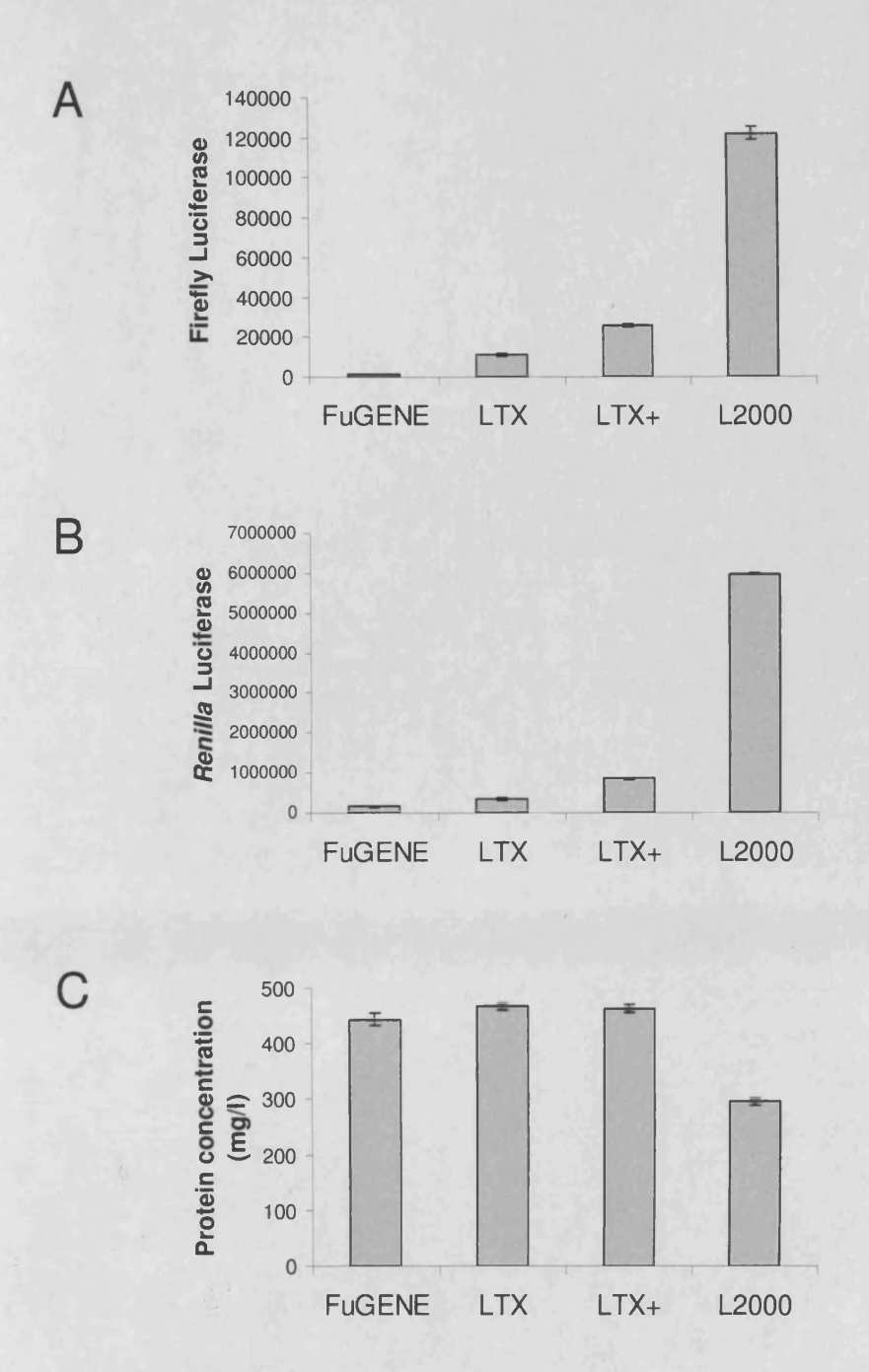
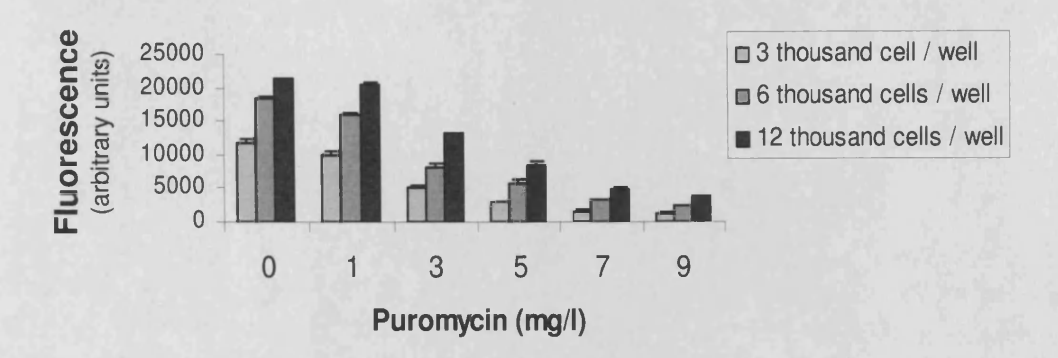


Figure 2.4. Selection of an optimal transfection method for plasmid DNA delivery to HK-2 cells. HK-2 cells were transfected with a mix of two reporter plasmids (one containing four SBEs in the promoter of the firefly luciferase gene, and one for high constitutive expression of *Renilla* luciferase) at 3:1 ratio. Following 48 hour incubation, Dual Luciferase Assay was used to measure firefly (A)and *Renilla* (B) luciferase activities. Additionally, as an indirect measure of cell viability after transfection, total protein concentration in lysates was estimated with Bradford assay (C). The experiment was performed in triplicate; SEM is shown.





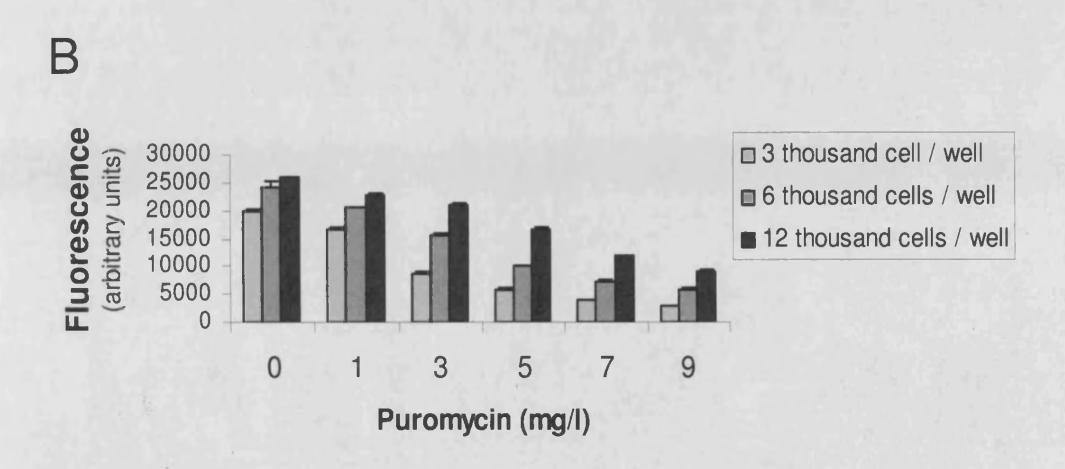


Figure 2.5. HK-2 cell resistance to puromycin. HK-2 cells were plated at three different densities on 96-well-plates. Various concentrations of puromycin were added to medium immediately after plating the cells (A), or 24 hours later (B). To assess the effect of puromycin on the cell viability, AlamarBlue test was performed 72 hours later. The experiment was performed in triplicate; SEM is shown.

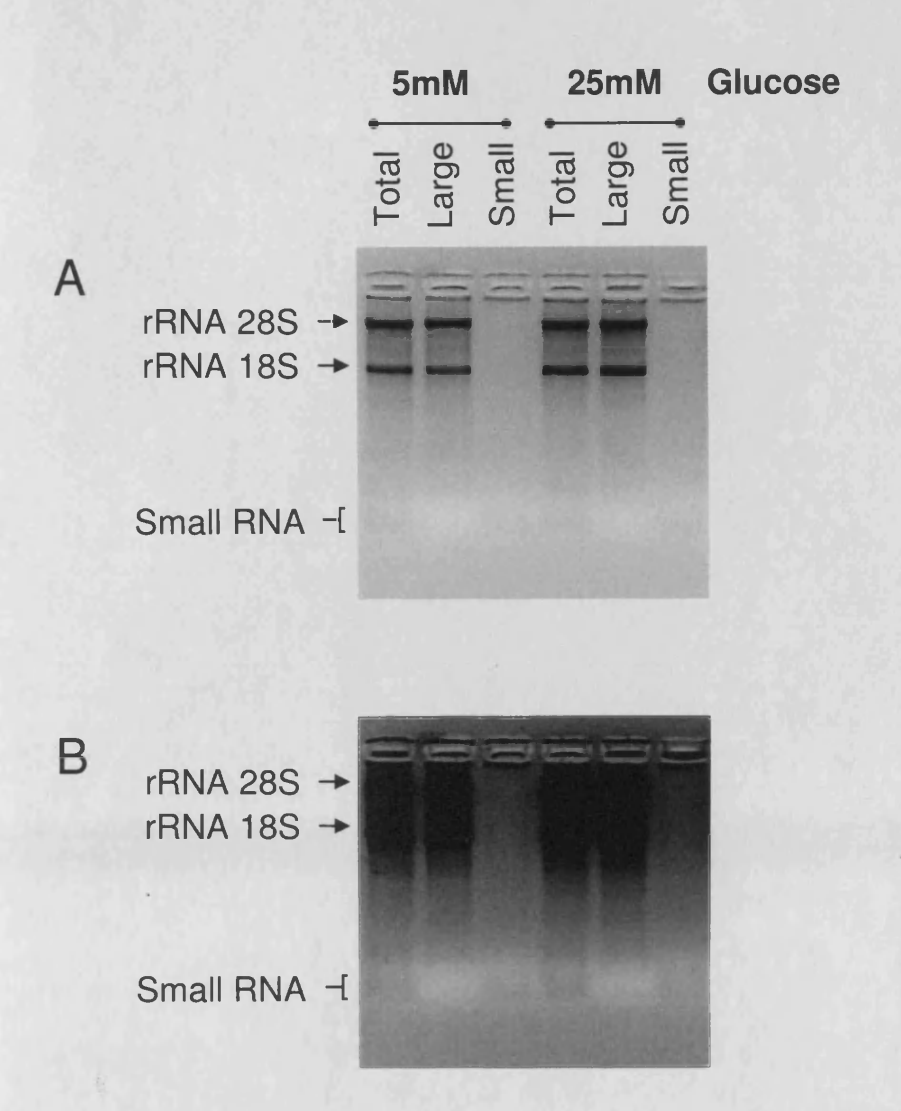
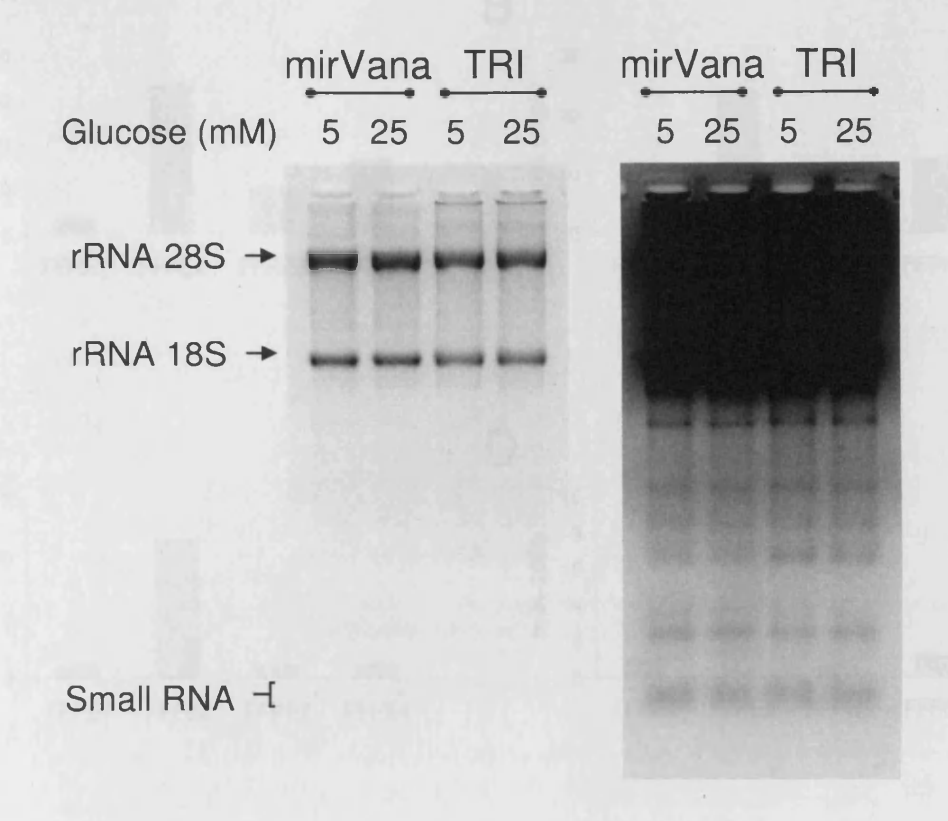


Figure 2.6. RNA extraction using mirVana miRNA Isolation Kit (Ambion). Total, large (> 200 nt), and small (< 200 nt) RNA fractions were isolated from HK-2 cells (control or treated with high concentration of glucose for 48 hours), as described in the text. The RNA fractions were separated on a 3% (w/v) agarose gel containing ethidium bromide, and visualised in UV light. The same gel photographed with low (A) or high (B) light intensity is shown. The two rRNA species: 28S and 18S, and the small RNA fraction (quickly migrating RNA, not detected in the large RNA preparations) are indicated.

A



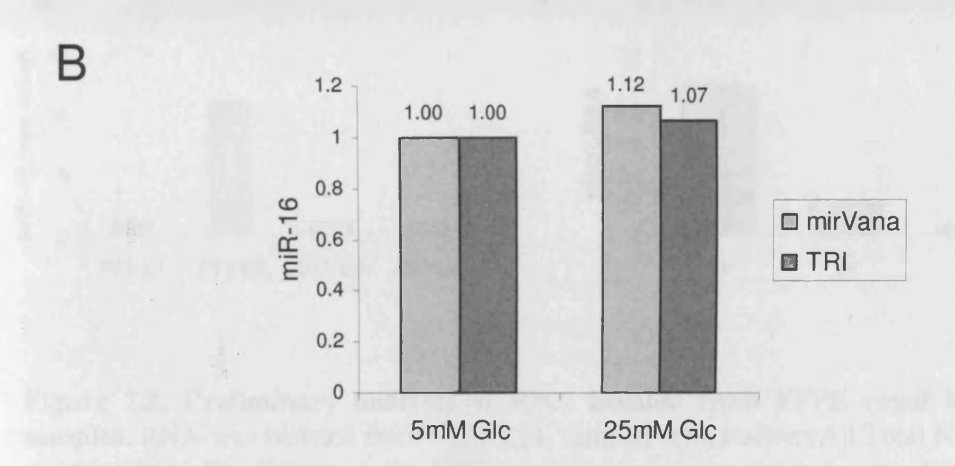


Figure 2.7. Comparison of two RNA isolation methods. Total RNA was isolated from HK-2 cells (control or treated with high concentration of glucose for 48 hours) using mirVana miRNA Isolation Kit (Ambion) or TRI Reagent (Sigma). The extracted RNA was separated on an agarose gel and photographed with low or high light intensity (A). Additionally, both RNA preparations were used for miR-16 quantification by stem-loop qRT-PCR (B).

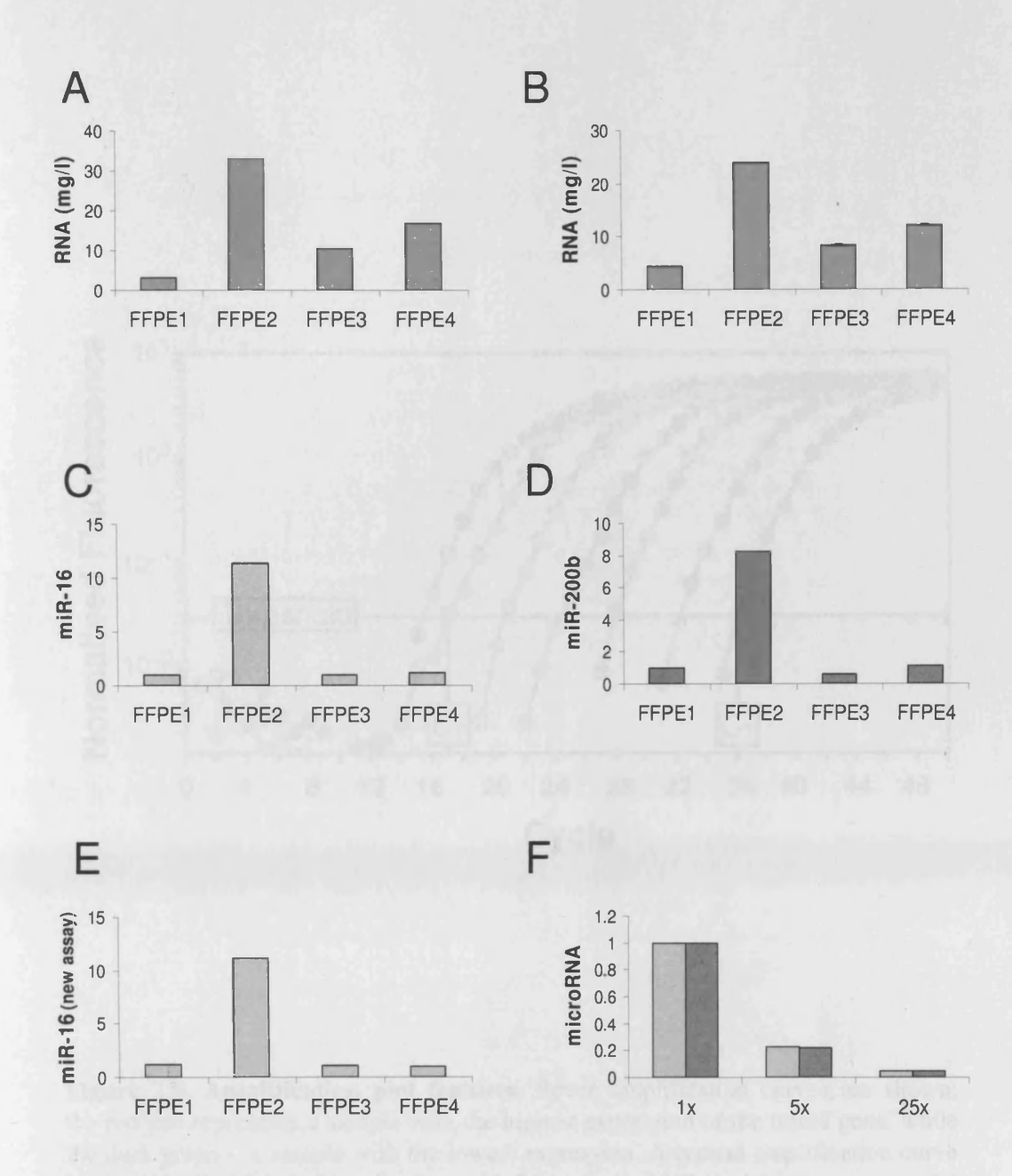


Figure 2.8. Preliminary analysis of RNA isolated from FFPE renal biopsy samples. RNA was isolated from four FFPE samples with RecoverAll Total Nucleic Acid Isolation Kit. Subsequently, RNA concentration was estimated using Agilent's 2100 bioanalyser with PicoChip (A) or Invitrogen Quant-iT RNA Assay (B). Additionally, miR-16 (C) and miR-200b (D) expression in those samples was measured with TaqMan stem-loop qRT-PCR. The performance of a new SYBR Green-based assay for detection of miR-16 was tested in those samples (E). Finally, miR-16 (lighter bars) and miR-200b (darker bars) were measured after 5 or 25-fold dilution of cDNA to demonstrate that the detection is quantitative and there were no PCR inhibitors present in the samples.

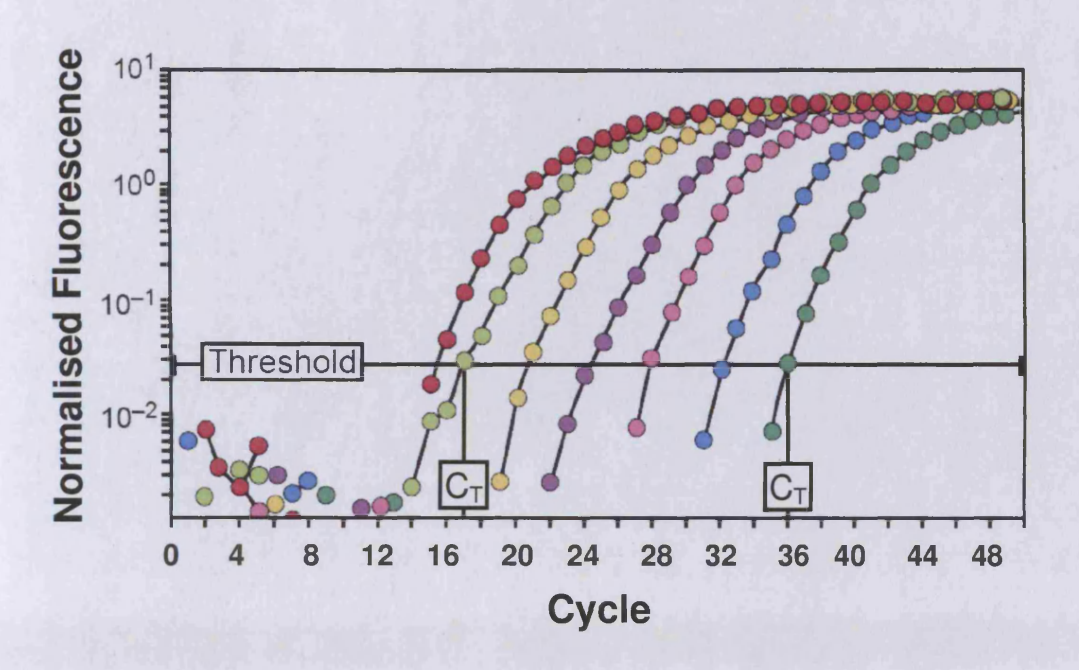


Figure 2.9. Amplification plot features. Seven amplification curves are shown; the red one represents a sample with the highest expression of the tested gene, while the dark green – a sample with the lowest expression. A typical amplification curve starts with the phase of low/background fluorescence, followed by the exponential phase (please note that the scale on the Y axis is logarithmic), the linear phase, and finally the plateau. The threshold is the point at which a reaction reaches a fluorescent intensity above background. For the most accurate reading, it is set at the exponential phase of the amplification. The PCR cycle at which the sample reaches the threshold is known as the threshold cycle (C_T). For example, C_T of the sample represented by the light green amplification curve is approximately 17, and C_T of the sample with the lowest expression of the gene of interest (dark green) is close to 36. As explained in the text, the fold-difference in the gene expression between these two samples equals $2^{(36-17)}$ =524288. The amplification plot comes from the work by N. Walker [197].

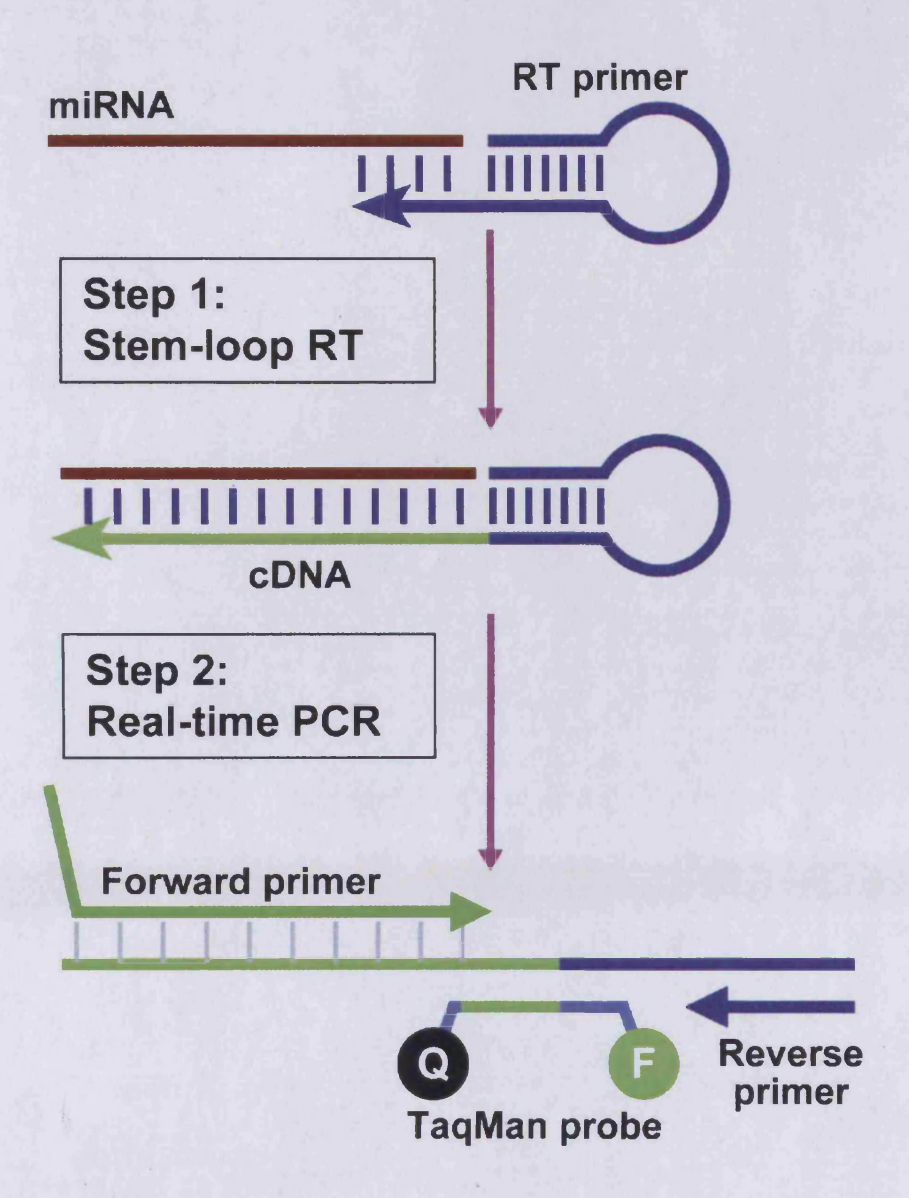
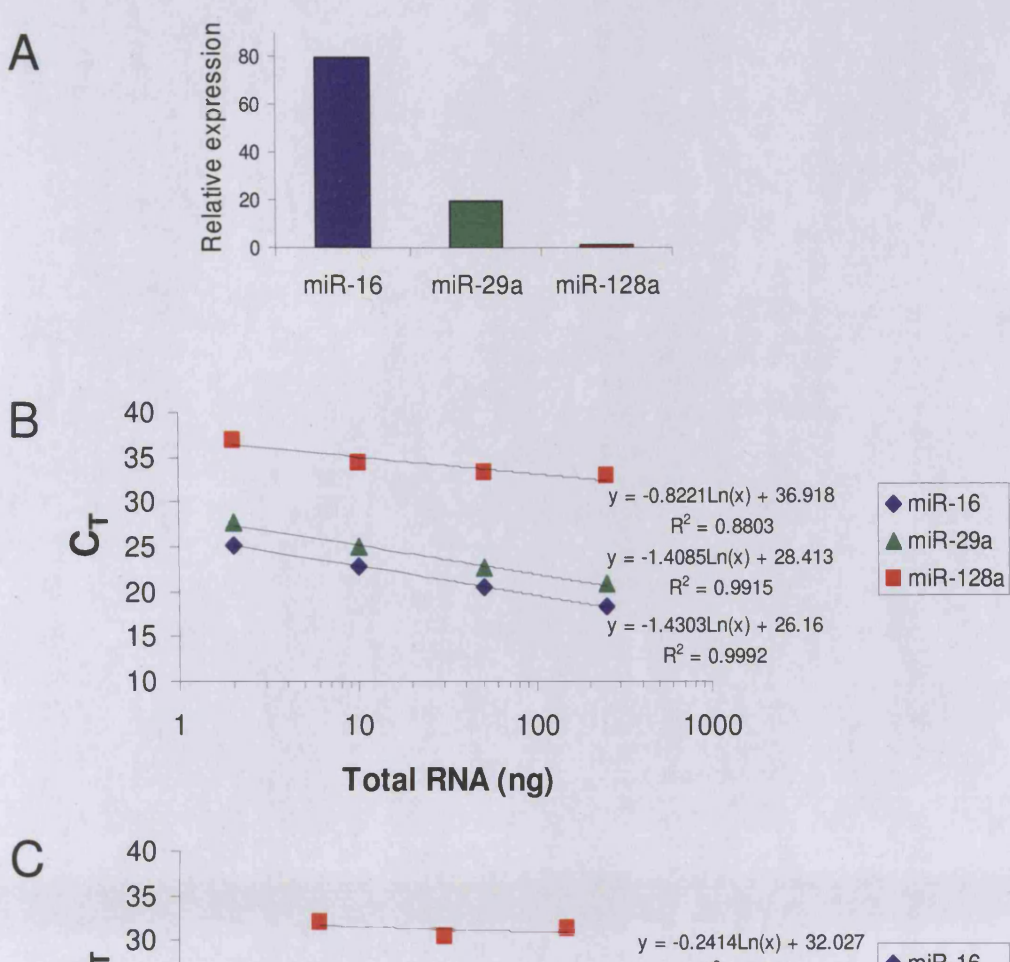


Figure 2.10. Schematic overview of the stem-loop qRT-PCR microRNA detection system. Quantification of microRNAs with this method consists of two steps. The first includes an RT reaction with a long RT-primer, forming a stem-loop structure, containing at the 3' end a few nucleotides complementary to the 3' end of a particular microRNA. The second step is a quantitative PCR with a forward primer specific to the microRNA, and a reverse primer of the same sequence as a fragment of the long RT-primer. In TaqMan MicroRNA Assays (Applied Biosystems), a source of fluorescence is a TaqMan probe, binding to the region between the two PCR primers. The scheme was taken from the article originally describing this method [187].



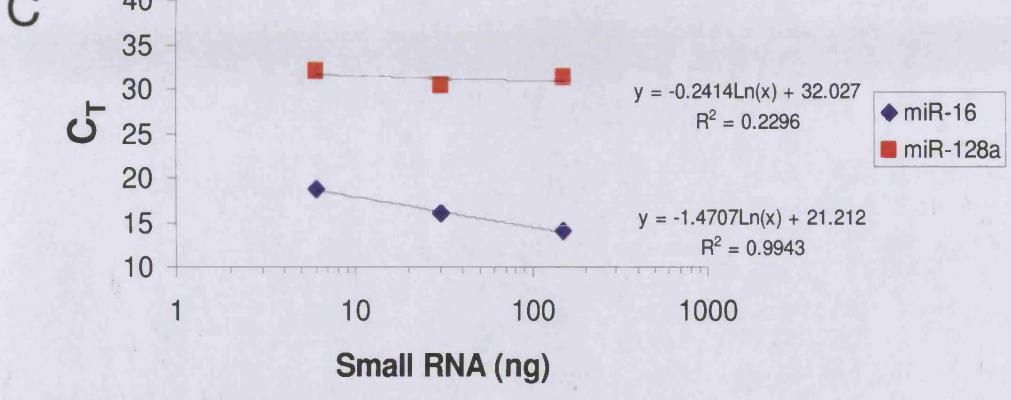


Figure 2.11. Evaluation of the performance of TaqMan MicroRNA Assays (**Applied Biosystems**). Three microRNAs were selected for analysis based on their expression in HK-2 cells according to the microarray results (A). The reactions were performed on 2, 10, 50, or 250 ng of total RNA isolated from HK-2 cells (B). The efficiencies were as follows: 101% for miR-16, 103% for miR-29a, and 237% for the least abundant of the three, miR-128a. The assay was then used with 6, 30, or 150 ng of small RNA (C). The calculated efficiency of miR-128a detection was 6196%, while miR-16, used here as a positive control, was amplified with the efficiency 97%.

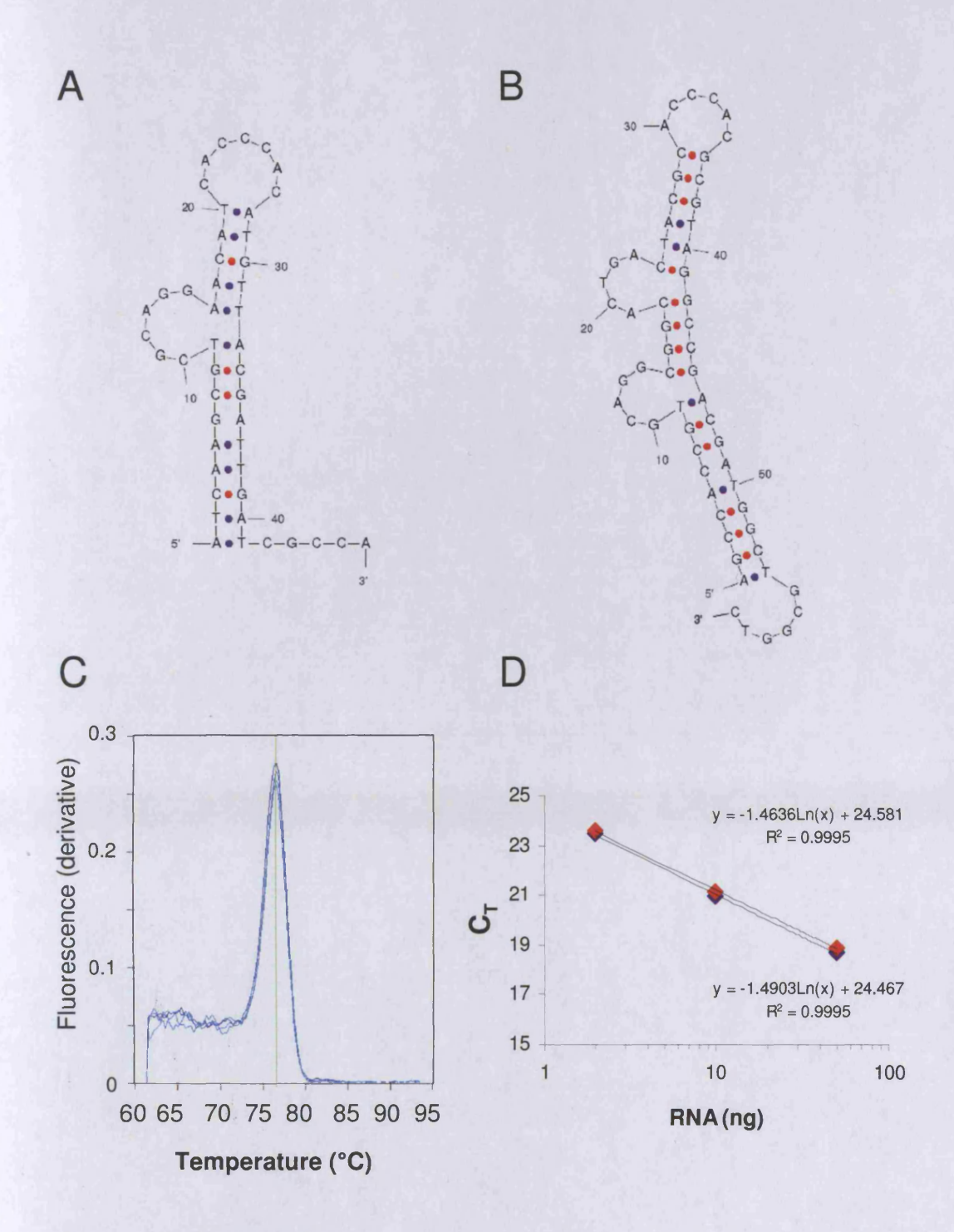


Figure 2.12. Design and validation of SYBR Green-based stem-loop qRT-PCR for microRNA detection. Predicted secondary structures of RT-primers for miR-16 (A) and miR-663 (B) detection are shown. (C) Melting curve analysis following miR-16 quantification with the new assay, demonstrating that only a single product is amplified. (D) Comparison of performance of the new miR-16 assay (red diamonds) with the TaqMan MicroRNA Assay (blue diamonds).

Name	Sequence (5' -> 3')	Comments					
siRNA							
CD44	CGTGGAGAAAAATGGTCGC	ID: n/a					
Dicer1	TGCTTGAAGCAGCTCTGGA	[198]					
Dicer2	CCATATGAGCGACAGCAGT	ID: 137010					
Dicer3	GCAAATCTTTCATCTCAAT	ID: 137012					
SMAD3	n/a	ID: 115717					
TRBP	TCTACGAAATTCAGTAGGA	[199]					
Scrambled1	GCGTATCGTAAGCAGTACT	Negative Control #1					
Synthet	Synthetic microRNAs (Pre-miR miRNA Precursors)						
miR-608	miR-608 AGGGGTGGTGTTGGGACAGCTCCGT						
miR-663	AGGCGGGGCGCGCGGGACCGC						
miR-LAT	GTGGCGGCCCGGGGCC						
MicroRNA inhibitors (Anti-miR miRNA Inhibitors)							
miR-192	GGCTGTCAATTCATAGGTCAG						
miR-200b	TCATCATTACCAGGCAGTATTA						
Negative Control	n/a	Negative Control #1					

Table 2.1. Small RNA used in this study. All molecules were ordered from Ambion. For double-stranded RNA, only sequence of the sense strand is given.

Plasmid	Inserts or PCR-primers (5' -> 3')				
psiSTRIKE U6-Puromycin (Promega)					
shDicer (short-hairpin RNA silencing Dicer based on Dicer3 siRNA)	A:ACCGCAAATCTTTCATCTCAATAAGTTCTCTATTGAGATG AAAGATTTGCTTTTTC B:TGCAGAAAAAAGCAAATCTTTCATCTCAATAGAGAACTTAT TGAGATGAAAAAGATTTG				
shGW182 (short-hairpin RNA silencing GW182 based on siRNA from [200])	A:ACCGAAATGCTCTGGTCCGCTAAAGTTCTCTTAGCGGAC CAGAGCATTTCTTTTC B:TGCAGAAAAAGAAATGCTCTGGTCCGCTAAGAGAACTTTA GCGGACCAGAGCATTT				
pre-miR-192 (miR-192 stem-loop precursor)	A:ACCGTGCACAGGGCTCTGACCTATGAATTGACAGCCAGT GCTCTCGTCTCCCCTCTGGCTGCCAATTCCATAGGTCACAG GTATGTTCGCCTTTTTC B:TGCAGAAAAAGGCGAACATACCTGTGACCTATGGAATTG GCAGCCAGAGGGGAGACGAGAGCACTGGCTGTCAATTCAT AGGTCAGAGCCCTGTGCA				
pre-miR-200b (miR-200b stem-loop precursor)	A:ACCGCTCGGGCAGCCGTGGCCATCTTACTGGGCAGCAT TGGATGGAGTCAGGTCTCTAATACTGCCTGGTAATGATGAC GGCGGAGCCCTGCACTTTTTC B:TGCAGAAAAAGTGCAGGGCTCCGCCGTCATCATTACCAG GCAGTATTAGAGACCTGACTCCATCCAATGCTGCCCAGTAA GATGGCCACGGCTGCCCGAG				
shScrambled1 (negative control based on Scrambled1 siRNA)	A:ACCGCGTATCGTAAGCAGTACTAAGTTCTCTAGTACTGCT TACGATACGCTTTTTC B:TGCAGAAAAAGCGTATCGTAAGCAGTACTAGAGAACTTA GTACTGCTTACGATACG				
shScrambled2 (negative control based on the reversed miR-16 sequence)	A:ACCGATCGTCGTGCATTTATAACCGCAAGTTCTCTGCGG TTATAAATGCACGACGATCTTTTTC B:TGCAGAAAAAGATCGTCGTGCATTTATAACCGCAGAGAA CTTGCGGTTATAAATGCACGACGAT				
shScrambled3 (negative control based on miR-192 scrambled by siRNA Wizard v2.6, InvivoGen)	A:ACCGCCAATCTCGTAGCCTATAGAAAGTTCTCTTCTATAG GCTACGAGATTGGCTTTTTC B:TGCAGAAAAAGCCAATCTCGTAGCCTATAGAAGAGAACTT TCTATAGGCTACGAGATTGG				
pGL3-Control (Promega)					
pGL3-Control-Xbal/EcoRl	A:CTAGAACTGGAGAGTACGTGAATTCTATTGA B:CTAGTCAATAGAATTCACGTACTCTCCAGTT				
3'UTR ZEB1 (~1.7 knt 3'UTR of ZEB1 PCR- amplified from HK-2 genomic DNA)	F:CATCGAACTAGTCAAAATAAATCCGGGTGTGCCT R:GTCCTAGAATTCACAGCAGTTCAGGCTTGTTGA				
3'UTR ZEB2 (~1.4 knt 3'UTR of ZEB2 PCR- amplified from HK-2 genomic DNA)	F:CATCGATCTAGATAAACTACTGCATTTTAAGCTTCCTATT R:GTCCTAGAATTCAGTTTGGCTACATTTTTATTCGAG				

Table 2.2. Plasmids generated for this study and sequences of the oligonucleotides used in cloning. The bold letters A and B indicate inserts, while F and R precede sequences of PCR-primers.

Sample no	Biopsy	Group *	Age	Sex	Date of biopsy	eGFR ml/min	∆ eGFR ml/min/yr	Fibrosis score
1	H2016.92	NP	66	М	1992	70	4.38	1.29
2	H529.92	NP	39	М	1992	48	4.55	-
3	H098.92	Р	42	F	1992	56	5.7	1.29
4	H2636.92	LP	73	М	1992	5	n/a	1.29
5	H2627.92	NP	56	М	1992	59	0.58	0.86
6	H503.93	Р	69	М	1993	14	9	2.14
7	H368.93	LP	75	М	1993	7	n/a	2.57
8	H264.94	NP	76	F	1994	17	1.02	1.14
9	H005.94	Р	27	F	1994	12	7	1
10	H1232.93	LP	60	F	1993	6	n/a	2.86
11	H278.94	NP	72	F	1994	13	4.01	-
12	H488.94	P	55	F	1994	12	7.1	1.86
13	H342.94	LP	40	М	1994	. 7	n/a	1.86
14	H267.95	NP	49	М	1995	57	0.3	0.29
15	H173.95	Р	74	М	1995	20	10.1	-
16	H260.95	LP	35	F	1995	5	n/a	1.71
17	H068.96	NP	52	М	1996	59	4.75	1
18	H213.96	P	59	F	1996	15	10.3	2.71
19	H062.97	NP	62	М	1997	49	2.37	0
20	H314.96	P	52	М	1996	92	11	1.14
21	H065.97	NP	58	М	1997	43	2.6	0.29
22	H053.98	NP	51	М	1998	36	0.71	0.71
23	H045.97	P	55	М	1997	93	9.53	0
24	H277.96	LP	50	М	1996	8	n/a	2
25	H102.98	NP	40	F	1998	67	1.1	0.43
26	H081.97	P	62	М	1997	46	9.24	1.143
27	H073.97	LP	53	М	1997	6	n/a	1.86

(Continued on the next page)

(Continued)

Sample no	Biopsy	Group*	Age	Sex	Date of biopsy	eGFR ml/min	∆ eGFR ml/min/yr	Fibrosis score
28	H123.98	NP	52	М	1998	32	0.5	0.6
29	H145.97	P	58	М	1997	61	6.2	0.57
30	H354.97	LP	45	М	1997	9	n/a	2.29
31	H184.99	NP	25	М	1999	45	3.8	0.71
32	H064.98	Р	48	М	1998	27	16	-
33	H069.99	LP	77	М	1999	10	n/a	1.71
34	H196.99	NP	60	М	1999	25	1.8	1
35	H183.99	P	44	М	1999	24	7	1.57
36	H191.00	NP	59	М	2000	31	0.9	1.29
37	H248.99	P	57	М	1999	30	7	1
38	H202.00	NP	47	М	2000	60	0.75	0.43
39	H130.00	P	29	М	2000	28	14.1	1.29
40	H196.00	P	77	F	2000	17	10	1.43

^{*} NP - non-progressors, P - progressors, LP- late presenters

Table 2.3. Patient characteristics. Samples used in the microRNA profiling experiment are in italics. eGFR – estimated glomerular filtration rate.

Gene	Assay ID/ Primer Sequences (5' -> 3')	Comments
l. TaqMan	assays	
	mRNA detection	
CD44	ID: Hs00174139_m1	
E-cadherin	ID: Hs00170423_m1	
RPLP0	PN: 4326314E	
	microRNA and small RNA detection	
let-7a	ID: 000377	
miR-16	ID: 000391	
miR-26a	ID: 000405	
miR-29a	ID: 002112	
miR-106b	ID: 000442	
miR-128a	ID: 002216	
miR-192	ID: 000491	
miR-200b	ID: 002251	
miR-608	ID: 001571	
snRNA U6	ID: 001093	
		<u> </u>
II. SYBR (Green assays	
	mRNA detection	
ACTB	F:GACCCAGATCATGTTTGAGACCTT,R:CAGAGGCGTACAGGGATAGCA	
B2M	F:ATGAGTATGCCTGCCGTGTG,R:CATGTCTCGATCCCACTTAACTATCTT	
Dicer	F:TTGGGGAATACTCAAACCTAGAAG,R:GCGACATAGCAAGTCATAATGAGA	
E-cadherin	F:TCCCAATACATCTCCCTTCACA,R:ACCCACCTCTAAGGCCATCTTT	
GAPDH	F:CCTCTGACTTCAACAGCGACAC,R:TGTCATACCAGGAAATGAGCTTGA	
HPRT1	F:GCAGTATAATCCAAAGATGGTCAAG,R:TCAAGGGCATATCCTACAACAAAC	
PAI-1	F:TCTCTGCCCTCACCAACATTC,R:CGGTCATTCCCAGGTTCTCT	
SMAD3	F:ACCACGCAGAACGTCAACA,R:CGATGGGACACCTGCAAC	by D.D.Luo
TBP	F:CACAGTGAATCTTGGTTGTAAACTTG,R:GGTTCGTGGCTCTCTTATCCTC	
TFRC	F:GGCACAGCTCTCCTATTGAAAC,R:CACTCCAACTGGCAAAGATAATG	
TGF-beta	F:CCTTTCCTGCTTCTCATGGC,R:ACTTCCAGCCGAGGTCCTTG	by D.Fraser
TRBP	F:GGCCCTCAAACACCTCAAAG,R:GGAATGTCCTCAGGCAGTGAA	
Vimentin	F:GGAGAAATTGCAGGAGGAGATG,R:AAGGTCAAGACGTGCCAGAGA	
ZEB1	F:CAGGCAGATGAAGCAGGATGT,R:TGACAGCAGTGTCTTGTTGTAG	
ZEB2	F:CCTTCTGCGACATAAATACGAACA,R:AGTACGAGCCCGAGTGTGAGA	
	microRNA and small RNA detection	
miR-16	RT:ATCAAGCGTCGCAGGAACATCACCCACATGTTACGATTGATCGCCA F:TAGCAGCACGTAAATATTGG,R:AGCGTCGCAGGAACATCA	
miR-21	RT:ATCAAGCGTCGCAGGAACATCACCCACATGTTACGATTGATT	
	F:TAGCTTATCAGACTGATGTTG,R:CGTCGCAGGAACATCACC RT:ATCAAGCGTCGCAGGAACATCACCCACATGTTACGATTGATT	
miR-29a 	F:TAGCACCATCTGAAATCGG,R:CGTCGCAGGAACATCACC	
miR-34a	RT:ATCAAGCGTCGCAGGAACATCACCCACATGTTACGATTGATACAACC F:TGGCAGTGTCTTAGCTGG,R:CGTCGCAGGAACATCACC	
miR-663	RT:AGCCACCGTGCAGGCGGCACTGACTACGCACCCACGCGTAGGCCGACGATGGCTGCGGTC	
	F:AGGCGGGGCGCCGCGGA,R:CCACCGTGCAGGCGCACTGACTACGCACC	

Table 2.4. Quantitative PCR assays used in this study. TaqMan assays were purchased from Applied Biosystems. All SYBR Green assays were designed as described in Methods, unless stated otherwise.

Antibody	Supplier (ID)	Dilution				
Immunofluorescence						
1 ° Mouse monoclonal (HECD-1) to E-cadherin	abcam (ab1416)	1:50				
2° Alexa Fluor 555 goat anti- mouse IgG	Molecular Probes / Invitrogen (A-21424)	1:1000				
Western blot						
1 ° Mouse monoclonal (13D6) to Dicer	abcam (ab14601)	1:100				
2° HRP goat anti-mouse IgG	Santa Cruz Biotech. (sc-2005)	1:1000				
1° Rabbit polyclonal·(H-108) to E-cadherin	Santa Cruz Biotech. (sc-7870)	1:1000				
1° Rabbit polyclonal to GAPDH	abcam (ab9485)	1:1000				
2° HRP goat anti-rabbit IgG	abcam (ab6721)	1:10000				

Table 2.5. Antibodies used for immunofluorescence and Western blot. The source of antibodies and optimal dilutions are shown.

CHAPTER THREE:

CHANGES IN MICRORNA EXPRESSION IN RESPONSE TO PROFIBROTIC STIMULI IN VITRO AND IN VIVO

3.1 Introduction

Several lines of evidence suggest that microRNAs compete with each other for the components of the miRISC complex. Moreover, it has been reported that microRNA turnover rates depend on availability of their target mRNAs [202]. Thus, a microRNA abundance in a cell or tissue very likely reflects its actual activity there. It is no surprise then that the most common strategy to identify microRNAs important in a particular process relies on evaluation of microRNA expression. Before the start of my project, there had been approximately 400 known human microRNAs and very limited data available regarding their expression in the kidney or in fibrotic processes (for more details see 1.5).

Previous extensive characterisation of proximal tubular epithelial cell responses to high concentration of glucose and other stimuli potentially related to diabetic nephropathy had taken place in this and other laboratories, as laid out in the introduction. Other investigators had shown extensive mRNA changes in proximal tubular epithelial cells in response to elevated glucose [203]. Before I started this project, the laboratory had collaborated with Ambion in a beta test of a novel array for microRNA profiling. It was decided to study effects of glucose on microRNA expression in the immortalised human proximal tubular epithelial cell line, HK-2.

Preliminary experiments done before the start of my project

To characterise expression of 212 human microRNAs in HK-2 cells, and evaluate changes in response to glucose, an analysis with a new microRNA microarray (mirVana miRNA Bioarray V1, Ambion) was performed by Asuragen, Inc. (Figure 3.1). The results demonstrated expression of approximately 50% (105) of the tested human microRNAs in HK-2 cells. Furthermore, high concentration of glucose induced profound changes in microRNA expression. In particular, 31 microRNAs were significantly, and more than 2-fold changed (all downregulated) in HK-2 cells cultured for 48 hours in medium containing high concentration of glucose.

The aim of this chapter was to determine the significance of those data, as well as to further characterise changes in microRNA expression in response to profibrotic stimuli *in vitro* and *in vivo*.

3.2 Results

3.2.1 MicroRNA expression in proximal tubular epithelial cells

MicroRNA expression in response to high concentration of glucose

In order to validate the preliminary results, five microRNAs (miR-16, miR-26a, miR-29a, miR-106b, and miR-128a) were selected. The choice was based both on their expression, according to the microarray data, and target predictions by PicTar. Their relative abundance, change in expression after 48 hour culture in medium with high concentration of glucose, and potential targets implicated in renal fibrosis are listed in Table 3.1.

For quantitative detection of the selected microRNAs in HK-2 cells, stem-loop qRT-PCR system was chosen and its accuracy verified, as described in Methods (see 2.2.3.2). Detection of the least abundant of the chosen microRNAs, miR-128a, using that assay was not quantitative. Therefore, the results presented below demonstrate expression only of the other four microRNAs.

Expression of miR-16, miR-26a, miR-29a, and miR-106b was examined in HK-2 cells exposed to 25 or 5 mM glucose for indicated time points (Figure 3.2A). Instead of expected 86-89% decrease, no statistically significant differences in microRNA expression between high-glucose treated and control cells were found.

Additionally, in separate experiments, cells were growth-arrested for 72 instead of 48 hours, cultured in medium without insulin, in different culture dishes or in different volume of medium, exposed to 35 mM glucose, or to 25 mM glucose from three independent sources, in all cases giving similar results (Figure 3.2B-G).

Having noticed the discrepancy between the preliminary data (7-9 fold change in response to glucose) and the qRT-PCR results (no difference between the two experimental groups), it was important to establish whether the cells responded to 25 mM glucose in a previously characterised way. Therefore, TGF-beta secretion to medium by HK-2 cells exposed to 25 or 5 mM glucose for four to seven days was measured by ELISA (Figure 3.3). The cells cultured in high-glucose medium secreted significantly more TGF-beta than control cells, reproducing published data [55].

Review of the data from the first microRNA microarrays with Asuragen, Inc. led them to suggest a potential technical error with the arrays, and to agree to repeat the microRNA profiling on new samples (three control and three from HK-2 cells treated with 25 mM glucose for 48 hours), using a new version (V2) of Ambion mirVana miRNA Bioarray.

The results showed no significant difference in expression of any of 328 tested human microRNAs in response to glucose (Figure 3.4), consistent with the qRT-PCR results. Nevertheless, the microarrays provided a list of 103 microRNAs expressed by HK-2 cells, which was used in later experiments. A complete listing of expression data is available online as a supplementary material for my paper [204].

MicroRNA expression in response to TGF-beta

The above data suggested that glucose alone did not alter microRNA expression in HK-2 cells in short-term culture. Extensive data implicates TGF-beta as a key mediator of renal fibrosis, induced by glucose and many other stimuli, as laid out in Chapter One. To examine if TGF-beta can influence microRNA expression in HK-2 cells, the four previously selected microRNAs, miR-16, miR-26a, miR-29a, and miR-106b, were quantified by stem-loop qRT-PCR in TGF-beta-treated cells (Figure 3.5). Two of them, miR-26a and miR-29a, were substantially (~50%) and significantly downregulated by treatment with 10 ng/ml TGF-beta for four days. Encouraged by those results, I selected five additional microRNAs for analysis. These were: let-7a, miR-21, miR-34a, miR-192, and miR-200b. They were all detected in HK-2 cells in the microarray experiment, and had some interesting properties, as found in literature (Table 3.2). Their expression was measured by qRT-PCR in HK-2 cells following stimulation with 10 ng/ml TGF-beta for four days (Figure 3.6A). Three of them were significantly changed by TGF-beta. The biggest, over 60% difference was found in miR-192 expression, which decreased in stimulated cells, while expression of miR-200b was only ~30% lower than in control cells. The only microRNA significantly upregulated by TGF-beta was miR-21. No statistically significant change was found in let-7a and miR-34a expression.

To ensure that equal amounts of RNA were used in both experimental groups, total RNA concentration prior to the stem-loop RT step was measured with Qubit fluorometer. Additionally, the small nuclear RNA U6 was measured by stem-loop qRT-PCR (Figure 3.6B). In all the future experiments involving HK-2 cell stimulation

with TGF-beta, miR-16, found to be stable in those conditions, was used for microRNA normalisation.

To get more insight into the regulation of the two most promising microRNAs, miR-192 and miR-21, HK-2 cells were stimulated with 1 or 10 ng/ml TGF-beta or 25 mM glucose for 12, 24, 48, or 96 hours. Then RNA was isolated and miR-192 and miR-21 expression was measured using stem-loop qRT-PCR (Figure 3.7). Consistent with the repeated microarray data, there was no substantial difference in expression of the tested microRNAs in response to high concentration of glucose. On the other hand, TGF-beta caused profound changes in miR-192 and miR-21 expression, increasing gradually with time. The greatest down- or upregulation of miR-192 or miR-21, respectively, was observed at the longest time-point examined, when using the higher dose of TGF-beta.

3.2.2 MicroRNA expression in kidney biopsies from patients with diabetic nephropathy

In parallel to the investigation of TGF-beta-induced changes in microRNA expression in vitro, I had an extraordinary opportunity to look at microRNA expression in formalin-fixed, paraffin-embedded (FFPE) renal biopsy samples from patients with diabetic nephropathy.

This opportunity arose because of the recent work of an MD student in the laboratory (Dr Aled Lewis) who had recruited 40 patients who had previously undergone a renal biopsy and had a diagnosis of diabetic nephropathy, and had performed a detailed histopathologic study of the archived biopsy material. The data is reported

in Lewis et al. [181]. The patients had been divided by Dr Lewis into three groups, depending on the rate of loss of renal function (as established by calculation of eGFR; see 1.2.2) in follow up. These were non-progressors (loss of eGFR < 5 ml/min/year), progressors (> 5 ml/min/year), and late presenters (eGFR at the time of biopsy < 15 ml/min). For more details on the samples and patients see 2.1.2.

RNA was isolated from 40 FFPE samples (cut into 20 µm sections by CBS), using a technique allowing for maximum recovery of microRNAs, as described in Methods (2.2.1.2). Agilent's 2100 bioanalyser together with the RNA PicoChip Kit was used then by CBS to assess RNA diversity between samples in terms of its integrity and concentration (Figure 3.8A). Although the RNA concentrations varied greatly, the electropherograms were similar for all samples, showing that the majority of the isolated RNA was relatively short (< 200 nt), with no sign of large RNA species such as rRNA.

Subsequently, expression of miR-16, which is highly and stably expressed in HK-2 cells, was examined by stem-loop qRT-PCR in those samples in order to establish if they were suitable for microRNA analysis by that method (Figure 3.8B). As in the reactions a constant volume was used, rather than constant RNA amount, the differences in quantity of detected miR-16 between individual samples were large, but the signal was of good quality. Interestingly, when the RNA concentration determined with Agilent's 2100 bioanalyser was compared with the relative expression of miR-16 in those samples, the ratio of RNA concentration to miR-16 appeared constant for all biopsies collected after 1996 (Figure 3.8C). In older samples, however, miR-16 expression was disproportionally low. Therefore, further analysis was performed on the biopsies obtained in 1996 or later.

RNA from the three patient groups: non-progressors (n=9), progressors (n=9), and late presenters (n=4), was pooled, so that the pooled samples for each group contained 200 ng of RNA, with proportionately equal representation of each biopsy. The pooled RNA was subjected to microRNA profiling using a qPCR-based array (TaqMan Low Density Array, Applied Biosystems), performed by CBS. Of 365 microRNAs examined, 103 were detected. The microRNA expression patterns varied across the groups (Figure 3.9A,B). The greatest difference in microRNA expression was observed for miR-192, which was over 3-fold downregulated in late presenters compared to both non-progressors and progressors (Figure 3.9C).

To validate the array data, miR-192 was quantified in all 22 individual biopsy samples with stem-loop qRT-PCR (Figure 3.10A). miR-16 was identified by geNorm [195] (see 2.4.3) as one of the three most stably expressed microRNAs in the array; therefore, it was used for normalisation of miR-192 expression. miR-192 was 67% lower in late presenters than in the other two groups, in keeping with data from the pooled array studies, and suggesting loss of miR-192 in advanced diabetic nephropathy.

Subsequently, association between miR-192 expression and structural or functional clinical parameters, obtained by Lewis et al. [181], was tested. Significant correlations were found between fibrosis score and miR-192 expression (Figure 3.10B, Pearson Correlation Coefficient: -0.704, p < 0.001), and between eGFR and miR-192 expression (Figure 3.10C, Pearson Correlation Coefficient: 0.768, p < 0.001).

3.3 Discussion

This chapter was intended to provide a starting point for investigation of microRNA role in renal fibrosis. Since at the beginning of the project microRNA expression in normal or fibrotic kidney was not well explored, an ideal strategy was to look for microRNAs regulated by profibrotic stimuli among all microRNAs discovered in humans. As in the middle of 2006 there were already over 400 different human microRNAs described (the miRBase release 8.1 [106]), a special high-throughput technique was needed to accomplish that.

The first generation of commercially available microRNA arrays were hybridisation-based arrays, similar to the typical microarrays used for mRNA detection. The main disadvantage of that method was the requirement of large quantities of good quality RNA. That excluded the possibility of global analysis of microRNA expression in non-surgically obtained renal samples. Surgical nephrectomy specimens, on the other hand, would provide enough RNA, but as profound changes in microRNA expression had been reported following a prolonged period of tissue hypoxia [205], they were not ideal for the study. Therefore, initially, microRNA role in the kidney was investigated in the well-established and successfully used in the department *in vitro* model of renal fibrosis, employing immortalized proximal tubular epithelial cells stimulated with profibrotic stimuli, typically high concentration of glucose or TGF-beta.

MicroRNA profiling by hybridisation array was a relatively new and challenging field at that time, mostly due to the size of the microRNAs. Optimal probe characteristics, array printing, sample preparation and labeling, and hybridisation also needed to be determined. Ambion, and their daughter company Asuragen, the company with which the collaborative beta test was performed, remain an industry leader in microRNA technology. At their first review of the initial array studies, no technical problems were identified. However, subsequent re-analysis gave clear pointers of technical issues with the arrays.

For the repetition of the microRNA profiling approximately one year later, the company used an optimized procedure and a new version of Ambion mirVana miRNA Bioarrays. The new arrays contained more probes for human microRNAs (328 vs. 212) and more control probes (61 vs. 4).

The array data together with the individual qRT-PCR assay results showed that high concentration of glucose in the short term did not influence microRNA expression in proximal tubular epithelial cell line. This was a rather unexpected finding, since elevated glucose had been reported to cause significant alterations in HK-2 cell gene expression [203]. The other available data suggest, however, that most of the effects on HK-2 cells can be observed after longer culture in high glucose medium than 48 hours, and often may be attributed to newly synthesized TGF-beta [206]. Further experiments confirm that in a short term TGF-beta may be necessary to see a change in microRNA expression in those cells.

The enormous progress rate in the microRNA field in the recent years has influenced the final outcome of this chapter in two ways. Firstly, the accumulating literature about function of individual microRNAs in various systems enabled a fine selection of candidate microRNAs that might be involved in fibrotic processes in the kidney, when a screen for TGF-beta-regulated microRNAs using a high-throughput technique could not be employed for economic reasons. Secondly, at the beginning of 2008

another method for global microRNA expression studies became available. That was a qRT-PCR-based array (TaqMan Low Density Array, TLDA, Applied Biosystems), allowing for simultaneous detection of 365 human microRNAs. Importantly, the technique was much more sensitive than hybridisation-based arrays; only 80 ng of sample RNA was needed for analysis. This made microRNA profiling theoretically feasible in FFPE renal biopsy samples collected over years from nephrology patients for routine evaluation. Such samples from 40 patients with diabetic nephropathy had been previously characterised histologically in the department and were available for further study. Although it was highly probable that there would be enough RNA from those samples, its quality, after fixation procedure and long storage (8-16 years), might have made them unsuitable for analysis.

The encouragement came from two reports comparing microRNA profiles in FFPE and fresh frozen tissue samples, demonstrating that microRNAs were well-preserved in the FFPE samples and could be successfully detected by hybridisation-based array or qRT-PCR [207, 208]. Preliminary analysis done on the 40 FFPE kidney biopsy samples confirmed that the isolated microRNAs can be easily detected by qRT-PCR. However, in older samples, eventually excluded from further analysis, the qRT-PCR signal compared with RNA concentration was remarkably low, suggesting that microRNAs in those old samples were damaged, possibly by oxidation during prolonged storage. Alternatively, the older fixation procedure might have been less efficient or included some inhibitors of PCR reaction. Very similar observations to mine have been made recently in a study comparing microRNA expression in FFPE lymph nodes from three decades [209].

The final microRNA profiling experiment using the qRT-PCR-based array, in addition of being the first demonstration that microRNAs can be globally analysed

in archival FFPE kidney biopsy samples, revealed multiple differences in microRNA expression depending on the rate of disease progression in follow up period (comparison: non-progressors of fibrosis vs. progressors) or severity at the presentation (late presenters vs. combined non-progressors and progressors). Renal biopsy is a complex mixture of cells that might vary depending for example on the relative amounts of cortex vs. medulla, or tubules vs. glomeruli vs. blood vessel, in each biopsy. In spite of this, one of the microRNAs identified in the array experiment as differentially expressed between early and late stages of diabetic nephropathy, miR-192, when examined in individual samples was still downregulated in the late presenters group and its expression inversely correlated with fibrosis and decrease in eGFR. Furthermore, the subsequent work in the department revealed that this was relatively specific to miR-192, since expression of another microRNA, miR-200b, in the biopsies did not correlate with either fibrosis or eGFR [204]. In addition, miR-192 loss in advanced diabetic nephropathy was confirmed by in situ hybridisation, which also demonstrated presence of miR-192 mostly in glomeruli and tubules [204].

These results suggest that miR-192 is a potential new biomarker in diabetic nephropathy, and validate the approach of measuring microRNAs in routinely processed renal biopsy tissue, analogously to studies of microRNA expression in cancer specimens, no less complex, that are soon to enter clinical practise. The data also imply that the other changes in microRNA expression found in the experiment are very likely to be meaningful and will be a fruitful area for further investigations. Sadly, limitations in time and materials permitted a detailed characterisation only of one of many microRNAs potentially important in renal fibrosis, miR-192, in this thesis.

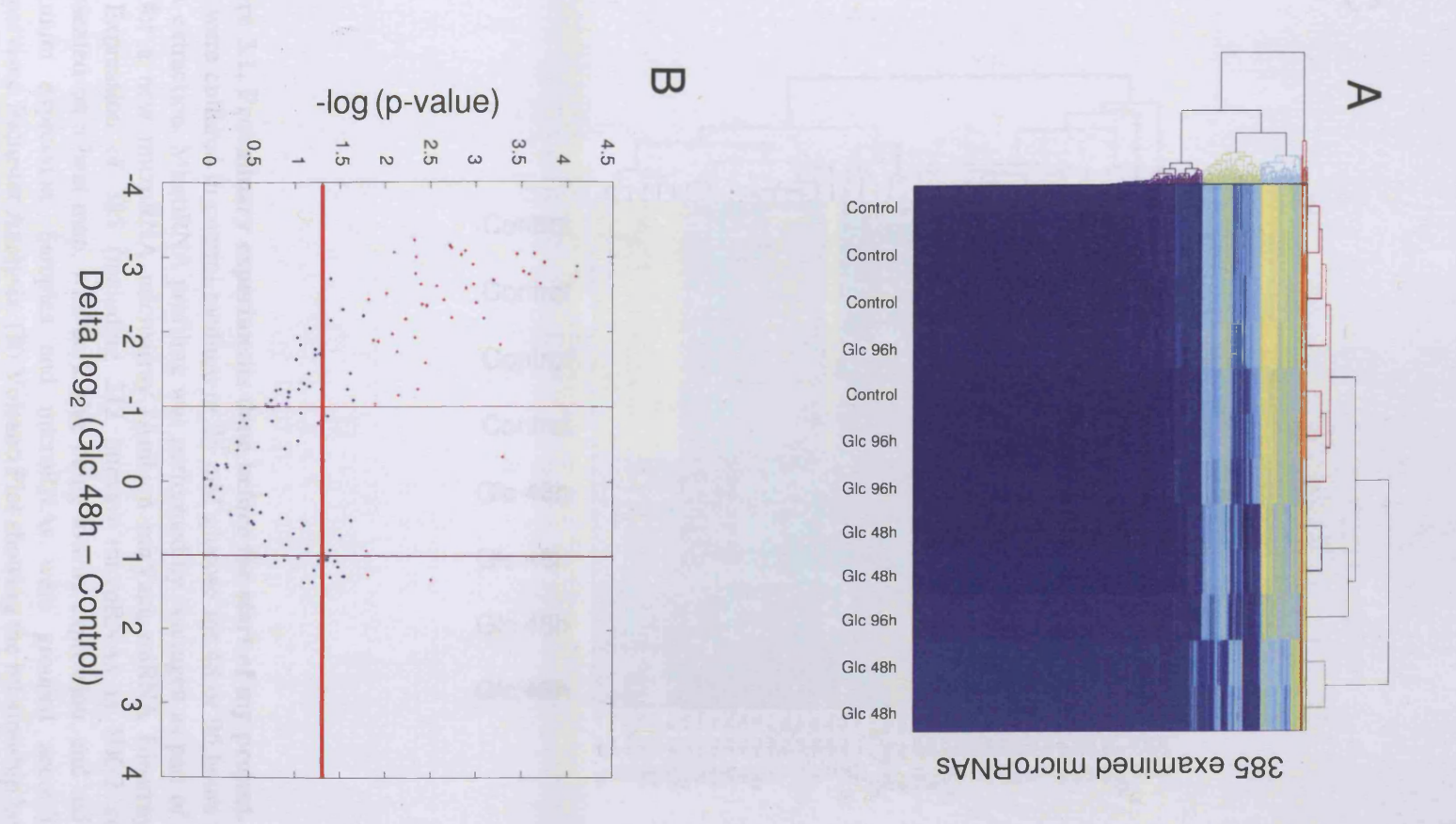
Expression of miR-192 has been previously reported to be relatively specific to the kidney [143], and to be present in the renal cortex rather than medulla [147]. Its expression has been studied also in diabetic nephropathy. Surprisingly, two groups working on this subject came to the opposite conclusions [151, 154]. Kato et al. observed upregulation of miR-192 in glomeruli from mouse models of diabetic nephropathy as well as in vitro in mesangial cells treated with TGF-beta [151]; whereas Kantharidis et al. presented results consistent with mine. Namely, he noted downregulation of miR-192 in mouse diabetic kidney, and in cultured mesangial and proximal tubular epithelial cells stimulated with TGF-beta [154]. Additionally, two recent papers from one laboratory pointed to a potential role of miR-192 in other renal disorders [156, 157]. The authors reported that in patients with IgA nephropathy miR-192 was upregulated when compared with control, inversely correlated with the rate of decline in eGFR and with glomerulosclerosis [156]. In patients with hypertensive nephrosclerosis they noticed an increase in miR-192, as well as its correlation with proteinuria [157]. The discrepancies between the existing data suggest that miR-192 regulation and role in the kidney is complex and, very likely, worth investigating.

Surprisingly, miR-215, miR-216a, and miR-217, the other microRNAs that have been implicated in diabetic nephropathy (see Table 1.2), were not detected in the renal biopsy tissue (and miR-377 was not examined). Since control samples from the normal kidney were not available for this study, it is conceivable that miR-215, decreased in the kidney of diabetic mice and in TGF-beta-treated mesangial and proximal tubular epithelial cells [151, 154], could potentially be expressed in the normal kidney and would be lost during the course of diabetic nephropathy. This, however, would not explain the lack of miR-216a and miR-217, which have

been found upregulated in glomeruli of diabetic mice and in TGF-beta-treated mesangial cells [152]. Most likely, distinct techniques, parts of the kidney/cell types investigated, and perhaps differences between species account for the inconsistency.

The results presented in this chapter identified microRNAs for further study, and suggested that microRNA quantification might provide useful prognostic information for patients with diabetic nephropathy. The major finding was the identification of miR-192 as downregulated by profibrotic factors both in short term *in vitro*, following stimulation of proximal tubular epithelial cell line with TGF-beta, and in long term *in vivo*, in course of diabetic nephropathy. Investigation of miR-192 function in the fibrotic process in the kidney will be the focus of Chapter Five.

(Continued on the next page)





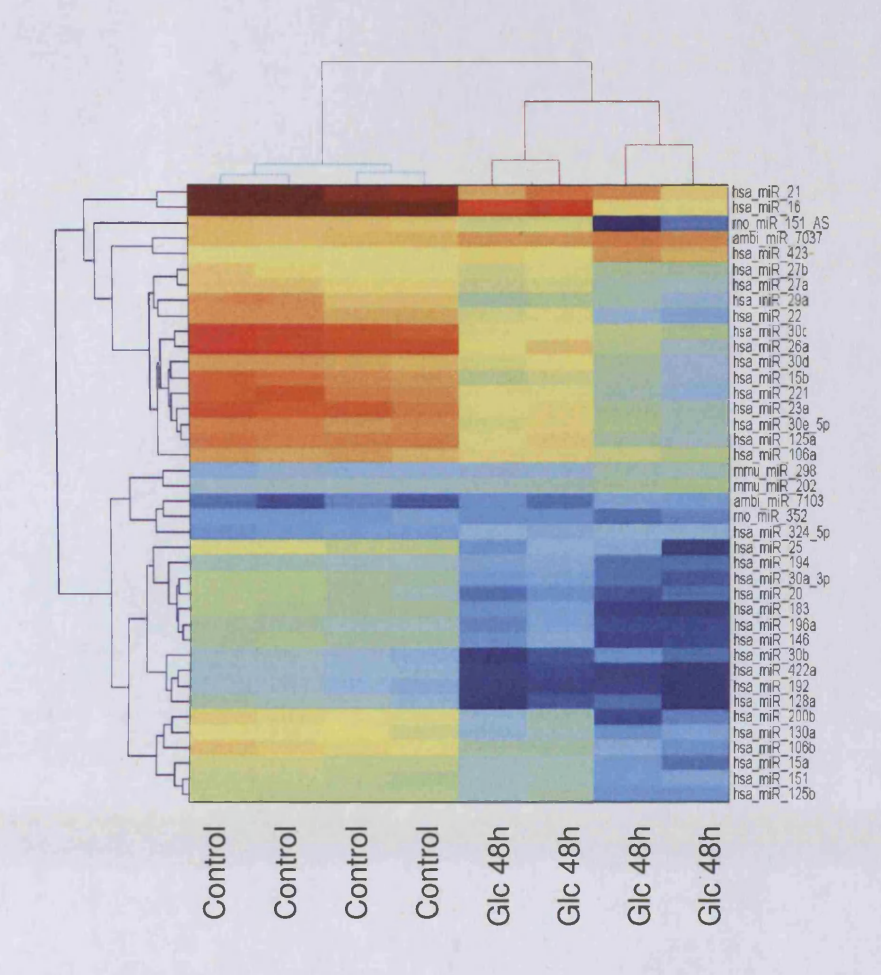
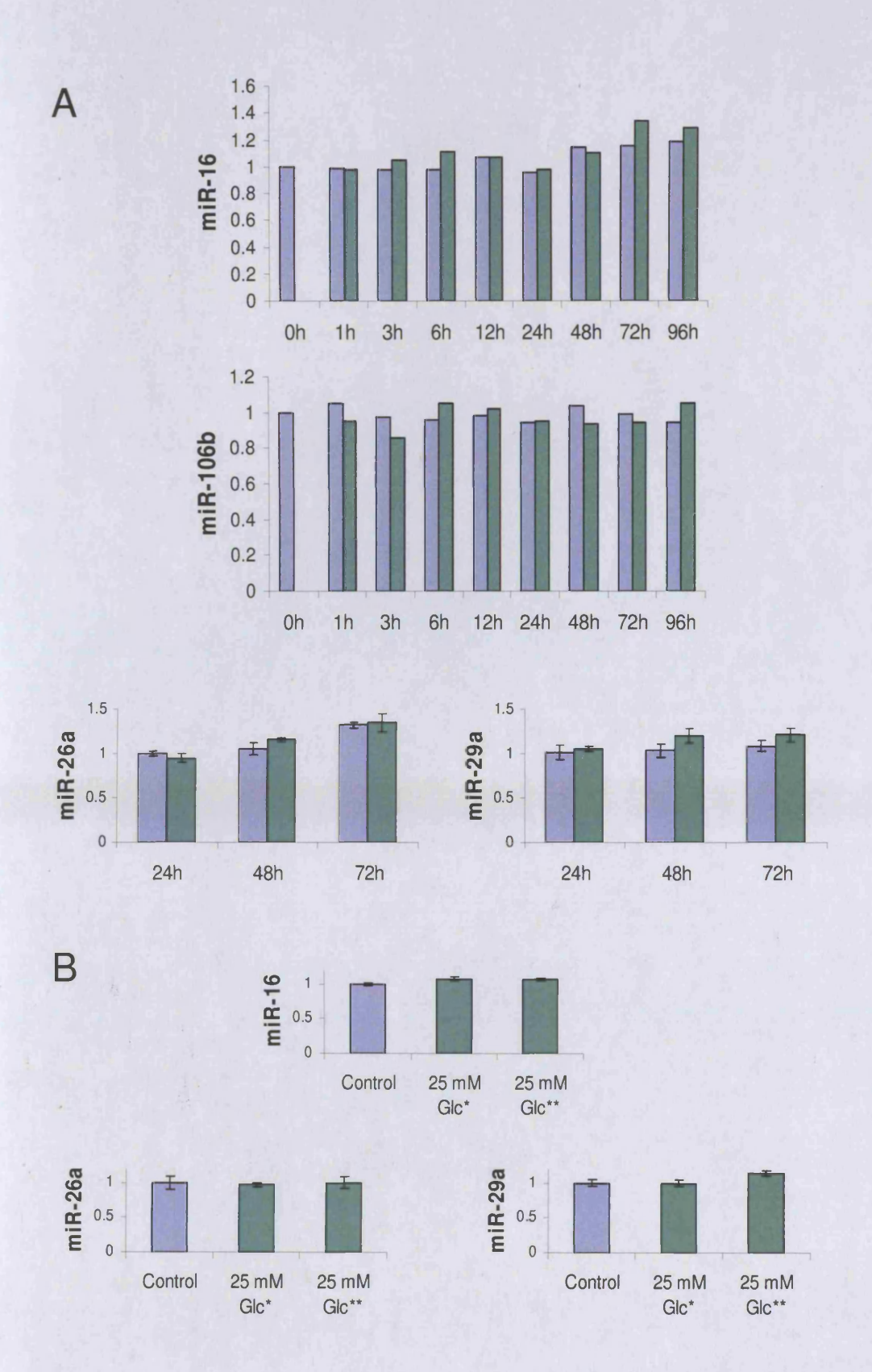


Figure 3.1. Preliminary experiments done before the start of my project. HK-2 cells were cultured in control medium or 25 mM glucose for 48 or 96 hours before RNA extraction. MicroRNA profiling was performed by Asuragen as part of a beta test for a new microRNA microarray (Ambion mirVana miRNA Bioarray V1). (A) Expression of 385 (including 212 human) microRNAs in HK-2 cells is represented on a heat map, with dark blue being low/no expression, and red being maximum expression. Samples and microRNAs were grouped according to unsupervised Bicluster Analysis. (B) Volcano Plot showing the relationship between change in microRNA expression between two groups (25 mM glucose and control) and statistical significance. Horizontal red line represents p = 0.05 threshold. (C) Expression of 40 microRNAs most altered by 25 mM glucose at 48 hours displayed as in (A).



(Continued on the next page)

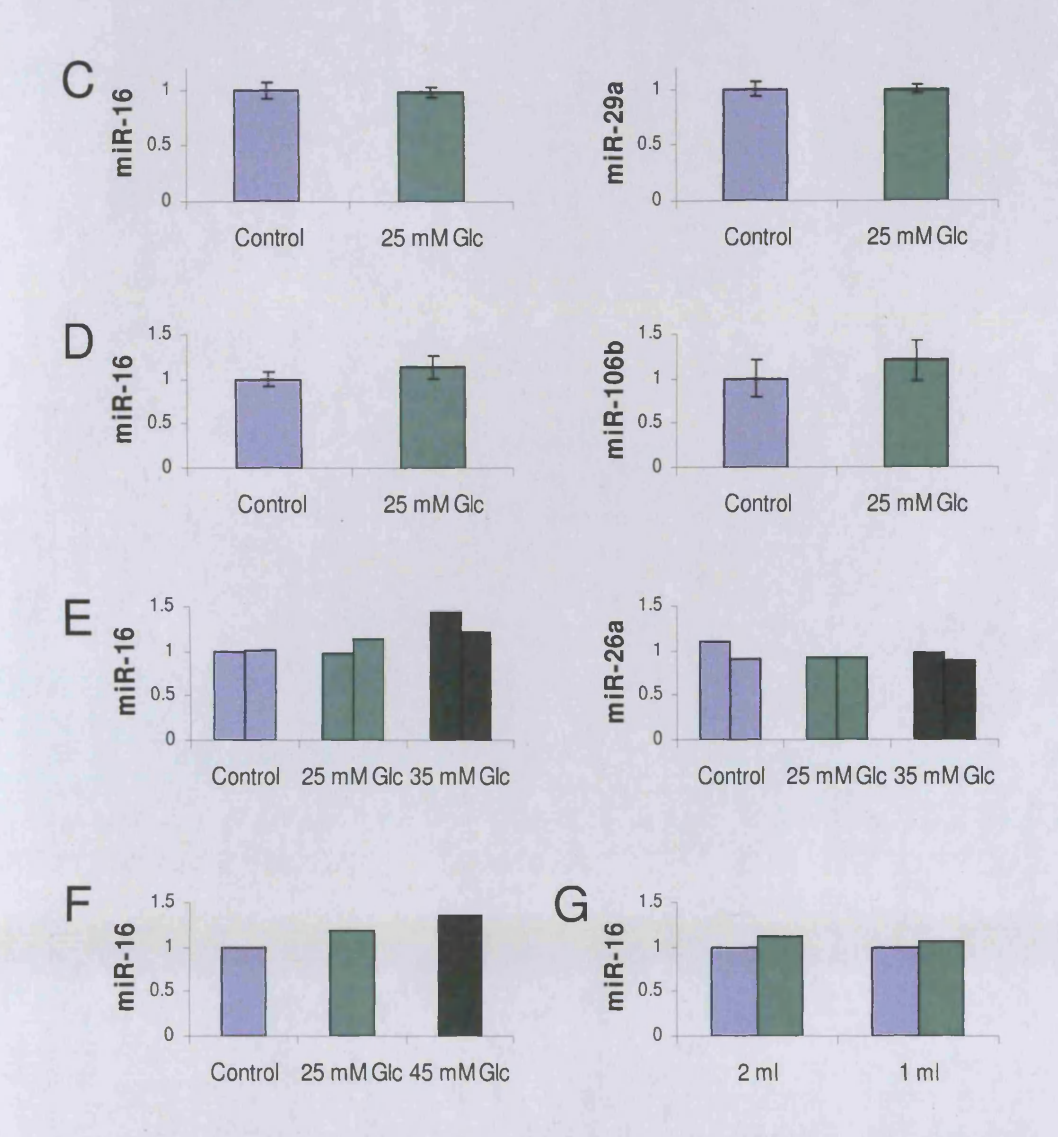
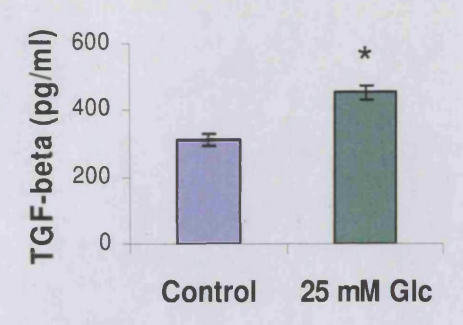


Figure 3.2. Expression of selected microRNAs in HK-2 cells cultured in medium with high glucose concentration. After 48-hour-culture in medium without FCS, confluent HK-2 cells were cultured in control medium (blue bars) or medium with 25 mM glucose (green bars) for 48 hours unless stated otherwise. Expression of miR-16, miR-106b, miR-26a, and miR-29a was examined using stem-loop qRT-PCR, as described in Methods. (A) Cells were stimulated with 25 mM glucose for 1 to 96 hours, as indicated on the graph. (B) Glucose used for stimulation came from two other independent sources. (C) Cells were plated before the experiment on T25 flasks instead of usual 6-well-plates. (D) Cells were growth-arrested for 72 rather than 48 hours. (E) Higher concentration of glucose (35 mM) was used. (F) Cells were stimulated with 25 or 45 mM glucose in medium without insulin. (G) Smaller volume (1 ml rather than usual 2 ml) of culture medium was used. Error bars (where shown) represent SEM, n=3. No significant change in microRNA expression between samples cultured in control and high glucose medium was found.

A



B

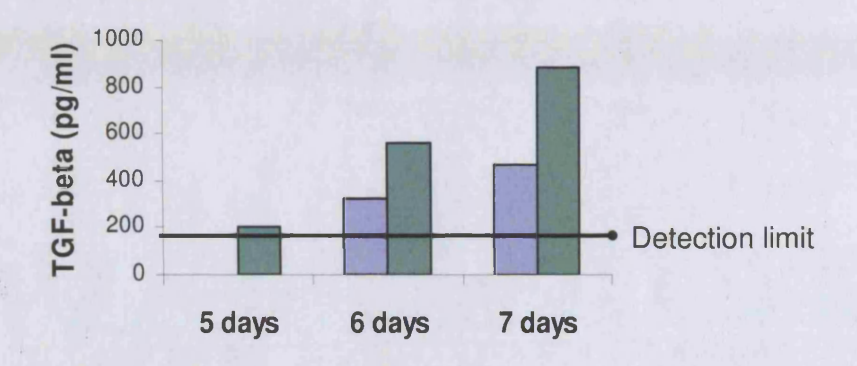
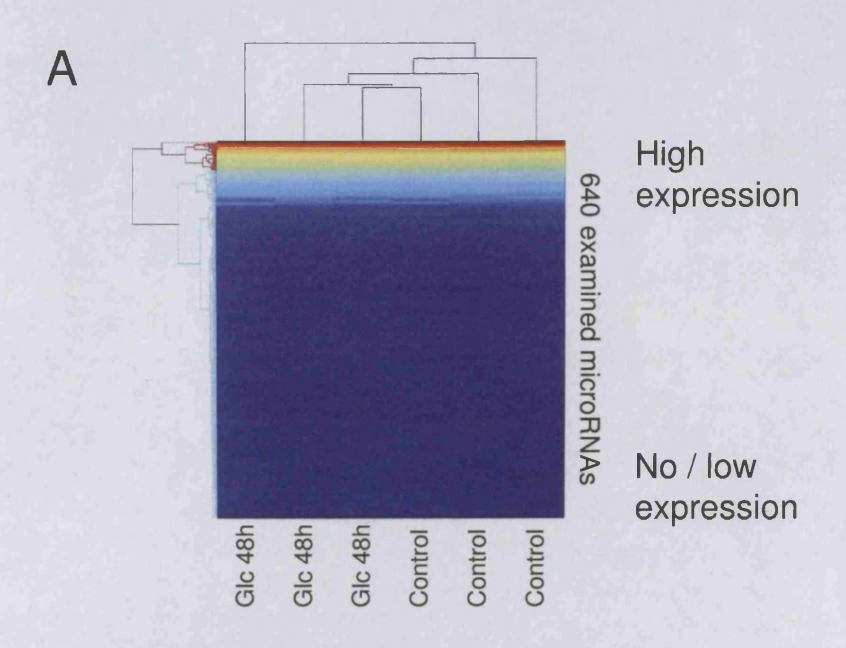


Figure 3.3. TGF-beta secretion by HK-2 cells cultured with 25 mM glucose. HK-2 cells were cultured on a 6-well-plate. After 48 hours without FCS, they were cultured in 1.2 ml medium containing 5 mM (blue bars) or 25 mM glucose (green bars) for four days (A) or as indicated on the chart (B). Medium was replaced every second day until the day 4, and then was collected after 24, 48, or 72 hours. The concentration of latent TGF-beta in medium was measured by ELISA. The error bars (A) represent SEM, n=3. An asterisk indicates p < 0.05.



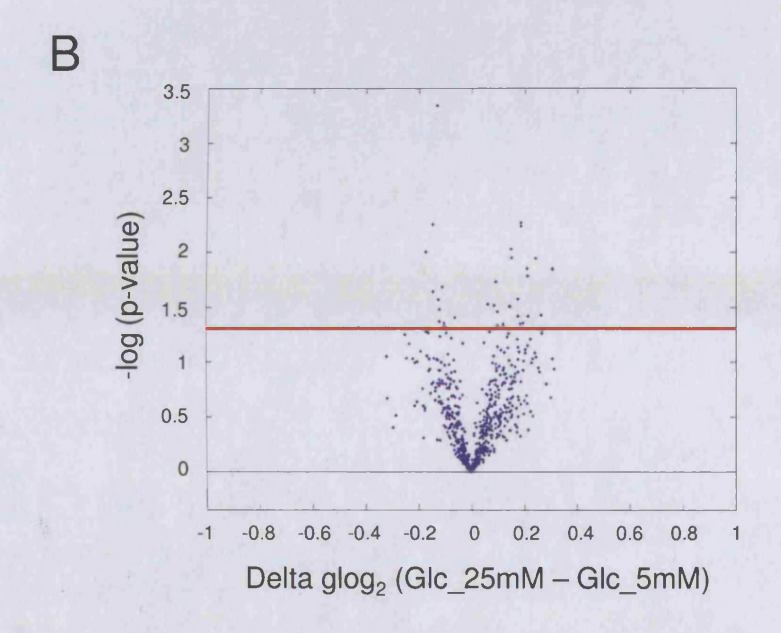
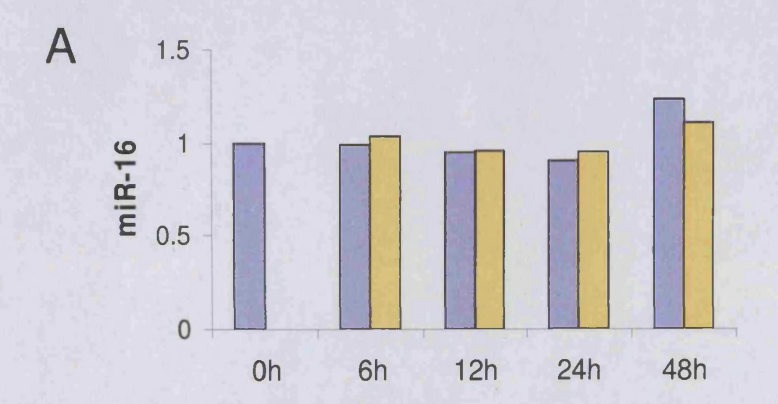
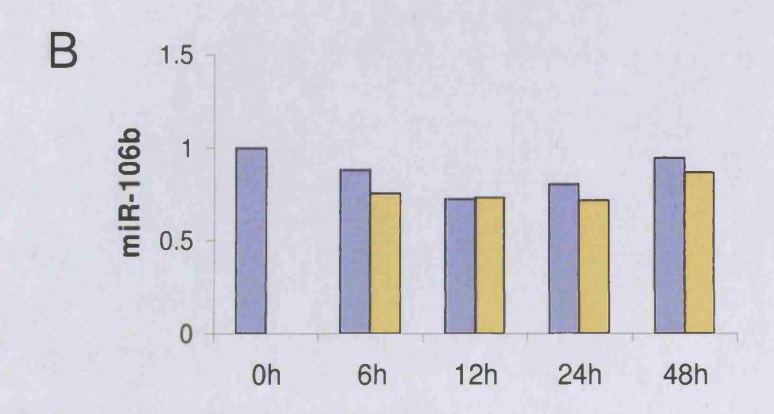


Figure 3.4. MicroRNA profiling in proximal tubular cells. HK-2 cells were cultured in 25 mM glucose or control medium for 48 hours before RNA extraction. MicroRNA profiling was done by Asuragen using Ambion mirVana miRNA Bioarray V2. (A) Expression of 640 (including 328 human) microRNAs in HK-2 cells is represented on a heat map scale, with dark blue being low/no expression, and red being maximum expression. Samples and microRNAs were grouped according to unsupervised Bicluster Analysis. (B) Volcano Plot shows the relationship between change in microRNA expression between the two groups (25 mM glucose and control) and statistical significance (-log of uncorrected p-values). Horizontal red line represents p = 0.05 threshold.





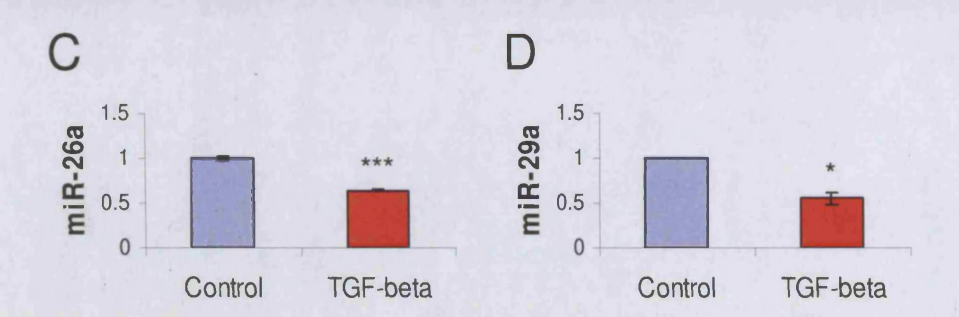


Figure 3.5. Expression of selected microRNAs in HK-2 cells stimulated with TGF-beta. After 48-hour-culture in medium without FCS, confluent HK-2 cells were cultured in control medium (blue bars) or stimulated with TGF-beta at the final concentration of 1 ng/ml (yellow bars) or 10 ng/ml (red bars) for indicated time points (A,B) or 96 hours (C,D). Expression of miR-16 (A), miR-106b (B), miR-26a (C), and miR-29a (D) was examined using stem-loop qRT-PCR. Error bars (C,D) represent SEM, n=3. Statistical significance is indicated with asterisks as follows: p < 0.05, *** p < 0.0005.

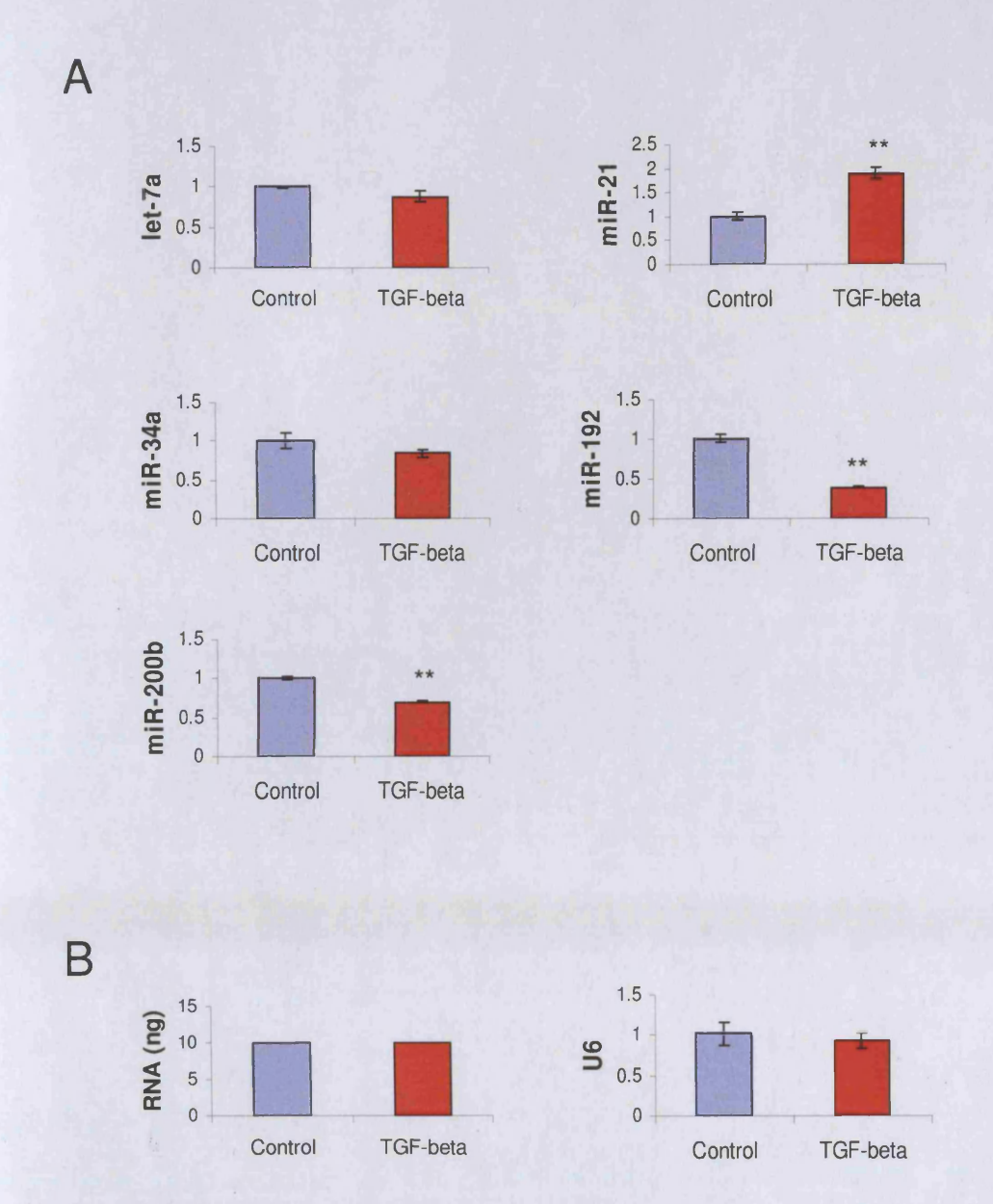
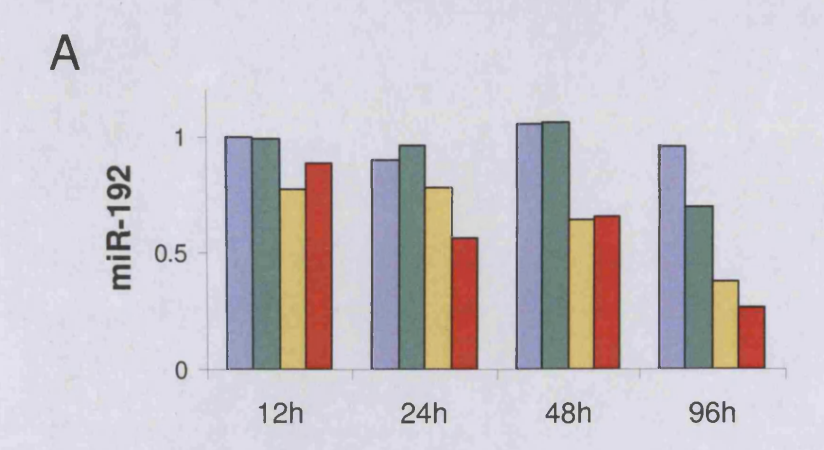


Figure 3.6. Expression of newly selected microRNAs in HK-2 cells stimulated with TGF-beta. After 48-hour-culture in medium without FCS, confluent HK-2 cells were cultured in control medium (blue bars) or stimulated with 10 ng/ml TGF-beta (red bars) for 96 hours. (A) Expression of let-7a, miR-21, miR-34a, miR-192, and miR-200b was examined using stem-loop qRT-PCR. (B) RNA amount used in RT reactions (intended 10 ng) was quantified in each sample using Quant-iT RNA Assay (Invitrogen). Additionally small nuclear RNA U6 was quantified using stem-loop qRT-PCR. The experiment was performed in triplicate; SEM is shown. ** indicates p < 0.005.



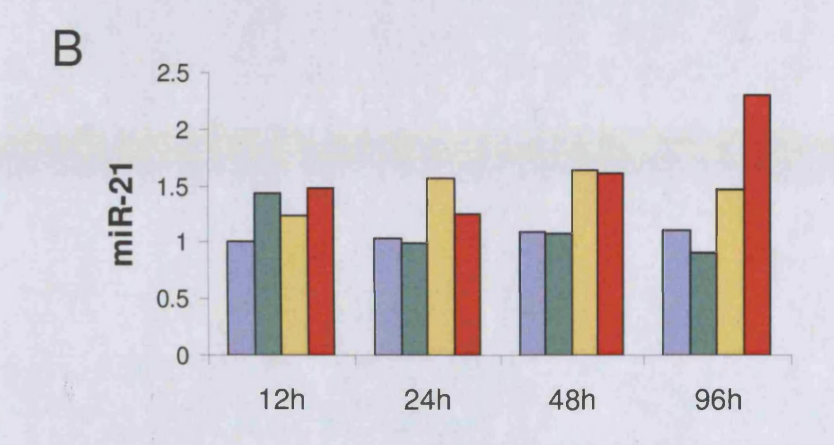
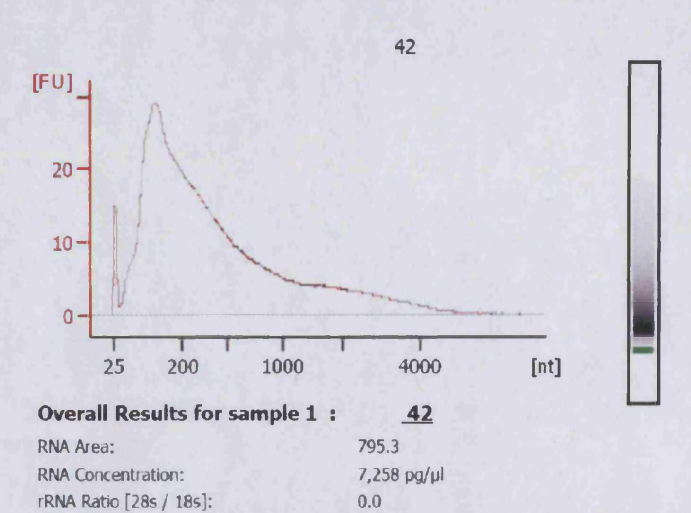


Figure 3.7. Expression of miR-192 and miR-21 in HK-2 cells stimulated with profibrotic stimuli. After 48-hour-culture in medium without FCS, confluent HK-2 cells were cultured in control medium (blue bars), medium with 25 mM glucose (green bars), or stimulated with TGF-beta at the final concentration of 1 ng/ml (yellow bars) or 10 ng/ml (red bars) for indicated time points. Expression of miR-192 (A) and miR-21 (B) was examined using stem-loop qRT-PCR. miR-16 was used for normalisation.

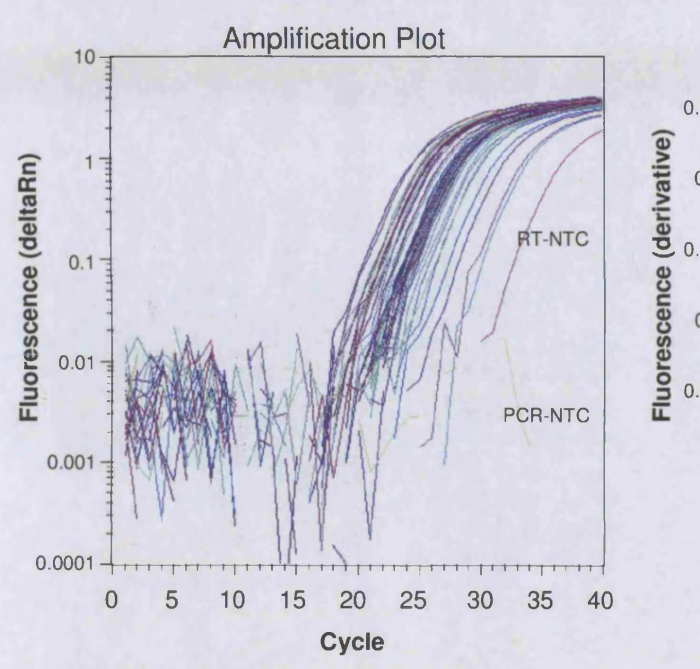
A Electropherogram Summary

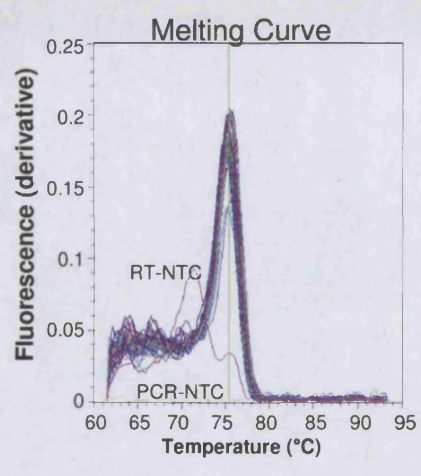
RNA Integrity Number (RIN):



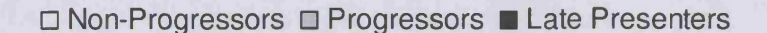
2.2 (B.02.02)

B





(Continued on the next page)



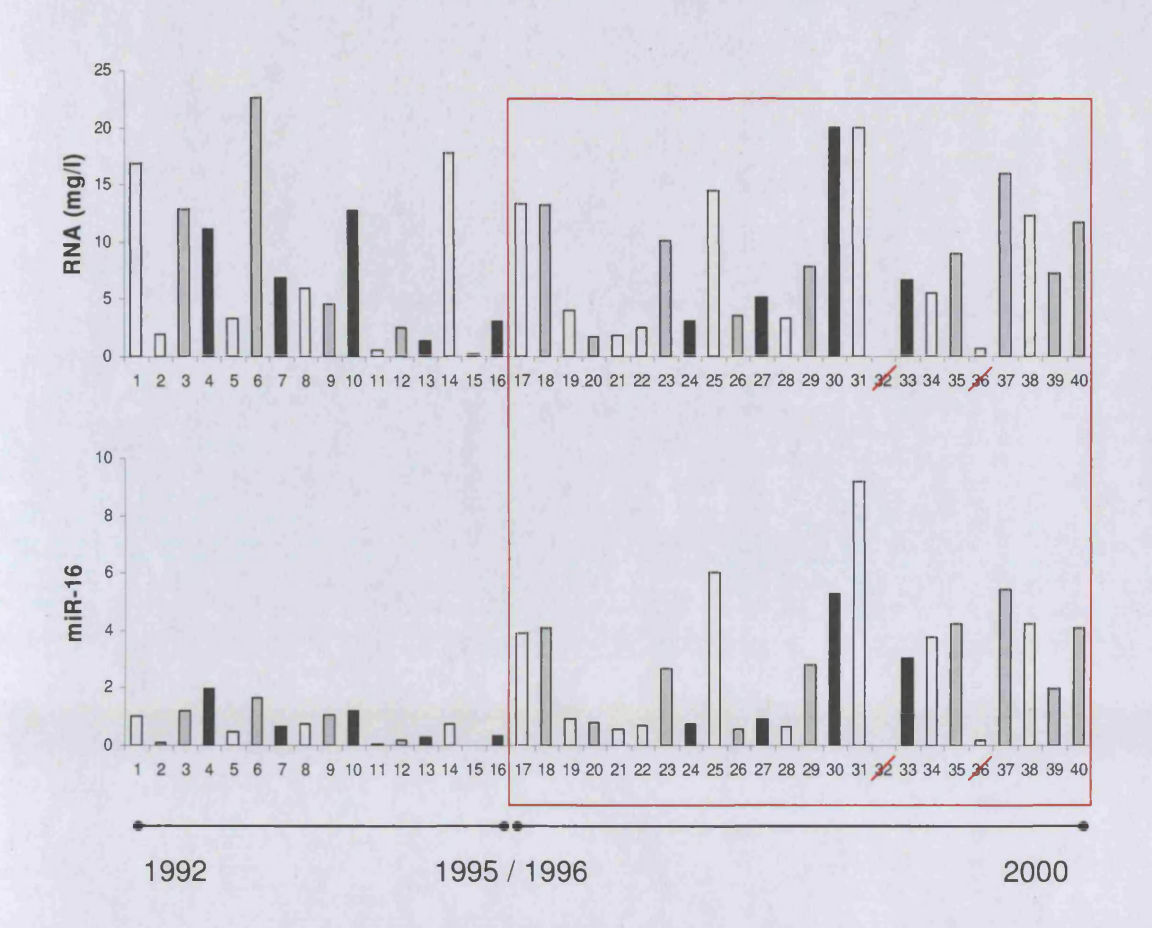
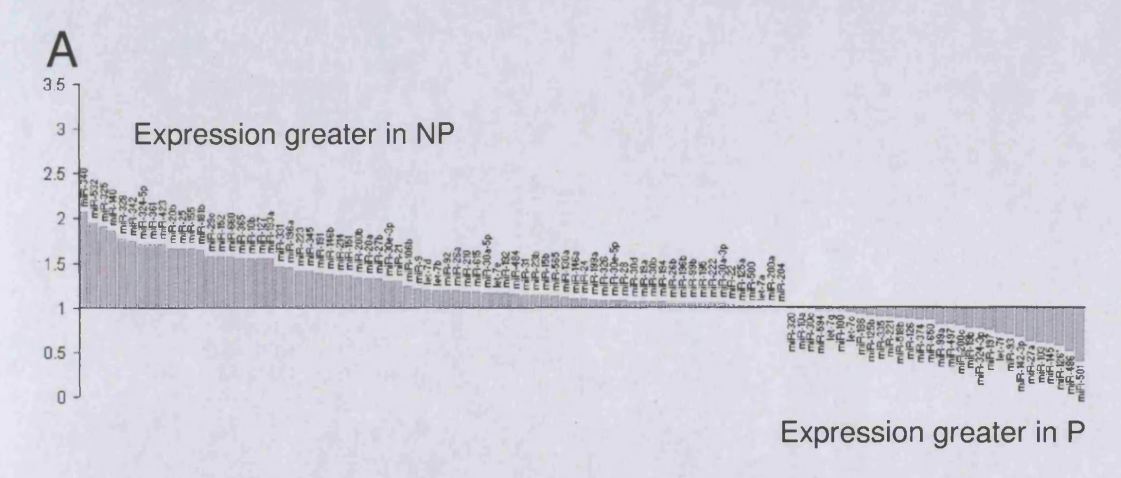
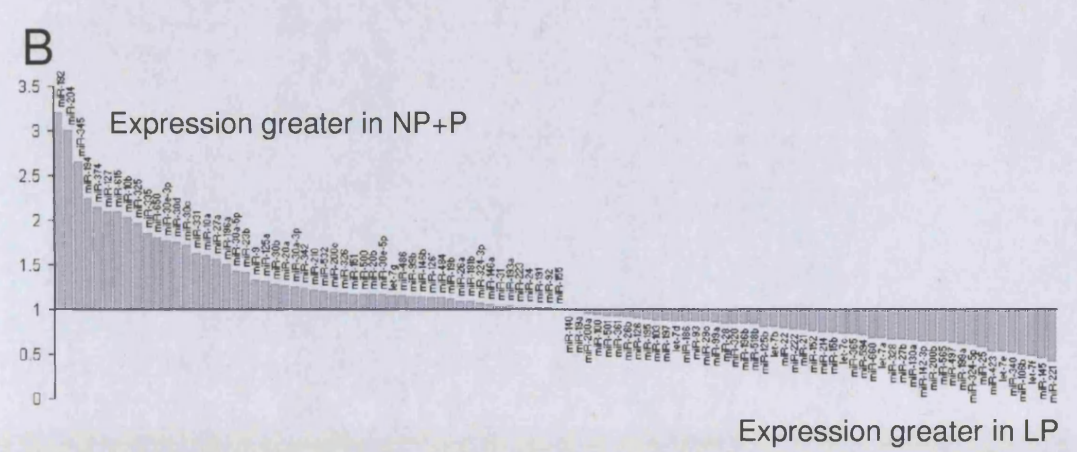


Figure 3.8. Quantification and quality control of RNA isolated from FFPE renal biopsy tissue from patients with diabetic nephropathy. RNA was isolated from FFPE renal tissue from 40 patients with diabetic nephropathy. (A) Microfluidics analysis of RNA integrity was performed by CBS using Agilent's 2100 bioanalyser together with the RNA PicoChip Kit. A representative electropherogram is shown. On the right the results are displayed as they would appear on an agarose gel. (B) miR-16 expression was measured in the 40 samples by stem-loop qRT-PCR. Amplification plot and melting curves are shown, demonstrating proper amplification and a single product of the reaction in all samples, but not in negative controls. (C) Comparison of RNA concentration estimated with RNA PicoChip and expression of miR-16 by stem-loop qRT-PCR. The red box indicates samples which were used in further experiments (from the biopsies taken in or after 1996, except for samples 32 and 36 with very low RNA concentration).





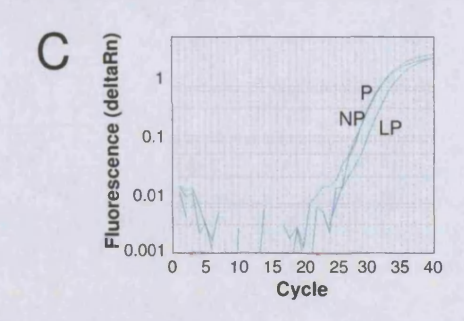


Figure 3.9. TaqMan Low Density Array determination of microRNA expression in renal biopsy tissue from patients with diabetic nephropathy. Renal biopsies from diabetic nephropaths were separated into three groups on the basis of progression following biopsy: non-progressors (NP, n=9), progressors (P, n=9), and late presenters (LP, n=4). Expression of 365 microRNAs was quantified in pooled RNA for each group using TaqMan Low Density Array Human MicroRNA Panel v1.0 (Applied Biosystems). Fold-expression values are displayed for microRNAs detected ($C_T < 33$). (A) Comparison of P vs. NP. (B) Comparison of combined earlier stage biopsies (NP+P) vs. LP. (C) Amplification plot demonstrating lower miR-192 expression in LP in comparison with NP and P.

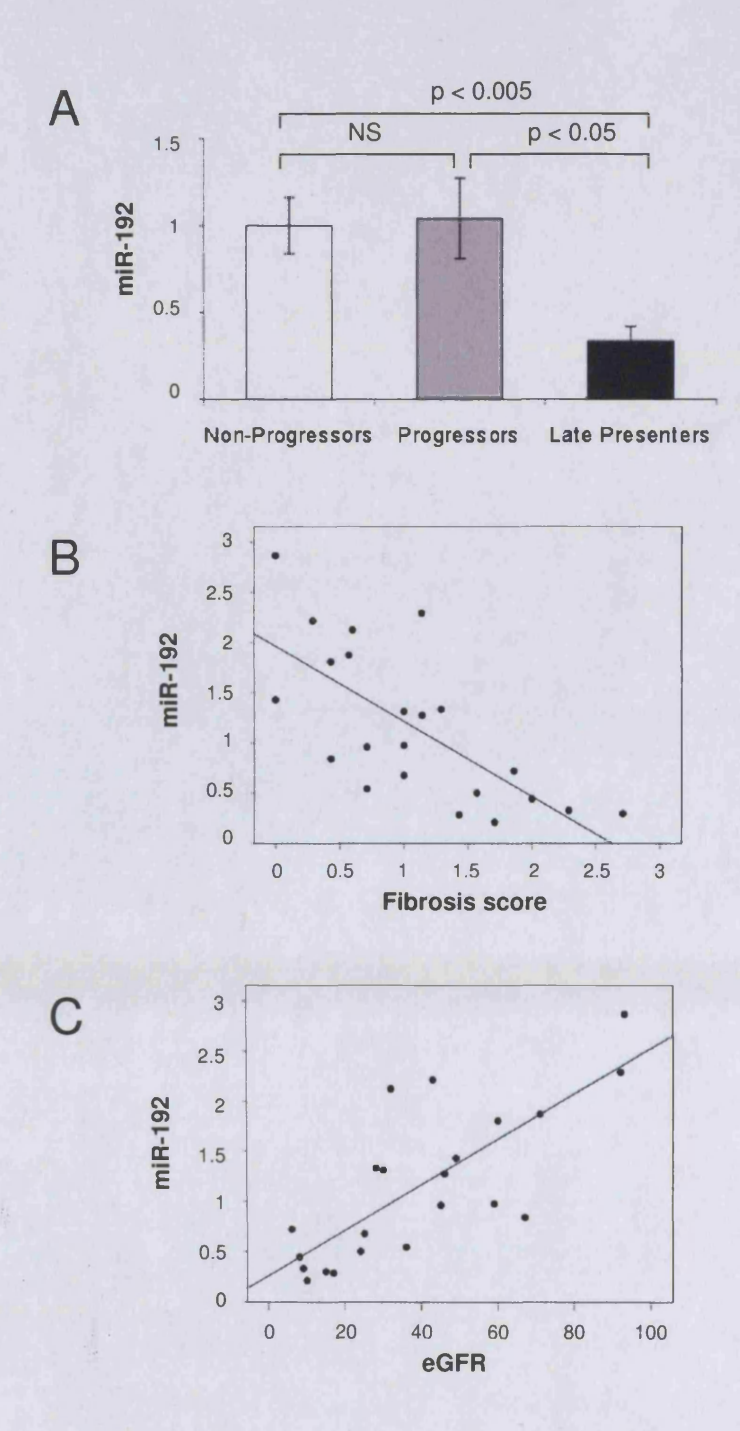


Figure 3.10. Expression of miR-192 in individual kidney biopsies and its correlation with severity of kidney disease. (A) miR-192 was examined in individual samples pooled for use in microRNA profiling (9 non-progressors, 9 progressors, 4 late presenters) by stem-loop qRT-PCR, using miR-16 as an endogenous control. Mean ± SEM is shown. (B) Plot of miR-192 expression vs. fibrosis score, Pearson Correlation Coefficient -0.704, p < 0.001. (C) Plot of miR-192 expression vs. eGFR, Pearson Correlation Coefficient 0.768, p < 0.001. Fibrosis score and eGFR were determined by Lewis et al. [181].

MicroRNA	Array signal* (Control)	Expression ratio* (Glucose 5/25mM)	Some predicted microRNA targets implicated in renal fibrosis**	
miR-16	13.1	6.857	activin A receptor, type II (ACVR2), TGFB-induced factor 2 (TALE family homeobox) (TGIF2), collagen, type XII alpha 1, and type XXIV alpha 1 (COL12A1, COL24A1), SMAD, mothers against DPP homolog 5, 3 and 7 (Drosophila) (SMAD5, SMAD3, SMAD7), PAI-1 mRNA-binding protein (PAI-RBP1), laminin gamma 1 (LAMC1), hyaluronan synthase 2 (HAS2), serum/glucocorticoid regulated kinase (SGK), bone morphogenetic protein receptor, type IA (BMPR1A), transforming growth factor, beta receptor III (TGFBR3), insulin-like growth factor 2 receptor (IGF2R)	
miR-26a	11.2	8.414	SMAD, mothers against DPP homolog 1 and 4 (Drosophila) (SMAD1, SMAD4), PAI-1 mRNA-binding protein (PAI-RBP1), platelet-derived growth factor receptor, alpha polypeptide (PDGFRA), collagen, type XXII alpha 1, and type I alpha 2, and type XIX alpha 1 (COL22A1, COL1A2, COL19A1), hyaluronan synthase 2 (HAS2)	
miR-29a	9.7	7.581	collagen, type I alpha 1, and type IV alpha 5, and type III alpha 1, and type I alpha 2, and type IV alpha 1, and type V alpha 2, and type II alpha 1, and type IX alpha 1, and type II alpha 1, and type IX alpha 1, and type II alpha 1, and type XV alpha 1, and type VII alpha 1, and type VI alpha 3, and type VI alpha 3, and type XIX alpha 1 (COL1A1, COL4A5, COL3A1, COL1A2, COL4A1, COL5A2, COL2A1, COL5A3, COL19A1), serum/glucocorticoid regulated kinase (SGK), transforming growth factor beta 1 induced transcript 4 (TGFB1I4), platelet derived growth factor C (PDGFC), transforming growth factor, beta 3 (TGFB3), laminin gamma 1 (LAMC1)	
miR-106b	9.0	8.704	hyaluronan binding protein 4 (HABP4), peroxisome proliferative activated receptor, alpha (PPARA), BMP and activin membrane-bound inhibitor homolog (Xenopus laevis) (BAMBI), SMAD, mothers against DPP homolog 6, 7and 5 (Drosophila) (SMAD6, SMAD7, SMAD5), hyaluronan synthase 2 (HAS2), platelet-derived growth factor receptor, alpha polypeptide (PDGFRA), bone morphogenetic protein receptor, type II (BMPR2), activin A receptor, type IB (ACVR1B), TGF-beta induced apotosis protein 2 (TAIP-2), TGFB inducible early growth response 2 (TIEG2), collagen, type IV, alpha 3 (Goodpasture antigen) (COL4A3)	
miR-128a	6.2	5.687	bone morphogenetic protein receptor, type II (BMPR2), epidermal growth factor receptor (EGFR), peroxisome proliferative activated receptor, gamma (PPARG), latent transforming growth factor beta binding protein 1 (LTBP1), collagen, type III alpha 1 (COL3A1), platelet-derived growth factor receptor, alpha polypeptide (PDGFRA), insulin receptor (INSR), hyaluronan and proteoglycan link protein 1 (HAPLN1), activin A receptor, type I (ACVR1), insulin receptor substrate 1 (IRS1)	

Table 3.1. Selection of microRNAs for further analysis.

^{*} Results obtained before the start of my project.
** Predictions by PicTar [191], as described in Methods.

MicroRNA	Function / special features*	Ref
let-7a	Tumour suppressor. Conserved from worms to mammals. One of the most studied microRNAs. Believed to be a master regulator of cell proliferation pathways.	[210]
miR-21	Oncogene ("oncomiR"). Promotes cell growth and proliferation in various cancers. Upregulated in keratinocytes following stimulation with TGF-beta.	[142, 211]
miR-34a	Tumour suppressor. Induced by p53 in response to DNA damage and oncogenic stress. Causes cell-cycle arrest in tumour-derived and primary cells.	[212]
miR-192	Upregulated in glomeruli of mouse model of diabetic nephropathy, as well as in mesangial cells stimulated with TGF-beta. Responsible for an increase in collagen 1-alpha 2 synthesis after TGF-beta stimulation in mesangial cells.	[152]
miR-200b	Ectopic expression of miR-200c in breast and lung cancer cell lines resulted in an increase in E-cadherin (according to the microarray data, in HK-2 cells miR-200b is the most abundant among the miR-200 family members).	[213]

^{*} Reported before October 2007.

Table 3.2. Selection of microRNAs potentially regulated by TGF-beta.

CHAPTER FOUR:

ATTEMPTS TO REPRESS EXPRESSION OR FUNCTION OF ALL MICRORNAS IN PROXIMAL TUBULAR EPITHELIAL CELLS

4.1 Introduction

There are several common elements in biosynthesis and mode of action of all microRNAs. Therefore, one might predict that blocking a single enzyme crucial for either of those processes will be sufficient to globally reduce microRNA expression or function. The observed changes would then suggest physiological roles of microRNAs in the studied model. In fact, many discoveries regarding microRNA functions have been made by investigating the effects of general microRNA inhibition.

Choosing the right protein for blockade is of fundamental importance in this approach. As described earlier (see 1.4.3), following microRNA-specific transcription of pri-microRNAs, there are a few major steps in microRNA biosynthesis shared by most microRNAs. These are sequentially: i) processing of pri-microRNA by the Microprocessor complex (comprising of the endonuclease Drosha and the RNA-binding protein DGCR8), giving approximately 70-nucleotide-long stem-loop structure called pre-microRNA, ii) nuclear export by Exportin-5, and iii) cleavage of the pre-microRNA by Dicer. The mature microRNA is then loaded with help of Dicer, TRBP, and PACT into the miRISC complex and may perform its functions.

A number of proteins are involved in those steps. Inhibition of some of them, e.g. Drosha, DGCR8, Exportin-5, Dicer, TRBP, Argonautes (Ago1-4), or GW182, has been shown to affect microRNA maturation or action [214-216]. However, the majority of them would not be ideal to study the role of microRNAs in biological processes because of their other important functions in the cell. In particular, Drosha

is involved in rRNA processing [217], while Exportin-5 transfers to the cytoplasm also other short RNA species containing a mini-helix motif, such as tRNA. [218]. Until recently, inhibition of Dicer seemed to be a perfect option. It was known solely for its function in processing of precursors of short silencing RNAs: microRNAs and siRNAs. For a long time it was commonly accepted that the latter type of processing did not occur in mammalian cells in physiological conditions. Instead, it was associated either with viral infection or transfection with artificial long double-stranded RNA. The presence of endogenous siRNAs in mammals was described for the first time in 2008 [219, 220]. Until then however, manipulation of Dicer expression seemed to give easily interpretable results and became the most commonly used method to study microRNA functions. That was also the reason why in this chapter I focused mainly on Dicer inhibition.

There is a single Dicer gene in humans. It encodes a rather large protein of predicted molecular weight of 217 kDa, consisting of nearly two thousand amino acid residues. It belongs to the RNase III family, which is a group of enzymes that specifically recognise and cleave double-stranded RNA into short discrete fragments of 21-27 nucleotides in length [221]. Crucial for Dicer hydrolytic activity are two ribonuclease domains characteristic to the whole RNase III family (often called the RNase III domains) and one PAZ domain binding to the end of double-stranded RNA. Each RNase III domain catalyses cleavage of one RNA strand, together generating products with the characteristic two-nucleotide-long overhangs at the 3' ends [221]. After the cleavage, presumably using its HExD/H-box helicase domain, Dicer helps the two strands of the short double-stranded RNA to separate. Subsequently, by interaction with the components of the miRISC complex and other

supporting proteins, it facilitates the loading of one of the strands into the miRISC complex.

The importance of Dicer and microRNAs in various processes has been highlighted by a number of Dicer knockout and knockdown experiments. The most spectacular examples include embryonic lethality of Dicer knockout mice [135], death of cardiac-specific Dicer knockout mice prenatally or shortly after birth due to defects in heart development [137], or fatal defects in brain development after Dicer conditional knockout in mouse neocortex [138]. In addition, in 2008, so after completion of the experiments presented below, three independent groups reported that conditional Dicer knockdown in renal podocytes results in advanced kidney failure and mouse death at six to eight weeks, providing evidence that Dicer is essential for normal kidney function [148-150].

This chapter was meant to facilitate the subsequent functional studies of individual microRNAs selected in Chapter Three. This would be achieved by finding out which of the processes related to renal fibrosis were microRNA-dependent, i.e. were affected following knockdown of Dicer or, as justified later, TRBP or GW182 in HK-2 cells.

4.2 Results

4.2.1 Transient knockdown of Dicer or TRBP using siRNA

Dicer knockdown

In order to inhibit microRNA biosynthesis, transient knockdown of Dicer was carried out in HK-2 cells using specific siRNA, as described in the literature [198].

To start with, a time course experiment was performed to establish the best time needed to observe maximal reduction in Dicer and mature microRNA expression. Total RNA was extracted from cells 24, 48, 72, or 96 hours after transfection with 18 nM Dicer-specific or control siRNA. Expression of Dicer and miR-16 (as an example of mature microRNA) was examined by qRT-PCR (Figure 4.1). Although Dicer expression was substantially lower in samples with Dicer knockdown at all four time points, there was no accompanying difference in miR-16 expression. That result might suggest that microRNA half-life in HK-2 cells was longer than the last time point (96 hours). Therefore, a double (sequential) transfection was performed. The cells were transfected with 18 nM siRNA against Dicer or control siRNA, or left untransfected. After 72 hours the transfection was repeated. The cells were lysed and RNA extracted 72 hours later. Dicer and miR-16 expression were analysed by qRT-PCR (Figure 4.2). The double transfection results were similar

to the previous, in that Dicer expression was markedly reduced, whereas the expression of miR-16 was not.

In the next attempt, I tested if higher siRNA concentrations would result in a better inhibition of the microRNA biosynthesis pathway. In addition to 18 nM final siRNA concentration, 30 nM (the most commonly used in the department) and 100 nM (maximum recommended by the manufacturer) concentrations were examined. The analysis was performed 72 hours after transfection by qRT-PCR (Figure 4.3). Again, Dicer expression was clearly reduced, but there was no difference in miR-16 expression, regardless the siRNA concentration.

Assuming that the observed lack of reduction in the microRNA expression was due to incomplete (approximately 70%) downregulation of Dicer, I tried two additional siRNAs specific to Dicer. HK-2 cells were transfected with all three kinds of siRNAs separately or in combination. After 72 hours, Dicer and miR-16 expression was examined by qRT-PCR (Figure 4.4). Even though Dicer knockdown was slightly more efficient when using the new siRNAs, it was still not sufficient to cause a difference in miR-16 expression.

As it was conceivable that the change in Dicer expression at the mRNA level was not followed by a change in the actual protein concentration, I also looked at Dicer at the protein level. The cells were transfected as previously, using the most effective of the three siRNAs. Subsequently, Dicer protein was examined by Western blot (Figure 4.5). The results confirmed the considerable downregulation of Dicer by the siRNA, yet the protein was still detectable.

Inhibition of TRBP (alone or together with Dicer)

Since inhibition of Dicer on its own did not result in the expected decrease in microRNA expression, another gene involved in microRNA biogenesis was silenced – alone or in combination with Dicer. The selected gene was TRBP (the human immunodeficiency virus transactivating response RNA-binding protein), known to co-operate with Dicer in the process of microRNA loading into the miRISC complex [199]. Moreover, TRBP has been shown to stabilise Dicer posttranscriptionally, and its knockdown in HeLa cells resulted in reduction of expression of various microRNAs, including miR-16 [199].

HK-2 cells were transfected with siRNA specific to TRBP, Dicer, or both at the same time. After 72 hours, expression of TRBP, Dicer, and three microRNAs of different abundances in HK-2 cells (miR-16, miR-26a, miR-200b) was examined by qRT-PCR (Figure 4.6). Despite substantial downregulation of both Dicer (75%) and TRBP (60%), the three microRNAs were unaffected.

4.2.2 Long-term knockdown of Dicer or GW182 with shRNA

Dicer downregulation

One of possible reasons why the transient Dicer knockdown with siRNA did not have any impact on microRNA expression was that the microRNAs could have especially long half-lives in HK-2 cells. In such situation, only long-term inhibition of Dicer would result in noticeable microRNA reduction. Therefore, HK-2 cells were stably transfected with short-hairpin RNA (shRNA) designed to silence Dicer (based on the best Dicer-specific siRNA) or control shRNA, as described in Methods. Dicer and miR-16 expression was examined 3, 19, and 43 days after transfection in a mixed population of stably transfected cells by qRT-PCR (Figure 4.7). In cells expressing Dicer-specific shRNA, Dicer expression was decreasing with time, but there was still no effect on miR-16.

Subsequently, single lines that stably express Dicer-specific shRNA were selected as described in Methods. About two months after transfection, cells were lysed and RNA extracted from six single lines. For comparison, also mixed populations of cells stably transfected with Dicer-specific or control shRNA were used. As the cell lines differed in their growth rate (three quickly, and three slowly growing), cell confluence and their number was only approximately equal in all samples at the time of the lysis. Therefore, instead of choosing a single endogenous control for qRT-PCR, like in the majority of experiments, six genes listed as possible endogenous controls by Applied Biosystems were used. These included GAPDH, RPLPO, TBP, B2M,

HPRT1, and U6. After leaving out B2M, which was unexpectedly upregulated in one of the samples, the signal from the other controls was averaged and used for normalisation of Dicer, miR-16, miR-26a, and miR-200b expression (Figure 4.8). The results showed that even in the line with the greatest downregulation of Dicer (78% knockdown), microRNA expression was not affected.

Attempt to reduce GW182 expression

As Dicer and TRBP knockdown did not cause the expected inhibition of microRNA biosynthesis, GW182, acting downstream of those genes, was then chosen for knockdown. GW182 is a component of the miRISC complex. It directs the complex together with a target mRNA to P-bodies, where the mRNA is either stored (but not translated) or degraded [222]. It has been shown that GW182 is required for microRNA function and its knockdown impairs silencing of reporters containing microRNA-binding sites in their 3'UTR [200].

Using siRNA sequence from that report [200], plasmid containing GW182-specific shRNA was constructed. HK-2 cells were stably transfected with that or control shRNA. After 2 or 25 days the cells were lysed and expression of GW182 was analysed by qRT-PCR (Figure 4.9). Since the change in GW182 expression was very small, the impact of GW182 knockdown on microRNA activity was not examined.

4.3 Discussion

Global inhibition of microRNA synthesis or function in HK-2 cells, if successful, would be a valuable tool for investigation of microRNA role in renal fibrosis. Firstly, it could confirm that microRNAs are not just expressed, but also functional in the kidney. Secondly, it would be possible to tell which of the processes contributing to the fibrosis are controlled by microRNAs.

Despite a considerable Dicer downregulation by siRNA or shRNA, microRNA expression was not changed in any of the attempts described above. The most likely explanation is that the remaining ~25% of Dicer was enough to perform all its functions in HK-2 cells. If that was the case, the improvement of knockdown efficiency could solve the problem. In fact, RNA interference, although previously employed successfully by other groups [198], is not an ideal method to achieve Dicer knockdown. Dicer is used in both siRNA and microRNA pathways, so I attempted to silence the machinery necessary for gene silencing.

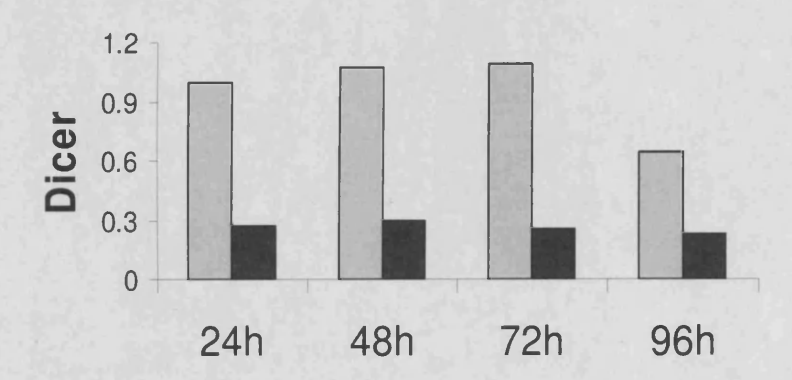
Among other strategies that have been used so far, blocking Dicer translation with a modified oligonucleotide complementary to the translation initiation start within Dicer mRNA seems to be very promising. However, this could be used only for short term experiments, so it would not be efficient in cells with long-lived microRNAs.

Another conceivable method would be a targeted disruption of the human Dicer locus in HK-2 cells using AAV vector. Interestingly, in the study describing this approach, only 55 of 97 detected microRNAs were found to be significantly downregulated in cells lacking functional Dicer [223]. Similarly, conditional Dicer knockout

in mouse retina demonstrated that biogenesis of some microRNAs is more Dicerdependent than of the others [224]. Perhaps, the lack of effect of Dicer inhibition on the expression of select microRNAs reflects the fact that another gene of similar function to Dicer exists in mammals.

Experiments demonstrating effects of global microRNA downregulation in a studied model were very popular a few years ago. Their main purpose was to show that microRNAs play a role in a particular organ or process. Nowadays, it is generally accepted that regulation by microRNAs is remarkably widespread. Therefore, instead of wondering if microRNAs are involved in process X, researchers would rather ask now which of them are involved in X and what their mRNA targets are. These are also the questions I will address in the next chapter.





В

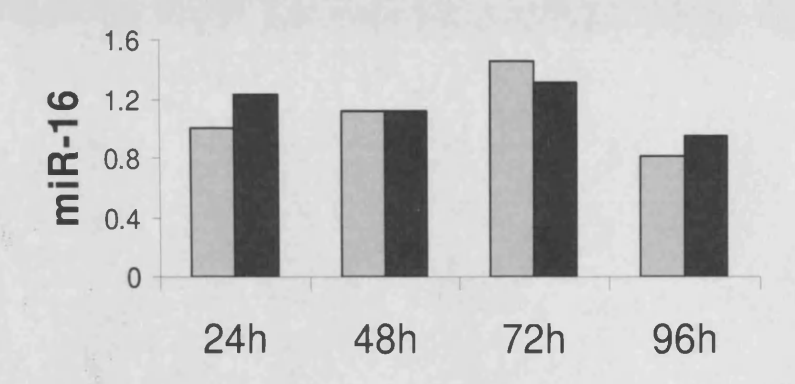
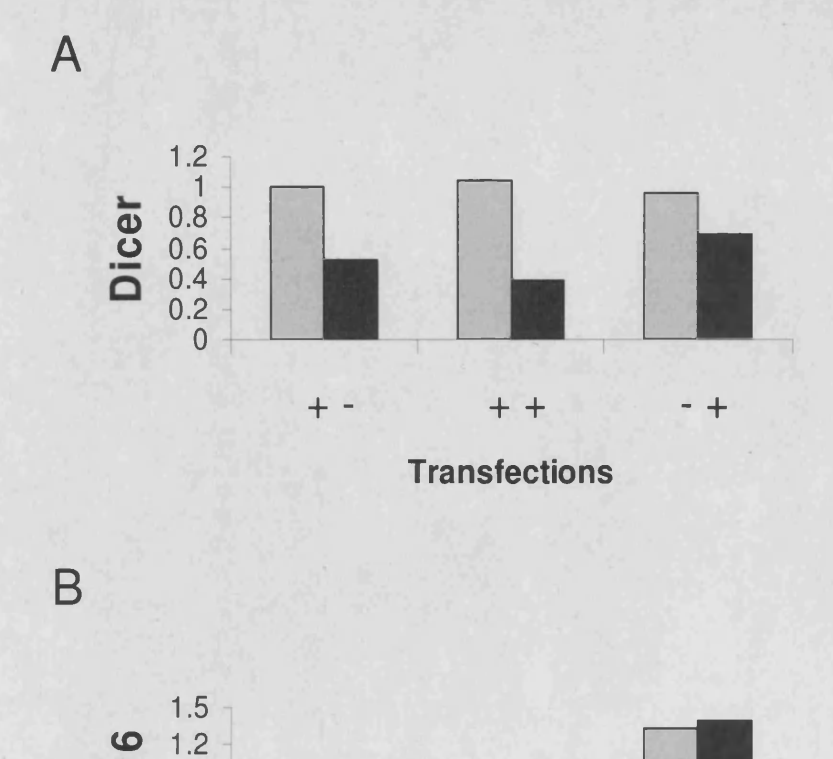
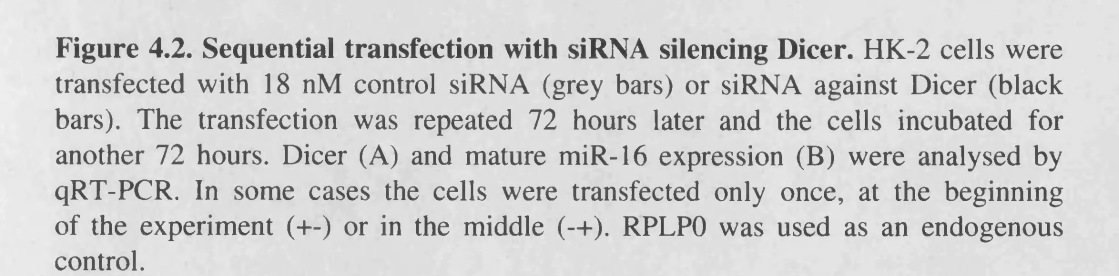


Figure 4.1. Transient Dicer knockdown – time course. HK-2 cells were transfected with 18 nM control siRNA (grey bars) or siRNA against Dicer (black bars). Expression of Dicer (A) and mature miR-16 (B) was examined 24, 48, 72, or 96 hours after transfection by qRT-PCR. RPLP0 was used for normalisation.

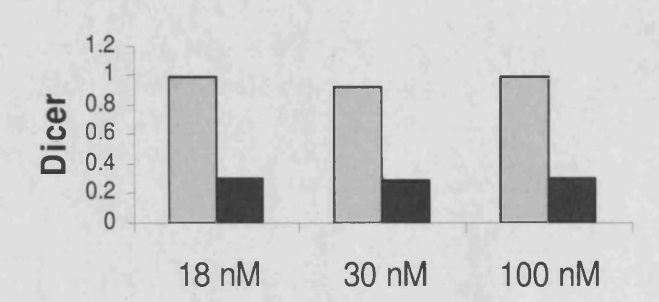


0.9 0.6 0.3



Transfections

Α



В

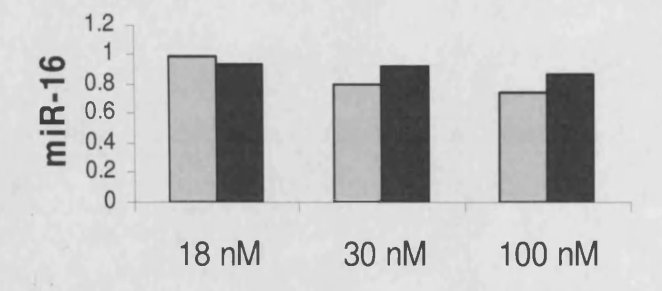
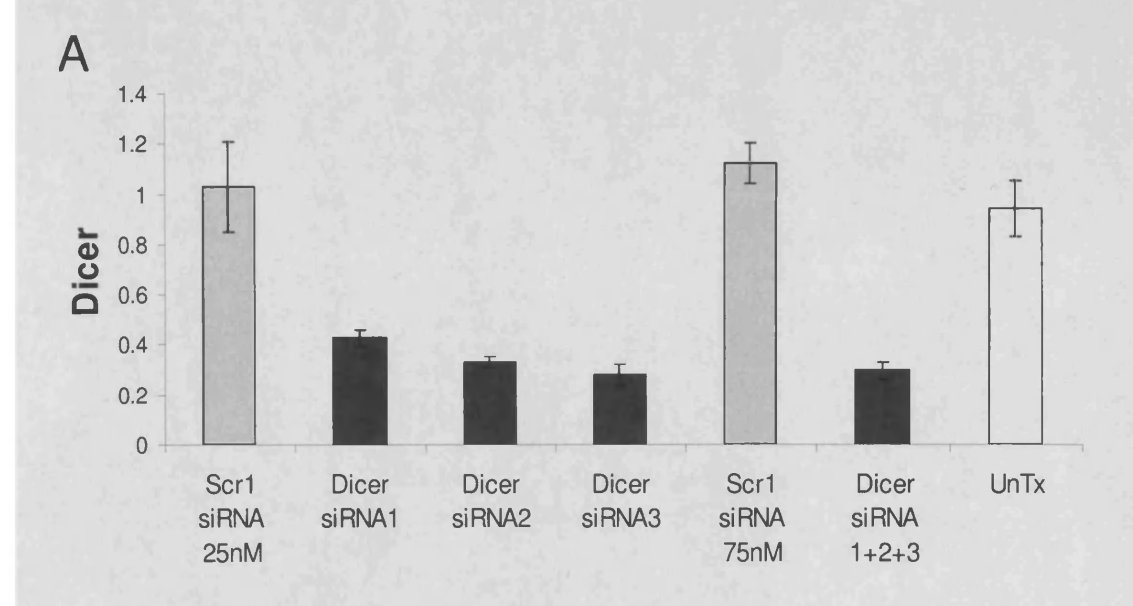


Figure 4.3. Transient Dicer knockdown – dose response. HK-2 cells were transfected with indicated concentrations of control siRNA (grey bars) or siRNA silencing Dicer (black bars). Expression of Dicer (A) and mature miR-16 (B) was measured 72 hours later by qRT-PCR. RPLP0 was used as an endogenous control.



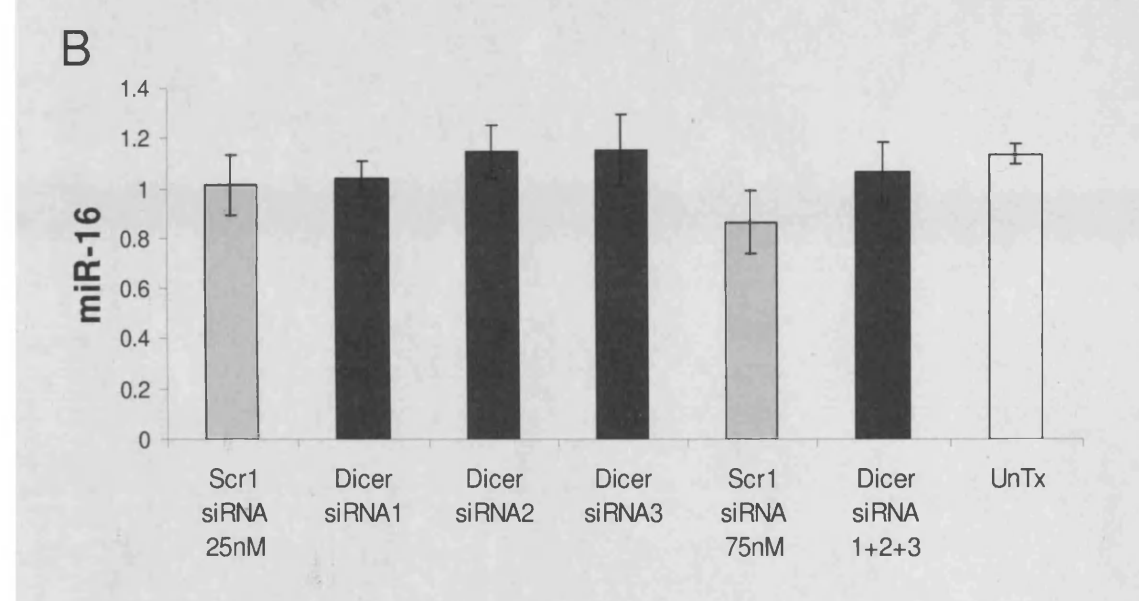


Figure 4.4. Transient Dicer knockdown using three siRNAs against Dicer. HK-2 cells were transfected with 25 nM of siRNA against Dicer (siRNA1-3), alone or in combination. Cells transfected with 25 nM or 75 nM control siRNA (Scr1), and untransfected cells (UnTx) were used as controls. Dicer (A) and mature miR-16 (B) expression was examined 72 hours after transfection by qRT-PCR. RPLP0 was used for normalisation. Averaged values from three independent transfections +/- SEM are shown.

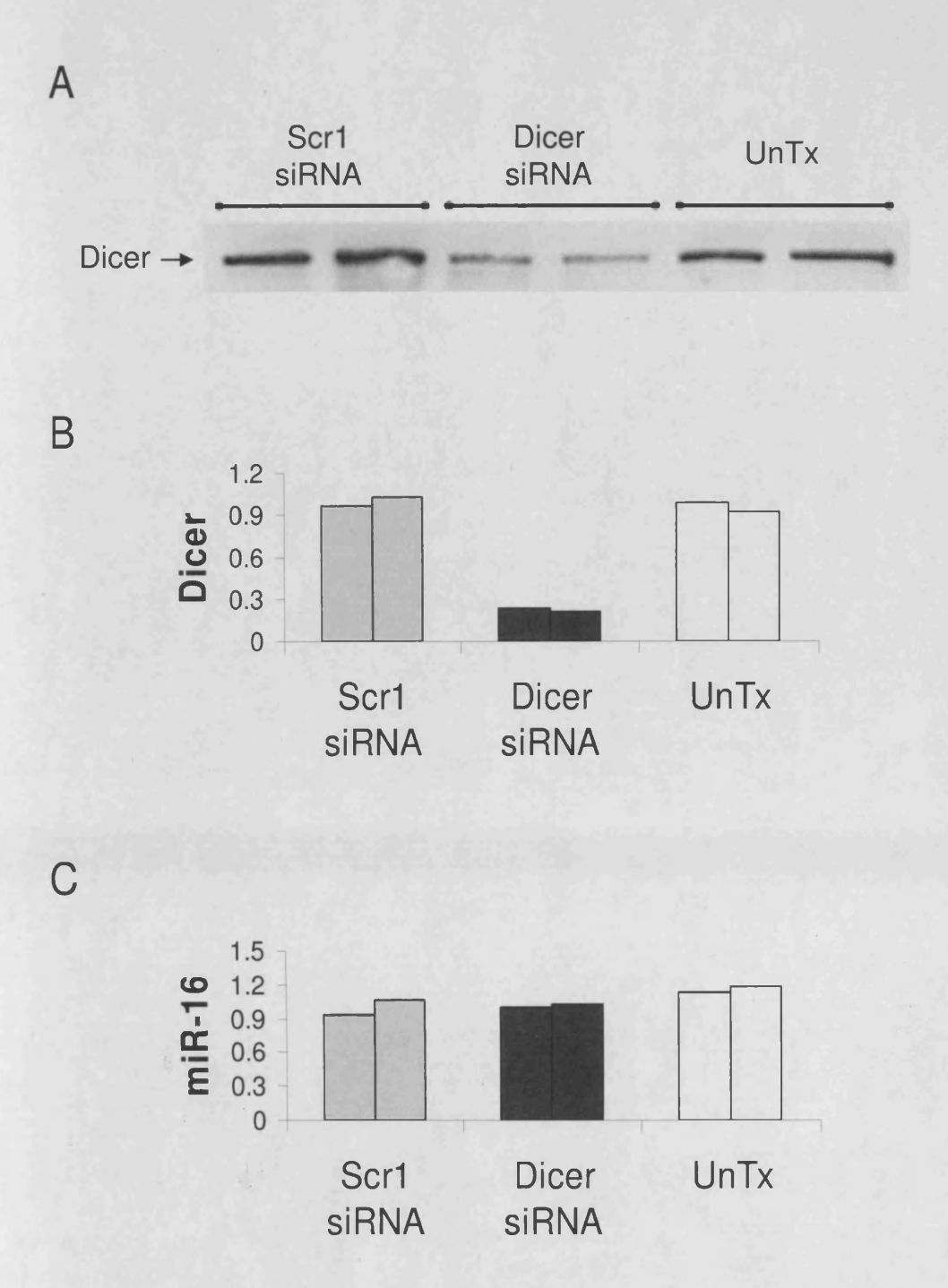


Figure 4.5. Transient Dicer knockdown at the protein level. HK-2 cells were transfected with indicated concentrations of control siRNA (Scr1), siRNA silencing Dicer (siRNA3), or left untransfected. Dicer expression was analysed by Western blot 72 hours later (A). Additionally, expression of Dicer (B) and mature miR-16 (C) was examined by qRT-PCR. The experiment was carried out in duplicate.

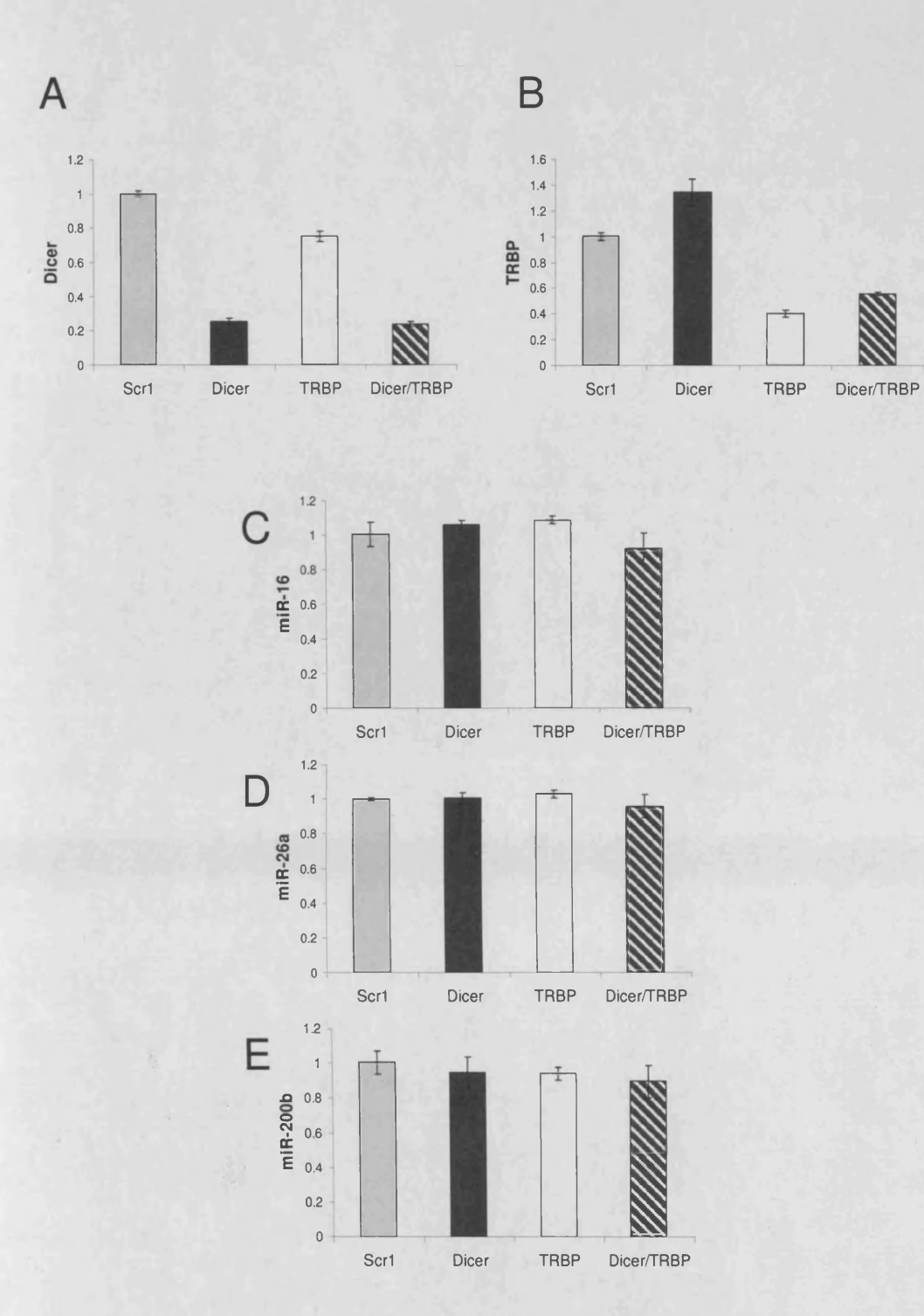


Figure 4.6. Transient knockdown of Dicer and TRBP. HK-2 cells were transfected with 25 nM control siRNA (Scr1), siRNA against Dicer (siRNA3), siRNA against TRBP, or combination of Dicer and TRBP siRNAs. Expression of Dicer (A), TRBP (B), mature miR-16 (C), miR-26a (D), and miR-200b (E) was analysed by qRT-PCR 72 hours after transfection. RPLP0 was used for normalisation. The experiment was performed in triplicate; SEM is shown.

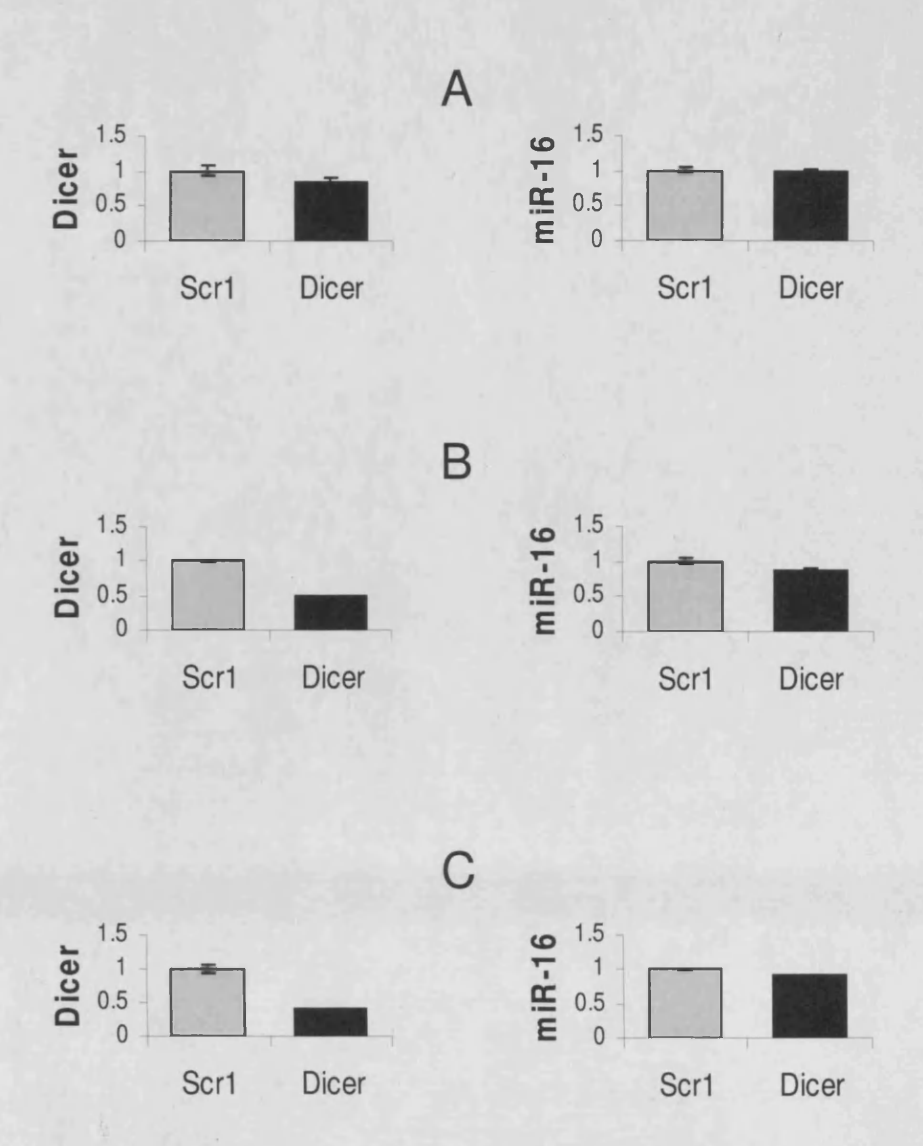
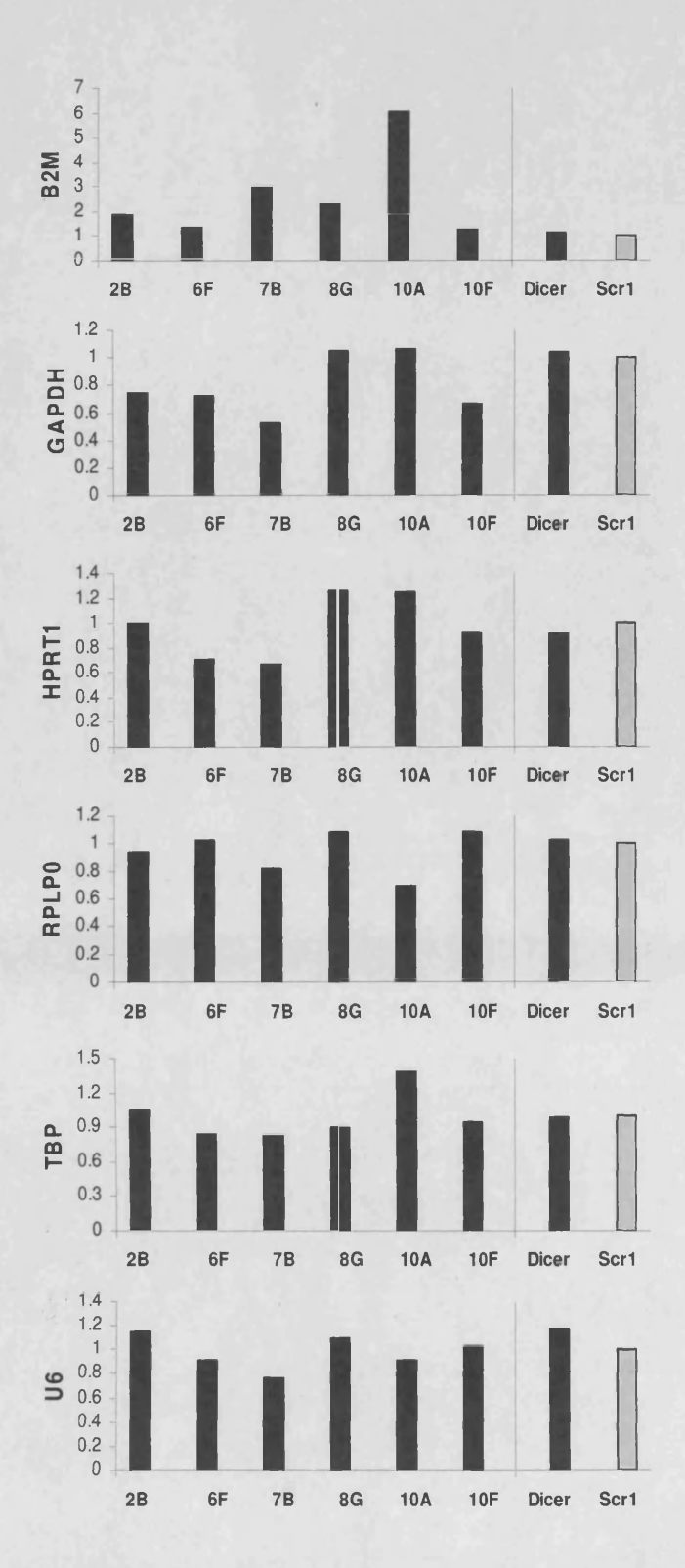


Figure 4.7. Long-term Dicer knockdown. HK-2 cells were transfected with the siSTRIKE U6 plasmid for expression of shRNA silencing Dicer (based on siRNA3) or a control shRNA (based on Scrambled1 siRNA). Expression of Dicer and mature miR-16 was analysed 3 (A), 19 (B), and 43 days (C) after transfection by qRT-PCR in a mixed population of transfected cells. Puromycin was used to eliminate untransfected cells, as described in Methods (see 2.1.1.5). GAPDH was used as an endogenous control. The experiment was performed in triplicate; SEM is shown.





(Continued on the next page)

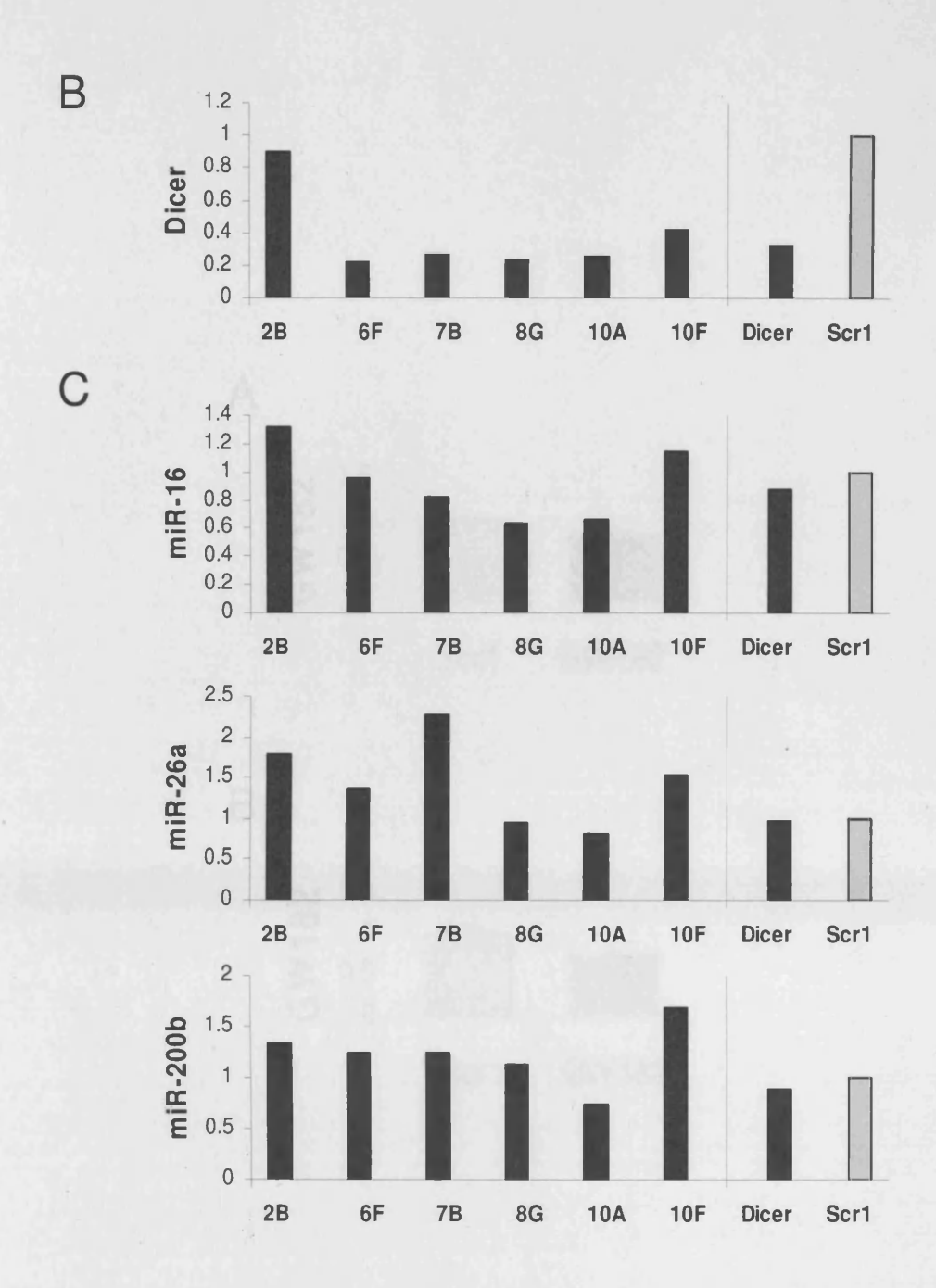
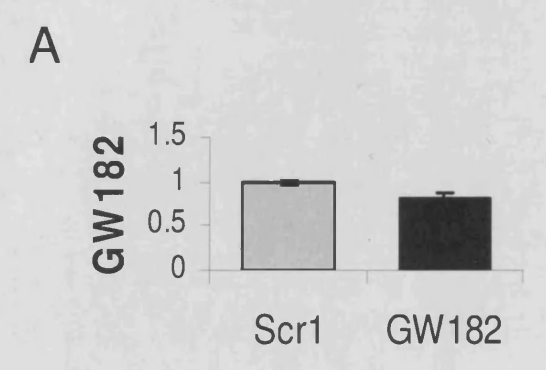


Figure 4.8. Selection of single lines that stably express shRNA silencing Dicer. Single lines were obtained from HK-2 cells stably expressing shRNA against Dicer, as described in Methods (see 2.1.1.5). Three quickly (2B, 6F, 10F), and three slowly growing (7B, 8G, 10A) lines were analysed by qRT-PCR together with mixed populations of cells that stably express shRNA against Dicer or control shRNA (Scr1). Expression of six potential endogenous controls: B2M, GAPDH, HPRT1, RPLP0, TBP, and U6 was examined (A). Dicer (B) and three mature microRNAs (C) were subsequently normalised to the combination of them all except B2M.



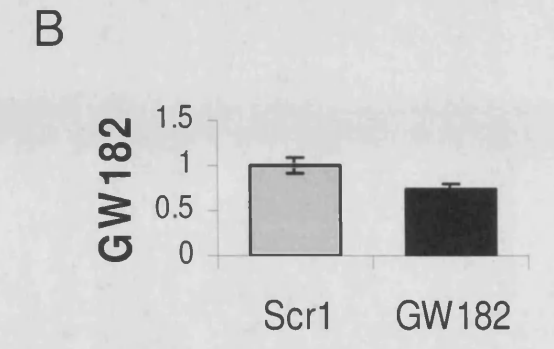


Figure 4.9. GW182 knockdown. HK-2 cells were transfected with the siSTRIKE plasmids for expression of shRNA silencing GW182 or a control shRNA (Scr1). Expression of GW182 was analysed 2 (A), and 25 days (B) after transfection by qRT-PCR in a mixed population of transfected cells. For the longer time point, puromycin was used to eliminate untransfected cells. GW182 expression was normalised to GAPDH. The experiment was performed in triplicate; SEM is shown.

CHAPTER FIVE:

MICRORNA FUNCTION IN THE KIDNEY: THE ROLE OF MIR-192 IN EMT

5.1 Introduction

In Chapter Three I examined microRNA expression in proximal tubular epithelial cell line following treatment with profibrotic stimuli, as well as in renal biopsy samples from patients with diabetic nephropathy. That combined strategy led to identification of miR-192 as a potentially important factor in kidney fibrosis.

Human miR-192 gene was initially predicted by computational methods and subsequently validated experimentally by cloning from human normal colorectal mucosae in 2003 [225]. So far, according to the miRBase release 14 [106], miR-192 homologs have been identified in eleven vertebrate species, from fishes through frogs to mammals.

The precursor of human miR-192 has been localized to an intergenic region on chromosome 11. It forms a microRNA cluster with miR-194, i.e. its primary transcript comprises also of miR-194 precursor, which is located approximately 100 bp apart from pre-miR-192 [226]. This may suggest similar expression patterns for those two microRNAs. In addition, due to similarity of their seed regions, miR-192 and miR-215 are predicted to have similar targets/functions, and therefore constitute one gene family. Notably, expression of all those three microRNAs, miR-192, miR-194, and miR-215, has been reported to be highly specific to the kidney in human [143]. Furthermore, miR-192 and miR-194 have been found enriched in rat renal cortex [147].

The first insight into miR-192 function came from a study by Kato et al. showing that in renal mesangial cells miR-192 contributes to fibrosis by inhibition of ZEB2, one of the E-box repressors, which otherwise binds to the promoter region

of collagen 1-alpha 2 and negatively regulates its synthesis [151]. Interestingly, the E-box repressors are best known for their function in E-cadherin regulation in both cancer and fibrosis contexts [227, 228]. It has been suggested that repression of E-cadherin in renal epithelial cells results in a comprehensive epithelial-to-mesenchymal transition (EMT) [229, 230], which is a key step in fibrogenesis in the kidney. Thus, one might predict that in different settings ZEB2 inhibition by miR-192 may as well prevent renal fibrosis by upregulation of E-cadherin. Indeed, at the American Society of Nephrology Meeting in 2008 another group demonstrated that TGF-beta downregulates miR-192 in mesangial and proximal tubular epithelial cells, as well as in a mouse model of diabetes [154]. In the proximal tubular epithelial cells that was associated with an increase in ZEB2 and downregulation of E-cadherin [154]. Consistent with this, my results showed downregulation of miR-192 after short- or long-term exposure to profibrotic stimuli *in vitro* or *in vivo*, respectively. This drew my attention to EMT.

EMT and its opposite: mesenchymal-to-epithelial transition (MET), are highly conserved processes crucial for morphogenesis in multicellular organisms [231]. During EMT, polarized epithelial cells are converted into motile mesenchymal cells, loosely embedded in an extracellular matrix. An early and, according to some authors, central to EMT change at the molecular level when a cell loses its epithelial phenotype is a decrease in E-cadherin expression, which normally connects epithelial cells via the adherens junctions [231]. The loss of E-cadherin is usually followed by actin reorganization, increase in expression of mesenchymal markers, e.g. vimentin and extracellular matrix genes, and enhanced cell migration and invasion [34].

EMT is regulated by several growth factors, cytokines, hormones, and other extracellular factors in a cell-type-dependent manner. Accordingly, numerous intracellular signal transduction pathways have been reported for EMT, including the TGF-beta pathway, the Wnt pathway, the Notch pathway, and signals from Tyrosine Kinase Receptors [232]. As a result, many genes involved in cellular adhesion, extracellular matrix deposition, cell migration and invasion are transcriptionally altered. The best-studied example is the transcriptional repression of E-cadherin. The promoter region of E-cadherin contains the so-called E-box elements, which in cells undergoing EMT are bound by some of a few zinc-finger transcriptional repressors, called the E-box repressors, such as ZEB1, ZEB2, Snail, Slug, and Twist, depending on the cellular context [231].

In addition to normal development, EMT has been shown to play an important role also in various pathologies, including chronic kidney disease. The presence of EMT in renal fibrosis was first demonstrated in 1995 by Strutz et al. [233]. The authors showed that tubular epithelial cells in a mouse model of anti-tubular basement membrane disease could express Fsp1, a cytoskeleton-associated protein normally expressed by fibroblasts but not epithelia [233]. Subsequent work by Hui Lan's group from the Tokai University, Japan, demonstrated that EMT occurs in rats after 5/6 nephrectomy, as alpha-smooth muscle actin and actin filaments were detected in tubular epithelia of the remnant kidney three weeks after nephrectomy [234]. In accordance with animal studies, epithelial cells with some EMT features have been also observed in human biopsy tissue from various kidney disorders [235, 236]. Importantly, their number was associated with serum creatinine and degree of interstitial damage, suggesting that EMT participates in the fibrotic process in humans [236]. All these studies, however, failed to prove that the cells potentially

undergoing EMT were not in fact an infiltration of interstitial myofibroblasts. It was an elegant work by Iwano et al. [237] that showed, using sophisticated genetic approaches, that interstitial fibroblasts could be derived from tubular epithelial cells after obstructive injury. Moreover, the authors estimated that among Fsp1-positive fibroblasts in the fibrotic kidney as many as 36% are derived from epithelial cells, 14-15% from the bone marrow, and the rest from local proliferation [237]. Considering the fact that EMT leads to an increase in a number of myofibroblasts as well as tubular atrophy, it emerges as an important mechanism in renal fibrosis.

Strong evidence suggests that EMT also promotes tumour progression. Properties of cells that have undergone EMT allow them to detach from the primary tumour, get into the circulation, and eventually re-acquire an epithelial phenotype to form a metastasis. In keeping with that, loss of E-cadherin, the main feature of EMT, has been linked to an aggressive phenotype and poor clinical prognosis in various cancers [238, 239]. Remarkably, in 2008 four independent groups, using different models, demonstrated that microRNAs of the miR-200 family prevent EMT by directly targeting the E-box repressors ZEB1 and ZEB2 [240-243].

Since my data suggested that expression of the miR-200 family was not altered in progression of diabetic nephropathy, and miR-192 has been ultimately shown to target both ZEB1 and ZEB2 [151, 244], it was conceivable that in the kidney miR-192 might play a major role in regulation of EMT. The aim of the present chapter was to investigate this possibility.

5.2 Results

5.2.1 Characterisation of HK-2 cell response to TGF-beta

To facilitate subsequent investigation of miR-192 role in EMT, I set out to further characterise TGF-beta-induced changes in HK-2 cells.

In the initial experiment, HK-2 cells were stimulated with 10 ng/ml TGF-beta for 96 hours. At that time the morphology of the treated cells, as seen under a microscope, was evidently altered; the cells were bigger and their shape resembled that of fibroblasts (this has been reported previously by numerous groups; for example see Figure 2a in [241]). RNA extracted from those cells was analysed by qRT-PCR (Figure 5.1).

Firstly, it was important to select a proper endogenous control for normalisation of the genes of interest (Figure 5.1A). Seven genes commonly used as endogenous controls in various systems were tested: ACTB, B2M, GAPDH, HPRT1, RPLP0, TBP, and TFRC. Among these, B2M, RPLP0, and GAPDH were identified as the most stable genes by geNorm VBA applet for Microsoft Excel [195], as described in Methods. In the next experiments involving HK-2 cell stimulation with TGF-beta, GAPDH was typically used.

Having chosen the endogenous control, I examined expression of EMT markers: E-cadherin, vimentin, and PAI-1 (Figure 5.1B). In cells stimulated with TGF-beta, the epithelial marker E-cadherin was profoundly downregulated (31% remaining), while the both mesenchymal markers were significantly upregulated (1.6- or 64-fold

increase in vimentin or PAI-1, respectively). The data confirmed that TGF-beta induced changes characteristic to EMT in HK-2 cells.

Then, expression of the two E-cadherin repressors ZEB1 and ZEB2, reported to be regulated directly by miR-192 and the miR-200 family, was examined (Figure 5.1C). ZEB2 was almost 2-fold upregulated by TGF-beta, while ZEB1 was not increased at the mRNA level.

Subsequently, the analysis was repeated on cells treated with TGF-beta for 12, 24, 48, or 96 hours (Figure 5.2). The results demonstrated that expression of the majority of the tested genes was similar at the consecutive time points. The exceptions were E-cadherin, gradually decreasing with time in TGF-beta-treated cells, and ZEB1, which was modestly upregulated at 24 hours.

5.2.2 Manipulation of miR-192 (and miR-200b) expression in HK-2 cells

To investigate the role of miR-192 in TGF-beta-induced EMT in HK-2 cells, its expression was altered in those cells by transfection with a specific inhibitor or, in separate experiments, its precursor. Manipulation of miR-192 expression in HK-2 cells was combined with stimulation with TGF-beta to answer two related questions:

- i. Does miR-192 inhibition reproduce the effects of TGF-beta?
- ii. Does miR-192 overexpression prevent the effects of TGF-beta?

Additionally, to determine if the miR-200 family is involved in regulation of EMT in the kidney, miR-200b (the most abundant member of the miR-200 family in HK-2 cells) was studied in parallel.

Inhibition of miR-192 and miR-200b

For inhibition of miR-192 and miR-200b, chemically modified single stranded nucleic acids complementary to the microRNAs (Anti-miR miRNA Inhibitors, Ambion) were used. HK-2 cells were transfected with the inhibitors at final concentration 100 nM (the maximum dose recommended by the manufacturer). Expression of E-cadherin, ZEB1, and ZEB2 was analysed 48 or 96 hours later by qRT-PCR (Figure 5.3). No substantial difference in expression of any of the genes tested was found between control cells and those with the blocked microRNAs.

The experiment was repeated with five times higher dose of the miR-192 inhibitor (as found in literature [240]), but no effect on E-cadherin, ZEB1, and ZEB2 was observed (data not shown).

Overexpression of miR-192 and miR-200b

In parallel, the effects of miR-192 or miR-200b overexpression on HK-2 cell response to TGF-beta were studied. To increase the amount of those microRNAs, the cells were transfected with plasmids containing the stem-loop microRNA precursors expressed by the human U6 promoter. Analysis of expression of the mature microRNAs by stem-loop qRT-PCR confirmed that 72 hours after transfection they were clearly upregulated (Figure 5.4). Despite approximately 10-fold or 8-fold increase in miR-192 or miR-200b, respectively, E-cadherin expression was not altered in control and TGF-beta stimulated cells.

Since the plasmids used in that experiment also contained a puromycin resistance gene, it was possible to investigate long-term effects of enforced expression

of miR-192 and miR-200b in HK-2 cells. Approximately four weeks after transfection, E-cadherin expression was analysed by qRT-PCR in control and TGF-beta-treated puromycin-resistant cells (Figure 5.5). This time, although increases in the microRNA expression were very subtle and statistically non-significant, E-cadherin was significantly 5- or over 2-fold upregulated by miR-192 and miR-200b, respectively. Treatment with TGF-beta for 96 hours reduced E-cadherin in all experimental groups. Importantly, the cells with enforced expression of miR-192 expressed after stimulation 2.5 times more E-cadherin than unstimulated control cells.

For more detailed characterisation of the observed effects, the kinetics of changes in miR-192 and E-cadherin expression was examined by qRT-PCR in cells overexpressing miR-192 (Figure 5.6). Consistent with the transient transfection results (Figure 5.4) as well as with the changes observed after four weeks (Figure 5.5), early after transfection there was a great increase in miR-192, but no difference in E-cadherin expression. However, already two weeks after transfection, miR-192 was present only in a slightly higher amount than in control cells, while E-cadherin was markedly upregulated and this increased with time.

To ensure that the observed effect on E-cadherin depends on miR-192 (or miR-200b in Figure 5.5) and not on the sequence of the control short-hairpin RNA used, two other controls were tested in a separate transfection experiment. Mixed population of puromycin-resistant cells transfected with three different controls or miR-192 precursor were analysed four weeks after transfection by qRT-PCR (Figure 5.7). Expression of miR-192 and E-cadherin was similar in all three controls and, consistently with the previous stable transfection, was lower than in cells overexpressing miR-192.

It was very likely that in the mixed population of stably-transfected cells there would be cells producing large amounts of miR-192, as well as those expressing the puromycin resistance gene but no miR-192 precursor. Therefore, single lines that stably overexpressed miR-192 were selected as described in Methods. Three lines with the highest miR-192 expression were used in the subsequent experiments. The same was attempted for miR-200b, but among six preliminarily selected lines, two died before analysis, one was dying at the time, and three others did not express more miR-200b than control. That was consistent with the observation by Hurteau et al. [213], that three weeks after transfection of MDA-MB-231 and A549 cells with miR-200c the cells begun to detach from the plates and died. Therefore, no more attempts to obtain single lines overexpressing miR-200b were made.

Expression of miR-192 and E-cadherin was examined by qRT-PCR in the three single lines overexpressing miR-192 (Figure 5.8). The results demonstrated approximately 5-fold increase in miR-192, and 17-fold increase in E-cadherin in the selected lines in comparison with control. Additionally, miR-192 prevented TGF-beta-induced downregulation of E-cadherin.

To confirm those findings at the protein level, E-cadherin was assessed in control and miR-192 overexpressing single lines, treated or not with TGF-beta for 96 hours, by Western blot (Figure 5.9A) and immunofluorescence (Figure 5.9B). Both techniques clearly showed large increase in E-cadherin in miR-192-overexpressing cells. Moreover, stimulation of cells with TGF-beta reduced E-cadherin, but it was still more abundant than in unstimulated control cells.

To investigate the mechanism responsible for the observed upregulation of E-cadherin, expression of two E-cadherin repressors and validated direct targets

of miR-192 [151, 244], ZEB1 and ZEB2, was examined by qRT-PCR (Figure 5.10A). ZEB1 and ZEB2 were substantially downregulated in all three lines overexpressing miR-192.

The above data was consistent with the hypothesis that miR-192 directly inhibits translation and/or causes degradation of the ZEB1 and ZEB2 transcripts; this in turn results in an increase in E-cadherin expression. To confirm that miR-192 interacts directly with 3'UTR of ZEB1 and ZEB2, reporter plasmids with those 3'UTRs downstream the firefly luciferase coding sequence were constructed as described in Methods, and the effect of miR-192 overexpression on the luciferase activity was examined (Figure 5.10B). Unexpectedly, I found no difference in translation of transcripts with 3'UTR of ZEB1 or ZEB2 between control cells and those stably expressing miR-192 precursor.

Finally, expression of the other two EMT markers, vimentin and PAI-1, was analysed in cells overexpressing miR-192 by qRT-PCR (Figure 5.11). ZEB2 has been shown to contribute to vimentin regulation in breast cancer [245]. Consistent with that, vimentin expression decreased in unstimulated cells that overexpressed miR-192. However, miR-192 largely failed to prevent TGF-beta-mediated vimentin upregulation. Also PAI-1 expression was unaffected by miR-192, suggesting that the effect of miR-192 on E-cadherin was specific, and did not represent a general opposition of TGF-beta-dependent effects.

5.3 Discussion

In Chapter Three I demonstrated decreased miR-192 expression *in vivo* in advanced diabetic nephropathy, and *in vitro* in HK-2 cells treated with TGF-beta. The goal of this chapter was to find causal links between loss of miR-192 expression and development of tubulointerstitial fibrosis. EMT is likely to be a key phenomenon in progressive renal fibrosis, downstream of TGF-beta. miR-192 had been shown to directly target ZEB1 and ZEB2 [151, 244], similarly as the miR-200 family members, strongly implicated in prevention of EMT in cancer [240-243]. This led me to study the potential role of miR-192 in maintaining a differentiated epithelial phenotype in proximal tubular cells, and whether its loss contributed to TGF-beta-dependent EMT in these cells.

I used a standard approach for identification of a microRNA function. I attempted to inhibit miR-192 in HK-2 cells by a complementary oligonucleotide and check if this could reproduce TGF-beta effect on the main EMT marker E-cadherin. In parallel, I tested if miR-192 overexpression in HK-2 cells would prevent TGF-beta-induced EMT-like changes in those cells.

The inhibition experiments did not reveal any difference in E-cadherin expression after miR-192 blockade. The most obvious explanation for this would be that the technique (either the inhibitor delivery or its interaction with miR-192) did not work properly. As there was no method available, other than functional assays, to confirm that, alternative explanations should also be considered. For instance, miR-192 inhibition alone might have not been sufficient for E-cadherin downregulation; perhaps other TGF-beta-induced changes, such as modulation

of the E-box repressors other than ZEB1 and ZEB2, were necessary or could accelerate miR-192 action. Maybe in transient transfection there was not enough time for the changes to occur. Finally, miR-192 might have not been involved in regulation of E-cadherin. In light of the overexpression results, however, this option seems very unlikely.

Enforced expression of miR-192 also did not cause any change in E-cadherin expression in a short term. To my knowledge, ZEB1 and ZEB2 protein half-lives have not been investigated in HK-2 cells. Therefore, it is difficult to predict when the effects of miR-192 on ZEB1 and ZEB2 would result in detectable E-cadherin upregulation. My results suggest that this happens between one and two weeks after transfection. However, the data comes from a mixed population of stably transfected cells, some of them not expressing miR-192, so one could expect that in cells expressing high amounts of supplementary miR-192, the increase in E-cadherin may be visible earlier. This highlights the main advantage of using single lines rather than a mixed population of transfected cells. For that reason, the major experiments in this chapter were done on single lines stably overexpressing miR-192.

In those lines, E-cadherin expression was found to be profoundly upregulated both at mRNA and protein levels. Most importantly, miR-192 prevented E-cadherin downregulation by TGF-beta. It would be tempting to speculate that miR-192 introduction into the kidney of patients with a chronic kidney disease might be useful in stopping the progression of the disease. However, miR-192 overexpression did not seem to affect the whole process of EMT, as judged by lack of effect on the other EMT markers tested. Furthermore, miR-192 has been shown to be upregulated in animal models of diabetic nephropathy and have a profibrotic effect in murine mesangial cells [151]. Interestingly, the authors of that report have demonstrated that

miR-192 exerted its profibrotic effect in mesangial cells via downregulation of ZEB2, showing that miR-192 function in the kidney is very complex and context-dependent.

The most likely mechanism of the upregulation of E-cadherin in miR-192-overexpressing cells includes inhibition of ZEB1 and ZEB2 by miR-192; subsequently, lower amounts of those repressors would result in an increased E-cadherin transcription. This hypothesis was based mainly on the reports demonstrating that miR-192 directly targets ZEB1 and ZEB2 [151, 244], and the massive evidence showing that ZEB1 and ZEB2 negatively regulate E-cadherin transcription [227, 228]. Consistently, ZEB1 and ZEB2 are both markedly downregulated at the mRNA level in miR-192-overexpressing HK-2 cells. Additionally, the work of my colleague, Dong Dong Luo, shows that the other transcriptional repressors of E-cadherin previously implicated in EMT, namely Snail, Slug, and Twist, or their regulator HMGA2 [246] are not influenced by miR-192 overexpression [204].

Surprisingly, the attempt to confirm that miR-192 directly interacts with 3'UTR of ZEB1 or ZEB2 using reporter plasmids was not successful. Subsequent experiments with those plasmids demonstrated that they also did not respond to TGF-beta (data not shown), suggesting a possible technical problem with the plasmids. Although their sequences were confirmed by sequencing, it has been reported recently that microRNA mechanism of action (whether they affect an initiation or elongation stage of translation) depends on the nuclear history of mRNA, and may differ for identical transcripts if they are derived from different promoters [247]. Perhaps, using a different core plasmid than pGL3 it would be

possible to observe a decrease in ZEB1 and ZEB2 translation in miR-192 overexpressing lines.

Interestingly, and in some way in accordance with the observation by Kong et al. [247], the results presented in this chapter suggest that regulation of exogenous miR-192 expression by TGF-beta depends on whether or not the construct for expression of miR-192 precursor is integrated into the genome. In single lines that stably overexpressed miR-192, it was downregulated by TGF-beta similarly as the endogenous microRNA. Strikingly, in transient transfection with the same plasmid, TGF-beta did not cause any effect on exogenous miR-192 expression.

As stable transfection resembles the natural situation well, it is conceivable that the mechanism of regulation by TGF-beta seen in miR-192-overexpressing lines is at least in part relevant to the regulation of endogenous miR-192 expression. The fact that exogenous miR-192 was markedly downregulated by TGF-beta despite replacement of the natural miR-192 promoter with the constitutive U6 promoter, suggests posttranscriptional regulation of miR-192 by TGF-beta. Recently, TGF-beta has been reported to influence processing of miR-21 precursor via interaction of SMAD proteins with Drosha [119]. It is not known at present how widespread the posttranscriptional regulation of microRNAs by TGF-beta is, but certainly would be worth investigating.

The miR-200 family has been strongly implicated in EMT in cancer [240-243]. Moreover, the described mechanism of E-cadherin regulation by the miR-200 family members was the same as the mechanism proposed above for miR-192. Therefore, it was interesting to see how miR-192 compared with miR-200 in the kidney. For that

reason miR-200b, the most abundant miR-200 family member in HK-2 cells, was functionally analysed together with miR-192. Transient transfections with miR-200b inhibitor or precursor did not affect E-cadherin, similarly as short-term manipulation of miR-192 expression. Due to inability to generate cell lines that stably express miR-200b precursor, also reported in the literature before [213], the effects of miR-200b on HK-2 cell phenotype could not be investigated fully. The obtained results, however, tend to suggest that miR-192 is at least not less important in EMT in the kidney than miR-200b. This notion is supported also by the lack of correlation between severity of renal fibrosis and miR-200b expression, as found in Chapter Three.

In this chapter I showed that miR-192 is involved in control of the early EMT marker, E-cadherin, in proximal tubular epithelial cells, and proposed a likely mechanism for that regulation. The data clearly show that high expression of miR-192 prevents some of TGF-beta-induced changes, and might therefore have implications for future therapies. It is also highly probable that the changes in miR-192 expression observed *in vivo* in the course of diabetic nephropathy are functionally linked to the progression of the disease.



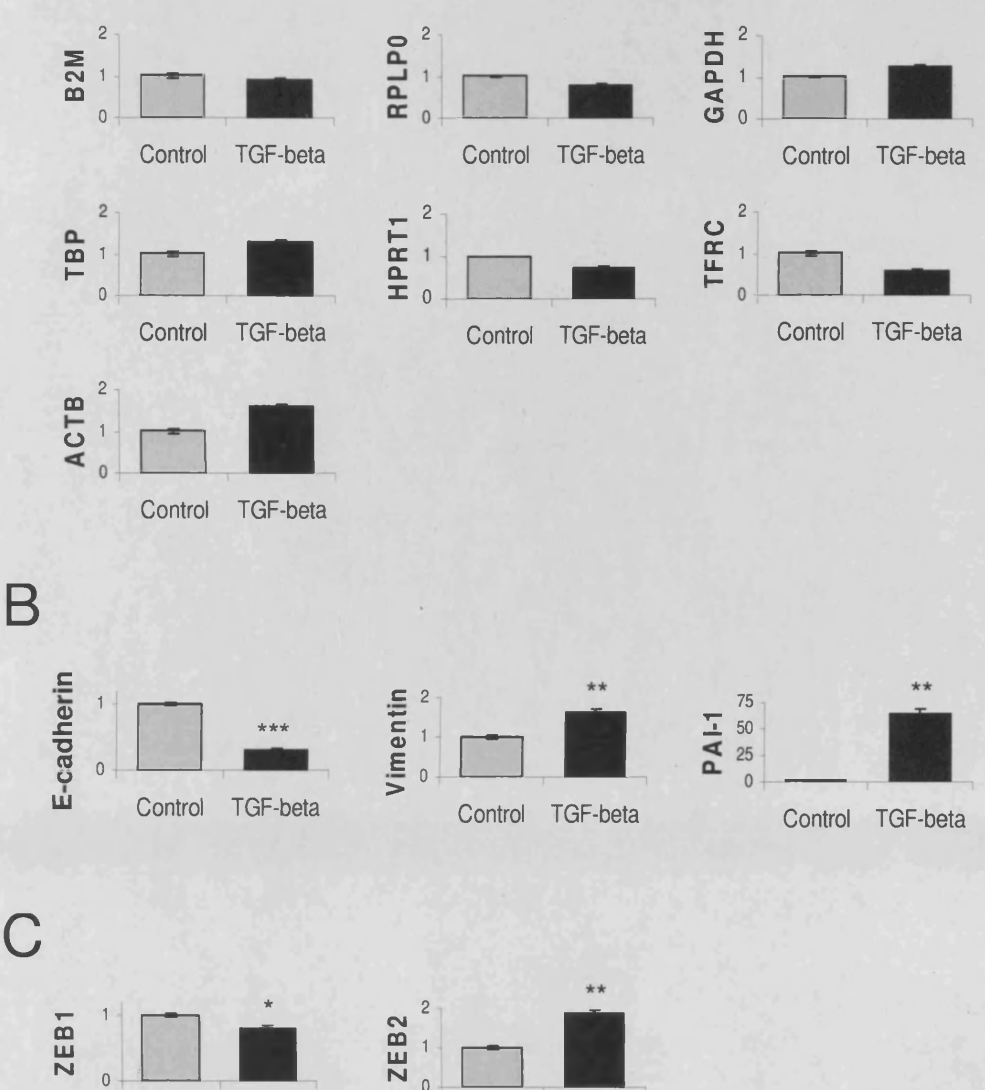


Figure 5.1. Characterisation of HK-2 response to TGF-beta by qRT-PCR. HK-2 cells were cultured without serum for 48 hours, and then incubated with 10 ng/ml TGF-beta (black bars) or control medium (grey bars) for 96 hours. (A) Selection of a suitable endogenous control. The tested genes are shown in order of their relative stability, as found using geNorm [195]. GAPDH was used for normalisation in this and subsequent experiments. (B) Expression of the EMT markers: E-cadherin, vimentin, and PAI-1. (C) Expression of E-cadherin repressors and known miR-192 direct targets: ZEB1 and ZEB2. The experiment was performed in triplicate; SEM is shown. Significance levels are marked with asterisks as follows: *p<0.05, ***p<0.005, ***p<0.0055.

Control

TGF-beta

Control TGF-beta

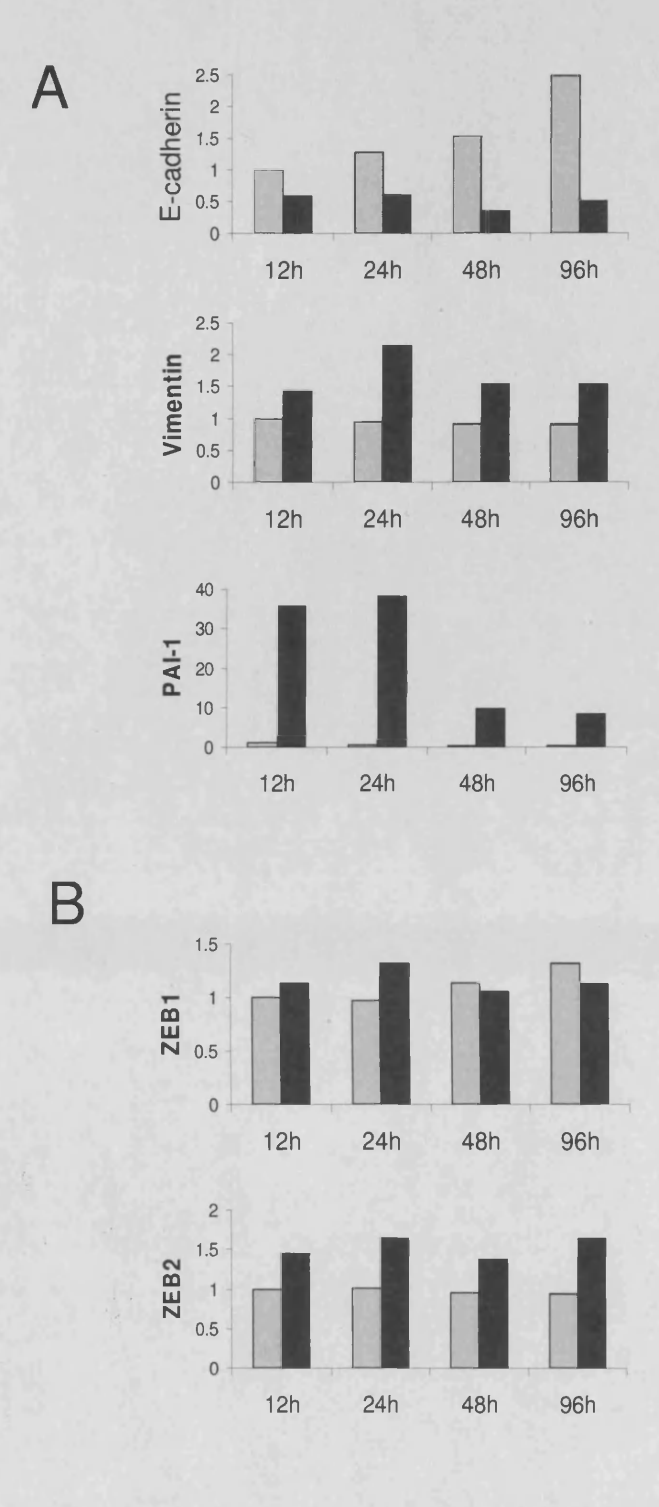


Figure 5.2. Characterisation of HK-2 response to TGF-beta by qRT-PCR – time course. HK-2 cells were cultured without serum for 48 hours, and then incubated with 10 ng/ml TGF-beta (black bars) or control medium (grey bars) for indicated time points. Expression of the EMT markers (A) and the E-cadherin repressors (B) was normalised to GAPDH.

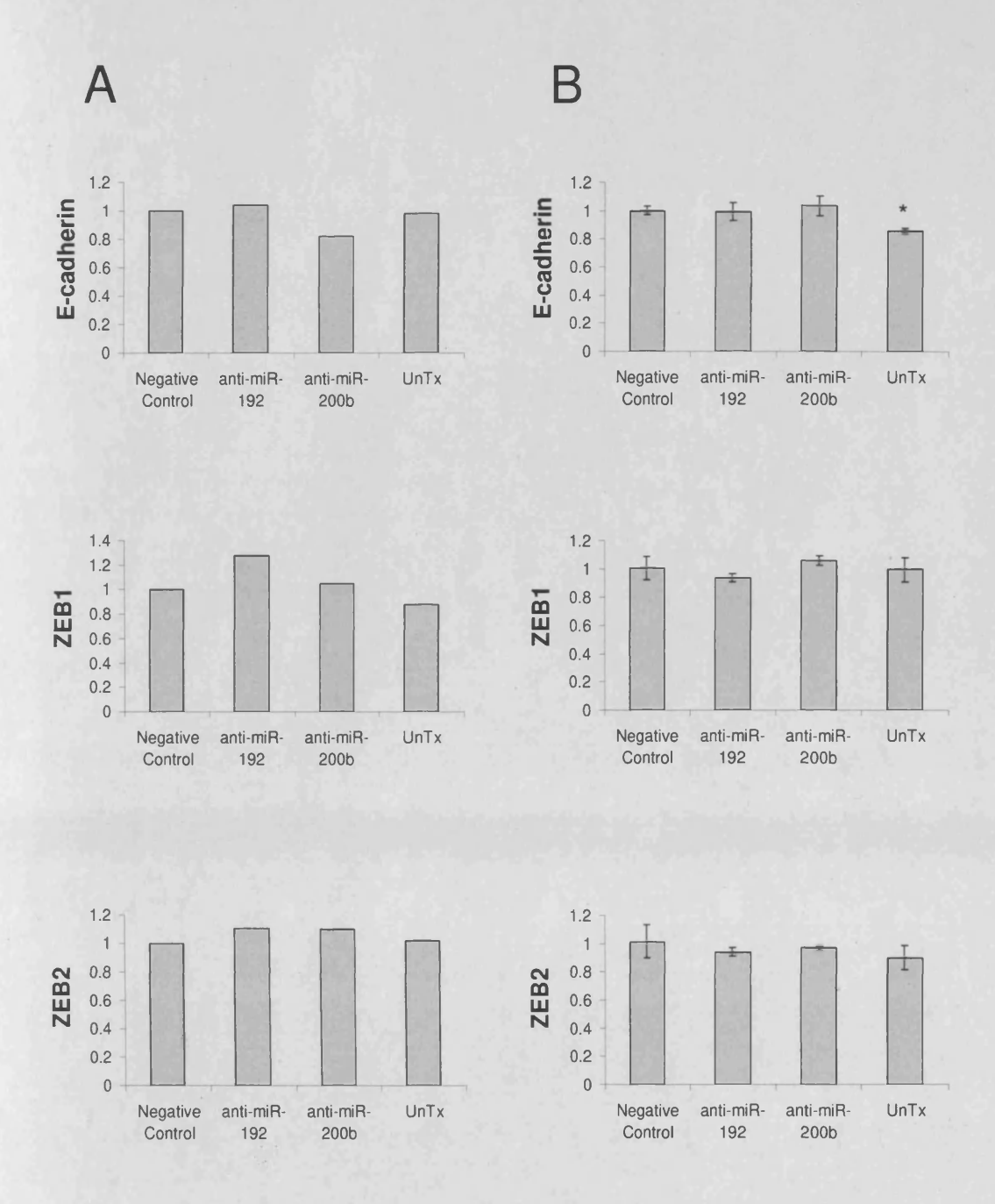


Figure 5.3. Inhibition of miR-192 or miR-200b in HK-2 cells. HK-2 cells were transfected with 100 nM anti-miR-192 or anti-miR-200b inhibitors. Expression of E-cadherin, ZEB1, and ZEB2 was examined by qRT-PCR 48 (A) or 96 hours (B) after transfection. Error bars (B) represent SEM, n=3. A significant difference (p < 0.05) was marked with an asterisk.

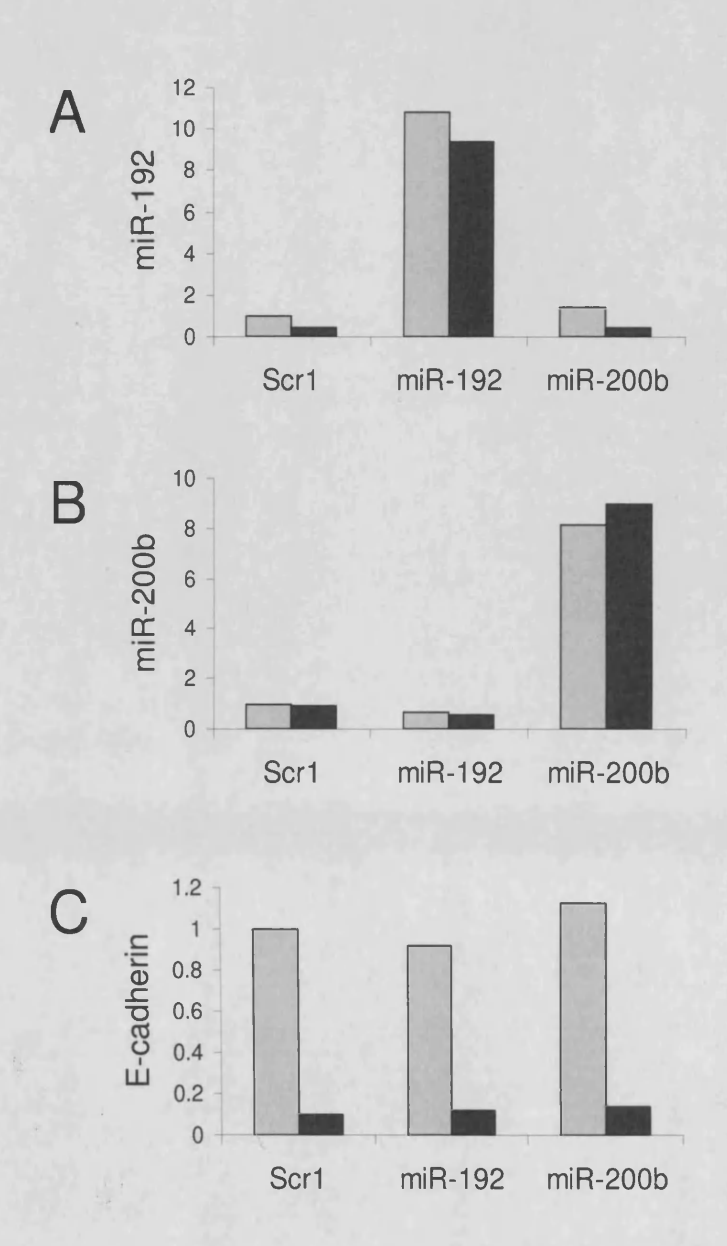


Figure 5.4. Transient overexpression of miR-192 and miR-200b in HK-2 cells. HK-2 cells were transfected with plasmids for expression of miR-192 or miR-200b precursors, or a control shRNA (Scr1), using Lipofectamine LTX+. 24 hours after transfection, they were stimulated (black bars) or not (grey bars) with 10 ng/ml TGF-beta for 48 hours. Expression of mature miR-192 (A) and miR-200b (B) was examined by stem-loop qRT-PCR and normalised to the small nuclear RNA, U6. (C) E-cadherin expression was measured by qRT-PCR and normalised to GAPDH. The experiment was repeated for miR-192.

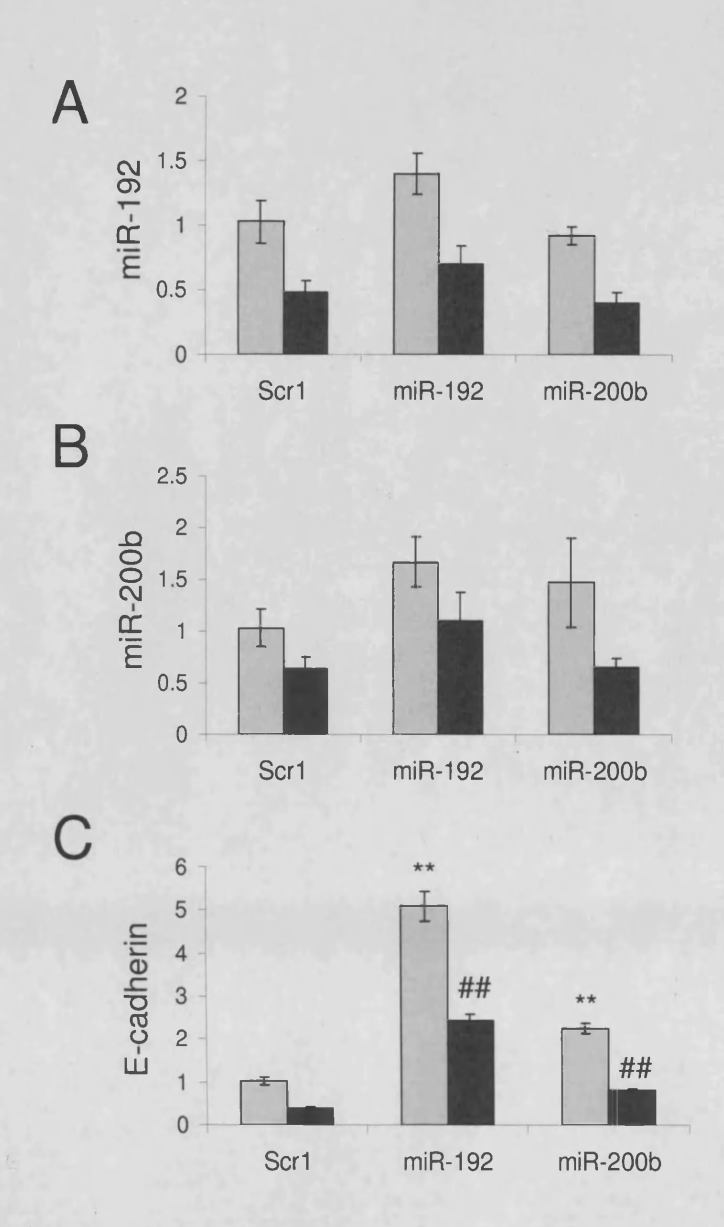
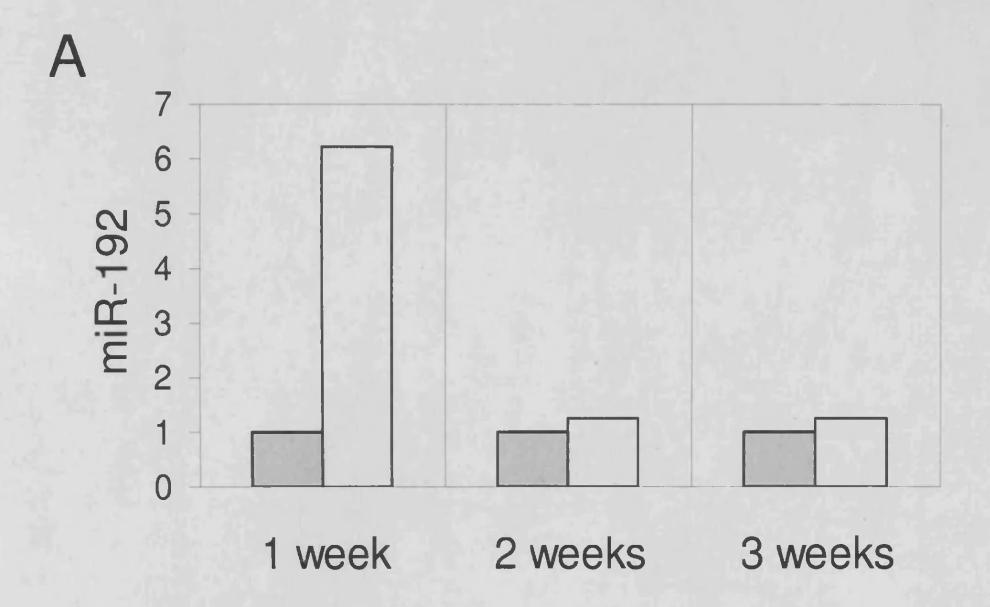


Figure 5.5. Stable overexpression of miR-192 and miR-200b in HK-2 cells. HK-2 cells were stably transfected with plasmids for expression of miR-192 or miR-200b precursors, or a control shRNA (Scr1). Approximately four weeks after transfection, mixed populations of stably transfected cells were cultured in medium without FCS for 48 hours and then stimulated with 10 ng/ml TGF-beta (black bars) or cultured in control medium (grey bars) for 96 hours. Expression of mature miR-192 (A) and miR-200b (B) was examined by stem-loop qRT-PCR and normalised to U6. (C) E-cadherin expression was measured by qRT-PCR and normalised to GAPDH. The experiment was carried out in triplicate; SEM is shown. Significance levels were estimated among TGF-beta-stimulated and unstimulated cells, respectively, and are indicated as follows: ** p < 0.005 (for comparison with unstimulated Scr1), ## p < 0.005 (for comparison with TGF-beta-treated Scr1).



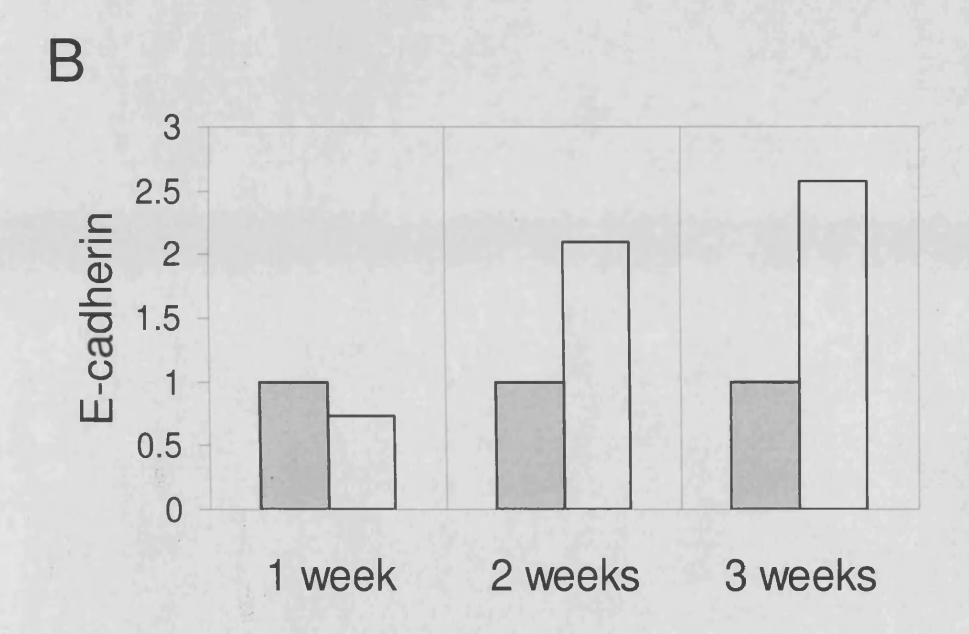
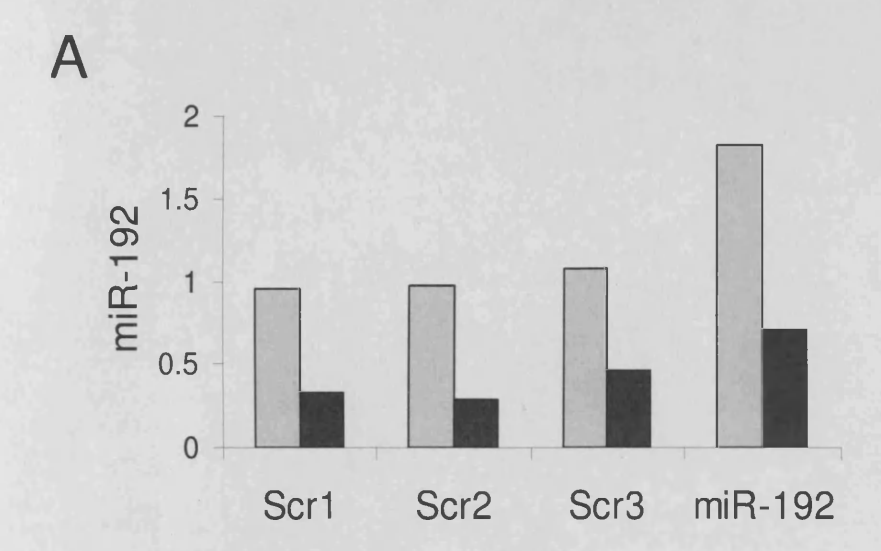


Figure 5.6. Stable overexpression of miR-192 – kinetics. HK-2 cells were stably transfected with plasmids for expression of miR-192 precursor (white bars), or control shRNA (grey bars). Expression of mature miR-192 (A) and E-cadherin (B) was examined one, two, and three weeks after transfection by qRT-PCR. miR-192 was normalised to miR-16, while E-cadherin – to GAPDH.



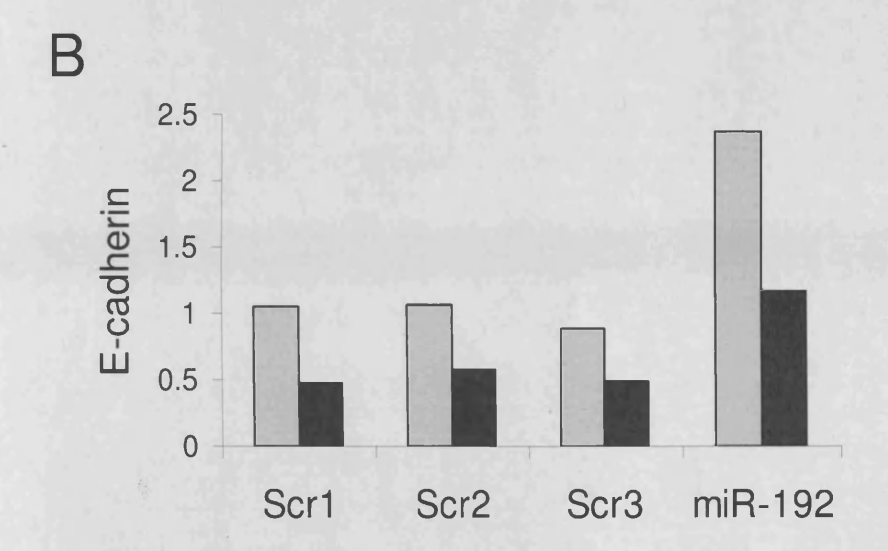
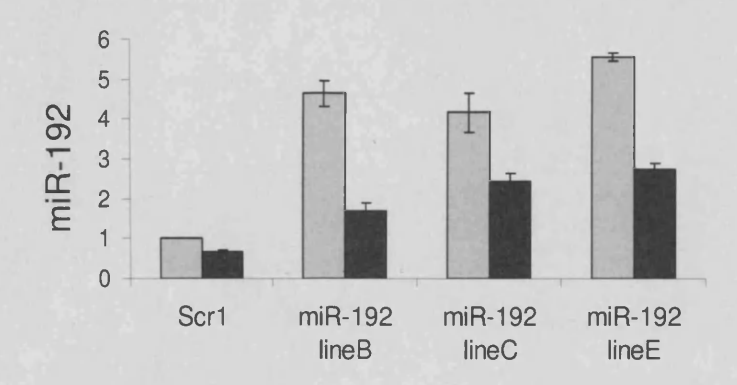


Figure 5.7. Comparison of three shRNAs expressed by control cells in stable transfection experiments. HK-2 cells were stably transfected with plasmids for expression of miR-192 precursors, or three different control shRNAs (Scr1-3). Approximately four weeks after transfection, mixed populations of stably transfected cells were cultured in medium without FCS for 48 hours and then stimulated with 10 ng/ml TGF-beta (black bars) or cultured in control medium (grey bars) for 96 hours. (A) Expression of mature miR-192 was examined by stemloop qRT-PCR and normalised to U6. (B) E-cadherin expression was measured by qRT-PCR and normalised to GAPDH.

A



B

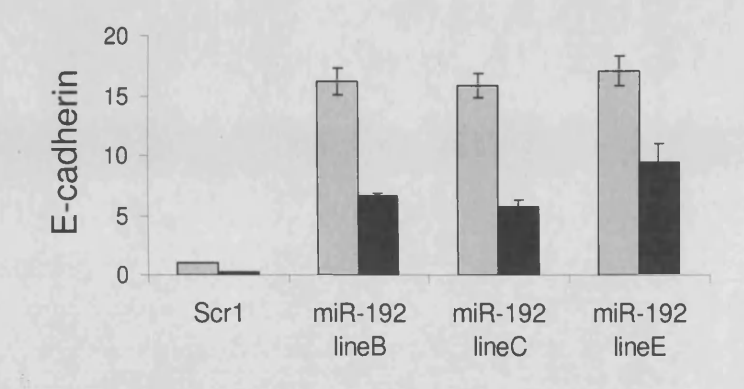
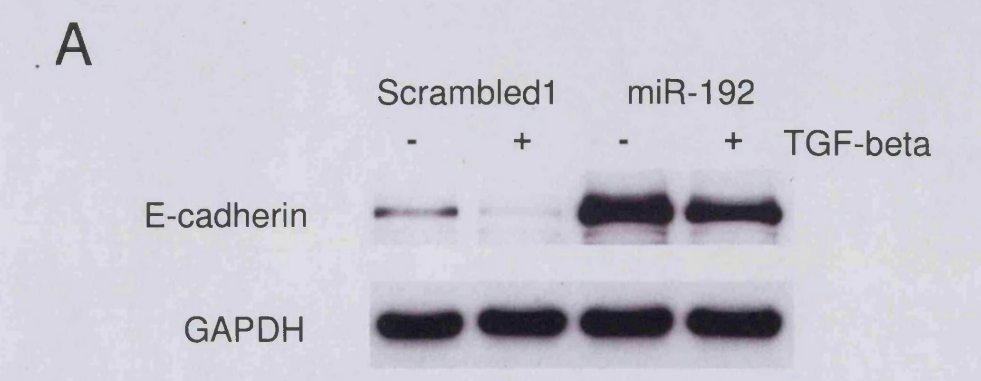


Figure 5.8. Expression of E-cadherin in single lines that stably overexpress miR-192 – at the mRNA level. Single lines stably expressing miR-192 precursor were obtained from the mixed population of stably transfected cells, as described in Methods. Three lines (B, C, E) and mixed Scr1 were cultured in medium without FCS for 48 hours and then stimulated with 10 ng/ml TGF-beta (black bars) or cultured in control medium (grey bars) for 96 hours. Expression of mature miR-192 (A) and E-cadherin (B) was examined by qRT-PCR. miR-192 was normalised to miR-16, and E-cadherin – to GAPDH. The experiment was performed in triplicate; SEM is shown.



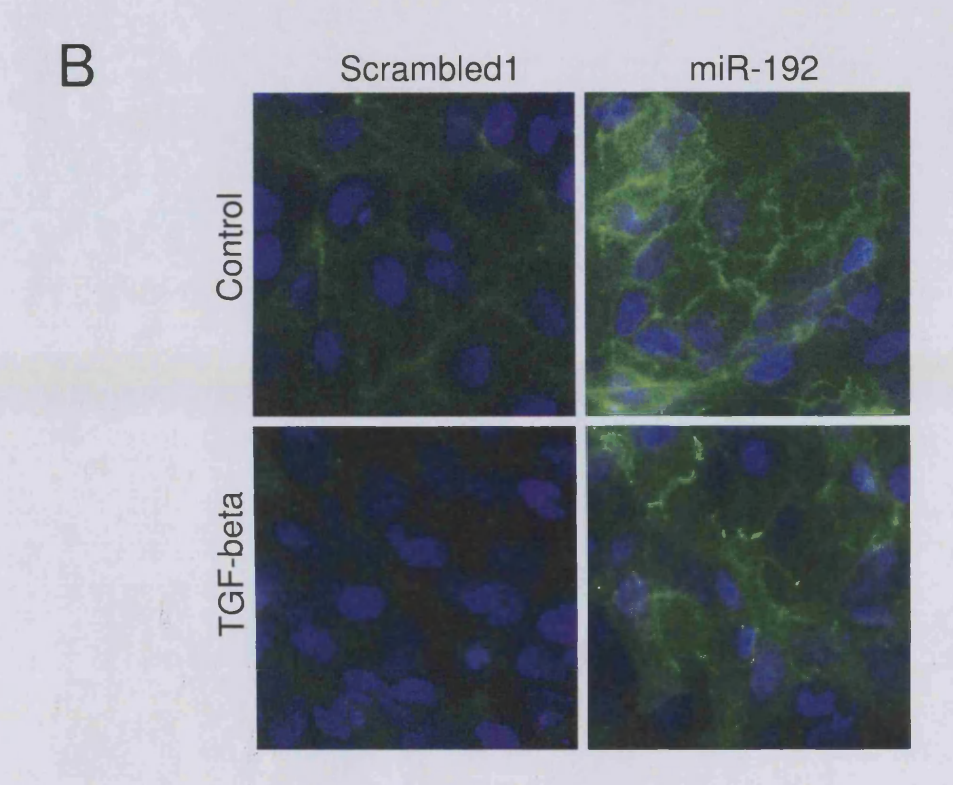


Figure 5.9. Expression of E-cadherin in single lines that stably overexpress miR-192 – at the protein level. Three stable lines with enforced miR-192 expression and control cells (Scrambled1) were prepared and stimulated with TGF-beta as described in Figure 5.8 legend. Then E-cadherin protein was examined by Western blot (A) or immunofluorescence (B). E-cadherin expression in all three lines was similar; only line B is shown. The experiments were repeated at least three times. Magnification in panel B was 400x.

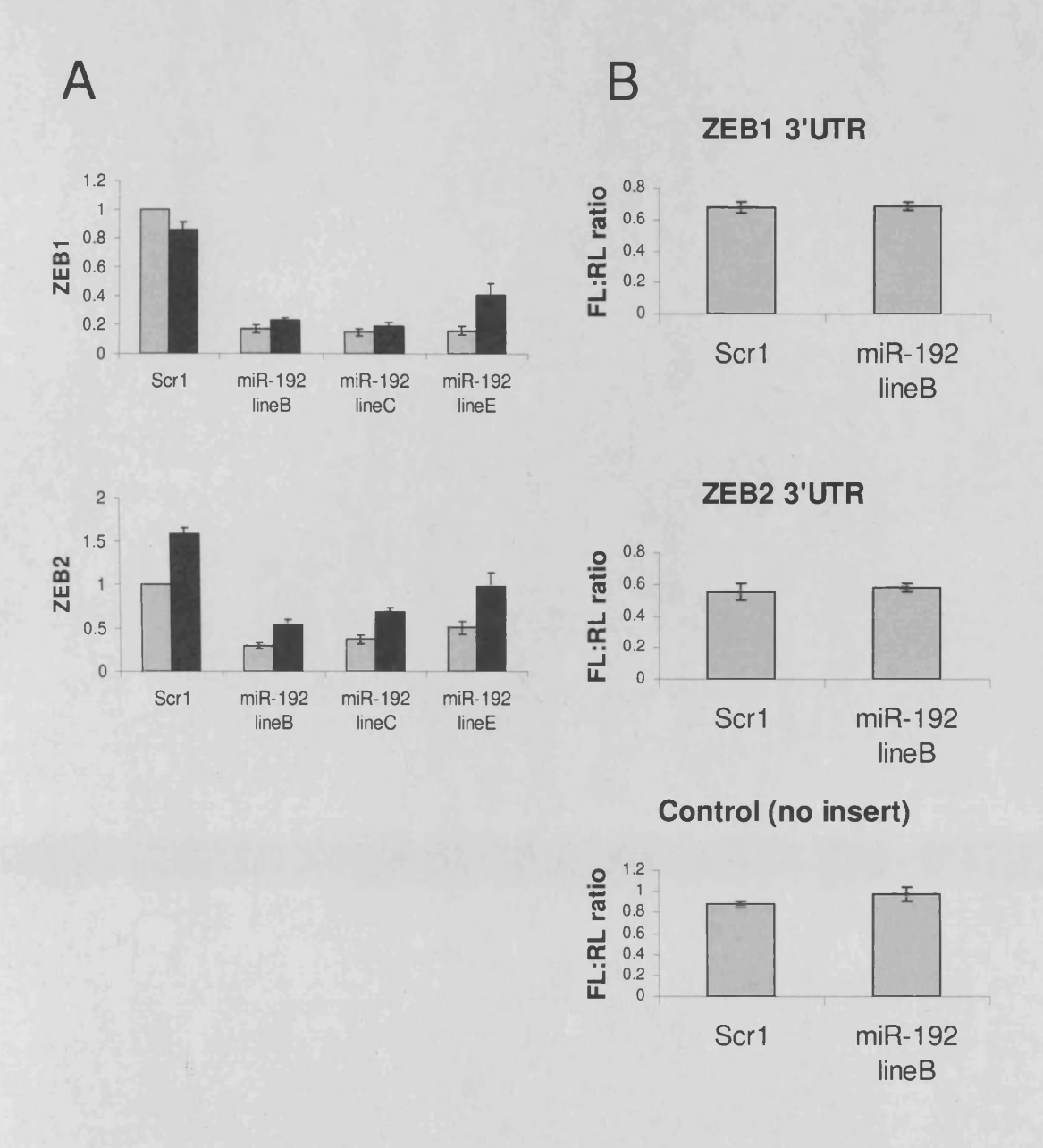
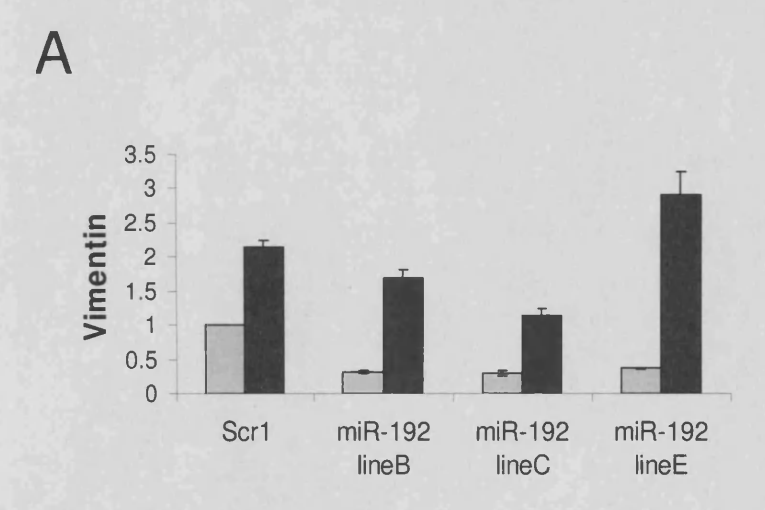


Figure 5.10. Regulation of ZEB1 and ZEB2 expression by miR-192. Three stable lines with enforced miR-192 expression and control cells (Scr1) were prepared as described in Figure 5.8 legend. (A) ZEB1 and ZEB2 expression was examined in control (grey bars) or TGF-beta-treated cells (black bars) by qRT-PCR. GAPDH was used for normalisation. (B) Control cells (Scr1) and one line stably overexpressing miR-192 were transfected with pGL3 reporter plasmids containing ZEB1 3'UTR, ZEB2 3'UTR, or pGL3 without any insert downstream the firefly luciferase CDS. To control for transfection efficiency, pRL plasmid encoding *Renilla* luciferase was used. Activity of firefly and *Renilla* luciferases was measured 24 hours after transfection as described in Methods. The experiments were performed in triplicate; SEM is shown.



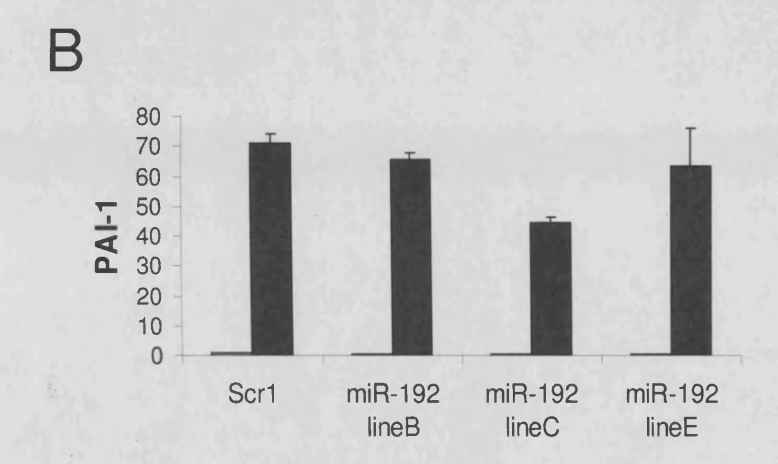


Figure 5.11. Expression of other EMT markers in single lines that stably overexpress miR-192. Three stable lines (B, C, E) with enforced miR-192 expression, and control cells (Scr1) were prepared as described in Figure 5.8 legend. They were cultured in medium without FCS for 48 hours and then stimulated with 10 ng/ml TGF-beta (black bars) or cultured in control medium (grey bars) for 96 hours. Expression of vimentin (A) and PAI-1 (B) was examined by qRT-PCR and normalised to GAPDH. The experiment was performed in triplicate; SEM is shown.

CHAPTER SIX:

ROLE OF MICRORNAS IN POSTTRANSCRIPTIONAL REGULATION OF TGF-BETA SYNTHESIS

6.1 Introduction

TGF-beta plays a crucial role in the initiation and progression of renal fibrosis. Thus, inhibition of its expression seems to be the most obvious therapeutic strategy. That, however, has been proven problematical, mostly because of the complexity of TGF-beta effects on the organism. Despite long and extensive studies on TGF-beta expression and actions, it is still difficult to predict all the outcomes of TGF-beta manipulation *in vivo*. A profound understanding of TGF-beta biology must precede any trials of that kind.

Up to now, numerous studies have shown that regulation of TGF-beta expression occurs at various levels, including the posttranscriptional step [248-250]. The precise mechanisms of such regulation are in most cases not known, and typically the results do not exclude the possibility that microRNAs are involved. In particular, a few years before the discovery of microRNAs, in 1990, Ruth Wager and Richard Assoian reported an RNase system in U937 cells that causes selective degradation of TGF-beta transcript, and is inhibited during phorbol ester-induced differentiation [175]. Looking at the results, one could speculate that the system employs some microRNAs expressed by non-activated U937 cells and downregulated by phorbol esters.

Search for microRNAs potentially targeting TGF-beta mRNA using the most popular microRNA target prediction programs available at the end of 2006 (PicTar, miRanda, TargetScan) gave a negative result. Therefore, my main strategy for identification of TGF-beta-regulating microRNAs relied on the recent (back then) and extremely interesting finding by Gupta et al. that a viral microRNA causes degradation of human TGF-beta transcript [251]. The authors have shown that miR-LAT, a microRNA

encoded in the herpes simplex virus 1 latency associated transcript, prevents apoptosis in neural cells via downregulation of TGF-beta and SMAD3 at the mRNA level. Importantly, they have suggested that those changes in expression are a direct effect of miR-LAT, and identified conserved GC-rich regions in 3'UTRs of both transcripts potentially interacting with miR-LAT. The paper was retracted at the beginning of 2008 [252], potentially explaining some of the negative data relating to miR-LAT presented below.

In this chapter I set out to establish if there are any human microRNAs that regulate TGF-beta generation, acting similarly to miR-LAT.

6.2 Results

6.2.1 *In silico* search for human microRNAs similar to miR-LAT

In order to find human microRNAs similar to miR-LAT, the miRBase [106], a database of all published microRNA sequences, was searched using SSEARCH algorithm (see 2.4.2). A few human microRNAs were identified. Three of them: miR-608, miR-663, and miR-769_3p, which showed the greatest similarity to miR-LAT, were examined further.

To confirm that those microRNAs are likely to interact with TGF-beta transcript, a microRNA target prediction program was used. Since all three microRNAs were newly described, the majority of available programs of that kind, including PicTar, did not take them into account. Therefore, RNA22 program [193], allowing for testing any microRNA and target sequences, was chosen. The program found two microRNA binding sites within TGF-beta transcript for miR-608, two for miR-663, and one for miR-769_3p. As expected, those sites were in the same conserved GC-rich region as described for miR-LAT [251] (Figure 6.1).

Binding of miR-608, miR-663, and miR-769_3p to TGF-beta mRNA as predicted by RNA22 was visualised using RNAfold program from Vienna RNA Secondary Structure Package [194] (Figure 6.2B,C,D). For comparison, miR-LAT interaction with TGF-beta, as described by Gupta et al. [251], is also shown (Figure 6.2A).

6.2.2 Expression of miR-608 and miR-663 in HK-2 and U937 cells

Having identified the microRNAs that can potentially modulate TGF-beta synthesis, an important point was to find out if they are expressed by our model cells – HK-2 cells. That had to be determined experimentally, since those microRNAs were too novel to be examined through the microRNA profiling with microarrays, and no published data was available regarding their abundance in the kidney.

In addition to HK-2 cells, their expression was also evaluated in U937 cells, in which possible evidence for a microRNA-based system for TGF-beta regulation had been found, as noted above [175].

miR-608, miR-663, and miR-769-3p were recently described at the time of investigation, and a commercial assay existed only for miR-608. Similar assays for the other two microRNAs were unavailable, so the detection system for miR-663 was designed in house especially for this project (see 2.2.3.2).

miR-608 expression

As there was no information about basal miR-608 expression in HK-2 cells, to validate the commercial TaqMan assay for miR-608 detection, RNA isolated from cells transfected with synthetic miR-608 was used. Three amounts of the total RNA (10, 2, and 0.4 ng) were used in RT reactions (Figure 6.3). The performance of the assay, judged as described in Methods, was entirely satisfactory.

Subsequently, miR-608 expression was measured in untransfected and non-activated HK-2 and U937 cells (Figure 6.4A). The results for both cell types show that there is either very little miR-608 in those cells, or it is not detectable. Since the fluorescence signal was in all cases very weak and not reproducible among replicates, there was a suspicion that it comes from non-specific PCR products. To determine that, after a quantitative PCR run (40 cycles), a few randomly picked PCR products were separated on an agarose gel, together with DNA size markers and the proper product of the reaction (with RNA from cells transfected with synthetic miR-608) (Figure 6.4B). Analysis of the gel confirmed that there were various non-specific PCR products present, and they were probably responsible for the weak fluorescence signal observed.

miR-663 expression

The qRT-PCR SYBR Green-based system for miR-663 detection was designed as described in Methods. To optimise and validate the system, RNA from HK-2 cells transfected with synthetic miR-663 was used. Similarly to the miR-608 assay validation, three amounts of total RNA (1000, 200, and 40 ng) were examined (Figure 6.5A). Additionally, after the PCR run melting curve analysis was performed to ensure that only one PCR product was present, giving acceptable results (Figure 6.5B).

The assay was then used to determine the basal miR-663 expression in HK-2 and U937 cells (Figure 6.6). Unfortunately, as in case of the miR-608 detection, performance of the assay was compromised when the microRNA concentration was much lower than in the transfected cells (Figure 6.6A,B). In particular, some non-specific, longer than expected PCR products appeared. To overcome this problem, the reactions were next carried out using small RNA fraction rather than total RNA (Figure 6.6C,D). As expected, after the modification only one, most likely the specific product was seen, suggesting the presence of miR-663 in the examined cell types. However, the lack of proper correlation between RNA input and the fluorescence signal raised some doubts about the quantitative character of the assay.

6.2.3 Effects of enforced expression of miR-608 and miR-663 in HK-2 cells on TGF-beta

Considering the finding that miR-608 and miR-663 are presumably not highly (if at all) expressed by HK-2 cells, the microRNA inhibitors could not be used to establish if those microRNAs can regulate TGF-beta synthesis. Instead, the cells were transfected with the synthetic microRNAs.

Effects on TGF-beta and SMAD3 at the mRNA level

In the work of Gupta et al., transfection of neuroblastoma cells with a fragment of the LAT gene containing miR-LAT was shown to cause downregulation of TGF-beta and SMAD3 transcripts [251]. To check if the human microRNAs similar to miR-LAT would do the same in HK-2 cells, the cells were transfected with synthetic miR-608 and miR-663. Subsequently, TGF-beta and (in some experiments) SMAD3 were examined by qRT-PCR.

To begin with, HK-2 cells were transfected with miR-608 at the final concentration of 30 nM (within the range recommended by the supplier, and most commonly used in siRNA experiments in the department). RNA was extracted from the cells every 24 hours for four days. Finally, TGF-beta expression was measured (Figure 6.7). There was no substantial difference between the cells transfected with miR-608 and control cells at any time point.

It was important then to establish if the delivery of the microRNAs to the cells is efficient. Since the synthetic microRNAs are structurally very similar to siRNAs,

a very effective siRNA targeting CD44 was used as a positive control (Figure 6.8). As expected, that siRNA caused reduction of CD44 mRNA by 96% 24 hours after the transfection, while there was no significant change in TGF-beta. These results suggest that the transfection was very efficient, and the siRNA effect on CD44 – specific. Similar transfection with miR-608 or miR-663 resulted in modest, but statistically significant reduction of TGF-beta mRNA (by 13% or 19%, respectively), and no significant change in CD44.

Additional experiment was performed to confirm the results, find out if miR-608 and miR-663 have synergistic effect on TGF-beta, and to check if they can substantially affect SMAD3 mRNA (Figure 6.9). Again, the differences in TGF-beta and SMAD3 expression between control cells and cells transfected with the microRNAs were far less profound than those shown for miR-LAT by Gupta et al. [251].

Effects on TGF-beta at the protein level

Since microRNAs were best known for their effect on translation rather than mRNA stability, the lack of great change in TGF-beta at the mRNA level following transfection with the synthetic miR-608 or miR-663 did not exclude the possibility that the microRNAs affect TGF-beta synthesis at the translational step. Therefore, TGF-beta secretion to medium by control cells and cells transfected with synthetic miR-608 was measured by ELISA. Unstimulated HK-2 cells plated at the low density required for transfection did not produce enough TGF-beta for detection (data not shown). Therefore, in subsequent experiments, HK-2 cells were stimulated with PMA for 24 hours after transfection, to stimulate TGF-beta synthesis. In these experiments,

TGF-beta concentration in the medium collected 24 hours later was not significantly different between the control and miR-608 overexpressing cells (Figure 6.10).

6.2.4 Function of exogenous miR-LAT in HK-2 cells

The lack of great effects of miR-608 and miR-663 on TGF-beta synthesis in HK-2 cells provoked the question if miR-LAT itself could affect TGF-beta in those cells. It had been reported that microRNA actions were sometimes cell type specific, depending on expression of other potential target genes and other modulators of microRNA activity [253-255]. Therefore, there was a possibility that another model system would be necessary to study regulation of TGF-beta by the microRNAs similar to miR-LAT.

Effects on TGF-beta and SMAD3 mRNA

To start with, the effect of miR-LAT on TGF-beta and SMAD3 transcripts in HK-2 cells was examined. The cells were transfected with synthetic miR-LAT, miR-608, or miR-663. Following 24 hour incubation, TGF-beta and SMAD3 mRNAs were quantified by qRT-PCR (Figure 6.11). The differences between the samples were in all cases very small, and the only statistically significant change was about 20% increase in TGF-beta after transfection with miR-LAT. The data was clearly inconsistent with the findings by Gupta et al. [251].

Effects on SMAD-dependent transcription

To confirm that miR-LAT did not behave in HK-2 cells as described for neuroblastoma cells, one more experiment inspired by that original paper was performed. A reporter plasmid containing four SMAD-binding elements in the promoter region of the firefly luciferase gene was used to determine if miR-LAT affected the SMAD-dependent transcription in HK-2 cells (Figure 6.12). Whether the plasmid and small RNA were delivered to the cells consecutively or simultaneously, miR-LAT did not change HK-2 cell response to TGF-beta. As a positive control, siRNA against SMAD3 was co-transfected with the reporter plasmid, and in both cases almost completely abolished the SMAD-dependent transcription after stimulation with TGF-beta (Figure 6.12).

6.3 Discussion

The aim of this chapter was to determine if TGF-beta synthesis was regulated by microRNAs. Typical approach to this problem would include the use of microRNA target prediction programs to select a few promising microRNAs, and subsequent experimental verification. In case of TGF-beta, however, this approach was not valid, as the most popular microRNA target prediction programs did not find any microRNAs that could potentially interact with TGF-beta mRNA.

A few features of its transcript make TGF-beta a poor candidate for a microRNA-regulated gene. First of all, the 3'UTR, most commonly targeted by microRNAs, is relatively short (137 nucleotides). Many of the known microRNA targets have very long 3'UTRs, often exceeding 1000 nucleotides, allowing for a complex regulation by a large number of microRNAs. Furthermore, over a half of TGF-beta 3'UTR is highly GC-rich (containing only about 10% of A or T residues). Sequences of that kind tend to form stable secondary structures, which make them inaccessible to small RNAs [256].

In view of that, the finding by Gupta et al. [251] that the viral microRNA miR-LAT regulates human TGF-beta synthesis, binding to the GC-rich part of its transcript, came as a great surprise. It also suggested there might be some human microRNAs that could act similarly to miR-LAT.

To identify such microRNAs I searched the publicly available database of all known microRNAs, and found a few human microRNAs of similar sequence to miR-LAT. All of them were newly described at that time. There were no predicted mRNA targets for them or literature regarding their function. Since many molecular biology techniques are not suited for manipulation or analysis of nucleic acids with very high contents of G and C residues, the fact that those microRNAs were all GC-rich provided a possible explanation why they were not well-studied, while they could be actually abundant or of great importance.

The difficulty of investigating those microRNAs was already evident when I intended to determine their expression in HK-2 cells. The stem-loop TaqMan assays (Applied Biosystems), the best performing system for microRNA detection by qRT-PCR, were initially unavailable for the three most promising microRNAs. Luckily, during the course of the study, the assay for miR-608 became available. Yet, there is still

(more than two years later) no TaqMan assay for miR-663. Therefore, after a disappointing test of a different commercial microRNA detection system (NCode SYBR Green qRT-PCR Kit, Invitrogen, for details see 2.2.3.2), a stem-loop SYBR Green assay for miR-663 detection was designed in the laboratory. The uniquely high G and C content of miR-663 (containing only one residue different than G or C) made this much more challenging than the design of other qRT-PCR microRNA assays for the project. In particular, that required an increase in length of the stem-loop RT-primer, altered RT conditions, and 15°C higher annealing and extension temperature during PCR reaction (see 2.2.3.2).

Both assays, for miR-608 and miR-663 detection, performed well when the RNA from HK-2 cells used in the reaction was enriched with the appropriate synthetic microRNAs. However, the basal amount of the microRNAs in HK-2 cells was apparently too small to allow for a proper quantification. Consistently, in the later microRNA profiling in the kidney biopsies (see Chapter Three) miR-608 was not detected (while miR-663 was not examined). Also, U937 cells, likely to have a functional microRNA-based system for regulation of TGF-beta generation [175], did not seem to express either of those microRNAs in large quantities.

The expression data suggest that miR-608 and miR-663 are not highly expressed by HK-2 cells. However, there is still a possibility that the weak signal observed is a consequence of the microRNAs high GC contents rather than their low abundances. For a strict comparison of expression of different microRNAs, an absolute quantification system would be needed.

Even assuming that miR-608 and miR-663 were not abundant in HK-2 cells, it was still worth checking if they could regulate TGF-beta synthesis in those cells. Firstly, microRNA effects are often cell type specific, so finding a microRNA that when

overexpressed would affect TGF-beta synthesis in proximal tubular epithelial cells, would be of great value for nephrology. Secondly, seeing an effect of miR-608 or miR-663 on TGF-beta would provide an enormous motivation to search for a tissue or cell type highly expressing the microRNA.

For that reason, a number of experiments were performed using synthetic miR-608 and miR-663. Disappointingly, these microRNAs had a very subtle effect on TGF-beta synthesis in HK-2 cells at the mRNA and protein level. Moreover, synthetic miR-LAT also did not behave in HK-2 cells the same way as described in the paper. The potential explanation for that discrepancy would be that effects of a microRNA seen in one cell type might be different from those found in another [253-255]. In this case, however, the real reason was most likely revealed by the retraction of the original paper at the beginning of 2008 [252].

Recent re-evaluation of the data suggests that, despite the retraction, the results might be actually of some use. In the middle of the year 2008, two highly informative papers about microRNA function were published in *Nature* [125, 134]. The authors for the first time used a large-scale mass-spectrometry-based approach to look at the influence of microRNAs on the protein output. They found that a single microRNA could repress approximately one thousand genes, but usually those changes were very modest. Testing both overexpression and knockdown of a particular microRNA, they observed mainly inverse effects on the protein production, suggesting that those small effects were not accidental. As many of the affected genes could be arranged into functional groups, those small changes might have an important impact on the cell.

Looking again at the results of the transfection of HK-2 cells with miR-608 and miR-663, one might wonder if the very small differences in TGF-beta are not real

effects of the microRNAs. Especially that statistical analysis of the data from three transfection experiments (each done in triplicate) shows that the downregulation of TGF-beta by 15% by miR-663 is statistically significant (Figure 6.13). In keeping with that, TargetScan (release 5.1) [257], currently the best validated microRNA target prediction program, predicts TGF-beta as a target of miR-663. Although my data show that its effect on TGF-beta was rather modest, miR-663 may be highly important for TGF-beta-related processes, given that microRNAs often regulate many genes of similar function. Furthermore, cooperative regulation by multiple microRNAs could possibly lead to a greater decrease in TGF-beta. According to the TargetScan predictions, another microRNA, miR-744, is also likely to control TGF-beta synthesis. The potential interactions of miR-663 and miR-744 with TGF-beta mRNA are a subject of intensive investigations in the department at the moment.

Additionally, there is more and more evidence now that microRNA-binding sites may be also located within the CDS or 5'UTR of a transcript. As those regions are not routinely considered by microRNA target prediction programs yet, there is a chance that TGF-beta regulation occurs also via non-canonical interaction with microRNAs.

agacage gagg gec ecg ggggg gaggggg acg ecc ecg tecg ggg cacce ecc egget etgggaggaggacgagctggtcgggagaagaggaaaaaaacttttqagacttttccqttqccgctg ggagccggaggcgcggggacctcttqqcqacqctqccccqcqaqqaqqcaqqacttqqqqac $\verb|teaggcgccccattccggaccagccctcgggagtcgccgacccggcctcccgcaaagactttt|$ ccccagacctcgggcgcaccccctgcacgccqccttcatccccqqcctqtctcctqaqcccccq $\verb|tcaagaccacccaccttctggtaccagatcgcgcccatctaggttatttccgtgggatactgag|$ acaccccggtccaagcctcccctcaccactgcgcccttctccctgaggacctcagctttccc $\verb|tcgaggccctcctaccttttgccgggagacccccagccctgcaggggcggggcctccccacca|\\$ $\verb|caccagccctgttcgcgctctcggcagtgccggggggggcgcctcccccATGccgccctccgg|$ gctgcggctgctgctgctgctgctaccqctqctgtqqctactqqtqctqacqcctqqccggccg gccgcgggactatccacctgcaagactatcgacatggagctggtgaagcggaagcgcatcgagg $\verb|ccatccgcggccagatcctgtccaagctgcggctcgccagcccccgagccagggggggtgcc||$ gcccggcccgctgcccgaggccgtgctcgccctgtacaacaqcacccgcgaccgggtggccggg gagagtgcagaaccggagcccgagcctgaggccgactactacgccaaggaggtcacccgggtgc $\tt gttcttcaacacatcagagctccgagaagcggtacctgaacccgtgttgctctcccgggcagag$ ctgcgtctgctgaggctcaagttaaaagtggagcagcacgtggagctgtaccagaaatacagca a ca attect ggc gatacet cag ca acc ggc t gct ggc acc cag cgact cgc cag ag t ggt t at case to consider a consideration of the considerttttgatgtcaccggagttgtgcggcagtggttgagccgtggaggggaaattgagggctttcgc $\verb|cttagcgcccactgctcctgtgacagcagggataacactgcaagtggacatcaacgggttca||$ $\verb|ctaccggccgcgaggtgacctggccaccattcatggcatgaaccggcctttcctgcttctcat|\\$ $\tt ggccaccccgctggagagggcccagcatctgcaaagctcccggcaccgccgagccctggacacc$ aggacctcggctggaagtggatccacgagcccaagggctaccatgccaacttctgcctcgggccctqccctacatttqqaqcctqqacacqcaqtacaqcaaggtcctgqccctgtacaaccaqcat aacccgggcgcctcggcgcgcgtgctgcgtgccgcaggcgctggagccgctgcccatcgtgt ${\tt actacgtgggccgcaagcccaaggtggagcagctgtccaacatgatcgtgcgctcctgcaagtg}$ cagcTGAqqtcccqccccqccccqccccqccccqqcccqqccccaccccqccccqcccc gctgccttgcccatgggggctgtatttaaggacacccgtgccccaagcccacctggggccccat

Figure 6.1. Human TGF-beta transcript. Start and stop codons are in uppercase. The binding site for miR-LAT, according to Gupta et al. [251], is in italics. Two predicted miR-608-binding sites are underlined, two predicted miR-663-binding sites are red, and one predicted binding site for miR-769_3p is bold. TGF-beta mRNA sequence was obtained from NCBI (NM_000660.4).

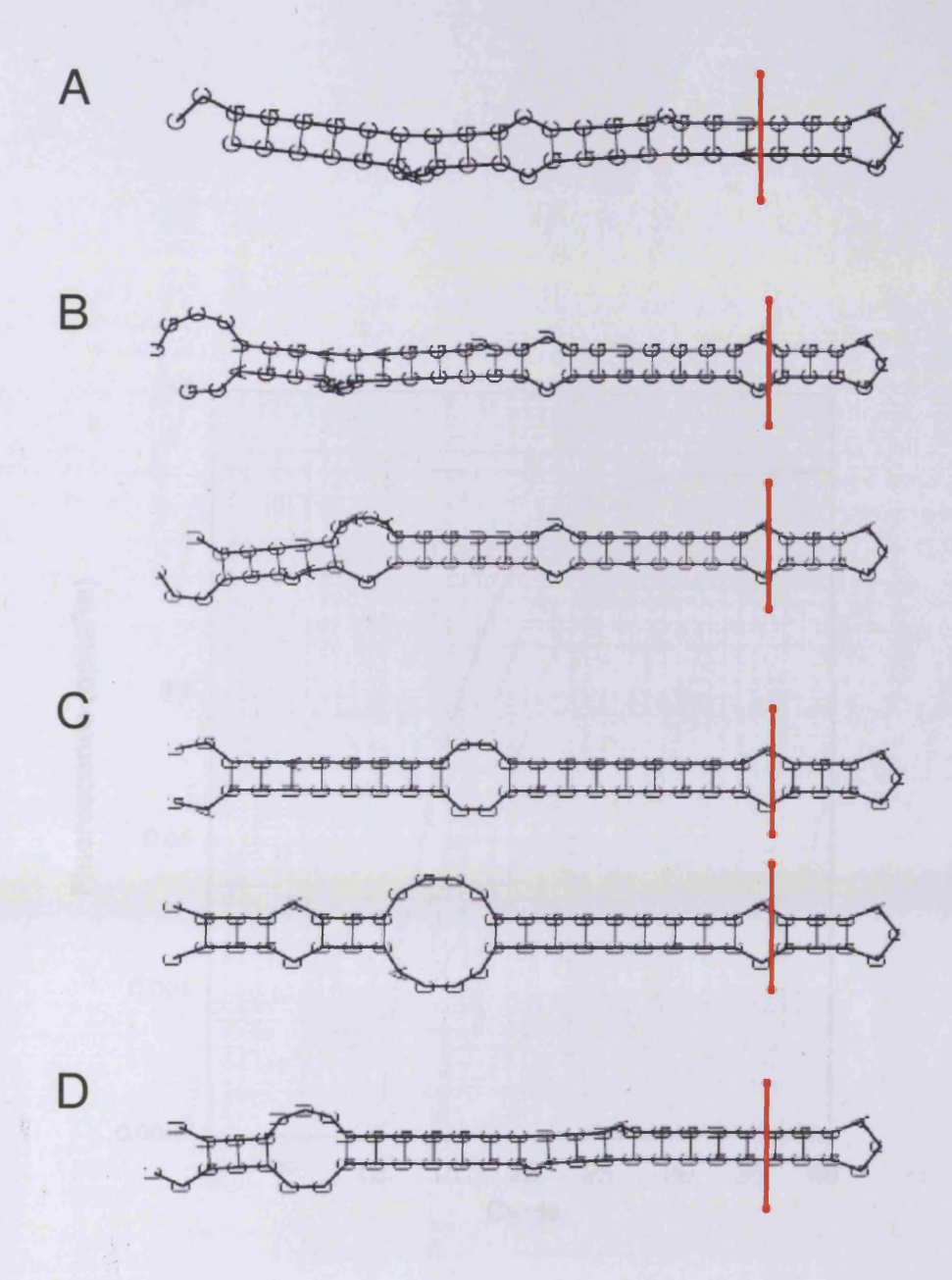


Figure 6.2. Predicted interactions between microRNAs and TGF-beta mRNA. Binding of miR-LAT (A), miR-608 (B), miR-663 (C), and miR-769_3p (D) to TGF-beta transcript as predicted by RNA22 was visualised using RNAfold program from Vienna RNA Secondary Structure Package [194]. For each predicted interaction, microRNA sequence (top) was linked to a fragment of TGF-beta (bottom) via a 9-nucleotide-long unrelated sequence (right from the red line), as justified in Methods.

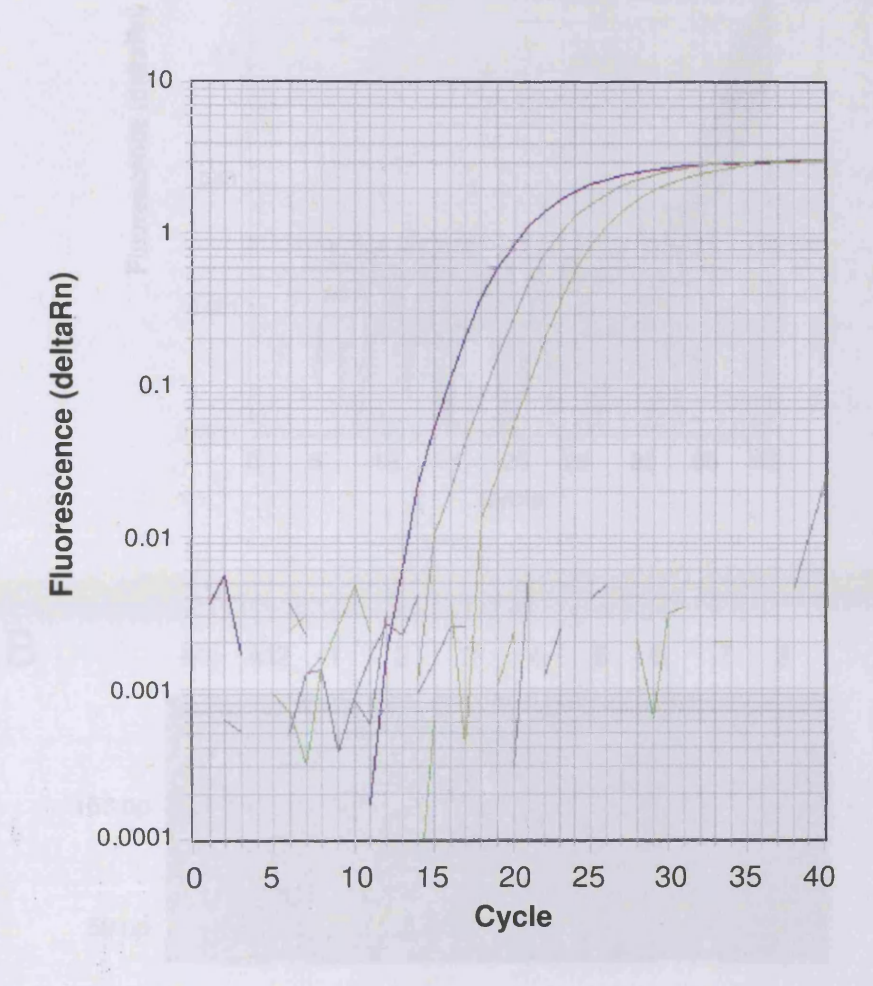
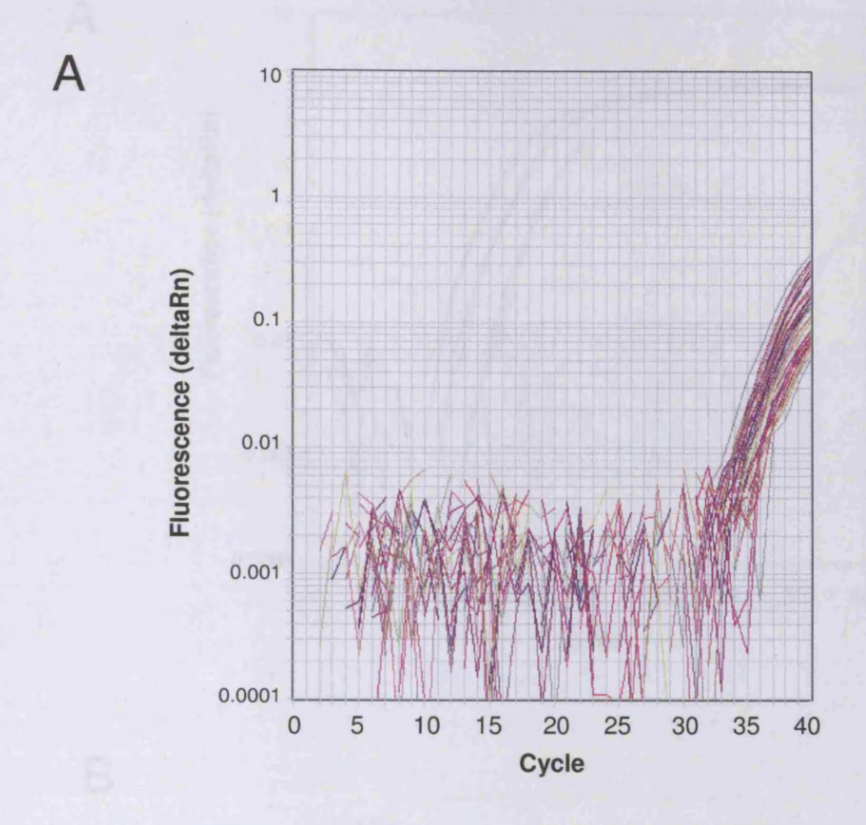


Figure 6.3. Validation of the commercial TaqMan qRT-PCR assay for miR-608 detection. The reaction was performed on three amounts of total RNA: 10, 2, 0.4 ng, isolated from HK-2 cells transfected with synthetic miR-608, as described in Methods. Amplification curves are shown for each sample, and also for three negative controls (-RT, RT-NTC, PCR-NTC).



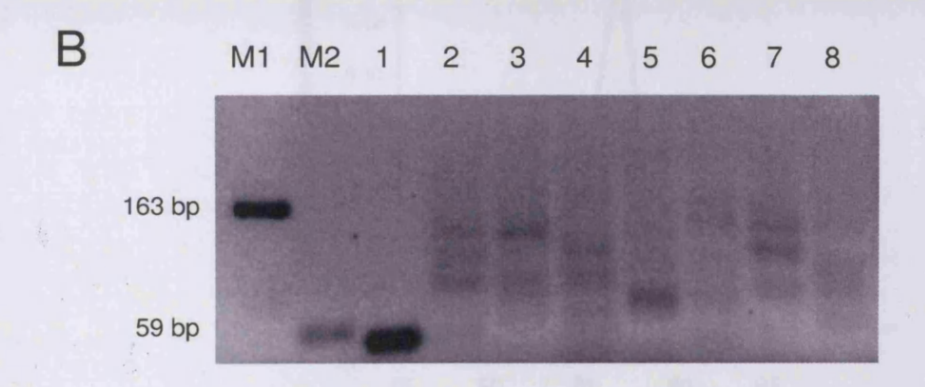
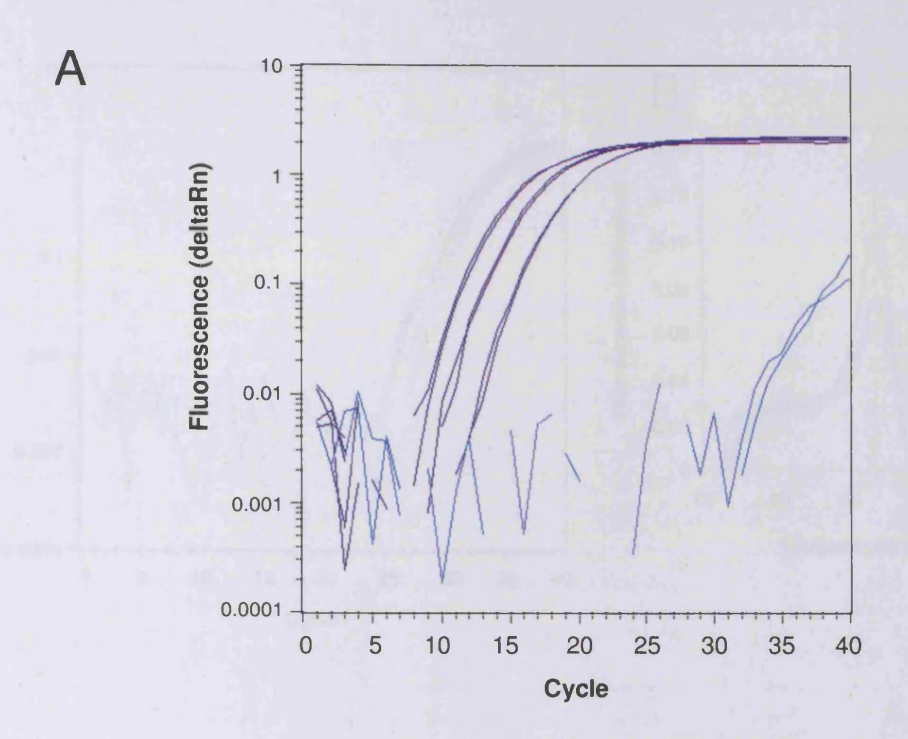


Figure 6.4. Expression of miR-608 in HK-2 and U937 cells. Expression of miR-608 was examined in untransfected HK-2 cells (6 samples in triplicate) and U937 cells (6 samples in triplicate) using the TaqMan qRT-PCR assay validated above. (A) Amplification curves are shown. (B) Seven randomly chosen qRT-PCR products (lanes 2-8) were separated on an agarose gel together with size markers (M1 – 163 bp, M2 – 59 bp) and qRT-PCR product of the reaction performed on RNA from HK-2 cells transfected with synthetic miR-608 (lane 1).



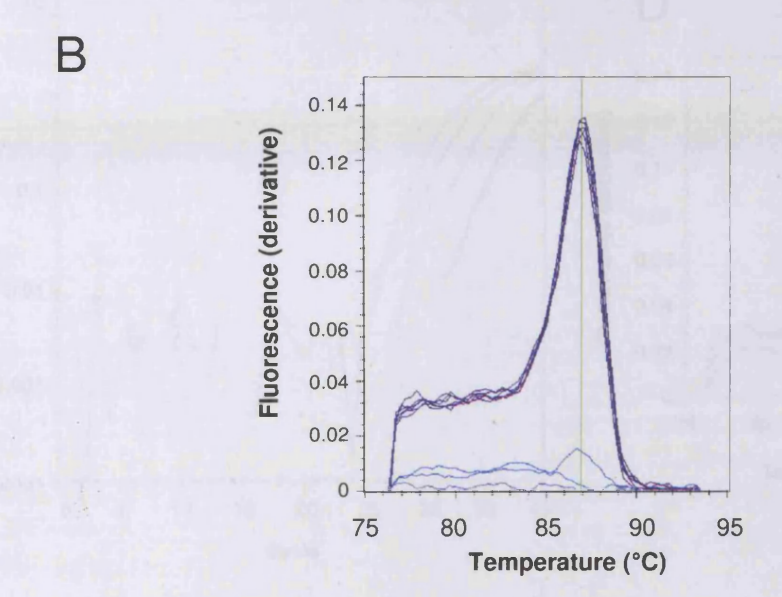


Figure 6.5. Validation of the miR-663 stem-loop qRT-PCR system designed for this project. The reaction was performed on three amounts of total RNA: 1000, 200, 40 ng (in duplicate), isolated from HK-2 cells transfected with synthetic miR-663, as described in Methods. Amplification curves (A) and melting curves (B) are shown for each sample, as well as for three negative controls (-RT, RT-NTC, PCR-NTC).

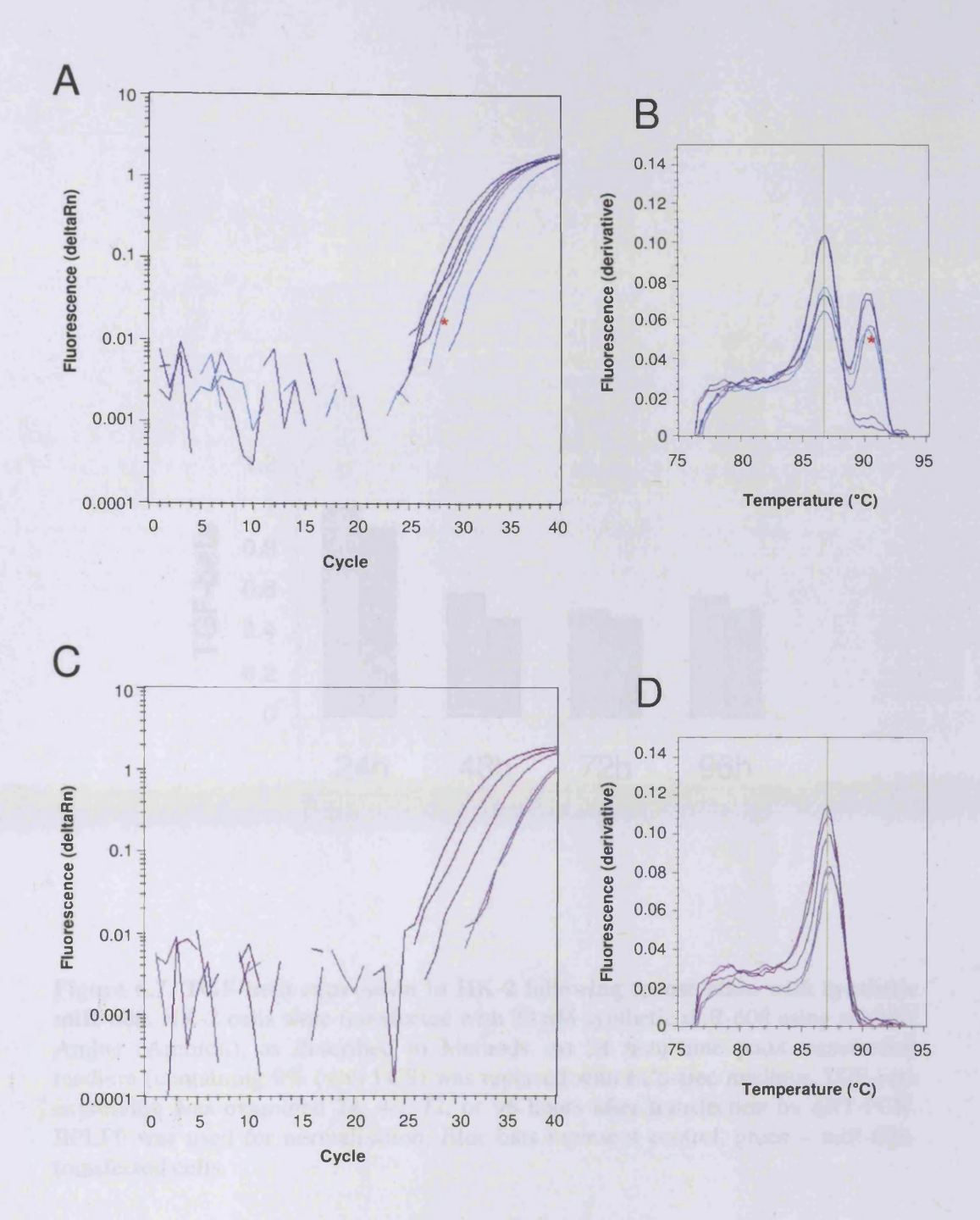


Figure 6.6. Expression of miR-663 in HK-2 and U937 cells. (A,B) Expression of miR-663 was examined in untransfected HK-2 cells using 1000, 500, 250, 125, 62.5 ng total RNA, and in U937 cells using 250 ng total RNA (red asterisk) with the qRT-PCR assay validated above. (C,D) The quantification of HK-2 cell miR-663 was repeated using small instead of total RNA fraction (100, 50, 25, 12.5, 6.25 ng). Amplification plots (A,C) and melting curves (B,D) are shown.

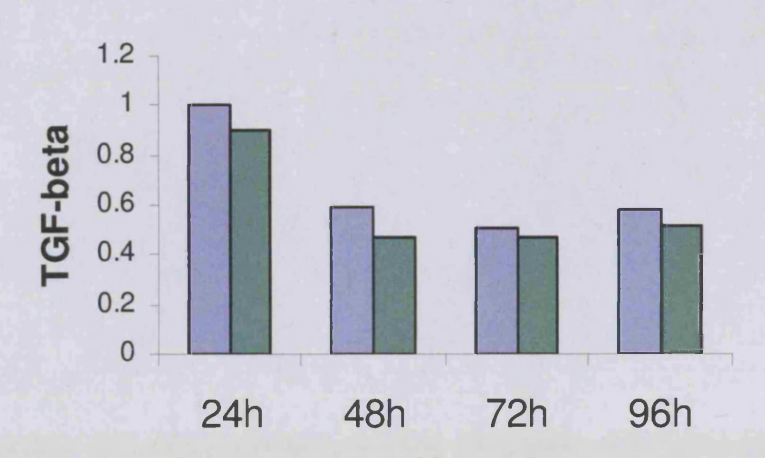
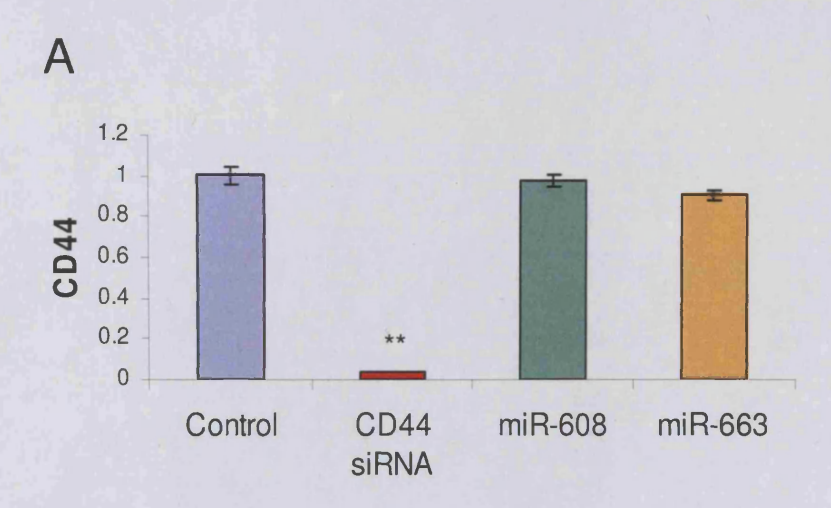


Figure 6.7. TGF-beta expression in HK-2 following transfection with synthetic miR-608. HK-2 cells were transfected with 30 nM synthetic miR-608 using siPORT Amine (Ambion), as described in Methods. At 24 hour-time point transfection medium (containing 9% (v/v) FCS) was replaced with FCS-free medium. TGF-beta expression was examined 24, 48, 72, or 96 hours after transfection by qRT-PCR. RPLPO was used for normalisation. Blue bars represent control, green – miR-608-transfected cells.



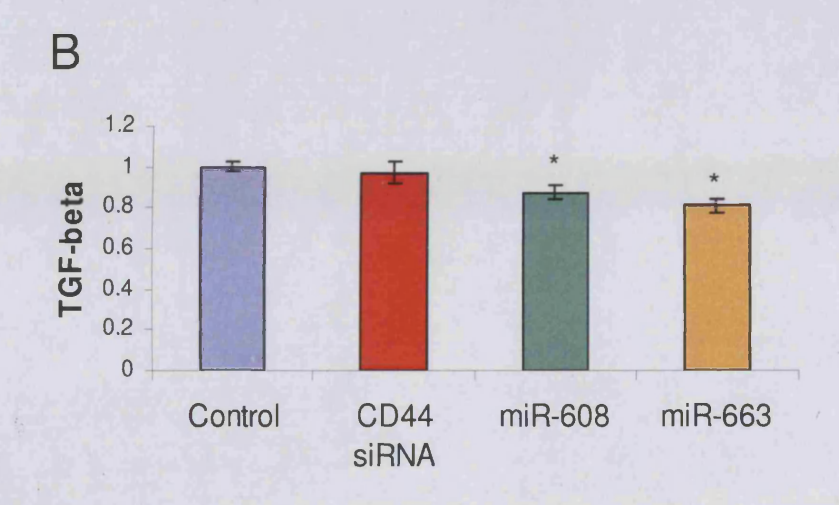
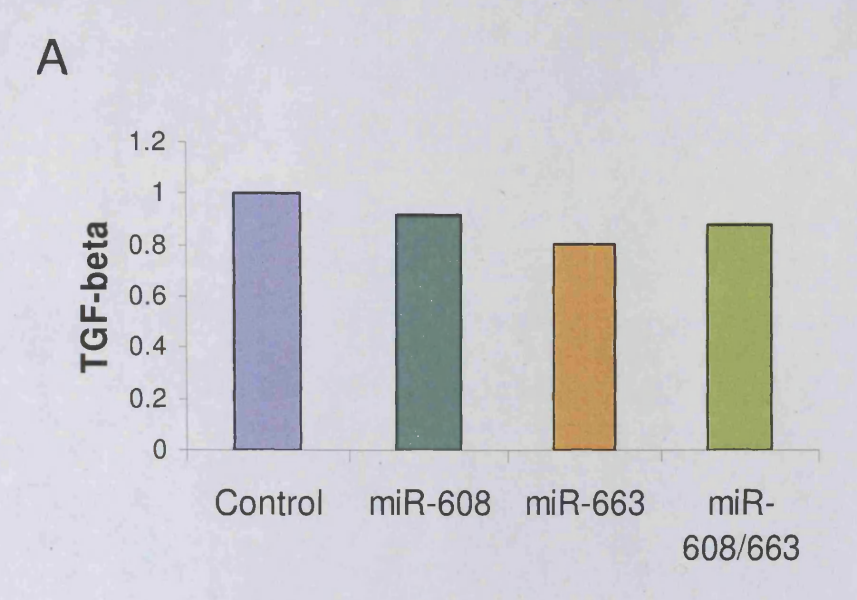


Figure 6.8. Transfection with synthetic miR-608 or miR-663. HK-2 cells were transfected with 30 nM miR-608, miR-663, or – to ensure the transfection was efficient – siRNA silencing CD44. After 24 hours CD44 (A) and TGF-beta (B) expression was tested with qRT-PCR. RPLP0 was used for normalisation. The experiment was performed in triplicate; SEM is shown. The statistical significance is indicated as follows: *p < 0.05, **p < 0.005.



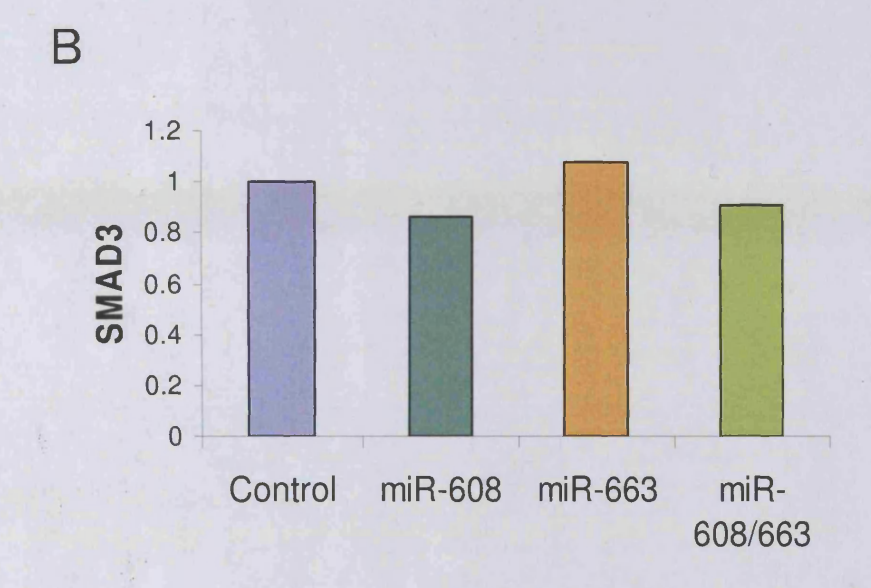
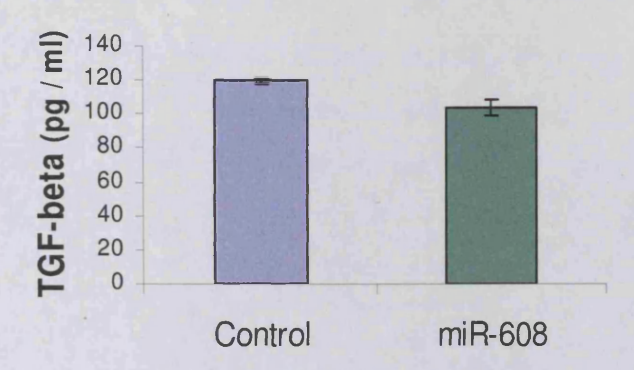


Figure 6.9. Effects of miR-608 and/or miR-663 on TGF-beta and SMAD3. HK-2 cells were transfected with 30 nM miR-608, miR-663, or miR-608 and miR-663 together (15 nM each). After 24 hours the transfection medium was replaced with FCS-free medium and the cells were incubated for another 24 hours. TGF-beta (A) and SMAD3 (B) expression was examined by qRT-PCR. RPLP0 was used for normalisation.





B

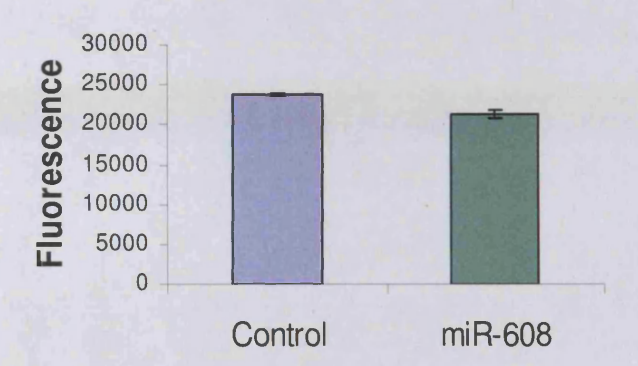
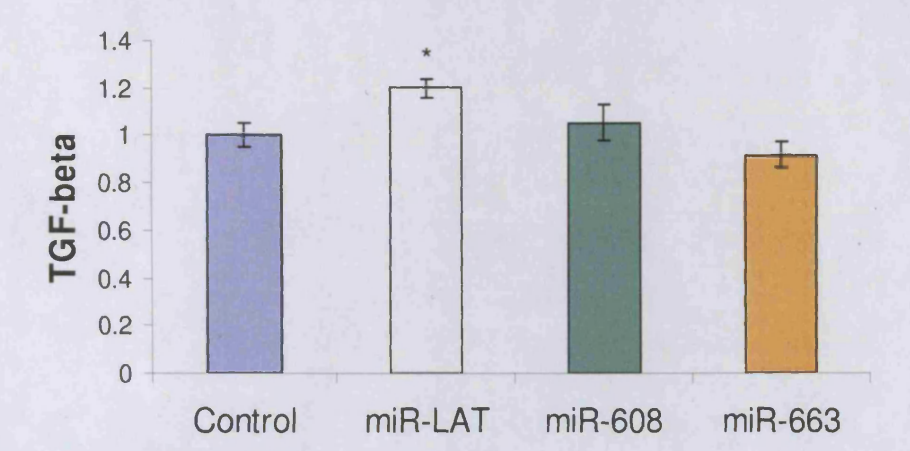


Figure 6.10. Effect of miR-608 on TGF-beta at the protein level. HK-2 cells were transfected with 30 nM miR-608. After 24 hours the cells were stimulated with 160 nM PMA in 0.5 ml FCS-free medium per well (12-well-plates). (A) TGF-beta secreted to medium was examined by ELISA. (B) AlamarBlue assay was used to normalise TGF-beta secretion for cell number. The transfection was performed in triplicate. For each sample ELISA was done in duplicate, and AlamarBlue in triplicate. After the normalisation, the difference between TGF-beta secretion in control and miR-608 transfected cells was non-significant.





B

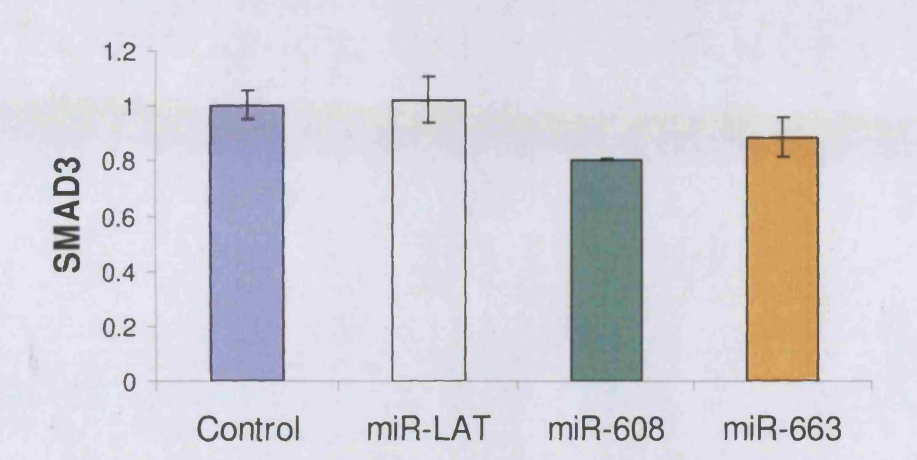


Figure 6.11. Effect of synthetic miR-LAT on TGF-beta and SMAD3. HK-2 cells were transfected with 30 nM miR-LAT, miR-608, or miR-663. TGF-beta (A) and SMAD3 (B) expression was examined 24 hours later by qRT-PCR. RPLP0 was used for normalisation. The experiment was performed in triplicate; SEM is shown. Asterisk indicates p < 0.05.

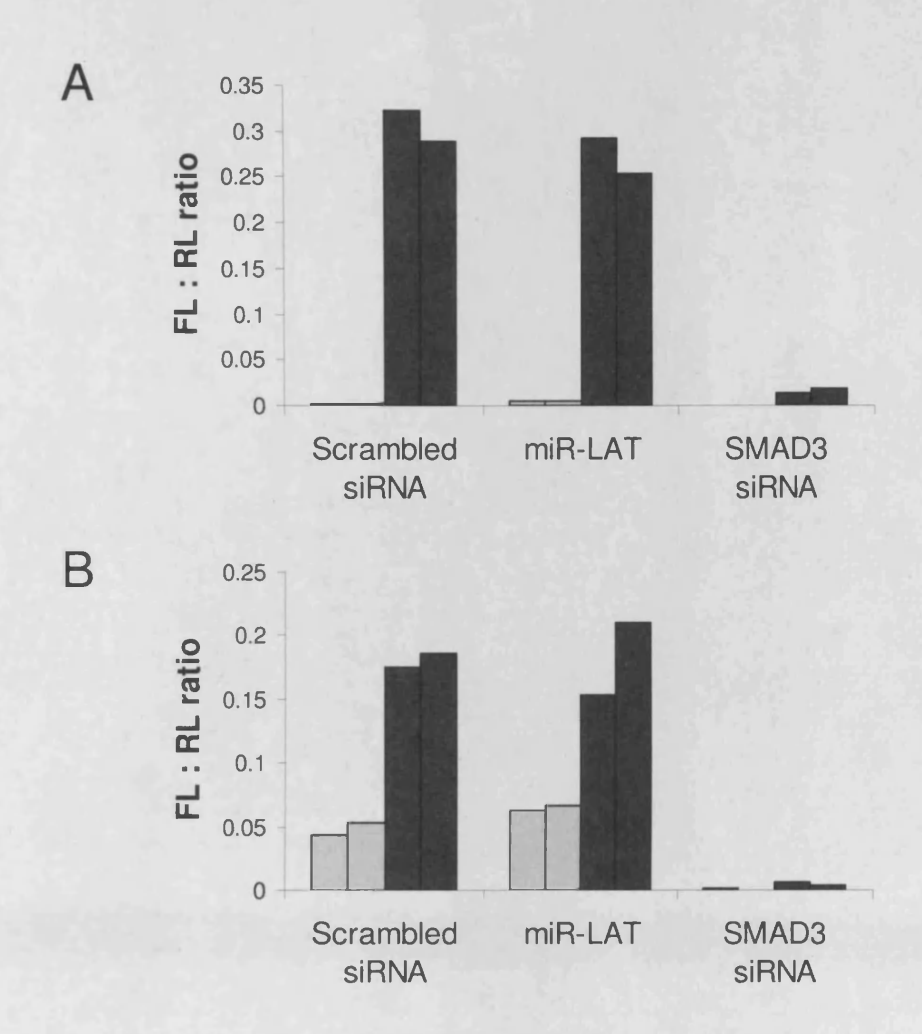


Figure 6.12. Effect of synthetic miR-LAT on SMAD-dependent transcription. (A) HK-2 cells were transfected with 30 nM Scrambled siRNA (negative control), miR-LAT, or SMAD3 siRNA (positive control). After 40 hours cells were transfected with a mix (9:1) of TGF-beta responsive reporter plasmid (with four SMAD-binding elements in the promoter region of the firefly luciferase) and control plasmid (for constitutive expression of Renilla luciferase). 24 hours after the second transfection, the cells were stimulated with 1 ng/ml TGF-beta (black bars) or not (grey bars) for six hours. Then, activities of firefly and Renilla luciferases were examined using Dual Luciferase Assay (Promega). (B) HK-2 cells were transfected with 30 nM Scrambled siRNA, miR-LAT, or SMAD3 siRNA together with the mix of the two plasmids used in (A). The transfection medium was replaced with fresh FCS-free medium and the cells were incubated for 48 hours. They were incubated with 1 ng/ml TGF-beta (black bars) or control medium (grey bars) for six hours. Activities of firefly and Renilla luciferases were measured as described above. Both experiments were performed in duplicate and both were repeated with the same results.



Figure 6.13. Effect of miR-608 and miR-663 on TGF-beta mRNA - summary. The data from three transfection experiments presented above (each in triplicate) were averaged, SEM calculated, and statistical significance was tested. Two asterisks indicate p < 0.005.

CHAPTER SEVEN:

GENERAL DISCUSSION

The aim of my thesis was to determine the role of microRNAs in renal fibrosis. At the start of the project, in 2006, microRNAs were emerging as potentially important factors in various physiological and pathological processes; however, there was very little known about their expression and function in the kidney, in particular in tubulointerstitial fibrosis. In my thesis, I have characterised global microRNA expression *in vitro* in proximal tubular epithelial cells and *in vivo* in kidney biopsy samples, and identified microRNAs altered by profibrotic stimuli. Furthermore, I have linked the changes in miR-192 expression with its role in regulation of E-cadherin in proximal tubular epithelial cells, indicating that miR-192 may prevent EMT in the kidney. Finally, I have examined the possibility that TGF-beta, a crucial cytokine in renal fibrosis, is directly regulated by microRNAs.

One of the major strengths of this work, making it unique among all studies on microRNAs in the kidney published so far, was the use of FFPE renal biopsy samples as a source of RNA for microRNA profiling. This technical advance can be widely applied within nephrology. Storage of FFPE kidney biopsies has been a routine practice in numerous countries for many years; a vast collection of such samples exists and – as my data show – they could be successfully used for retrospective studies of various kidney disorders. Thus far, limited RNA availability has precluded hybridisation-based microRNA analysis in non-surgically obtained kidney specimens. For this reason, microRNA expression in human kidneys has been studied mostly in tissue obtained at surgical nephrectomy. A key advantage of renal biopsy tissue over nephrectomy specimens is the relatively rapid fixation, which eliminates the risk that substantial changes in microRNA expression occurring after a prolonged period of tissue hypoxia [205] will affect the results.

Extensive characterisation of microRNA expression in malignancy shows that microRNA profiling has promise as a clinical tool for diagnostic and prognostic evaluation, as well as for identification of potential therapeutic targets. My results suggest that this holds true also for non-malignant diseases such as diabetic nephropathy. I have found a number of microRNAs that were differentially expressed between patients with early and late stage of diabetic nephropathy, and between patients with slow and fast progression of the disease. The greatest difference was found in expression of miR-192, which was downregulated in kidney samples from patients with severe diabetic nephropathy, and thus was examined further in this thesis.

Analysis of miR-192 expression in individual kidney biopsies revealed that it correlates well with renal function (eGFR) and inversely correlates with renal fibrosis (fibrosis score). Furthermore, *in vitro* work showed that miR-192 is downregulated also by short-term treatment with TGF-beta in proximal tubular epithelial cells. Subsequent manipulation of miR-192 expression in those cells demonstrated that miR-192 is involved in regulation of E-cadherin expression, most likely by targeting directly two E-cadherin transcriptional repressors: ZEB1 and ZEB2. Since downregulation of E-cadherin is the first and crucial step of EMT, and EMT is strongly implicated in pathogenesis of renal fibrosis, my data suggest that miR-192 might prevent the fibrosis in the kidney.

As discussed in detail earlier, the role of miR-192 in diabetic nephropathy has been also studied by two other research groups [151, 154], revealing that miR-192 action may be context-dependent and not necessarily beneficial for the kidney. All the groups, however, point to miR-192 importance in diabetic nephropathy and a need for further investigation. In the context of proximal tubular epithelial cell

biology, there are still a few unanswered questions. For instance, the mechanism of miR-192 downregulation by TGF-beta is not fully understood. My miR-192 overexpression data presented in Chapter Five suggest that miR-192 is regulated posttranscriptionally. In addition, a preliminary *in silico* analysis of the miR-192 promoter region identified multiple binding sites for SMADs, HNF-1alpha, SP1 and SP3, as well as E-boxes that could potentially interact with ZEB1, ZEB2, or other E-box repressors, indicating that endogenous miR-192 is also very likely regulated by TGF-beta at the level of transcription. This, together with the possibility that miR-192 has also other targets and functions in proximal tubular epithelial cells, is under investigation in the department now.

MicroRNA-192, identified by microRNA expression profiling as downregulated in severe diabetic nephropathy, was subsequently found to play a potentially important role in renal fibrosis. This implies that other changes in microRNA expression found in that experiment, i.e. two microRNAs different more than two-fold between non-progressors and progressors, and eleven between late presenters and early stage biopsies, are very likely to be meaningful too. Moreover, even if their detailed characterisation fails to extend the existing knowledge about mechanisms driving kidney fibrosis, they could still be used as biomarkers in diabetic nephropathy and possibly other kinds of chronic kidney disease.

Currently, diagnosis of chronic kidney disease is based mainly on serum creatinine in combination with urinary findings, such as proteinuria. These, however, change substantially only in advanced disease, so do not allow for very early detection, which is critical for effective management of the condition. Additionally, there is no well-established prognostic biomarker, which could help to distinguish between

patients with quick and low rate of disease progression, so that the treatment could be adjusted appropriately.

In the last years, there has been a great interest in microRNAs as biomarkers for various diseases, mostly cancers (for review see [258]). Strikingly, recent reports have demonstrated the presence of microRNAs in bodily fluids, including urine [259, 260]. Furthermore, analysis of microRNA expression in urine samples has been already successfully employed to identify potential bladder cancer biomarkers [261]. It is tempting to speculate that expression of microRNAs identified in this study as potentially important in diabetic nephropathy, including miR-192, would be changed not only in renal biopsy tissue, but also in urine samples. That could eventually lead to a quick, reliable and – most of all – non-invasive method for diagnosis or prognosis in chronic kidney disease.

Renal fibrosis, as a result of chronic kidney disease, is a complex condition, which is mediated by a whole network of molecular, cellular, and physiological mechanisms. A single microRNA is capable of regulating multiple components of a pathway or multiple pathways. Therefore, microRNAs are particularly good candidates for global regulators of such disorders and they certainly deserve more attention in the context of renal fibrosis. The long-term goal is to define functions of all microRNAs expressed in the normal and fibrotic kidney by identifying and validating their targets, and to examine their potential as future therapeutic, diagnostic or prognostic clinical tools. My work presented in this thesis, together with a few reports on the subject published in parallel, constitutes a good starting point to achieve that.

REFERENCES

- [1] W.F. Boron and E.L. Boulpaep, *Medical Physiology: A Cellular and Molecular Approach*, Updated Edition, Saunders, 2004.
- [2] C. Lote, The renin-angiotensin system and regulation of fluid volume, *Surgery*, **24** (2006), 154-159.
- [3] P.E. de Jong, M. van der Velde, R.T. Gansevoort and C. Zoccali, Screening for chronic kidney disease: Where does Europe go?, *Clin J Am Soc Nephrol*, 3 (2008), 616-623.
- [4] M.W. Taal and B.M. Brenner, Predicting initiation and progression of chronic kidney disease: Developing renal risk scores, *Kidney Int*, **70** (2006), 1694-1705.
- [5] W. Bakker, E. Eringa, P. Sipkema and V. van Hinsbergh, Endothelial dysfunction and diabetes: roles of hyperglycemia, impaired insulin signaling and obesity, *Cell Tissue Res*, **335** (2009), 165-189.
- [6] J.E. Shaw, R.A. Sicree and P.Z. Zimmet, Global estimates of the prevalence of diabetes for 2010 and 2030, *Diabetes Res Clin Pract*, 87 (2010), 4-14.
- [7] B.F. Schrijvers, A.S. De Vriese and A. Flyvbjerg, From hyperglycemia to diabetic kidney disease: The role of metabolic, hemodynamic, intracellular factors and growth factors/cytokines, *Endocr Rev*, **25** (2004), 971-1010.
- [8] D. Nitsch, R. Burden, R. Steenkamp, D. Ansell, C. Byrne, F. Caskey, P. Roderick and T. Feest, Patients with diabetic nephropathy on renal replacement therapy in England and Wales, *QJM*, **100** (2007), 551-560.
- [9] G. Wolf, New insights into the pathophysiology of diabetic nephropathy: from haemodynamics to molecular pathology, *Eur J Clin Invest*, **34** (2004), 785-796.
- [10] P. Fioretto, M.W. Steffes, D.E.R. Sutherland, F.C. Goetz and M. Mauer, Reversal of lesions of diabetic nephropathy after pancreas transplantation, *New Engl J Med*, **339** (1998), 69-75.
- [11] P. Hovind, P. Rossing, L. Tarnow, U.M. Smidt and H.H. Parving, Progression of diabetic nephropathy, *Kidney Int*, **59** (2001), 702-709.
- [12] R. Zatz, B.R. Dunn, T.W. Meyer, S. Anderson, H.G. Rennke and B.M. Brenner, Prevention of diabetic glomerulopathy by pharmacological amelioration of glomerular capillary hypertension, *J Clin Invest*, 77 (1986), 1925-1930.
- [13] E.J. Lewis, L.G. Hunsicker, R.P. Bain, R.D. Rohde and The Collaborative Study Group., The effect of angiotensin-converting-enzyme inhibition on diabetic nephropathy, *New Engl J Med*, **329** (1993), 1456-1462.
- [14] L. Foggensteiner, S. Mulroy and J. Firth, Management of diabetic nephropathy, *J R Soc Med*, **94** (2001), 210-217.

- [15] S. Adler, Diabetic nephropathy: Linking histology, cell biology, and genetics, *Kidney Int*, **66** (2004), 2095-2106.
- [16] Wellcome Trust Case Control Consortium, Genome-wide association study of 14,000 cases of seven common diseases and 3,000 shared controls, *Nature*, 447 (2007), 661-678.
- [17] C. Hasslacher, E. Ritz, P. Wahl and C. Michael, Similar risks of nephropathy in patients with type I or type II diabetes mellitus, *Nephrol Dial Transplant*, 4 (1989), 859-863.
- [18] A.S. Levey, J. Coresh, E. Balk, A.T. Kausz, A. Levin, M.W. Steffes, R.J. Hogg, R.D. Perrone, J. Lau and G. Eknoyan, National Kidney Foundation practice guidelines for chronic kidney disease: evaluation, classification, and stratification, *Ann Intern Med*, **139** (2003), 137-147.
- [19] A.A. Eddy, Molecular basis of renal fibrosis, *Pediatr Nephrol*, **15** (2000), 290-301.
- [20] S.M. Mauer, M.W. Steffes, E.N. Ellis, D.E. Sutherland, D.M. Brown and F.C. Goetz, Structural-functional relationships in diabetic nephropathy, *J Clin Invest*, 74 (1984), 1143-1155.
- [21] P. Fioretto and M. Mauer, Histopathology of diabetic nephropathy, Semin Nephrol, 27 (2007), 195-207.
- [22] E. Galkina and K. Ley, Leukocyte recruitment and vascular injury in diabetic nephropathy, *J Am Soc Nephrol*, **17** (2006), 368-377.
- [23] K.A. Nath, The tubulointerstitium in progressive renal disease, *Kidney Int*, **54** (1998), 992-994.
- [24] S.N. Wang, J. Lapage and R. Hirschberg, Glomerular ultrafiltration and apical tubular action of IGF-I, TGF-beta, and HGF in nephrotic syndrome, *Kidney Int*, **56** (1999), 1247-1251.
- [25] L. Chen, R.A. Boadle and D.C. Harris, Toxicity of holotransferrin but not albumin in proximal tubule cells in primary culture, *J Am Soc Nephrol*, 9 (1998), 77-84.
- [26] A.C. Alfrey, D.H. Froment and W.S. Hammond, Role of iron in the tubulo-interstitial injury in nephrotoxic serum nephritis, *Kidney Int*, **36** (1989), 753-759.
- [27] L. Biancone, S. David, V.D. Pietra, G. Montrucchio, V. Cambi and G. Camussi, Alternative pathway activation of complement by cultured human proximal tubular epithelial cells, *Kidney Int*, **45** (1994), 451-460.
- [28] C. Zoja, M. Morigi, M. Figliuzzi, I. Bruzzi, S. Oldroyd, A. Benigni, P. Ronco and G. Remuzzi, Proximal tubular cell synthesis and secretion of endothelin-1 on challenge with albumin and other proteins, *Am J Kidney Dis*, **26** (1995), 934-941.
- [29] Y. Wang, J. Chen, L. Chen, Y.C. Tay, G.K. Rangan and D.C. Harris, Induction of monocyte chemoattractant protein-1 in proximal tubule cells by urinary protein, *J Am Soc Nephrol*, 8 (1997), 1537-1545.

- [30] S. Tang, N.S. Sheerin, W. Zhou, Z. Brown and S.H. Sacks, Apical proteins stimulate complement synthesis by cultured human proximal tubular epithelial cells, *J Am Soc Nephrol*, **10** (1999), 69-76.
- [31] S.D. Ricardo, M.E. Levinson, M.R. DeJoseph and J.R. Diamond, Expression of adhesion molecules in rat renal cortex during experimental hydronephrosis, *Kidney Int*, **50** (1996), 2002-2010.
- [32] R.A. Weiss, M.P. Madaio, J.E. Tomaszewski and C.J. Kelly, T cells reactive to an inducible heat shock protein induce disease in toxin-induced interstitial nephritis, *J Exp Med*, **180** (1994), 2239-2250.
- [33] A.O. Phillips, R. Steadman, K. Morrisey, J. Martin, L. Eynstone and J.D. Williams, Exposure of human renal proximal tubular cells to glucose leads to accumulation of type IV collagen and fibronectin by decreased degradation, *Kidney Int*, **52** (1997), 973-984.
- [34] Y. Liu, Epithelial to mesenchymal transition in renal fibrogenesis: pathologic significance, molecular mechanism, and therapeutic intervention, *J Am Soc Nephrol*, **15** (2004), 1-12.
- [35] F. Strutz and M. Zeisberg, Renal Fibroblasts and Myofibroblasts in Chronic Kidney Disease, *J Am Soc Nephrol*, 17 (2006), 2992-2998.
- [36] J. Massague, The transforming growth factor-beta family, *Annu Rev Cell Biol*, **6** (1990), 597-641.
- [37] M. Iwano, A. Kubo, T. Nishino, H. Sato, H. Nishioka, Y. Akai, H. Kurioka, Y. Fujii, M. Kanauchi, H. Shiiki and K. Dohi, Quantification of glomerular TGF-beta1 mRNA in patients with diabetes mellitus, *Kidney Int*, **49** (1996), 1120-1126.
- [38] T. Yamamoto, N.A. Noble, A.H. Cohen, C.C. Nast, A. Hishida, L.I. Gold and W.A. Border, Expression of transforming growth factor-beta isoforms in human glomerular diseases, *Kidney Int*, **49** (1996), 461-469.
- [39] K. Sharma and F.N. Ziyadeh, Renal hypertrophy is associated with upregulation of TGF-beta 1 gene expression in diabetic BB rat and NOD mouse, Am J Physiol Renal Physiol, 267 (1994), F1094-1001.
- [40] J.B. Kopp, V.M. Factor, M. Motes, P. Nagy, N. Sanderson, E.P. Bottinger, P.E. Klotman and S.S. Thorgeirsson, Transgenic mice with increased plasma levels of TGF-beta 1 develop progressive renal disease, *Lab Invest*, **74** (1996), 991-1003.
- [41] L. Yu, W.A. Border, I. Anderson, M. McCourt, Y. Huang and N.A. Noble, Combining TGF-beta inhibition and angiotensin II blockade results in enhanced antifibrotic effect, *Kidney Int*, **66** (2004), 1774-1784.
- [42] E. Van Obberghen-Schilling, N.S. Roche, K.C. Flanders, M.B. Sporn and A.B. Roberts, Transforming growth factor beta 1 positively regulates its own expression in normal and transformed cells, *J Biol Chem*, **263** (1988), 7741-7746.
- [43] L. Yu, W.A. Border, Y. Huang and N.A. Noble, TGF-beta isoforms in renal fibrogenesis, *Kidney Int*, **64** (2003), 844-856.

- [44] B. Schmierer and C.S. Hill, TGF-beta-SMAD signal transduction: molecular specificity and functional flexibility, *Nat Rev Mol Cell Biol*, 8 (2007), 970-982.
- [45] S. Gupta, M.R. Clarkson, J. Duggan and H.R. Brady, Connective tissue growth factor: Potential role in glomerulosclerosis and tubulointerstitial fibrosis, *Kidney Int*, **58** (2000), 1389-1399.
- [46] Y. Ito, J. Aten, R.J. Bende, B.S. Oemar, T.J. Rabelink, J.J. Weening and R. Goldschmeding, Expression of connective tissue growth factor in human renal fibrosis, *Kidney Int*, 53 (1998), 853-861.
- [47] B.L. Riser, M. Denichilo, P. Cortes, C. Baker, J.M. Grondin, J. Yee and R.G. Narins, Regulation of connective tissue growth factor activity in cultured rat mesangial cells and its expression in experimental diabetic glomerulosclerosis, *J Am Soc Nephrol*, 11 (2000), 25-38.
- [48] G. Wolf, E. Mueller, R.A. Stahl and F.N. Ziyadeh, Angiotensin II-induced hypertrophy of cultured murine proximal tubular cells is mediated by endogenous transforming growth factor-beta, *J Clin Invest*, **92** (1993), 1366-1372.
- [49] G. Carvajal, J. Rodriguez-Vita, R. Rodrigues-Diez, E. Sanchez-Lopez, M. Ruperez, C. Cartier, V. Esteban, A. Ortiz, J. Egido, S.A. Mezzano and M. Ruiz-Ortega, Angiotensin II activates the Smad pathway during epithelial mesenchymal transdifferentiation, *Kidney Int*, 74 (2008), 585-595.
- [50] R.J. Fern, C.M. Yesko, B.A. Thornhill, H.S. Kim, O. Smithies and R.L. Chevalier, Reduced angiotensinogen expression attenuates renal interstitial fibrosis in obstructive nephropathy in mice, *J Clin Invest*, **103** (1999), 39-46.
- [51] C.M. Richter, Role of endothelin in chronic renal failure developments in renal involvement, *Rheumatology*, **45** (2006), iii36-38.
- [52] A. Benigni, C. Zoja, D. Corna, S. Orisio, D. Facchinetti, L. Benatti and G. Remuzzi, Blocking both type A and B endothelin receptors in the kidney attenuates renal injury and prolongs survival in rats with remnant kidney, *Am J Kidney Dis*, **27** (1996), 416-423.
- [53] B. Hocher, C. Thoene-Reineke, P. Rohmeiss, F. Schmager, T. Slowinski, V. Burst, F. Siegmund, T. Quertermous, C. Bauer, H.H. Neumayer, W.D. Schleuning and F. Theuring, Endothelin-1 transgenic mice develop glomerulosclerosis, interstitial fibrosis, and renal cysts but not hypertension, *J Clin Invest*, **99** (1997), 1380-1389.
- [54] W.W. Tang, T.R. Ulich, D.L. Lacey, D.C. Hill, M. Qi, S.A. Kaufman, G.Y. Van, J.E. Tarpley and J.S. Yee, Platelet-derived growth factor-BB induces renal tubulointerstitial myofibroblast formation and tubulointerstitial fibrosis, *Am J Pathol*, **148** (1996), 1169-1180.
- [55] D. Fraser, N. Brunskill, T. Ito and A. Phillips, Long-term exposure of proximal tubular epithelial cells to glucose induces transforming growth factor-beta1 synthesis via an autocrine pdgf loop, Am J Pathol, 163 (2003), 2565-2574.

- [56] G. Ramesh and W.B. Reeves, TNF-alpha mediates chemokine and cytokine expression and renal injury in cisplatin nephrotoxicity, *J Clin Invest*, **110** (2002), 835-842.
- [57] S.K. Jo, S.A. Sung, W.Y. Cho, K.J. Go and H.K. Kim, Macrophages contribute to the initiation of ischaemic acute renal failure in rats, *Nephrol Dial Transplant*, **21** (2006), 1231-1239.
- [58] H.Y. Lan, D.J. Nikolic-Paterson, M. Zarama, J.L. Vannice and R.C. Atkins, Suppression of experimental crescentic glomerulonephritis by the interleukin-1 receptor antagonist, *Kidney Int*, **43** (1993), 479-485.
- [59] Y. Taniguchi, N. Yorioka, K. Yamashita, J. Kumagai, S. Kushihata, H. Oda and M. Yamakido, Hepatocyte growth factor localization in primary glomerulonephritis and drug-induced interstitial nephritis, *Nephron*, **73** (1996), 357-358.
- [60] S. Mizuno, T. Kurosawa, K. Matsumoto, Y. Mizuno-Horikawa, M. Okamoto and T. Nakamura, Hepatocyte growth factor prevents renal fibrosis and dysfunction in a mouse model of chronic renal disease, *J Clin Invest*, **101** (1998), 1827-1834.
- [61] H. Takayama, W.J. LaRochelle, S.G. Sabnis, T. Otsuka and G. Merlino, Renal tubular hyperplasia, polycystic disease, and glomerulosclerosis in transgenic mice overexpressing hepatocyte growth factor scatter factor (Abstract), *Lab Invest*, 77 (1997), 131-138.
- [62] W.W. Tang, G.Y. Van and M. Qi, Myofibroblast and alpha1(III) collagen expression in experimental tubulointerstitial nephritis, *Kidney Int*, **51** (1997), 926-931.
- [63] H. Kim, T. Oda, J. Lopez-Guisa, D. Wing, D.R. Edwards, P.D. Soloway and A.A. Eddy, TIMP-1 deficiency does not attenuate interstitial fibrosis in obstructive nephropathy, *J Am Soc Nephrol*, 12 (2001), 736-748.
- [64] J.J. Kanalas and U. Hopfer, Effect of TGF-beta 1 and TNF-alpha on the plasminogen system of rat proximal tubular epithelial cells, *J Am Soc Nephrol*, 8 (1997), 184-192.
- [65] W. Qi, X. Chen, P. Poronnik and C.A. Pollock, The renal cortical fibroblast in renal tubulointerstitial fibrosis, *Int J Biochem Cell Biol*, **38** (2006), 1-5.
- [66] J.P. Rerolle, A. Hertig, G. Nguyen, J.D. Sraer and E.P. Rondeau, Plasminogen activator inhibitor type 1 is a potential target in renal fibrogenesis, *Kidney Int*, **58** (2000), 1841-1850.
- [67] T. Oda, Y.O. Jung, H.S. Kim, X. Cai, J.M. Lopez-Guisa, Y. Ikeda and A.A. Eddy, PAI-1 deficiency attenuates the fibrogenic response to ureteral obstruction, *Kidney Int*, **60** (2001), 587-596.
- [68] B. Alberts, A. Johnson, J. Lewis, M. Raff, K. Roberts and P. Walter, *Molecular Biology of the Cell*, Fifth Edition, Garland Science, 2007.
- [69] R.D. Kornberg, Mediator and the mechanism of transcriptional activation, *Trends Biochem Sci*, **30** (2005), 235-239.

- [70] M.M. Babu, N.M. Luscombe, L. Aravind, M. Gerstein and S.A. Teichmann, Structure and evolution of transcriptional regulatory networks, *Curr Opin Struct Biol*, **14** (2004), 283-291.
- [71] D.I.K. Martin, Transcriptional enhancers on/off gene regulation as an adaptation to silencing in higher eukaryotic nuclei, *Trends Genet*, 17 (2001), 444-448.
- [72] L. Kuras, T. Borggrefe and R.D. Kornberg, Association of the Mediator complex with enhancers of active genes, *PNAS*, **100** (2003), 13887-13891.
- [73] L. Xu, C.K. Glass and M.G. Rosenfeld, Coactivator and corepressor complexes in nuclear receptor function, *Curr Opin Genet Dev*, **9** (1999), 140-147.
- [74] J.A. Goodrich and J.F. Kugel, Non-coding-RNA regulators of RNA polymerase II transcription, *Nat Rev Mol Cell Biol*, 7 (2006), 612-616.
- [75] C. Kanduri, J. Whitehead and F. Mohammad, The long and the short of it: RNA-directed chromatin asymmetry in mammalian X-chromosome inactivation, *FEBS Lett*, **583** (2009), 857-864.
- [76] J.C. Schwartz, S.T. Younger, N.B. Nguyen, D.B. Hardy, B.P. Monia, D.R. Corey and B.A. Janowski, Antisense transcripts are targets for activating small RNAs, *Nat Struct Mol Biol*, **15** (2008), 842-848.
- [77] A.D. Goldberg, C.D. Allis and E. Bernstein, Epigenetics: A landscape takes shape, *Cell*, **128** (2007), 635-638.
- [78] P. Anderson, Post-transcriptional regulons coordinate the initiation and resolution of inflammation, *Nat Rev Immunol*, **10** (2010), 24-35.
- [79] A.E. McKee and P.A. Silver, Systems perspectives on mRNA processing, *Cell Res*, 17 (2007), 581-590.
- [80] S. Buratowski, Connections between mRNA 3' end processing and transcription termination, *Curr Opin Cell Biol*, **17** (2005), 257-261.
- [81] S. Millevoi and S. Vagner, Molecular mechanisms of eukaryotic pre-mRNA 3' end processing regulation, *Nucl Acids Res* (In Press).
- [82] M. Chen and J.L. Manley, Mechanisms of alternative splicing regulation: insights from molecular and genomics approaches, *Nat Rev Mol Cell Biol*, **10** (2009), 741-754.
- [83] J.M. Gott and R.B. Emeson, Functions and mechanisms of RNA editing, *Annu Rev Genet*, **34** (2000), 499-531.
- [84] J.B. Li, E.Y. Levanon, J.K. Yoon, J. Aach, B. Xie, E. LeProust, K. Zhang, Y. Gao and G.M. Church, Genome-wide identification of human RNA editing sites by parallel DNA capturing and sequencing, *Science*, **324** (2009), 1210-1213.
- [85] M. Stewart, Ratcheting mRNA out of the nucleus, *Mol Cell*, **25** (2007), 327-330.
- [86] B.R. Cullen, Retroviruses as model systems for the study of nuclear RNA export pathways, *Virology*, **249** (1998), 203-210.

- [87] A.L. Silva and L. Romao, The mammalian nonsense-mediated mRNA decay pathway: To decay or not to decay! Which players make the decision?, *FEBS lett*, **583** (2009), 499-505.
- [88] C. van Vliet, E.C. Thomas, A. Merino-Trigo, R.D. Teasdale and P.A. Gleeson, Intracellular sorting and transport of proteins, *Prog Biophys Mol Biol*, 83 (2003), 1-45.
- [89] C. Andreassi and A. Riccio, To localize or not to localize: mRNA fate is in 3'UTR ends, *Trends Cell Biol*, **19** (2009), 465-474.
- [90] R. Parker and U. Sheth, P bodies and the control of mRNA translation and degradation, *Mol Cell*, **25** (2007), 635-646.
- [91] G.S. Wilkie, K.S. Dickson and N.K. Gray, Regulation of mRNA translation by 5'- and 3'-UTR-binding factors, *Trends Biochem Sci*, **28** (2003), 182-188.
- [92] R.J. Jackson, C.U.T. Hellen and T.V. Pestova, The mechanism of eukaryotic translation initiation and principles of its regulation, *Nat Rev Mol Cell Biol*, 11 (2010), 113-127.
- [93] R. Mendez and J.D. Richter, Translational control by CPEB: a means to the end, *Nat Rev Mol Cell Biol*, 2 (2001), 521-529.
- [94] M. Mann and O.N. Jensen, Proteomic analysis of post-translational modifications, *Nat Biotech*, **21** (2003), 255-261.
- [95] D.F. Steiner, D. Cunningham, L. Spigelman and B. Aten, Insulin biosynthesis: evidence for a precursor, *Science*, **157** (1967), 697-700.
- [96] M.A. Weiss, Proinsulin and the genetics of diabetes mellitus, *J Biol Chem*, **284** (2009), 19159-19163.
- [97] C. Giglione, O. Vallon and T. Meinnel, Control of protein life-span by N-terminal methionine excision, *EMBO J*, **22** (2003), 13-23.
- [98] C.T.N. Pham, Neutrophil serine proteases: specific regulators of inflammation, *Nat Rev Immunol*, **6** (2006), 541-550.
- [99] R.C. Lee, R.L. Feinbaum and V. Ambros, The C. elegans heterochronic gene lin-4 encodes small RNAs with antisense complementarity to lin-14, *Cell*, **75** (1993), 843-854.
- [100] B. Wightman, I. Ha and G. Ruvkun, Posttranscriptional regulation of the heterochronic gene lin-14 by lin-4 mediates temporal pattern formation in C. elegans, *Cell*, **75** (1993), 855-862.
- [101] B.J. Reinhart, F.J. Slack, M. Basson, A.E. Pasquinelli, J.C. Bettinger, A.E. Rougvie, H.R. Horvitz and G. Ruvkun, The 21-nucleotide let-7 RNA regulates developmental timing in Caenorhabditis elegans, *Nature*, **403** (2000), 901-906.
- [102] A.E. Pasquinelli, B.J. Reinhart, F. Slack, M.Q. Martindale, M.I. Kuroda, B. Maller, D.C. Hayward, E.E. Ball, B. Degnan, P. Muller, J. Spring, A. Srinivasan, M. Fishman, J. Finnerty, J. Corbo, M. Levine, P. Leahy, E. Davidson and G. Ruvkun, Conservation of the sequence and temporal expression of let-7 heterochronic regulatory RNA, *Nature*, 408 (2000), 86-89.

- [103] A. Molnar, F. Schwach, D.J. Studholme, E.C. Thuenemann and D.C. Baulcombe, miRNAs control gene expression in the single-cell alga Chlamydomonas reinhardtii, *Nature*, **447** (2007), 1126-1129.
- [104] B.R. Cullen, Viral and cellular messenger RNA targets of viral microRNAs, *Nature*, **457** (2009), 421-425.
- [105] S.D. Boyd, Everything you wanted to know about small RNA but were afraid to ask, *Lab Invest*, **88** (2008), 569-578.
- [106] S. Griffiths-Jones, H.K. Saini, S. van Dongen and A.J. Enright, miRBase: tools for microRNA genomics, *Nucl Acids Res*, **36** (2008), D154-158.
- [107] J. Lu, G. Getz, E.A. Miska, E. Varez-Saavedra, J. Lamb, D. Peck, A. Sweet-Cordero, B.L. Ebert, R.H. Mak, A.A. Ferrando, J.R. Downing, T. Jacks, H.R. Horvitz and T.R. Golub, MicroRNA expression profiles classify human cancers, *Nature*, **435** (2005), 834-838.
- [108] V.N. Kim, J. Han and M.C. Siomi, Biogenesis of small RNAs in animals, *Nat Rev Mol Cell Biol*, **10** (2009), 126-139.
- [109] D.P. Bartel, MicroRNAs: genomics, biogenesis, mechanism, and function, *Cell*, **116** (2004), 281-297.
- [110] Y. Lee, M. Kim, J. Han, K.H. Yeom, S. Lee, S.H. Baek and V.N. Kim, MicroRNA genes are transcribed by RNA polymerase II, *EMBO J*, **23** (2004), 4051-4060.
- [111] A. Lujambio, G.A. Calin, A. Villanueva, S. Ropero, M. Sanchez-Cespedes, D. Blanco, L.M. Montuenga, S. Rossi, M.S. Nicoloso, W.J. Faller, W.M. Gallagher, S.A. Eccles, C.M. Croce and M. Esteller, A microRNA DNA methylation signature for human cancer metastasis, *PNAS*, **105** (2008), 13556-13561.
- [112] A.M. Denli, B.B.J. Tops, R.H.A. Plasterk, R.F. Ketting and G.J. Hannon, Processing of primary microRNAs by the Microprocessor complex, *Nature*, 432 (2004), 231-235.
- [113] R. Yi, Y. Qin, I.G. Macara and B.R. Cullen, Exportin-5 mediates the nuclear export of pre-microRNAs and short hairpin RNAs, *Genes Dev*, **17** (2003), 3011-3016.
- [114] E. Bernstein, A.A. Caudy, S.M. Hammond and G.J. Hannon, Role for a bidentate ribonuclease in the initiation step of RNA interference, *Nature*, **409** (2001), 363-366.
- [115] J.G. Ruby, C.H. Jan and D.P. Bartel, Intronic microRNA precursors that bypass Drosha processing, *Nature*, **448** (2007), 83-86.
- [116] E. Berezikov, W.J. Chung, J. Willis, E. Cuppen and E.C. Lai, Mammalian mirtron genes, *Mol Cell*, **28** (2007), 328-336.
- [117] R.I. Gregory, K. Yan, G. Amuthan, T. Chendrimada, B. Doratotaj, N. Cooch and R. Shiekhattar, The Microprocessor complex mediates the genesis of microRNAs, *Nature*, **432** (2004), 235-240.

- [118] T. Fukuda, K. Yamagata, S. Fujiyama, T. Matsumoto, I. Koshida, K. Yoshimura, M. Mihara, M. Naitou, H. Endoh, T. Nakamura, C. Akimoto, Y. Yamamoto, T. Katagiri, C. Foulds, S. Takezawa, H. Kitagawa, K. Takeyama, B.W. O'Malley and S. Kato, DEAD-box RNA helicase subunits of the Drosha complex are required for processing of rRNA and a subset of microRNAs, Nat Cell Biol, 9 (2007), 604-611.
- [119] B.N. Davis, A.C. Hilyard, G. Lagna and A. Hata, SMAD proteins control DROSHA-mediated microRNA maturation, *Nature*, **454** (2008), 56-61.
- [120] D.J. Luciano, H. Mirsky, N.J. Vendetti and S. Maas, RNA editing of a miRNA precursor, RNA, 10 (2004), 1174-1177.
- [121] J. Winter, S. Jung, S. Keller, R.I. Gregory and S. Diederichs, Many roads to maturity: microRNA biogenesis pathways and their regulation, *Nat Cell Biol*, 11 (2009), 228-234.
- [122] Y. Kawahara, B. Zinshteyn, P. Sethupathy, H. Iizasa, A.G. Hatzigeorgiou and K. Nishikura, Redirection of silencing targets by adenosine-to-inosine editing of miRNAs, *Science*, **315** (2007), 1137-1140.
- [123] Y. Wang, G. Sheng, S. Juranek, T. Tuschl and D.J. Patel, Structure of the guide-strand-containing argonaute silencing complex, *Nature*, **456** (2008), 209-213.
- [124] M. Chekulaeva and W. Filipowicz, Mechanisms of miRNA-mediated post-transcriptional regulation in animal cells, *Curr Opin Cell Biol*, **21** (2009), 452-460.
- [125] M. Selbach, B. Schwanhausser, N. Thierfelder, Z. Fang, R. Khanin and N. Rajewsky, Widespread changes in protein synthesis induced by microRNAs, *Nature*, **455** (2008), 58-63.
- [126] J. Liu, M.A. Valencia-Sanchez, G.J. Hannon and R. Parker, MicroRNA-dependent localization of targeted mRNAs to mammalian P-bodies, *Nat Cell Biol*, 7 (2005), 719-723.
- [127] S. Vasudevan, Y. Tong and J.A. Steitz, Switching from repression to activation: microRNAs can up-regulate translation, *Science*, **318** (2007), 1931-1934.
- [128] U.A. Orom, F.C. Nielsen and A.H. Lund, MicroRNA-10a binds the 5 'UTR of ribosomal protein mRNAs and enhances their translation, *Mol Cell*, **30** (2008), 460-471.
- [129] N.P. Tsai, Y.L. Lin and L.N. Wei, MicroRNA mir-346 targets the 5'-untranslated region of receptor-interacting protein 140 (RIP140) mRNA and up-regulates its protein expression (Abstract), *Biochem J*, **424** (2009), 411-418.
- [130] J.J. Forman, A. Legesse-Miller and H.A. Coller, A search for conserved sequences in coding regions reveals that the let-7 microRNA targets Dicer within its coding sequence, *PNAS*, **105** (2008), 14879-14884.
- [131] X. Zhou, X. Duan, J. Qian and F. Li, Abundant conserved microRNA target sites in the 5'-untranslated region and coding sequence, *Genetica*, **137** (2009), 159-164.

- [132] D.H. Kim, P. Saetrom, O. Snove and J.J. Rossi, MicroRNA-directed transcriptional gene silencing in mammalian cells, *PNAS*, **105** (2008), 16230-16235.
- [133] R.F. Place, L.C. Li, D. Pookot, E.J. Noonan and R. Dahiya, MicroRNA-373 induces expression of genes with complementary promoter sequences, *PNAS*, **105** (2008), 1608-1613.
- [134] D. Baek, J. Villen, C. Shin, F.D. Camargo, S.P. Gygi and D.P. Bartel, The impact of microRNAs on protein output, *Nature*, **455** (2008), 64-71.
- [135] E. Bernstein, S.Y. Kim, M.A. Carmell, E.P. Murchison, H. Alcorn, M.Z. Li, A.A. Mills, S.J. Elledge, K.V. Anderson and G.J. Hannon, Dicer is essential for mouse development, *Nat Genet*, **35** (2003), 215-217.
- [136] Y. Zhao, J.F. Ransom, A. Li, V. Vedantham, M. von Drehle, A.N. Muth, T. Tsuchihashi, M.T. McManus, R.J. Schwartz and D. Srivastava, Dysregulation of cardiogenesis, cardiac conduction, and cell cycle in mice lacking miRNA-1-2, *Cell*, **129** (2007), 303-317.
- [137] J.F. Chen, E.P. Murchison, R. Tang, T.E. Callis, M. Tatsuguchi, Z. Deng, M. Rojas, S.M. Hammond, M.D. Schneider, C.H. Selzman, G. Meissner, C. Patterson, G.J. Hannon and D.Z. Wang, Targeted deletion of Dicer in the heart leads to dilated cardiomyopathy and heart failure, *PNAS*, 105 (2008), 2111-2116.
- [138] D. De Pietri Tonelli, J.N. Pulvers, C. Haffner, E.P. Murchison, G.J. Hannon and W.B. Huttner, miRNAs are essential for survival and differentiation of newborn neurons but not for expansion of neural progenitors during early neurogenesis in the mouse embryonic neocortex, *Development*, 135 (2008), 3911-3921.
- [139] T.C. Chang and J.T. Mendell, microRNAs in vertebrate physiology and human disease, *Annu Rev Genomics Hum Genet*, 8 (2007), 215-239.
- [140] S.M. Hammond, MicroRNAs as tumor suppressors, *Nat Genet*, **39** (2005), 582-583.
- [141] M.S. Kumar, J. Lu, K.L. Mercer, T.R. Golub and T. Jacks, Impaired microRNA processing enhances cellular transformation and tumorigenesis, *Nat Genet*, **39** (2007), 673-677.
- [142] M.L. Si, S. Zhu, H. Wu, Z. Lu, F. Wu and Y.Y. Mo, miR-21-mediated tumor growth, *Oncogene*, **26** (2006), 2799-2803.
- [143] Y. Sun, S. Koo, N. White, E. Peralta, C. Esau, N.M. Dean and R.J. Perera, Development of a micro-array to detect human and mouse microRNAs and characterization of expression in human organs, *Nucl Acids Res*, 32 (2004), e188.
- [144] J. Shingara, K. Keiger, J. Shelton, W. Laosinchai-Wolf, P. Powers, R. Conrad, D. Brown and E. Labourier, An optimized isolation and labeling platform for accurate microRNA expression profiling, RNA, 11 (2005), 1461-1470.

- [145] C.G. Liu, G.A. Calin, B. Meloon, N. Gamliel, C. Sevignani, M. Ferracin, C.D. Dumitru, M. Shimizu, S. Zupo, M. Dono, H. Alder, F. Bullrich, M. Negrini and C.M. Croce, An oligonucleotide microchip for genome-wide microRNA profiling in human and mouse tissues, *PNAS*, 101 (2004), 9740-9744.
- [146] P. Landgraf, M. Rusu, R. Sheridan, A. Sewer, N. Iovino, A. Aravin, S. Pfeffer, A. Rice, A.O. Kamphorst, M. Landthaler, C. Lin, N.D. Socci, L. Hermida, V. Fulci, S. Chiaretti, R. Foa, J. Schliwka, U. Fuchs, A. Novosel, R.-U. Mueller, B. Schermer, U. Bissels, J. Inman, Q. Phan, M. Chien, D.B. Weir, R. Choksi, G. De Vita, D. Frezzetti, H.I. Trompeter, V. Hornung, G. Teng, G. Hartmann, M. Palkovits, R. Di Lauro, P. Wernet, G. Macino, C.E. Rogler, J.W. Nagle, J. Ju, F.N. Papavasiliou, T. Benzing, P. Lichter, W. Tam, M.J. Brownstein, A. Bosio, A. Borkhardt, J.J. Russo, C. Sander, M. Zavolan and T. Tuschl, A mammalian microRNA expression atlas based on small RNA library sequencing, Cell, 129 (2007), 1401-1414.
- [147] Z. Tian, A.S. Greene, J.L. Pietrusz, I.R. Matus and M. Liang, MicroRNA-target pairs in the rat kidney identified by microRNA microarray, proteomic, and bioinformatic analysis, *Genome Res*, 18 (2008), 404-411.
- [148] J. Ho, K.H. Ng, S. Rosen, A. Dostal, R.I. Gregory and J.A. Kreidberg, Podocyte-specific loss of functional microRNAs leads to rapid glomerular and tubular injury, *J Am Soc Nephrol*, **19** (2008), 2069-2075.
- [149] S. Shi, L. Yu, C. Chiu, Y. Sun, J. Chen, G. Khitrov, M. Merkenschlager, L.B. Holzman, W. Zhang, P. Mundel and E.P. Bottinger, Podocyte-selective deletion of Dicer induces proteinuria and glomerulosclerosis, *J Am Soc Nephrol*, 19 (2008), 2159-2169.
- [150] S.J. Harvey, G. Jarad, J. Cunningham, S. Goldberg, B. Schermer, B.D. Harfe, M.T. McManus, T. Benzing and J.H. Miner, Podocyte-specific deletion of Dicer alters cytoskeletal dynamics and causes glomerular disease, *J Am Soc Nephrol*, 19 (2008), 2150-2158.
- [151] M. Kato, J. Zhang, M. Wang, L. Lanting, H. Yuan, J.J. Rossi and R. Natarajan, MicroRNA-192 in diabetic kidney glomeruli and its function in TGF-beta-induced collagen expression via inhibition of E-box repressors, *PNAS*, **104** (2007), 3432-3437.
- [152] M. Kato, S. Putta, M. Wang, H. Yuan, L. Lanting, I. Nair, A. Gunn, Y. Nakagawa, H. Shimano, I. Todorov, J.J. Rossi and R. Natarajan, TGF-beta activates Akt kinase through a microRNA-dependent amplifying circuit targeting PTEN, *Nat Cell Biol*, 11 (2009), 881-889.
- [153] Q. Wang, Y. Wang, A.W. Minto, J. Wang, Q. Shi, X. Li and R.J. Quigg, MicroRNA-377 is up-regulated and can lead to increased fibronectin production in diabetic nephropathy, *FASEB J*, **22** (2008), 4126-4135.
- [154] P. Kantharidis, B. Wang, S.M. Twigg and M.E. Cooper, The role of growth factors and miRNAs on EMT in diabetic disease, in: *The American Society of Nephrology Annual Meeting*, Philadelphia, US, 2008.

- [155] P. Pandey, B. Brors, P. Srivastava, A. Bott, S. Boehn, H.J. Groene and N. Gretz, Microarray-based approach identifies microRNAs and their target functional patterns in polycystic kidney disease, *BMC Genomics*, 9 (2008), 624.
- [156] G. Wang, B.C.H. Kwan, F.M.M. Lai, P.C.L. Choi, K.M. Chow, P.K.T. Li and C.C. Szeto, Intrarenal expression of microRNAs in patients with IgA nephropathy, *Lab Invest*, **90** (2009), 98-103.
- [157] G. Wang, B.C.H. Kwan, F.M.M. Lai, P.C.L. Choi, K.M. Chow, P.K.T. Li and C.C. Szeto, Intrarenal expression of miRNAs in patients with hypertensive nephrosclerosis, *Am J Hypertens*, 23 (2009), 78-84.
- [158] F. Gottardo, C.G. Liu, M. Ferracin, G.A. Calin, M. Fassan, P. Bassi, C. Sevignani, D. Byrne, M. Negrini, F. Pagano, L.G. Gomella, C.M. Croce and R. Baffa, Micro-RNA profiling in kidney and bladder cancers, *Urol Oncol*, 25 (2007), 387-392.
- [159] C. Nakada, K. Matsuura, Y. Tsukamoto, M. Tanigawa, T. Yoshimoto, T. Narimatsu, L.T. Nguyen, N. Hijiya, T. Uchida, F. Sato, H. Mimata, M. Seto and M. Moriyama, Genome-wide microRNA expression profiling in renal cell carcinoma: significant down-regulation of miR-141 and miR-200c, *J Pathol*, 216 (2008), 418-427.
- [160] Y. Huang, Y. Dai, J. Yang, T. Chen, Y. Yin, M. Tang, C. Hu and L. Zhang, Microarray analysis of microRNA expression in renal clear cell carcinoma, *Eur J Surg Oncol*, **35** (2009), 1119-1123.
- [161] T.F. Chow, Y.M. Youssef, E. Lianidou, A.D. Romaschin, R.J. Honey, R. Stewart, K.T. Pace and G.M. Yousef, Differential expression profiling of microRNAs and their potential involvement in renal cell carcinoma pathogenesis, *Clin Biochem*, 43 (2010), 150-158.
- [162] D. Juan, G. Alexe, T. Antes, H. Liu, A. Madabhushi, C. Delisi, S. Ganesan, G. Bhanot and L.S. Liou, Identification of a microRNA panel for clear-cell kidney cancer, *Urology* (In Press).
- [163] W. Sui, Y. Dai, Y. Huang, H. Lan, Q. Yan and H. Huang, Microarray analysis of microRNA expression in acute rejection after renal transplantation, *Transpl Immunol*, 19 (2008), 81-85.
- [164] D. Anglicheau, V.K. Sharma, R. Ding, A. Hummel, C. Snopkowski, D. Dadhania, S.V. Seshan and M. Suthanthiran, MicroRNA expression profiles predictive of human renal allograft status, *PNAS*, **106** (2009), 5330-5335.
- [165] R.F. Duisters, A.J. Tijsen, B. Schroen, J.J. Leenders, V. Lentink, I. van der Made, V. Herias, R.E. van Leeuwen, M.W. Schellings, P. Barenbrug, J.G. Maessen, S. Heymans, Y.M. Pinto and E.E. Creemers, miR-133 and miR-30 regulate connective tissue growth factor: implications for a role of microRNAs in myocardial matrix remodeling, *Circ Res*, 104 (2009), 170-178.

- [166] N. Liu, S. Bezprozvannaya, A.H. Williams, X. Qi, J.A. Richardson, R. Bassel-Duby and E.N. Olson, microRNA-133a regulates cardiomyocyte proliferation and suppresses smooth muscle gene expression in the heart, *Genes Dev*, 22 (2008), 3242-3254.
- [167] Encyclopædia Britannica., Kidney, in: Encyclopædia Britannica Online: http://www.britannica.com/EBchecked/topic/317358/kidney [Retrieved 15th January 2010], 2010.
- [168] J.S. Berns, Patient information: Chronic kidney disease., in: *UpToDate*, D.S. Basow, ed, Waltham, MA, 2009.
- [169] A. Williams, Functional aspects of animal microRNAs, *Cell Mol Life Sci*, **65** (2008), 545-562.
- [170] B.J.G. Pereira, M.H. Sayegh and P. Blake, *Chronic Kidney Disease*, *Dialysis*, & *Transplantation*, Second Edition, Saunders, 2005.
- [171] M.J. Ryan, G. Johnson, J. Kirk, S.M. Fuerstenberg, R.A. Zager and B. Torok-Storb, HK-2: An immortalized proximal tubule epithelial cell line from normal adult human kidney, *Kidney Int*, **45** (1994), 48-57.
- [172] L. Pirisi, K.E. Creek, J. Doniger and J.A. Dipaolo, Continuous cell lines with altered growth and differentiation properties originate after transfection of human keratinocytes with human papillomavirus type 16 DNA, *Carcinogenesis*, 9 (1988), 1573-1579.
- [173] S. Jones, S. Jones and A.O. Phillips, Regulation of renal proximal tubular epithelial cell hyaluronan generation: Implications for diabetic nephropathy, *Kidney Int*, **59** (2001), 1739-1749.
- [174] Y.C. Tian, D. Fraser, L. Attisano and A.O. Phillips, TGF-beta1-mediated alterations of renal proximal tubular epithelial cell phenotype, *Am J Physiol Renal Physiol*, **285** (2003), F130-142.
- [175] R.E. Wager and R.K. Assoian, A phorbol ester-regulated ribonuclease system controlling transforming growth factor beta 1 gene expression in hematopoietic cells, *Mol Cell Biol*, **10** (1990), 5983-5990.
- [176] C. Sundstrom and K. Nilsson, Establishment and characterization of a human histiocytic lymphoma cell line (U-937), *Int J Cancer*, **17** (1976), 565-577.
- [177] R. Hass, H. Gunji, R. Datta, S. Kharbanda, A. Hartmann, R. Weichselbaum and D. Kufe, Differentiation and retrodifferentiation of human myeloid leukemia cells is sssociated with reversible induction of cell cycle-regulatory genes, *Cancer Res*, **52** (1992), 1445-1450.
- [178] I. Olsson, U. Gullberg, I. Ivhed and K. Nilsson, Induction of differentiation of the human histocytic lymphoma cell line U-937 by 1alpha,25-dihydroxycholecalciferol, *Cancer Res*, **43** (1983), 5862-5867.
- [179] S. Schutze, P. Scheurich, C. Schluter, U. Ucer, K. Pfizenmaier and M. Kronke, Tumor necrosis factor-induced changes of gene expression in U937 cells. Differentiation-dependent plasticity of the responsive state, *J Immunol*, **140** (1988), 3000-3005.

- [180] E. Piek, A. Moustakas, A. Kurisaki, C.H. Heldin and P. ten Dijke, TGF-beta type I receptor/ALK-5 and Smad proteins mediate epithelial to mesenchymal transdifferentiation in NMuMG breast epithelial cells, *J Cell Sci*, **112** (1999), 4557-4568.
- [181] A. Lewis, R. Steadman, P. Manley, K. Craig, C. de la Motte, V. Hascall and A.O. Phillips, Diabetic nephropathy, inflammation, hyaluronan and interstitial fibrosis, *Histol Histopathol*, **23** (2008), 731-739.
- [182] W. Shih, W.H. Hines and E.G. Neilson, Effects of cyclosporin A on the development of immune-mediated interstitial nephritis, *Kidney Int*, 33 (1988), 1113-1118.
- [183] P. Chomczynski and N. Sacchi, Single-step method of RNA isolation by acid guanidinium thiocyanate-phenol-chloroform extraction, *Anal Biochem*, **162** (1987), 156-159.
- [184] S. Rozen and H. Skaletsky, Primer3 on the WWW for general users and for biologist programmers, in: *Bioinformatics: Methods and Protocols*, 1999, pp. 365-386.
- [185] J. Ye, S. McGinnis and T.L. Madden, BLAST: improvements for better sequence analysis, *Nucleic Acids Res*, 34 (2006), W6-9.
- [186] K.J. Livak and T.D. Schmittgen, Analysis of relative gene expression data using real-time quantitative PCR and the 2-[Delta][Delta]CT method, *Methods*, **25** (2001), 402-408.
- [187] C. Chen, D.A. Ridzon, A.J. Broomer, Z. Zhou, D.H. Lee, J.T. Nguyen, M. Barbisin, N.L. Xu, V.R. Mahuvakar, M.R. Andersen, K.Q. Lao, K.J. Livak and K.J. Guegler, Real-time quantification of microRNAs by stem-loop RT-PCR, *Nucleic Acids Res*, 33 (2005), e179.
- [188] R. Shi and V.L. Chiang, Facile means for quantifying microRNA expression by real-time PCR, *Biotechniques*, **39** (2005), 519-525.
- [189] M. Zuker, Mfold web server for nucleic acid folding and hybridization prediction, *Nucleic Acids Res*, **31** (2003), 3406-3415.
- [190] U.K. Laemmli, Cleavage of structural proteins during the assembly of the head of bacteriophage T4, *Nature*, 227 (1970), 680-685.
- [191] A. Krek, D. Grun, M.N. Poy, R. Wolf, L. Rosenberg, E.J. Epstein, P. MacMenamin, I. da Piedade, K.C. Gunsalus, M. Stoffel and N. Rajewsky, Combinatorial microRNA target predictions, *Nat Genet*, **37** (2005), 495-500.
- [192] T.F. Smith and M.S. Waterman, Identification of common molecular subsequences, *J Mol Biol*, **147** (1981), 195-197.
- [193] K.C. Miranda, T. Huynh, Y. Tay, Y.S. Ang, W.L. Tam, A.M. Thomson, B. Lim and I. Rigoutsos, A pattern-based method for the identification of microRNA binding sites and their corresponding heteroduplexes, *Cell*, **126** (2006), 1203-1217.
- [194] I.L. Hofacker, Vienna RNA secondary structure server, *Nucleic Acids Res*, **31** (2003), 3429-3431.

- [195] J. Vandesompele, K. De Preter, F. Pattyn, B. Poppe, N. Van Roy, A. De Paepe and F. Speleman, Accurate normalization of real-time quantitative RT-PCR data by geometric averaging of multiple internal control genes, *Genome Biol*, 3 (2002), 1-11.
- [196] Y. Benjamini and Y. Hochberg, Controlling the false discovery rate: A practical and powerful approach to multiple testing, *J R Stat Soc*, **57** (1995), 289-300.
- [197] N.J. Walker, A technique whose time has come, Science, 296 (2002), 557-559.
- [198] G. Hutvagner, J. McLachlan, A.E. Pasquinelli, E. Balint, T. Tuschl and P.D. Zamore, A cellular function for the RNA-interference enzyme Dicer in the maturation of the let-7 small temporal RNA, *Science*, **293** (2001), 834-838.
- [199] T.P. Chendrimada, R.I. Gregory, E. Kumaraswamy, J. Norman, N. Cooch, K. Nishikura and R. Shiekhattar, TRBP recruits the Dicer complex to Ago2 for microRNA processing and gene silencing, *Nature*, **436** (2005), 740-744.
- [200] J. Liu, F.V. Rivas, J. Wohlschlegel, J.R. Yates, R. Parker and G.J. Hannon, A role for the P-body component GW182 in microRNA function, *Nat Cell Biol*, 7 (2005), 1261-1266.
- [201] J. Huang, F. Wang, E. Argyris, K. Chen, Z. Liang, H. Tian, W. Huang, K. Squires, G. Verlinghieri and H. Zhang, Cellular microRNAs contribute to HIV-1 latency in resting primary CD4+ T lymphocytes, *Nat Med*, **13** (2007), 1241-1247.
- [202] S. Chatterjee and H. Grosshans, Active turnover modulates mature microRNA activity in Caenorhabditis elegans, *Nature*, **461** (2009), 546-549.
- [203] W. Qi, X. Chen, R.E. Gilbert, Y. Zhang, M. Waltham, M. Schache, D.J. Kelly and C.A. Pollock, High glucose-induced thioredoxin-interacting protein in renal proximal tubule cells is independent of transforming growth factor-beta1, Am J Pathol, 171 (2007), 744-754.
- [204] A. Krupa, R. Jenkins, D.D. Luo, A. Lewis, A. Phillips and D. Fraser, Loss of microRNA-192 promotes fibrogenesis in diabetic nephropathy, *J Am Soc Nephrol* (In Press).
- [205] R. Kulshreshtha, M. Ferracin, S.E. Wojcik, R. Garzon, H. Alder, F.J. Agosto-Perez, R. Davuluri, C.G. Liu, C.M. Croce, M. Negrini, G.A. Calin and M. Ivan, A microRNA signature of hypoxia, *Mol Cell Biol*, 27 (2007), 1859-1867.
- [206] M.V. Rocco, Y. Chen, S. Goldfarb and F.N. Ziyadeh, Elevated glucose stimulates TGF-beta gene expression and bioactivity in proximal tubule, *Kidney Int*, 41 (1992), 107-114.
- [207] J. Li, P. Smyth, R. Flavin, S. Cahill, K. Denning, S. Aherne, S. Guenther, J. O'Leary and O. Sheils, Comparison of miRNA expression patterns using total RNA extracted from matched samples of formalin-fixed paraffinembedded (FFPE) cells and snap frozen cells, *BMC Biotechnol*, 7 (2007), 36.

- [208] Y. Xi, G. Nakajima, E. Gavin, C.G. Morris, K. Kudo, K. Hayashi and J. Ju, Systematic analysis of microRNA expression of RNA extracted from fresh frozen and formalin-fixed paraffin-embedded samples, RNA, 13 (2007), 1668-1674.
- [209] U. Siebolts, H. Varnholt, U. Drebber, H.P. Dienes, C. Wickenhauser and M. Odenthal, Tissues from routine pathology archives are suitable for microRNA analyses by quantitative PCR, *J Clin Pathol*, **62** (2009), 84-88.
- [210] C.D. Johnson, A. Esquela-Kerscher, G. Stefani, M. Byrom, K. Kelnar, D. Ovcharenko, M. Wilson, X. Wang, J. Shelton, J. Shingara, L. Chin, D. Brown and F.J. Slack, The let-7 microRNA represses cell proliferation pathways in human cells, *Cancer Res*, 67 (2007), 7713-7722.
- [211] J. Zavadil, M. Narasimhan, M. Blumenberg and R.J. Schneider, Transforming growth factor-beta and microRNA: mRNA regulatory networks in epithelial plasticity, *Cells Tissues Organs*, **185** (2007), 157-161.
- [212] L. He, X. He, L.P. Lim, E. de Stanchina, Z. Xuan, Y. Liang, W. Xue, L. Zender, J. Magnus, D. Ridzon, A.L. Jackson, P.S. Linsley, C. Chen, S.W. Lowe, M.A. Cleary and G.J. Hannon, A microRNA component of the p53 tumour suppressor network, *Nature*, 447 (2007), 1130-1134.
- [213] G.J. Hurteau, J.A. Carlson, S.D. Spivack and G.J. Brock, Overexpression of the microRNA hsa-miR-200c leads to reduced expression of Transcription Factor 8 and increased expression of E-Cadherin, *Cancer Res*, **67** (2007), 7972-7976.
- [214] A. Shenoy and R. Blelloch, Genomic analysis suggests that mRNA destabilization by the Microprocessor is specialized for the auto-regulation of Dgcr8, *PLoS ONE*, 4 (2009), e6971.
- [215] E. Lund, S. Guttinger, A. Calado, J.E. Dahlberg and U. Kutay, Nuclear export of microRNA precursors, *Science*, **303** (2004), 95-98.
- [216] H. Su, M.I. Trombly, J. Chen and X. Wang, Essential and overlapping functions for mammalian Argonautes in microRNA silencing, *Genes Dev*, 23 (2009), 304-317.
- [217] S. Kadener, J. Rodriguez, K.C. Abruzzi, Y.L. Khodor, K. Sugino, M.T. Marr, S. Nelson and M. Rosbash, Genome-wide identification of targets of the drosha-pasha/DGCR8 complex, RNA, 15 (2009), 537-545.
- [218] A. Calado, N. Treichel, E.-C. Muller, A. Otto and U. Kutay, Exportin-5-mediated nuclear export of eukaryotic elongation factor 1A and tRNA, *EMBO J*, **21** (2002), 6216-6224.
- [219] O.H. Tam, A.A. Aravin, P. Stein, A. Girard, E.P. Murchison, S. Cheloufi, E. Hodges, M. Anger, R. Sachidanandam, R.M. Schultz and G.J. Hannon, Pseudogene-derived small interfering RNAs regulate gene expression in mouse oocytes, *Nature*, **453** (2008), 534-538.
- [220] T. Watanabe, Y. Totoki, A. Toyoda, M. Kaneda, S. Kuramochi-Miyagawa, Y. Obata, H. Chiba, Y. Kohara, T. Kono, T. Nakano, M.A. Surani, Y. Sakaki and H. Sasaki, Endogenous siRNAs from naturally formed dsRNAs regulate transcripts in mouse oocytes, *Nature*, **453** (2008), 539-543.

- [221] I.J. MacRae and J.A. Doudna, Ribonuclease revisited: structural insights into ribonuclease III family enzymes, *Curr Opin Struct Biol*, 17 (2007), 138-145.
- [222] L. Ding and M. Han, GW182 family proteins are crucial for microRNA-mediated gene silencing, *Trends Cell Biol*, 17 (2007), 411-416.
- [223] J.M. Cummins, Y. He, R.J. Leary, R. Pagliarini, L.A. Diaz, T. Sjoblom, O. Barad, Z. Bentwich, A.E. Szafranska, E. Labourier, C.K. Raymond, B.S. Roberts, H. Juhl, K.W. Kinzler, B. Vogelstein and V.E. Velculescu, The colorectal microRNAome, *PNAS*, **103** (2006), 3687-3692.
- [224] D. Damiani, J.J. Alexander, J.R. O'Rourke, M. McManus, A.P. Jadhav, C.L. Cepko, W.W. Hauswirth, B.D. Harfe and E. Strettoi, Dicer inactivation leads to progressive functional and structural degeneration of the mouse retina, *J Neurosci*, **28** (2008), 4878-4887.
- [225] M.Z. Michael, S.M. O' Connor, N.G. van Holst Pellekaan, G.P. Young and R.J. James, Reduced accumulation of specific microRNAs in colorectal neoplasia, *Mol Cancer Res*, 1 (2003), 882-891.
- [226] J. Krutzfeldt, N. Rajewsky, R. Braich, K.G. Rajeev, T. Tuschl, M. Manoharan and M. Stoffel, Silencing of microRNAs in vivo with `antagomirs', *Nature*, 438 (2005), 685-689.
- [227] J. Comijn, G. Berx, P. Vermassen, K. Verschueren, L. van Grunsven, E. Bruyneel, M. Mareel, D. Huylebroeck and F. van Roy, The two-handed E box binding zinc finger protein SIP1 downregulates E-cadherin and induces invasion, *Mol Cell*, 7 (2001), 1267-1278.
- [228] T. Shirakihara, M. Saitoh and K. Miyazono, Differential regulation of epithelial and mesenchymal markers by deltaEF1 proteins in epithelial mesenchymal transition induced by TGF-beta, *Mol Biol Cell*, **18** (2007), 3533-3544.
- [229] A.J. Evans, R.C. Russell, O. Roche, T.N. Burry, J.E. Fish, V.W.K. Chow, W.Y. Kim, A. Saravanan, M.A. Maynard, M.L. Gervais, R.I. Sufan, A.M. Roberts, L.A. Wilson, M. Betten, C. Vandewalle, G. Berx, P.A. Marsden, M.S. Irwin, B.T. Teh, M.A.S. Jewett and M. Ohh, VHL promotes E2 Box-dependent E-Cadherin transcription by HIF-mediated regulation of SIP1 and Snail, Mol Cell Biol, 27 (2007), 157-169.
- [230] B. Krishnamachary, D. Zagzag, H. Nagasawa, K. Rainey, H. Okuyama, J.H. Baek and G.L. Semenza, Hypoxia-inducible factor-1-dependent repression of E-cadherin in von Hippel-Lindau tumor suppressor-null renal cell carcinoma mediated by TCF3, ZFHX1A, and ZFHX1B, Cancer Res, 66 (2006), 2725-2731.
- [231] J.P. Thiery, Epithelial-mesenchymal transitions in tumour progression, *Nat Rev Cancer*, **2** (2002), 442-454.
- [232] J. Yang and R.A. Weinberg, Epithelial-mesenchymal transition: At the crossroads of development and tumor metastasis, *Dev Cell*, **14** (2008), 818-829.
- [233] F. Strutz, H. Okada, C.W. Lo, T. Danoff, R.L. Carone, J.E. Tomaszewski and E.G. Neilson, Identification and characterization of a fibroblast marker: FSP1, *J Cell Biol*, **130** (1995), 393-405.

- [234] Y.Y. Ng, T.P. Huang, W.C. Yang, Z.P. Chen, A.H. Yang, W. Mu, D.J. Nikolic-Paterson, R.C. Atkins and H.Y. Lan, Tubular epithelial-myofibroblast transdifferentiation in progressive tubulointerstitial fibrosis in 5/6 nephrectomized rats, *Kidney Int*, **54** (1998), 864-876.
- [235] K. Jinde, D.J. Nikolic-Paterson, X.R. Huang, H. Sakai, K. Kurokawa, R.C. Atkins and H.Y. Lan, Tubular phenotypic change in progressive tubulointerstitial fibrosis in human glomerulonephritis, *Am J Kidney Dis*, **38** (2001), 761-769.
- [236] M.P. Rastaldi, F. Ferrario, L. Giardino, G. Dell'Antonio, C. Grillo, P. Grillo, F. Strutz, G.A. Muller, G. Colasanti and G. D'Amico, Epithelial-mesenchymal transition of tubular epithelial cells in human renal biopsies, *Kidney Int*, 62 (2002), 137-146.
- [237] M. Iwano, D. Plieth, T.M. Danoff, C. Xue, H. Okada and E.G. Neilson, Evidence that fibroblasts derive from epithelium during tissue fibrosis, *J Clin Invest*, **110** (2002), 341-350.
- [238] P.A. Gregory, C.P. Bracken, A.G. Bert and G.J. Goodall, MicroRNAs as regulators of epithelial-mesenchymal transition, *Cell Cycle*, 7 (2008), 3112-3117.
- [239] A.K. Perl, P. Wilgenbus, U. Dahl, H. Semb and G. Christofori, A causal role for E-cadherin in the transition from adenoma to carcinoma, *Nature*, **392** (1998), 190-193.
- [240] U. Burk, J. Schubert, U. Wellner, O. Schmalhofer, E. Vincan, S. Spaderna and T. Brabletz, A reciprocal repression between ZEB1 and members of the miR-200 family promotes EMT and invasion in cancer cells, *EMBO Rep*, 9 (2008), 582-589.
- [241] P.A. Gregory, A.G. Bert, E.L. Paterson, S.C. Barry, A. Tsykin, G. Farshid, M.A. Vadas, Y. Khew-Goodall and G.J. Goodall, The miR-200 family and miR-205 regulate epithelial to mesenchymal transition by targeting ZEB1 and SIP1, *Nat Cell Biol*, **10** (2008), 593-601.
- [242] M. Korpal, E.S. Lee, G. Hu and Y. Kang, The miR-200 family inhibits epithelial-mesenchymal transition and cancer cell migration by direct targeting of E-cadherin transcriptional repressors ZEB1 and ZEB2, *J Biol Chem*, **283** (2008), 14910-14914.
- [243] S.M. Park, A.B. Gaur, E. Lengyel and M.E. Peter, The miR-200 family determines the epithelial phenotype of cancer cells by targeting the E-cadherin repressors ZEB1 and ZEB2, *Genes Dev*, **22** (2008), 894-907.
- [244] S. Yang, J. Du, Z. Wang, J. Yan, W. Yuan, J. Zhang and T. Zhu, Dual mechanism of deltaEF1 expression regulated by bone morphogenetic protein-6 in breast cancer, *Int J Biochem Cell Biol*, **41** (2009), 853-861.
- [245] S. Bindels, M. Mestdagt, C. Vandewalle, N. Jacobs, L. Volders, A. Noel, F.v. Roy, G. Berx, J.M. Foidart and C. Gilles, Regulation of vimentin by SIP1 in human epithelial breast tumor cells, *Oncogene*, **25** (2006), 4975-4985.
- [246] S. Thuault, U. Valcourt, M. Petersen, G. Manfioletti, C.H. Heldin and A. Moustakas, Transforming growth factor-beta employs HMGA2 to elicit epithelial-mesenchymal transition, *J Cell Biol*, **174** (2006), 175-183.

- [247] Y.W. Kong, I.G. Cannell, C.H. de Moor, K. Hill, P.G. Garside, T.L. Hamilton, H.A. Meijer, H.C. Dobbyn, M. Stoneley, K.A. Spriggs, A.E. Willis and M. Bushell, The mechanism of micro-RNA-mediated translation repression is determined by the promoter of the target gene, *PNAS*, **105** (2008), 8866-8871.
- [248] D. Fraser, L. Wakefield and A. Phillips, Independent regulation of transforming growth factor-beta1 transcription and translation by glucose and platelet-derived growth factor, Am J Pathol, 161 (2002), 1039-1049.
- [249] S.J. Kim, K. Park, D. Koeller, K.Y. Kim, L.M. Wakefield, M.B. Sporn and A.B. Roberts, Post-transcriptional regulation of the human transforming growth factor-beta 1 gene, *J Biol Chem*, **267** (1992), 13702-13707.
- [250] L. Scotto and R.K. Assoian, A GC-rich domain with bifunctional effects on mRNA and protein levels: implications for control of transforming growth factor beta 1 expression, *Mol Cell Biol*, **13** (1993), 3588-3597.
- [251] A. Gupta, J.J. Gartner, P. Sethupathy, A.G. Hatzigeorgiou and N.W. Fraser, Anti-apoptotic function of a microRNA encoded by the HSV-1 latencyassociated transcript, *Nature*, 442 (2006), 82-85.
- [252] A. Gupta, J.J. Gartner, P. Sethupathy, A.G. Hatzigeorgiou and N.W. Fraser, Anti-apoptotic function of a microRNA encoded by the HSV-1 latency-associated transcript (Retraction), *Nature*, **451** (2008), 600.
- [253] Q. Jing, S. Huang, S. Guth, T. Zarubin, A. Motoyama, J. Chen, F. Di Padova, S.C. Lin, H. Gram and J. Han, Involvement of microRNA in AU-rich element-mediated mRNA instability, *Cell*, **120** (2005), 623-634.
- [254] M. Kedde, M.J. Strasser, B. Boldajipour, J.A.F.O. Vrielink, K. Slanchev, C. le Sage, R. Nagel, P.M. Voorhoeve, J. van Duijse, U.A. Orom, A.H. Lund, A. Perrakis, E. Raz and R. Agami, RNA-binding protein Dnd1 inhibits microRNA access to target mRNA, Cell, 131 (2007), 1273-1286.
- [255] Y. Mishima, A.J. Giraldez, Y. Takeda, T. Fujiwara, H. Sakamoto, A.F. Schier and K. Inoue, Differential regulation of germline mRNAs in soma and germ cells by zebrafish miR-430, *Curr Biol*, **16** (2006), 2135-2142.
- [256] R. Kretschmer-Kazemi Far and G. Sczakiel, The activity of siRNA in mammalian cells is related to structural target accessibility: a comparison with antisense oligonucleotides, *Nucl Acids Res*, **31** (2003), 4417-4424.
- [257] B.P. Lewis, C.B. Burge and D.P. Bartel, Conserved seed pairing, often flanked by adenosines, indicates that thousands of human genes are microRNA targets, *Cell*, **120** (2005), 15-20.
- [258] W.C.S. Cho, MicroRNAs: Potential biomarkers for cancer diagnosis, prognosis and targets for therapy, *Int J Biochem Cell Biol* (In Press).
- [259] S. Gilad, E. Meiri, Y. Yogev, S. Benjamin, D. Lebanony, N. Yerushalmi, H. Benjamin, M. Kushnir, H. Cholakh, N. Melamed, Z. Bentwich, M. Hod, Y. Goren and A. Chajut, Serum microRNAs are promising novel biomarkers, *PLoS ONE*, 3 (2008), e3148.

- [260] H.S. Melkonyan, W.J. Feaver, E. Meyer, V. Scheinker, E.M. Shekhtman, Z. Xin and S.R. Umansky, Transrenal nucleic acids: from proof of principle to clinical tests, *Ann N Y Acad Sci*, **1137** (2008), 73-81.
- [261] M. Hanke, K. Hoefig, H. Merz, A.C. Feller, I. Kausch, D. Jocham, J.M. Warnecke and G. Sczakiel, A robust methodology to study urine microRNA as tumor marker: microRNA-126 and microRNA-182 are related to urinary bladder cancer, *Urol Oncol* (In Press).

APPENDIX: Buffers and Reagents

Reducing Gel Loading Buffer 3x		TBS (10x)	
0.5 M Tris-HCl, pH 6.8	1 ml	Tris	24.2 g/l
Glycerol	2.4 ml	NaCl	80 g/l
10% (w/v) SDS	4.8 ml	pH 7.4	
0.05% (w/v) Bromophenol Blue 2 drops			
Beta-mercaptoethanol	1.2 ml	Stripping Buffer	
		0.5 M Tris pH 6.8	5 ml/40 ml
Running Buffer (10x)		10% (w/v) SDS	8 ml/40 ml
Tris-HCl	30 g/l	Beta-mercaptoethanol	320µl/40ml
Glycine	144 g/l		
SDS	10 g/l	YTx2	
pH 8.3		Tryptone	16 g/l
		Yeast extract	10 g/l
Transfer Buffer (10x)		NaCl	5 g/l
Tris-HCl	30 g/l		
Glycine	144 g/l	YTx2 agar plates	
pH 8.3 (no adjustment necessary)		Tryptone	16 g/l
		Yeast extract	10 g/l
Transfer Buffer (1x)		NaCl	5 g/l
Transfer Buffer 10x	100 ml/l	Agar	20 g/l
Methanol	200 ml/l		